Green Chemistry

Cutting-edge research for a greener sustainable future
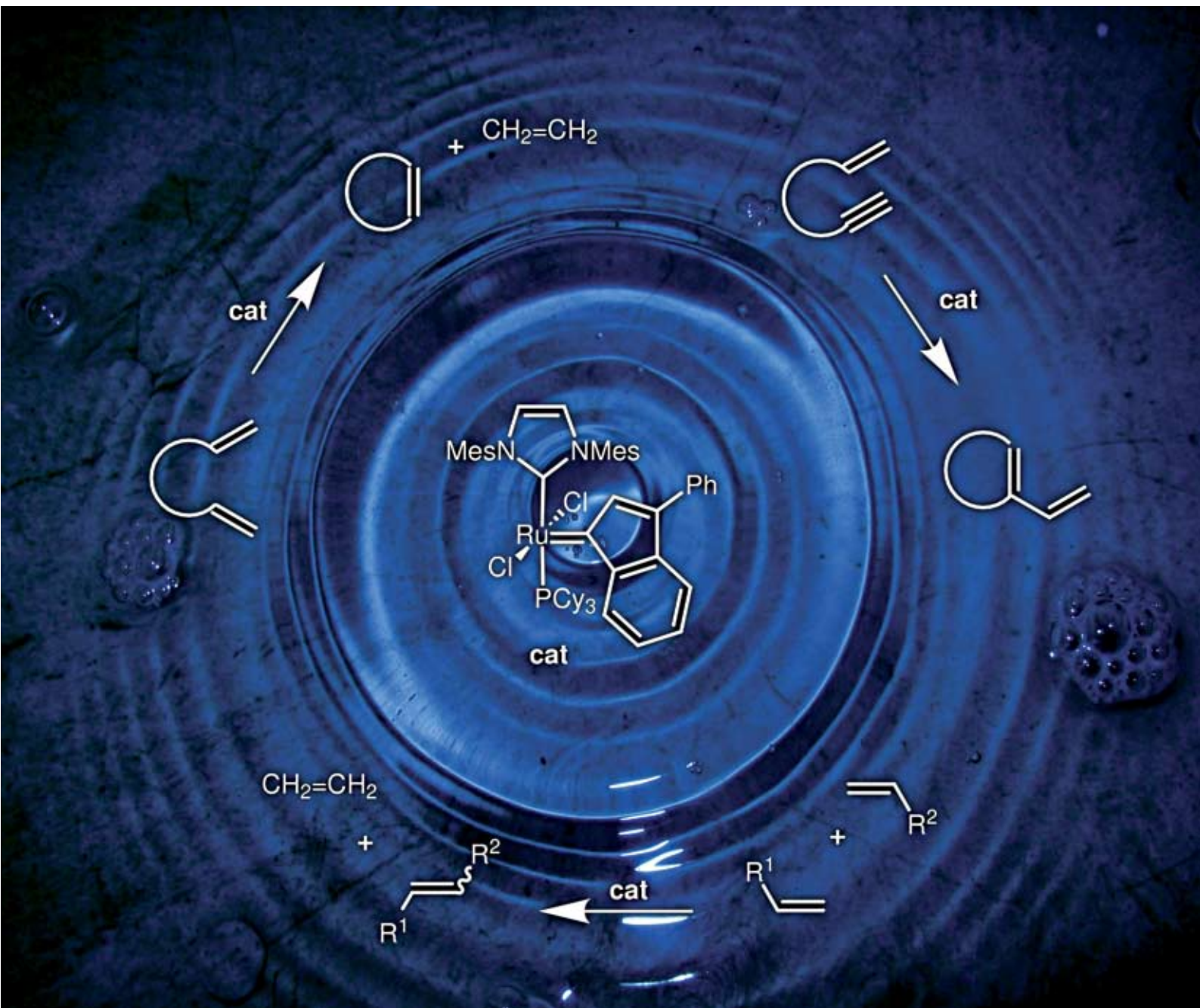
Grela *et al.*
Olefin metathesis in water using ultrasonication

Poliakoff *et al.*
24 principles of green engineering and chemistry

RSC Publishing

2ND EuCheMS Chemistry Congress

2008 SEPTEMBER 16 - 20 TORINO, ITALY

Chemistry: the Global Science

PLENARY LECTURES BY

Peter AGRE (Baltimore, USA)
Avelino CORMA (Valencia, Spain)
Jean M.J. FRÉCHET (Berkeley, USA)
Robert H. GRUBBS (Pasadena, USA)
Kyriacos C. NICOLAOU (La Jolla, USA)
Martyn POLIAKOFF (Nottingham, UK)
K. Barry SHARPLESS (La Jolla, USA)

KEYNOTE LECTURES BY

Varinder AGGARWAL (Bristol, UK))
Lucia BANCI (Florence, IT)
Matthias BELLER (Rostock, DE)
Richard CATLOW (London, UK)
Ken CAULTON (Bloomington, USA)
Fritz FRIMMEL (Karlsruhe, DE)
Dante GATTESCHI (Florence, IT)
Jana HAJSLOVA (Prague, CZ)
Dino MORAS (Illkirch, FR)
Ulrich STIMMING (Munich, DE)
Philip TAYLOR (Geel, BE)
Jun-ichi YOSHIDA (Kyoto, JP)

SCIENTIFIC COMMITTEE

Chair **Hartmut MICHEL** (DE)
Co-chair **Igor TKATCHENKO** (FR)

ORGANISING COMMITTEE

Chair **Giovanni NATILE** (IT)
Co-chair **Francesco DE ANGELIS** (IT)

LOCAL ORGANISING COMMITTEE

Chair **Lorenza OPERTI** (IT)
Co-chair **Salvatore COLUCCIA** (IT)

Special topic symposia:

ADVANCES IN SYNTHESIS

■ Organic Catalysis
■ Radical Reactivity in Transition Metal Chemistry
■ Reactions under Novel Conditions

ADVANCES IN UNDERSTANDING

■ Chemical Measurement Quality: Societal Impact
■ Cutting Edge Chemistry with Computers
■ Food Analysis: Pushing Detection Limits down to Nothing

CHEMISTRY AND LIFE SCIENCES

■ Biomolecular Interactions and Mechanisms
■ Drug Targeting and Delivery
■ Metal Homeostasis

ENERGY AND INDUSTRY

■ Biorefineries and Biotechnologies
■ Energy Production & Storage
■ New Trends for Agrochemicals

ENVIRONMENT

■ Greening Chemistry
■ Greenhouse Gases
■ Water Pollutants

MATERIALS AND DEVICES

■ Branched Polymers - Smart Functional Materials
■ Nanomaterials
■ Porous Materials

ORGANISING SECRETARIAT

Centro Congressi Internazionale s.r.l. - Corso Bramante 58/9 10126 Torino - I
tel +39 011.2446911 fax +39 011.2446900/44 - info@euchems-torino2008.it

www.euchems-torino2008.it

*EuCheMS, the European Association for Chemical and Molecular Sciences incorporates
50 member societies which in total represent some
150.000 individual chemists in academia, industry and government in over
35 countries across Europe.

Editorial Board news

As we move forward in 2008 we have two exciting announcements which we would like to share with the *Green Chemistry* readers.

Congratulations to Martyn Poliakoff CBE

As many of you may have seen Professor Martyn Poliakoff, Chair of the *Green Chemistry* Editorial Board, was awarded a CBE (Commander of the Order of the British Empire) in the 2008 New Year's honours list. He was awarded the CBE for his services to science and we would like to congratulate Martyn on receiving this award.

Martyn has been undertaking world leading research at The University of Nottingham for nearly 30 years and is one of the United Kingdom's most distinguished scientists. He has been associated with *Green Chemistry* since its launch and has served as Chair of the Editorial Board since 2006.

In addition to his role as Research Professor in Chemistry in Nottingham, he is an Honorary Professor of Chemistry at Moscow State University and has in recent years worked closely with research teams in developing nations. He is internationally renowned as a leader in the field of green chemistry—working to develop environmentally acceptable processes and materials. The main focus of his research is exploring the use of supercritical CO_2 ($scCO_2$) as an alternative to conventional solvents for reaction chemistry, so called 'clean technology'. His research group has been able to demonstrate the utilisation of supercritical fluids for reactions which are difficult or even impossible to achieve in conventional solvents.

Of the award Professor Poliakoff said: "Obviously I was delighted. It is a great honour to me and my colleagues and the whole field of chemistry."

Professor Steven Ley joins the team

We are also pleased to announce the appointment of Steven Ley to the *Green Chemistry* Editorial Board. Steven Ley is the BP (1702) Professor of Chemistry at the University of Cambridge, and is a Fellow of Trinity College. He is involved in a wide variety of research including: developing new synthetic methods and catalysts; supported reagents; carbohydrate chemistry; tricarbonyliron complexes in synthesis; the application of enzymes in synthesis; insect antifeedants; and the total synthesis of complex natural products. We welcome Steven to the *Green Chemistry* editorial board team and look forward to his input into the journal.

We very much hope that you have enjoyed the first two featured reviews of the year, and are looking forward to the exciting reviews and contributions we have scheduled during our 10th year of publishing.

Walter Leitner, Scientific Editor
Sarah Ruthven, RSC Editor

The 24 Principles of Green Engineering and Green Chemistry: "IMPROVEMENTS PRODUCTIVELY"

DOI: 10.1039/b719469m

Samantha Tang, Richard Bourne, Richard Smith and Martyn Poliakoff suggest a condensed 24 Principles of Green Chemistry and Green Engineering, with the mnemonic "IMPROVEMENTS PRODUCTIVELY"

Chemists and engineers working in the area of green chemistry are increasingly, and quite justifiably, asked to explain why their particular reaction, process or product is actually green. Already there is a lively debate on this topic[1] and sometimes the claim of a "green reaction" can ignite fierce controversy.[2]

In this context, the 12 Principles of Green Chemistry[3] have become a widely accepted set of criteria for the rapid assessment of the "greenness" of a given chemical route or for comparing the environmental acceptability of two rival processes. Unfortunately, the 12 principles do not explicitly include a number of important concepts, highly relevant to environmental impact; for example, the inherency of a product or process, the need for life cycle assessment, or the possibility of heat recovery from an exothermic reaction or heat integration. For this reason, Anastas and Zimmerman subsequently proposed a

set of 12 Principles of Green Engineering,[4] see Fig. 1.

The principles of both green chemistry and green engineering are rather lengthy and thus are not in a form that can be readily communicated to an audience in the middle of a lecture to emphasize an important point. This means that much of their value can be lost in debates over green technologies. Therefore, two years ago we proposed[5] a condensed version of the green chemistry principles which fitted onto a single PowerPoint slide and incorporated the mnemonic PRODUCTIVELY, Fig. 2. This cut-down set has proved really quite effective in presentations and has been adopted by others.

Here we present a companion set of the Green Engineering Principles, with the mnemonic IMPROVEMENTS, Fig. 3. We believe that these two sets of principles are now sufficiently manageable in their

Principles of Green Chemistry

P - Prevent wastes
R - Renewable materials
O - Omit derivatization steps
D - Degradable chemical products
U - Use safe synthetic methods
C - Catalytic reagents
T - Temperature, Pressure ambient
I - In-Process Monitoring
V - Very few auxiliary substances
E - E-factor, maximize feed in product
L - Low toxicity of chemical products
Y - Yes it's safe

Fig. 2 The condensed 12 Principles of Green Chemistry, taken from ref. 5.

condensed forms that, for the first time, they can be used together as a single set of 24 principles covering most of the key issues of green and sustainable chemistry and processing. With this combined set of principles for engineering and chemistry, it will be easier to include a discussion of environmental impact in lectures and presentations. Therefore, if a set of concepts becomes easier to communicate, then more people will both use and discuss them. Thus the entire field of green chemistry will benefit. Therefore we encourage you to use the principles to discuss your IMPROVEMENTS PRODUCTIVELY.

Samantha Y. Tang, Richard A. Bourne, and Martyn Poliakoff, School of Chemistry, The University of Nottingham, University Park , Nottingham, UK NG7 2RD *E.mail: samantha.tang@ nottingham.co.uk** and **Richard L. Smith**, Research Center of Supercritical Fluid Technology, Tohoku University, Aramaki

1   Designers need to strive to ensure that all material and energy inputs and outputs are as inherently non-hazardous as possible.
2   It is better to prevent waste than to treat or clean up waste after it is formed.
3   Separation and purification operations should be a component of the design framework.
4   System components should be designed to maximize mass, energy and temporal efficiency.
5   System components should be output pulled rather than input pushed through the use of energy and materials.
6   Embedded entropy and complexity must be viewed as an investment when making design choices on recycle, reuse or beneficial disposition.
7   Targeted durability, not immortality, should be a design goal.
8   Design for unnecessary capacity or capability should be considered a design flaw. This includes engineering "one size fits all" solutions.
9   Multi-component products should strive for material unification to promote disassembly and value retention (minimize material diversity).
10 Design of processes and systems must include integration of interconnectivity with available energy and materials flows.
11 Performance metrics include designing for performance in commercial "after-life".
12 Design should be based on renewable and readily available inputs throughout the life cycle.

Fig. 1   The 12 Principles of Green Engineering, taken from ref. 4.

Principles of Green Engineering

I - Inherently non-hazardous and safe
M - Minimize material diversity
P - Prevention instead of treatment
R - Renewable material and energy inputs
O - Output-led design
V - Very simple
E - Efficient use of mass, energy, space & time
M - Meet the need
E - Easy to separate by design
N - Networks for exchange of local mass & energy
T - Test the life cycle of the design
S - Sustainability throughout product life cycle

Fig. 3 The condensed 12 Principles of Green Engineering, based on those given in full in Fig. 1.

Aza Aoba-6-6-11, 980-8579, Aoba-ku, Sendai, Japan

References

1 R. van Noorden, *Chem. World*, 2007, **4**(6), 14.
2 D. G. Blackmond, A. Armstrong, V. Coombe and A. Wells, *Angew. Chem., Int. Ed.*, 2007, **46**, 37987.
3 P. T. Anastas and J. C. Warner, *Green Chemistry: Theory and Practice*, Oxford University Press, Oxford, 1998, p. 30.
4 P. T. Anastas and J. B. Zimmerman, *Environ. Sci. Technol.*, 2003, **37**, 94A.
5 S. L. Y. Tang, R. L. Smith and M. Poliakoff, *Green Chem.*, 2005, **7**, 761.

Professor Dr Roger A. Sheldon—65 years on

Ilya I. Moiseev, Shun-Ichi Murahashi, Martyn Poliakoff, Ken Seddon and Vytas K. Švedas reflect on a recent symposium held in honour of Roger Sheldon, a founding father of green chemistry and of this journal.

The Technical University of Delft has just celebrated the end of an epoch. Roger Sheldon, a founding father of green chemistry and of this journal, has formally retired from his position as Professor of Biocatalysis and Organic Chemistry.

His retirement was marked by a two-day symposium "A Journey in Green Chemistry and Catalysis" in Delft, on the 6th–7th December, 2007. It culminated in a formal University ceremony with Roger Sheldon delivering a valedictory lecture, "E-factors, Green Chemistry and Catalysis: Records of the Travelling Chemist", attended by over a hundred people (including most of the invited symposium speakers, attired in Dutch academic dress), followed by a series of orations honouring his achievements.

The symposium was a lively celebration of green chemistry, each speaker focusing on a different facet of Roger's contribution to the field. At Delft, Roger is affectionately known as 'Mr E-Factor' and this journal is proud to have published his review 'The E-Factor—15 years on' to mark the occasion.[1] The speakers and session chairs included the five authors of this report, Isabel Arends (who delivered an amusing and affectionate account of Roger's career), I. T. Horvath, A. Corma, M. Reetz, G. Huisman, L. L. Fischer, M. Schneider and H. van Bekkum. The topics covered solvents, catalysis, foods, biofuels and biocatalysis. This last topic highlighted Roger's great contribution to industrial biocatalysis, which is, perhaps, less widely known than the E-factor. A recurring theme in all of the lectures was the impact that Roger's seminal work continues to have on the chemical industry.

The whole event was distinguished by the combination of warmth, humour and scientific rigour which is the signature of Roger's persona. The authors were particularly delighted by the warm tribute by members of Roger's research group, one of whom dressed up as a giant parrot (see Fig. 1). The students' affection and respect for their supervisor was both a tribute and an inspiration to others. Many speakers acknowledged the great support that Roger's wife Jetty and their family have given him.

Fig. 1 Roger Sheldon advising one of his post-doctoral assistants, Linda Otten (dressed up as a giant parrot).

Ilya I. Moiseev, Kurnakov Institute of General and Inorganic Chemistry, Russian Academy of Science, Moscow, 119991, Russia ilya.moiseev@mail.ru, **Shun-Ichi Murahashi**, Department of Applied Chemistry, Okayama University of Science, Ridai-cho, 1-1, Okayama, Japan, E-mail: murahashi@high.ous.ac.jp, **Martyn Poliakoff**, The School of Chemistry, The University of Nottingham, Nottingham, UK NG7 2RD, E-mail: martyn.poliakoff@nottingham.ac.uk, **Kenneth R. Seddon**, The QUILL Research Centre, The Queen's University of Belfast, Belfast, UK BT9 5AG, E-mail: k.seddon@qub.ac.uk and **Vytas K. Švedas**, The School of Bioengineering and Bioinformatics and Belozersky Institute of Physicochemical Biology, Lomonosov Moscow State University, Moscow, 119992, Russia, E-mail: vytas@belozersky.msu.ru

References

1 R. A. Sheldon, *Green Chem.*, 2007, **9**, 1273–1283.

COMMUNICATION | www.rsc.org/greenchem | Green Chemistry

Olefin metathesis in water using acoustic emulsification

Łukasz Gułajski,[a] Paweł Śledź,[a,b] Anna Lupa[a,c] and Karol Grela*[a]

The performance of two commercially available olefin metathesis catalysts in water has been studied. Ultrasonication of the water-insoluble substrates and catalysts in water allowed the formation of stable emulsions without added surfactants, while the smooth catalytic metathesis took place in the water-insoluble emulsion droplets. Ring-closing (RCM), enyne and cross metathesis (CM) of a variety of substrates proceed with remarkable efficiency in water using acoustic emulsification.

Olefin metathesis is now a well-used methodology in organic synthesis. The recent development of molybdenum and ruthenium catalysts, such as Mo(=CHCMe$_2$Ph)[N(2,6-(i-Pr) OCMe(CF$_3$)$_2$]$_2$ (**1**), (PCy$_3$)$_2$Cl$_2$Ru=CHPh (**2**) and (SIMes)(PCy$_3$) Cl$_2$Ru=CHPh (**3**) (Cy = cyclohexyl, SIMes = 1,3-bis(2,4,6-trimethylphenyl)4,5-dihydroimidazolin-2-ylidene), has an important impact in organic chemistry.[1] Using catalysts **1–3**, chemists can now efficiently synthesize an impressive range of molecules that only a decade ago required significantly longer and tedious routes.[1]

Water has been widely investigated recently as a replacement for more conventional organic solvents, because of its low cost and its avoidance of organic vapors; it has thus been identified as a "green" solvent.[2,3] Furthermore, the aqueous olefin metathesis can be critical for some biological applications of olefin metathesis.[4] Unfortunately, like many other reactive organometallic compounds, catalyst **1** needs dry degassed organic solvents as reaction media, to avoid deactivation caused by oxygen and moisture.[1] Ru-based complexes are less sensitive to moisture, however their low solubility in aqueous media make aqueous olefin metathesis difficult. Some specially designed hydrophilic ruthenium complexes **4–9** have therefore been developed to solve this limitation (Fig. 1).[5] Alternatively, classical water-insoluble ruthenium initiators were used in mixed water/organic heterogeneous systems or in neat water in the presence of various surfactants, such as dodecyltrimethylammonium bromide, sodium dodecylsulfate (SDS) or with polydimethylsiloxane or without surfactants.[6]
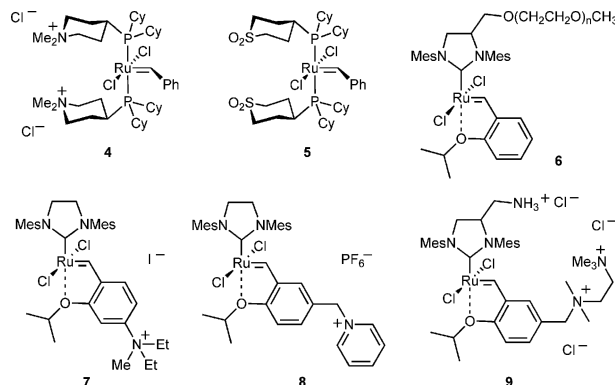
[a]Institute of Organic Chemistry, Polish Academy of Sciences, Kasprzaka 44/52, 01-224, Warsaw, Poland. E-mail: klgrela@gmail.com; Fax: +48 22 632 66 81; Tel: +48 22 3432117

[b]Warsaw University, Department of Chemistry, Pasteura 1, 02-093, Warsaw, Poland

[c]Faculty of Chemistry, Warsaw University of Technology (Politechnika), Noakowskiego 3, 00-664, Warsaw, Poland

Fig. 1 Selected polar catalysts for aqueous olefin metathesis.

Although some examples of metathesis in water without additives are known, in most cases the influential effect of the surfactant was observed.[6] Importantly, the micellar conditions make several water-insoluble substrates, such as lipophilic alkenes and dienes, compatible with water as a solvent.

We now describe a user-friendly protocol for effecting olefin metathesis *in water* at ambient temperature, in the absence of any co-solvents and surfactants. In this simplified protocol ultrasonication[7] of a water-insoluble substrate (or substrates) *floating on water* leads to the formation of an emulsion, in which smooth catalytic metathesis takes place after addition of water-insoluble commercially available Grubbs (**3**) and catMETium® IMesPCy (**10**) catalysts (Scheme 1).[8]
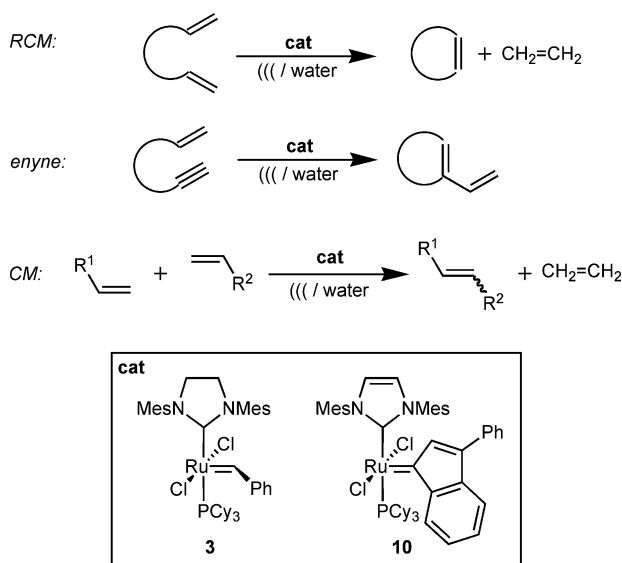
In a model experiment, to diene **11a** (oil, 0.5 mmol) floating on water (2.5 mL) catalyst **3** (solid, 5 mol%) was added and the reaction tube was sonicated forming a stable, pink-colored dispersion. After 5 h of sonication at 40 °C the crude reaction mixture was extracted with EtOAc and analyzed by GC (*n*-nonane was then added as an internal standard). We were pleased to find that metathesis of **11a** under such conditions proceeded with high selectivity, and the corresponding RCM product **12a** was formed quantitatively (Scheme 2).

We assumed that under such conditions the RCM reaction took place inside the water-insoluble droplets of diene **11a**. To check if water plays a role in the reaction, we repeated the same RCM reaction in the absence of any solvent (in neat **11a**) without sonication. GC and MS-ESI analysis of the crude product of the reaction revealed that a relatively large amount of oligomers **12a'**—products of the ADMET reaction—were formed under the solvent-less conditions (Scheme 2). It should
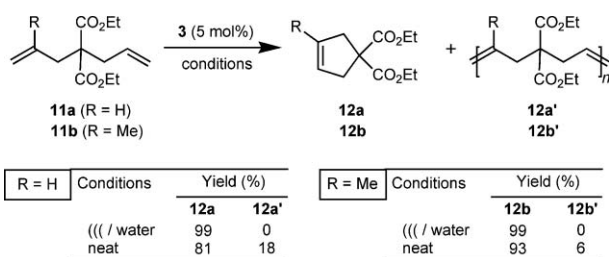
Scheme 1 Metathesis in water using acoustic emulsification. (((= ultrasound.

Scheme 2 RCM in aqueous sonicated emulsion and in neat **11a**. Conditions: sonicated emulsion: 5 mol% of catalyst, H_2O, $C_{substrate} = 0.2$ mol L^{-1}, 40 °C, 5 h, in air; neat **11a**, 25 °C, 5 h, in air.

be noted that under micellar conditions no oligomerisation was observed in the same reaction (Scheme 2).[9] Similar results have been found for another simple diene, **11b**, which cyclised cleanly in acoustically generated water emulsion, but formed some of the ADMET oligomers when reacted neat (Scheme 2; ADMET = acyclic diene metathesis polymerization).[9]

Other dienes, such as **11c, 11e** as well as enyne **11d**, sonicated in the presence of commercial catalysts **3** and **10** reacted cleanly leading to the expected products in good yields (Table 1). The yields were determined by NMR or GC analysis of the crude reaction mixtures. In selected cases, products were isolated by extraction with EtOAc and purified by column chromatography. Interestingly, while no remaining **3** has been detected after the reaction, in the case of more stable[10] **10**, up to 64% of the initial catalyst can be recovered after the reaction. The results presented in Table 1 (entries 1–7) show that the conditions developed by us are quite general for formation of 5- and 6-membered rings. Unfortunately, attempts to close bigger rings failed, as RCM of diene **11j** did not form the expected 16-membered Exaltolide® precursor **12j**, exclusively leading to formation of a complex mixture of oligomers,[9] instead (Table 1, entry 19).

Next, we decided to extend experiments in water to more challenging cross-metathesis (CM)[11] reactions of electron deficient substrates. This transformation is extremely rare in aqueous conditions, usually leading to poor conversions and low selectivities.[12] It was proposed that this failure can be caused by the insufficient stability of the electrophilic alkylidene intermediates formed in these reactions in a polar environment.[12] However, the present study reveals that CM of electron poor substrates is very possible in water, proceeding in very good yields and selectivities (Table 1, entries 11–16). To our best knowledge, such reactions represent the first successful example of the high-yielding aqueous CM between an alkene and an electron-deficient partner.[13] While this result is poorly understood, we speculate that under such conditions the sensitive ruthenium intermediates are "protected" inside the water-insoluble organic droplets, thus allowing higher turnovers. Interestingly, CM of **11f** and methyl acrylate was also possible without sonication, in a vigorously stirred water suspension, however under such conditions the reaction proceeded in lower conversion (entry 12). Next, we observed that 4-methoxystyrene undergoes quantitative self-metathesis reaction using acoustic emulsification (Table 1, entry 17). The advantageous effect of ultrasound was also visible in this case (entry 16).

The products of the small-scale screening reactions were isolated by EtOAc extraction from the aqueous solution. However, we observed that in many cases the crude products deposit as an oil on the water surface or precipitate from the water mixture as solids. In order to demonstrate that organic extraction can be avoided, we have attempted the self CM of styrene **11i** in a beaker immersed in the ultrasound-cleaner and after the reaction was complete, isolated the water-insoluble product by decantation (72% yield, GC purity >99%; Table 1, entry 17).

In summary, a new protocol for performing the environmentally friendly olefin metathesis has been proposed. The commercially available Grubbs and catMETium® IMesPCy catalysts show unprecedented activity in RCM, enyne and CM reactions in sonicated water emulsions. Further studies aiming to tame the ultrasound conditions for metathesis applications are currently under way.
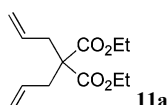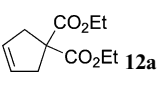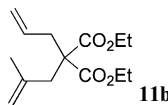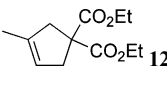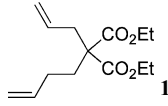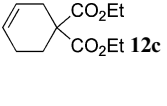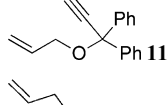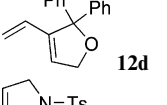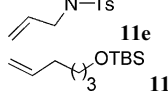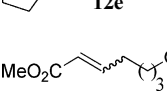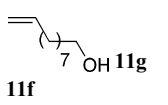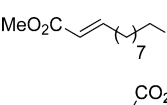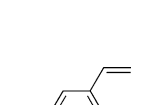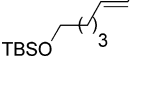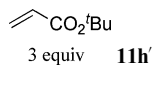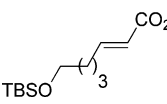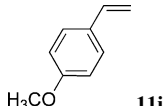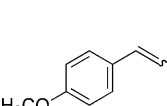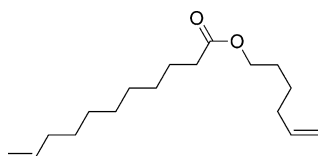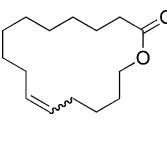
Experimental

Representative procedure for olefin metathesis

A reaction tube charged with **11f** (0.4 mmol), **11f'** (1.2 mmol) and non-degassed H_2O (0.8 mL) was immersed in a standard laboratory glassware cleaner and sonicated for 5 minutes. To the resulting suspension, the catalyst **3** or **10** (0.02 mmol, 5 mol%) was added as a solid and the resulting pink emulsion was sonicated at 40 °C in air. After 5 h, ethyl acetate (2.5 mL) was added and the heterogeneous mixture was passed through a cartridge containing a silica gel (1.2 g). The cartridge was then washed with an additional portion of ethyl acetate (10–15 mL). Volatiles were removed under reduced pressure to yield crude product **12f** which was subsequently purified by flash chromatography on silica gel (eluting with 10% EtOAc/c-hexane) to yield the analytically pure product as a colourless oil (62 mg, 76%).

Table 1 Metathesis reaction in aqueous sonicated emulsions[a]

Entry	Substrate	Product	Catalyst (mol%)	Yield[b](%)
1	11a	12a	3 (5)	99
2			3 (5)[c]	81[d]
3			10 (5)[e]	99
4	11b	12b	3 (5)	99
5			3 (5)[c]	93[f]
6			10 (5)[g]	64
7	11c	12c	3 (5)	99
8	11d	12d	3 (5)	65
9			10 (5)[h]	99
10	11e	12e	3 (5)	89 (86)[i]
11	11f / 11f′ (3 equiv)	12f	3 (5)[j]	86 (76)
12			3 (5)[j],[k]	76 (65)
13			10 (5)[l]	56
14	11f′ / 11g	12g	3 (5)	99
15			10 (5)[m]	90
16	11f / 11h′ (3 equiv)	12h	3 (5)[j],[n]	95 (81)
17	11i	12i	3 (5)	100 (72)[o]
18			3 (5)[k]	78
19	11j	12j	3 (5)	0[p]

[a] Condition: 5 mol% of catalyst, H_2O, $C_{substrate} = 0.2$ mol/L, 40 °C, 5h, ultrasounds, in air. [b] Yields were determined by GC or ^{1}H NMR, in parentheses are yields of isolated products. [c] Reaction performed without solvent. [d] 18% ADMET oligomers were formed. [e] 48% of catalyst **10** was recovered. [f] 6% ADMET oligomers were formed. [g] 55% of catalyst **10** was recovered. [h] 64% of catalyst **10** was recovered. [i] 86% of the crude product of 89% GC-purity was isolated by decantation of the water phase. [j] $C_{substrate} = 0.5$ mol L^{-1}. [k] Reaction conducted in intensively stirred water suspension, without ultrasonication. [l] 56% of catalyst **10** was recovered. [m] 33% of catalyst **10** was recovered. [n] 4% homodimer of **11f** was formed. [o] 72% of the crude product of 99% GC-purity was isolated by decantation of the water phase. [p] Product **12j** was not observed, only ADMET oligomers were formed.

Acknowledgements

Notes and references

1 (a) For selected reviews on olefin metathesis, see: T. M. Trnka and R. H. Grubbs, *Acc. Chem. Res.*, 2001, **34**, 18–29; (b) *Handbook of Metathesis*, ed. R. H. Grubbs, Wiley-VCH, Weinheim, Germany, 2003; (c) S. J. Connon and S. Blechert, *Angew. Chem., Int. Ed.*, 2003, **42**, 1900–1923; (d) D. Astruc, *New J. Chem.*, 2005, **29**, 42–56; (e) For an industrial perspective, see: A. M. Thayer, *Chem. Eng. News*, 2007, **85**(7), 37–47; (f) catalyst **1** and analogues: R. R. Schrock and A. H. Hoveyda, *Angew. Chem., Int. Ed.*, 2003, **42**, 4592–4633; (g) catalysts **2** and **3** and analogues: T. M. Trnka and R. H. Grubbs, *Acc. Chem. Res.*, 2001, **34**, 18–29.

2 (a) *Aqueous-Phase Organometallic Catalysis*, ed. B. Cornils and W. A. Hermann, Wiley-VCH, Weinheim, Germany, 2004; (b) C.-J. Li and T.-H. Chan, *Organic Reaction in Aqueous Media*, Wiley, New York, 1997; (c) *Organic Synthesis in Water*, ed. P. A. Grieco, Blackie Academic and Professional, London, 1998; (d) *Organic Reaction in Water*, ed. U. M. Lindström, Blackwell Publishing, Oxford, 2007.

3 For a review on sustainable aspects of olefin metathesis, see: H. Clavier, K. Grela, A. Kirschning, M. Mauduit and S. P. Nolan, *Angew. Chem., Int. Ed.*, 2007, **46**, 6786–6801.

4 (a) For example, see: E. J. Gordon, W. J. Sanders and L. L. Kiessling, *Nature*, 1998, **392**, 30–31; (b) M. Kanai, K. H. Mortell and L. L.

Kiessling, *J. Am. Chem. Soc.*, 1997, **119**, 9931–9932; (*c*) D. D. Manning, X. Hu, P. Beck and L. L. Kiessling, *J. Am. Chem. Soc.*, 1997, **119**, 3161–3162; (*d*) D. D. Manning, L. E. Strong, X. Hu, P. Beck and L. L. Kiessling, *Tetrahedron*, 1997, **53**, 11937–11952.

5 (*a*) Complex **4**: D. M. Lynn, B. Mohr and R. H. Grubbs, *J. Am. Chem. Soc.*, 1998, **120**, 1627–1628; (*b*) complex **5**: T. Rölle and R. H. Grubbs, *Chem. Commun.*, 2002, 1070–1071; (*c*) complex **6**: S. H. Hong and R. H. Grubbs, *J. Am. Chem. Soc.*, 2006, **128**, 3508–3509; (*d*) complex **7**: A. Michrowska, Ł. Gułajski, Z. Kaczmarska, K. Mennecke, A. Kirschning and K. Grela, *Green Chem.*, 2006, **8**, 685–688; (*e*) A. Michrowska, Ł. Gułajski and K. Grela, *Chem. Today*, 2006, **24**(6), 19–22; (*f*) **8**: D. Rix, F. Caïjo, I. Laurent, Ł. Gułajski, K. Grela and M. Mauduit, *Chem. Commun.*, 2007, 3771–3773; (*g*) compound **9**: J. P. Jordan and R. H. Grubbs, *Angew. Chem., Int. Ed.*, 2007, **46**, 5152–5155.

6 (*a*) D. M. Lynn, S. Kanaoka and R. H. Grubbs, *J. Am. Chem. Soc.*, 1996, **118**, 784–790; (*b*) V. Monteil, P. Wehrmann and S. Mecking, *J. Am. Chem. Soc.*, 2005, **127**, 14568–14659; (*c*) T. A. Kirkland, D. M. Lynn and R. H. Grubbs, *J. Org. Chem.*, 1998, **63**, 9904–9909; (*d*) K. J. Davis and D. Sinou, *J. Mol. Catal. A: Chem.*, 2002, **177**, 173–178; (*e*) M. T. Mwangi, M. B. Runge and N. B. Bowden, *J. Am. Chem. Soc.*, 2006, **128**, 14434–14435; (*f*) S. J. Connon, M. Rivard, M. Zaja and S. Blechert, *Adv. Synth. Catal.*, 2003, **345**, 572–575; (*g*) M. T. Zarka, O. Nuyken and R. Weberskirch, *Macromol. Rapid Commun.*, 2004, **25**, 858–862; (*h*) For early examples of ROMP in aqueous media initiated by poorly defined ruthenium complexes such as RuCl$_3$(H$_2$O)$_n$ or Ru(H$_2$O)$_6$(TsO)$_2$, see: B. M. Novak and R. H. Grubbs, *J. Am. Chem. Soc.*, 1988, **110**, 960–961; (*i*) B. M. Novak and R. H. Grubbs, *J. Am. Chem. Soc.*, 1988, **110**, 7542–7543; (*j*) M. A. Hillmeyer, C. Lepetit, D. V. McGrath, B. M. Novak and R. H. Grubbs, *Macromolecules*, 1992, **25**, 3345–3350; (*k*) K. H. Mortell, R. V. Weatherman and L. L. Kiessling, *J. Am. Chem. Soc.*, 1996, **118**, 2297–2298.

7 (*a*) For selected reviews on ultrasound in chemistry, see: T. J. Mason, *Chem. Soc. Rev.*, 1997, **26**, 443–451; (*b*) W. Bonrath and R. A. P. Schmidt, *Adv. Org. Synth.*, 2005, **1**, 81–117; (*c*) G. Cravotto and P. Cintas, *Chem. Soc. Rev.*, 2006, **35**, 180–196; (*d*) G. Cravotto and P. Cintas;, *Angew. Chem., Int. Ed.*, 2007, **46**, 5476–5478; (*e*) S. K. Ley, C. M. Low, *Ultrasound in Synthesis*, Springer, Berlin, 1989; (*f*) *Sonochemistry: The Uses of Ultrasound in Chemistry*, ed. T. J. Mason, The Royal Society of Chemistry, London, 1990; (*g*) for a recent example of an electrochemical reaction in aqueous media using acoustic emulsification, see: R. Asami, T. Fuchigami and M. Atobe, *Chem. Commun.*, 2008, DOI: 10.1039/b713859h.

8 Catalyst **3** (Materia Inc) and **10** (Evonik–Degussa GmbH) samples are available from Aldrich Inc. and Strem Chemicals Inc., respectively.

9 For an excellent study on formation of oligomers as intermediates in RCM, see: J. C. Conrad, M. D. Eelman, J. A. Duarte Silva, S. Monfette, H. H. Parnas, J. L. Snelgrove and D. E. Fogg, *J. Am. Chem. Soc.*, 2007, **129**, 1024–1025.

10 (*a*) M. Bieniek, A. Michrowska, D. L. Usanov and K. Grela, *Chem.– Eur. J.*, 2008, **14**, 806–818; (*b*) H. Clavier, S. P., *Chem.–Eur. J.*, 2007, **13**, 8029–8036; (*c*) For a review on ruthenium indenylidene complexes, see: V. Dragutan, I. Dragutan and F. Verpoort, *Platinum Met. Rev.*, 2005, **49**, 33–40.

11 (*a*) For reviews, see: A. J. Vernall and A. D. Abell, *Aldrichimica Acta*, 2003, **36**, 93–105; (*b*) see ref. 1c; (*c*) H. E. Blackwell, D. J. O'Leary, A. K. Chatterjee, R. A. Washenfelder, D. A. Bussmann and R. H. Grubbs, *J. Am. Chem. Soc.*, 2000, **122**, 58–71.

12 For an insight into this problem, see: S. J. Connon and S. Blechert, *Bioorg. Med. Chem. Lett.*, 2002, **12**, 1873–1876.

13 Recently, we have reported a single example of CM between **11f** and methyl acrylate promoted in water by polar ammonium-tagged catalyst **7**. This reaction was, however, less efficient than the related ultrasound-promoted reaction described herein (Table 1, entry 11). Ł. Gułajski, A. Michrowska, J. Narożnik, Z. Kaczmarska, L. Rupnicki and K. Grela, *Chem. Sus. Chem.*, 2008, DOI: 10.1002/cssc.200700111.

Microwave generation and trapping of acetylketene†

Indra Reddy Gudipati, Dhandapani Venkatram Sadasivam and David Martin Birney*

Microwave heating of 1 efficiently generates acetylketene (2) which reacted *in situ* with a range of alcohols, aldehydes and trifluoroacetophenone, giving products in high isolated yields.

Acetylketene (2) has been widely studied both for its fundamental interest as a reactive intermediate and because it is useful for the generation of β-ketoesters (5) and dioxinones (6) by trapping with alcohols and aldehydes respectively.[1–8] The existing methods for generating 2 require either toxic reagents for the synthesis of many precursors, or at best prolonged heating for thermal generation of 2. Herein, we describe the use of microwave heating to generate 2 and its *in situ* trapping. This methodology offers several distinct advantages of relevance to the formation of 2: shorter reaction times, less toxic solvents and reduced solvent volumes and higher yields than conventional methodology.

2,2,4-Trimethyl-4*H*-1,3-dioxin-4-one (1) is a convenient and atom efficient precursor for acetylketene (2); simple reflux in toluene gives 2, with only acetone as a byproduct, as shown in Scheme 1.[2] Although this reaction is reversible, 2 reacts with alcohols and aldehydes to form β-ketoesters (5 *via* the enols 4) and dioxinones (6) faster than with acetone to regenerate 1. Dimerization of 2 to form 3 is competitive with the formation of 1. In addition, it has been shown that the reaction of 2 with alcohols is faster than with aldehydes.[3]
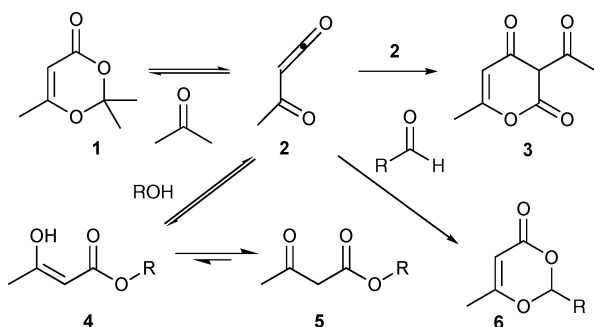
Scheme 1 Formation and trapping of acetylketene (2).

In view of the high yields, energy efficiency, and reduced solvent volume of microwave heating,[9] the formation and trapping of acetylketene 2 under these conditions was investigated. Microwave heating requires a polar solvent;[9] ethyl acetate was

chosen because it is relatively environmentally benign,[10] has a high dielectric constant and does not react with 2 under the reaction conditions. Molecular sieves (4 Å) were added to sequester any adventitous water. The initial optimization of the microwave reaction conditions was done by simply monitoring the disappearance of 1 and the concomitant formation of the dimer 3. Microwave heating of 1 in ethyl acetate in a closed pressure vessel at 120 °C for 20 min gave complete loss of 1; for consistency, these conditions were used in all subsequent reactions.

Alcohols react rapidly with 2 in a pseudopericyclic [4 + 2] cycloaddition,[4] first forming the enol tautomers 4, which subsequently tautomerizes to β-ketoesters 5 (Scheme 1).[5,6] Alcohols show significant selectivity, 1° > 2° > 3°, presumably due to steric crowding in the transition state.[3] Therefore, the generation of 2 from 1 and the trapping reactions of 2 with ethanol, 2-propanol and 2-methyl-2-propanol were studied under these microwave conditions (eqn (1)). To investigate the effect of solvent and concentration, the reaction was also studied in neat alcohols. Because yields have not been reported for the conventional thermolysis reactions of these alcohols, their reactions with 2 generated from 1 in refluxing toluene were also studied. The results are summarized in Table 1. As expected, the reaction times are significantly shorter for the microwave synthesis, as compared to conventional heating in refluxing toluene. The yields are consistently highest (up to 92%) for the microwave reactions in ethyl acetate as solvent. The somewhat reduced yield of 5c is not unexpected, given the steric hindrance of 2-methyl-2-propanol and its relatively slow reaction with 2.[3] It is somewhat surprising that the yields for the reactions in neat alcohol are lower than with ethyl aceate as solvent. Increasing the concentration of 1 (0.8 mL) in neat ethanol (total of 10 mL) led to a much lower yield (63%) as well as an unidentified byproduct.

$$\text{1} + \text{ROH} \xrightarrow[\text{EtOAc}]{\text{microwave}} \text{5a R = Et} \quad \text{5b R = }i\text{-Pr} \quad \text{5c R = }t\text{-Bu} \quad (1)$$

Table 1 Yields from microwave and conventional heating of 1 to give 2 and subsequent trapping with alcohols

Product	R	Microwave yield[a, b]	Neat alcohol yield[a, c]	Conventional yield[a, d]
5a	CH_3CH_2–	92%	85%	84%
5b	$(CH_3)_2CH$–	91%	72%	83%
5c	$(CH_3)_3C$–	72%	51%	58%

[a] Isolated yield. [b] 1 (0.2 mL, 1.5 mmol), 20 equiv. alcohol (ROH), ethyl acetate solvent to make 10 mL, 20 min 120 °C. [c] 1 (0.2 mL, 1.5 mmol), alcohol (ROH, to make 10 mL) as solvent and trap, 20 min 120 °C. [d] Toluene solvent, reflux, 8 h.

Texas Tech University, Department of Chemistry and Biochemistry, Lubbock, Texas, USA. E-mail: david.birney@ttu.edu; Fax: +1 806-742-1289; Tel: +1 806-742-3063

† Electronic supplementary information (ESI) available: Experimental procedures and spectral data for all compounds. See DOI: 10.1039/b718080b
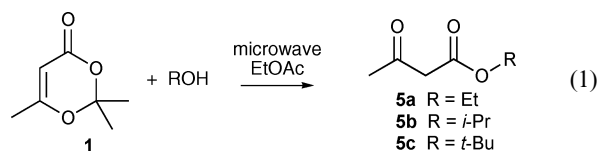
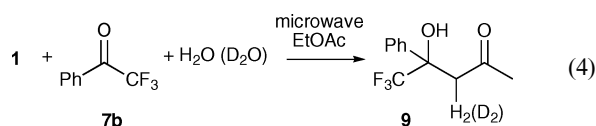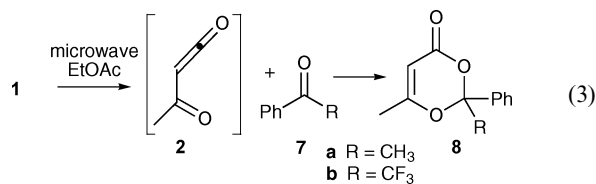**Table 2** Microwave and conventional heating of **1** to give **2** and subsequent trapping with aldehydes

Product	R	Microwave yield[a, b]	Conventional yield[a]
6a	(CH$_3$)$_3$C–	82%	60%[c]
6b	(CH$_3$)$_2$CHCH$_2$–	73%	
6c	(CH$_3$)$_2$CH–	53%[d]	10%[e]

[a] Isolated yield. [b] Ethyl acetate solvent, 20 min 120 °C. [c] Mesitylene solvent, reflux.[15] [d] An unidentified impurity was also obtained. [e] This is the combined yield of two diastereomers for the reaction of 2-methylbutanal with **2** generated from **1** under flash vacuum thermolysis conditions.[7]

Trapping with aldehydes was next examined, under the same reaction conditions (eqn (2)). The results are summarized in Table 2. Although the isolated yields are somewhat lower, they remain substantially higher than from conventional pyrolysis.[6,7] The yield of **6c** was decreased by the formation of an unidentified byproduct; **6a** and **6b** were obtained free from related impurities. The relative insensitivity of this reaction to steric bulk (*cf.* 82% yield of **6a**) is consistent with the planar, pseudopericyclic nature of the transition state for the [4 + 2] cycloaddition.[7,8]
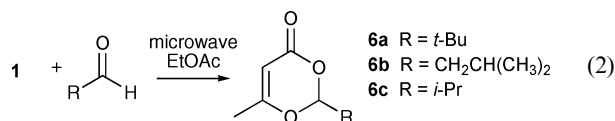

A qualitative understanding of the reactivity of **2** suggests that it should not react with most ketones; dimerization of **2** to give **3** occurs in competition with the reaction with acetone to regenerate **1**.[3] An electron deficient ketone (trifluoroacetophenone, **7b**) might be at the borderline of reactivity, while a stabilized ketone (acetophenone, **7a**) would not be expected to react. To investigate these qualitative ideas, trapping of **2** with **7a** and **7b** was attemped. The results are summarized in Table 3 and eqn (3) and (4). As expected, microwave heating of **1** in the presence of **7a** gave only the dimer **3**. However, microwave heating of **1** in dry ethyl acetate in the absence of molecular sieves and in the presence of **7b** gave the anticipated[11] [4 + 2] product **8b** in addition to dimer **3**. Interestingly, in the presence of molecular sieves, none of **8b** was obtained. Instead, **9** and **3** were formed. The formation of compounds such as **9** is, to the best of our knowledge, unprecedented in acylketene chemistry. Overall, this reaction is equivalent to an aldol condensation between the enolate of acetone and **7b**, without the use of strong base, or any other reagent. Thus, it may be considered to be an atom efficient (acetone and CO$_2$ are the only byproducts) and green aldol condensation.[12]

Table 3 Microwave and conventional heating of **1** to give **2** and subsequent trapping with ketones

Reactant	Trapped product[a]	Yield[b]	**3** as % of **1**[c]
7a	—	—	—
7b[d]	**8b**	49%	22%
7b[e]	**9**	44%	48%

[a] In all cases, dimer **3** was also obtained. [b] Isolated yield. Ethyl acetate solvent, 20 min 120 °C. [c] NMR yield of dimer **3** as a percentage of reactant **1** consumed. [d] No added water. [e] Added 4 Å molecular sieves, H$_2$O or D$_2$O.

The structure of **9** suggests both the addition of water to **2** as well as a decarboxylation. Indeed, deliberate addition of water also gave **9**. Addition of D$_2$O gave selective incorporation of approximately 70% deuterium in each of the diasterotopic positions in the methylene group as shown, with no evidence of deuteration in the methyl group. Resubmitting unlabelled **9** to the reaction conditions and microwave heating in the presence of D$_2$O did not lead to any deuterium incorporation. A proposed mechanism is outlined in Scheme 2. The rate of reaction of **2** with water has been measured and is extremely rapid.[6] Addition of alcohols to **2** initially forms the enol tautomer, thus formation of **10** is expected to be the fastest reaction of **2**. Then **10** is proposed to react with **7b** to form **11**. β-Ketoacids undergo rapid decarboxylation upon heating;[13] it appears that **10** survives long enough to undergo bimolecular reaction with **7b**. Decarboxylation of **11** would give **12** and, after tautomerization, **9**. While this tautomerization allows for the regioselective incorporation of a single deuterium, the observation of 70% enrichment at each diastereomeric position would require tautomerization to either **13** or **14** without decarboxylation.[14]
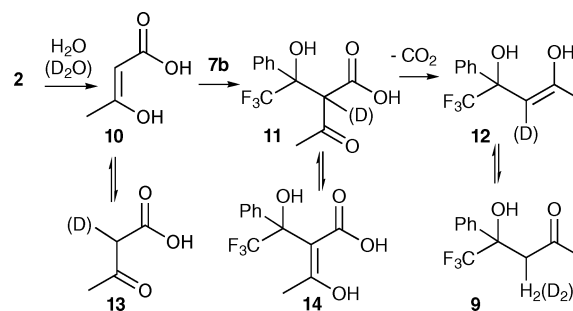
Scheme 2 Proposed mechanism for the formation of **9**.

Experimental

Microwave experiments were conducted in a Milestone START reactor, with IR temperature measurement. Unless otherwise stated, reactions were carried out as follows. Molecular sieves (4 Å, 3 g) were added to a 15 mL oven-dried pressure tube and flushed with nitrogen. Ethyl acetate (sufficient to make 10 mL final volume), 0.2 mL **1** (1.52 mmol) and 20 equivalents of trapping agent (30 mmol) were added and the tube was again flushed with nitrogen, sealed and then heated in the microwave reactor. Over 8 min, the temperature was raised to 120 °C, held for 20 min, and then cooled for 10 min. The solvent and excess trapping agent were removed under vacuum and the product

isolated by flash chromatography on silica gel. Details for specific reactions and spectral data are provided in the ESI.†

Notes and references

1 T. T. Tidwell, *Ketenes*, Wiley-Interscience, New York, 2nd edn, 2006; D. M. Birney, *J. Org. Chem.*, 1994, **59**, 2557; C. Wentrup, W. Heilmayer and G. Kollenz, *Synthesis*, 1994, 1219; J. S. Witzeman, *Tetrahedron Lett.*, 1990, **31**, 1401–1404; J. S. Witzeman and W. D. Nottingham, W. D., *J. Org. Chem.*, 1991, **56**, 1713; R. J. Clemens, *Chem. Rev.*, 1986, **86**, 241.
2 R. J. Clemens and J. S. Witzeman, *J. Am. Chem. Soc.*, 1989, **111**, 2186; R. J. Clemens and J. A. Hyatt, *J. Org. Chem*, 1985, **50**, 2431.
3 D. M. Birney, X. Xu, S. Ham and X. Huang, *J. Org. Chem.*, 1997, **62**, 7114.
4 D. M. Birney and P. E. Wagenseller, *J. Am. Chem. Soc.*, 1994, **116**, 6262.
5 B. Freiermuth and C. Wentrup, *J. Org. Chem.*, 1991, **56**, 2286.
6 A. D. Allen, M. A. McAllister and T. T. Tidwell, *Tetrahedron Lett.*, 1993, **34**, 1095.
7 W. W. Shumway, S. Ham, J. Moer, B. R. Whittlesey and D. M. Birney, *J. Org. Chem.*, 2000, **65**, 7731.
8 W. W. Shumway, N. K. Dalley and D. M. Birney, *J. Org. Chem.*, 2001, **66**, 5832.
9 C. O. Kappe and A. Stadler, *Microwaves in Organic and Medicinal Chemistry*, Wiley-VCH, 2005.
10 The LD_{50} for ethyl acetate is 11.3 mL kg^{-1} in rats. For comparison, the LD_{50}'s for toluene and ethanol are 7.53 and 10.6 mL kg^{-1} respectively, *The Merck Index*, Merck & Co., Rahway, New Jersey, 11th edn, 1989.
11 Compound **8** has been synthesized by conventional thermolysis of **1** with **7b**, but no yield was reported. M. Sato, F. Uehara, H. Kamaya, M. Murakami, C. Kaneko, T. Furuya and H. Kurihara, *Chem. Commun.*, 1996, 1063.
12 Indeed, compound **9** has previously been synthesized by a base catalyzed aldol condensation. J. P. Guthrie and J. A. Barker, *J. Am. Chem. Soc.*, 1998, **120**, 6698.
13 Extrapolation of the measured rates of decarboxylation of acetoacetic acid suggests a half-life of approximately 0.1 s for **13** at 120 °C. K. J. Pedersen, *J. Am. Chem. Soc.*, 1929, **51**, 2098.
14 In related work, Zhang and Curran have observed decarboxylation in the microwave heating of β-keto esters in water. They consider, but rule out acylketene intermediates, arguing that cyclohexanone does not trap the acylketene. We have previously shown that alcohols (in this case formed as a byproduct from the heating of β-keto esters) reacts selectively with **2** even in the presence of a large excess of cyclohexanone. Thus, we suggest that their results are in fact consistent with **2** + H_2O to give **10**, in their case followed by decarboxylation of **13**. D. P. Curran and Q. Zhang, *Adv. Synth. Catal.*, 2003, **345**, 329.
15 N. Haddad, I. Ruckman and Z. Abramovich, *J. Org. Chem.*, 1997, **62**, 7629.

Aerobic oxidation of benzyl alcohol in supercritical CO_2 catalyzed by perruthenate immobilized on polymer supported ionic liquid

Ye Xie, Zhaofu Zhang, Suqin Hu, Jinliang Song, Wenjing Li and Buxing Han*

The catalyst for aerobic oxidation of benzyl alcohol to produce benzyl aldehyde was prepared by immobilization of perruthenate on polymer supported 1-vinyl-3-butyl imidazolium chloride, and the catalytic reaction was conducted in supercritical (SC) CO_2, toluene and dichloromethane at 80 °C. The phase behavior of the reaction system with SC CO_2 as solvent was also determined. It was demonstrated that the catalyst was very active and highly selective. The reaction rate in SC CO_2 depended strongly on pressure and reached a maximum at about 14 MPa, which can be explained by the effect of pressure on the phase behavior of the reaction system, diffusivity of the components and solvent power of SC CO_2. The catalyst could be reused directly after extraction of the products using SC CO_2, and it was still active after several runs, although the yield decreased continuously with run times. This work integrated the advantages of green solvent, green supporting material and green oxidant.
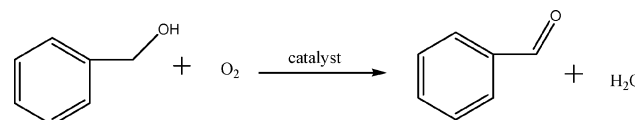
1. Introduction

Oxidation of alcohol to carbonyl compounds such as aldehydes, ketones or carboxylic acids is an important class of reactions. In industrial processes, oxidants or catalysts containing heavy metals such as Cr an Mn are utilized,[1] and large amounts of waste are produced to obtain the products.[2] Utilization of low toxic, highly active and selective catalysts and environmentally benign oxidants remains a challenge for chemists. Various metals including palladium, cobalt, copper, and vanadium have been reported to be catalysts for aerobic oxidation.[3] It has been known that Ru, especially tetra-*N*-propylammonium perruthenate (TPAP), is efficient and highly selective for reactions converting alcohol to the corresponding aldehyde or ketone.[4]

In recent years, reactions in supercritical fluids (SCFs) have received much attention. Supercritical (SC) CO_2 is more attractive because it is readily available, inexpensive, nontoxic, nonflammable, environmentally benign, and has a mild critical temperature (31.1 °C) and critical pressure (7.38 MPa).[5] It is considered as one of the ideal substitutes for conventional volatile organic solvents in chemical reactions, and many reactions have been successfully conducted in SC CO_2.[6]

Many ionic liquids (ILs) can be designed as green solvents, although many of them are toxic and harmful for the ecosystem.[7] The nonvolatile, nonflammable and easily recyclable nature of ILs makes them a suitable reaction media for many reactions.[8] In addition, functionalized ILs for special purposes have been reported frequently in recent years.[9]

The preparation of heterogeneous catalysts by immobilization of functional ILs has become an interesting topic, and some excellent research has been reported. For example, silica-supported ILs doped with perruthenate have been successfully used as catalysts for aerobic oxidation of alcohols to produce carbonyl compounds at 75 °C using 22.0 MPa SC CO_2 as the solvent, and satisfactory results were obtained.[4a] Silica-supported ILs doped with Rh catalytic species were used as the catalysts for hydrogenations[10] and hydroformylations,[11] and the reaction rates were faster than homogeneous reactions and separation of the catalysts and products were easier. Pd nanoparticles immobilized on BSA-15 molecular sieves by 1,1,3,3-tetramethylguanidinium lactate was used to catalyze hydrogenations at solvent-free conditions.[12] Polymeric materials can be used as supports of catalysts with some advantages,[13] and immobilization of ILs on polymers has also been reported. For example, imidazolium ILs was supported on polystyrene (PS) resin *via* covalent bonding.[14] The supported ILs were efficient catalysts for substitution reactions, and the supported ILs showed much higher catalytic activity than the free ILs. Hydrogenation catalysts were fabricated by impregnation of transition metals and ILs into poly-(diallyldimethylammonium chloride), which showed excellent activity.[15]

In previous work, we copolymerized IL 1-vinyl-3-butyl imidazolium chloride ([VBIM]Cl) with cross linker divinyl benzene (DVB) to prepare the cross-linked polymer supported IL(CPSIL), in which [VBIM]Cl was anchored on the DVB cross-linked polymer matrix by covalent bonds. The supported IL was very active, selective and a stable catalyst for the cycloaddition of CO_2 to epoxides.[16a] In the present work, we prepared a new catalyst by immobilizing RuO_4^- on CPSIL, which was achieved by exchanging of Cl^- in the CPSIL with RuO_4^- in solution. The catalyst was used for aerobic oxidation of benzyl alcohol to benzyl aldehyde (Scheme 1) using SC CO_2 as solvent. It was

Beijing National Laboratory for Molecular Science, Institute of Chemistry, Chinese Academy of Sciences, Beijing, 100080, China. E-mail: hanbx@iccas.ac.cn; Fax: +86 10-62562821; Tel: +86 10-62562821

Scheme 1 Aerobic oxidation of benzyl alcohol to produce benzyl aldehyde.

This journal is © The Royal Society of Chemistry 2008
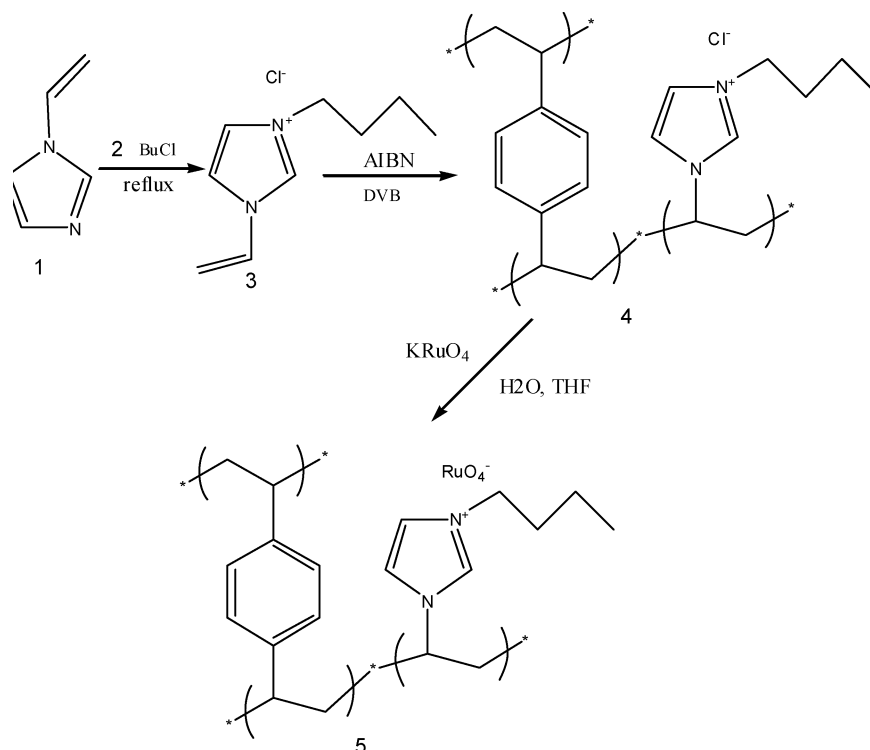
Scheme 2 Procedure to prepare the supported RuO_4^- catalyst.

demonstrated that the catalyst was very active and selective for the reaction in SC CO_2, and the reaction rate could be tuned effective by changing the pressure of CO_2.

2. Experimental section

2.1. Materials

CO_2 and O_2 were supplied by Beijing Analytical Instrument Factory with a purity of 99.99%. Toluene, dichloromethane, N,N-dimethylformamide, 1-butyl chloride and azobis(isobutyronitrile) (AIBN) were A.R. grade and produced by Beijing Chemical Plant. Divinyl benzene (DVB) was purchased from FLUKA. 1-Vinyl imidazole and $KRuO_4$ were provided by Aldrich, and benzyl alcohol was supplied by Sinpharm Chemical Reagent Co., Ltd. AIBN was recrystallized three times before use, other chemicals were used as received.

2.2. Preparation of 1-vinyl-3-butyl imidazolium chloride ([VBIM]$^+$Cl$^-$)

The experimental procedures were similar to that reported previously (Scheme 2).[16] In a typical experiment, 18.50 g (200 mmol) butylchloride and 5.50 g (58.3 mmol) 1-vinylimidazole were added into a 25 mL two-necked flask equipped with magnetic stirrer. The mixture was refluxed for 24 h in an oil bath at 70 °C under the protection of nitrogen with stirring. Then the reaction mixture was cooled down to room temperature. The upper phase was poured out and the solid residue was washed three times by ethyl acetate. Then the solid was dried at 50 °C for 12 h under vacuum to obtain the product [VBIM]$^+$Cl$^-$.

2.3. Preparation of crosslinked polymer supported ionic liquid (CPSIL)

The CPSIL was prepared by radical polymerization (Scheme 2).[16a] In the experiment, 3.2 g (24.6 mmol) crosslinker DVB, 0.5 g (2.68 mmol) [VBIM]$^+$Cl$^-$ and 0.05 g AIBN were dissolved in chloroform (150 mL) in a three-necked flask under nitrogen protection. The mixture was maintained at 70 °C and refluxed for 48 h with stirring. The CPSIL was formed, and it was collected by filtration, washed three times with tetrahydrofuran, acetone and methanol. Then the solid was dried under vacuum at 50 °C followed by grinding before using. The composition of the polymer was determined using a Flash EA1112 analyzer. Anal. Found: N: 1.79; C: Cl: 2.51.

2.4. Preparation of catalyst

The active component RuO_4^- was supported on the CPSIL by exchanging of Cl$^-$ in the CPSIL with RuO_4^- in solution (Scheme 2). In the experiment, 0.25 g $KRuO_4$ was dissolved in 40 mL mixed solvent of H_2O and THF (2 : 1) in a 100 mL flask, and then 2.0 g CPSIL prepared above was added into the flask under vigorous stirring. The mixture was treated by sonication for 10 min and continued stirring for 1 day to allow sufficient exchange of Cl$^-$ and RuO_4^-. The catalyst was obtained by filtration. The solid catalyst was washed with a mixed solvent of water and THF (H_2O : THF 2 : 1) and dried under vacuum at 70 °C for 2 days. The content of Ru in the catalyst was 4.53%, which was determined using ICP-AES (VISTA-MPX, Varian Corp., USA). The X-ray photoelectron spectrum (XPS) of the catalyst was collected on an ESCALab220i-XL spectrometer.

2.5. Procedures for oxidation reaction

The oxidation reaction was carried out in an 8 mL stainless steel reactor with magnetic stirrer. In a typical experiment, 0.16 g benzyl alcohol and 0.05 g catalyst were loaded into the reactor, and then O_2 was charged to 1 MPa at 25°C (caution: the mixing of high pressure O_2 and organic liquid is dangerous). After the reactor was heated to the desired temperature, CO_2 was compressed into the reactor to the desired pressure using a high pressure syringe pump (DB-80), and then the reaction mixture was stirred. After the reaction, the reactor was cooled in ice water and CO_2 was released passing through a cold trap with N,N-dimethylformamide. The solution in the cold trap and the reaction mixture in the reactor were mixed, and products were analyzed by GC (Agilent 6820) with dodecane as the internal standard. The product was also confirmed by NMR at room temperature on a Bruker 300 MHz NMR spectrometer using $CDCl_3$ as the solvent. ^1H NMR ($CDCl_3$, 300 MHz): δ_H 10.03 (1H,s), 7.90 (2H, d, $J = 7.3$ Hz), 7.65 (1H, t, $J = 7.4$), 7.55 (2H, t, $J = 7.4$).

3. Results and discussion
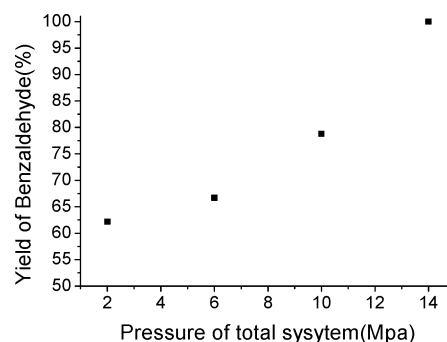
3.1. Influence of reaction time

Fig. 1 demonstrates the effect of reaction time on the yield of benzyl aldehyde. As expected, the yield increased with reaction time. The selectivity of the reaction was very high and no obvious byproducts were detected. Most of the alcohol was converted to the corresponding aldehyde in 24 h at 6 MPa and 80 °C.
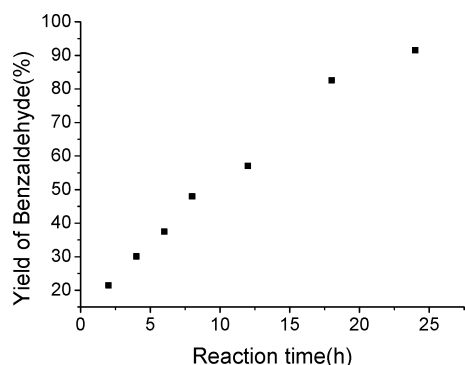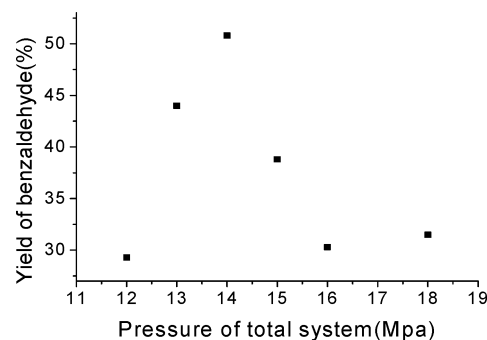

Fig. 1 Dependence of benzyl aldehyde yield on reaction time in CO_2 at 80 °C. Reaction conditions: 0.16 g benzyl alcohol, 0.05 g catalyst, 1 MPa O_2, 6 MPa total pressure.

3.2. Influence of pressure

Fig. 2 shows the effect of pressure on the yield of benzyl aldehyde with a reaction time of 4 h. Increase of CO_2 pressure could markedly accelerate the reaction rate up to 14 MPa, and a yield of >99% was achieved after 4 h at 14 MPa, as can be seen from Fig. 2. In order to study how pressure affected the reaction rate at higher pressure, we studied the yield with a shorter reaction time, and the results are presented in Fig. 3. At each pressure, the experiment was repeated at least three times. The repeatability was better than ±2%. The figure shows that there was a maximum in the yield vs. pressure curve at about 14 MPa, i.e., the yield increased with increasing pressure as pressure was

Fig. 2 Yield of benzyl aldehyde as a function of total pressure of reaction system at 80 °C. Reaction conditions: 0.0533 g benzyl alcohol, 0.050 g catalyst, 4 h reaction time, 1 MPa O_2.

Fig. 3 Dependence of benzyl aldehyde yield on total pressure of reaction system at 80 °C. Reaction conditions: 0.0266 g benzyl alcohol, 0.025 g catalyst, 2 h reaction time, 1 MPa O_2.

less than about 14 MPa, and decreased with increasing pressure at higher pressures.

It is well known that the solvent power of SC CO_2 changes with pressure. Therefore, the phase behavior of the reaction system may change with pressure of CO_2, which in turn affects the properties of chemical reactions.[17] In this work, we studied the phase behavior of the reaction system by preparing the mixtures of typical compositions in the reaction process. The view cell reported previously was used.[17] The catalyst was not added in the phase behavior study to avoid reaction. There were three components in the reaction system before reaction; CO_2, O_2 and benzyl alcohol, and there were five components during the reaction process; CO_2, O_2, benzyl alcohol, benzyl aldehyde, and H_2O, and there were four components after the benzyl alcohol was completely converted; CO_2, O_2, benzyl aldehyde and H_2O. The composition of the reaction system was a function of original molar ratio (before reaction) of CO_2 : O_2 : benzyl alcohol and the conversion of benzyl alcohol. At a fixed original ratio, the composition of the system was a function of conversion of benzyl alcohol, i.e. the composition of the reaction system at any conversion could be easily calculated and the phase behavior at different conversions could be determined by preparing mixtures. Fig. 4 shows the dependence of phase separation pressure of the reaction system on the conversion of benzyl alcohol. The original volume ratio of benzyl alcohol added and the view cell was the same as that in the reactor. There was one fluid phase in the reaction system above the phase separation pressure, and there were two fluid phases in the reaction system below the phase separation pressure. Fig. 4
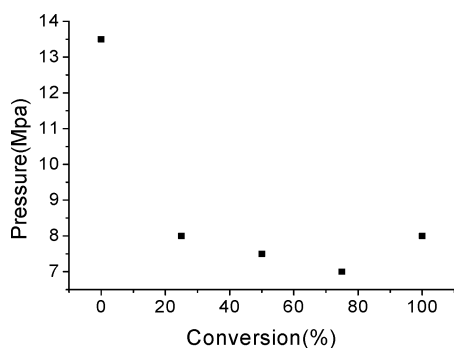
Fig. 4 Dependence of phase separation pressure of the reaction system on the conversion of benzyl alcohol. Conditions: 0.0266 g benzyl alcohol, 1 MPa O_2.

shows clearly that there was only one fluid phase above 13.5 MPa in the reaction process, and there could be two fluid phases at the lower pressures. The phase behavior of the reaction system can explain partially the maximum in Fig. 3, which is discussed qualitatively as follow.

The solubility of O_2 in liquids is usually very small because it is nonpolar and highly volatile. It is known that dissolution of CO_2 in liquids can enhance the solubility of other gases in liquids.[18] As pressure was lower than phase separation pressure, there were two fluid phases in the reaction system, benzyl alcohol-rich phase and CO_2-rich phase. The reaction took place in benzyl alcohol-rich phase because the catalyst was dispersed in this phase. With increasing pressure, the concentration of O_2 in the benzyl alcohol-rich phase might increase, which favored the reaction because O_2 was a reactant. At the same time, dissolution of CO_2 in the liquid phase resulted in increase in diffusion of the reactants, which also enhanced the reaction. However, dissolution of CO_2 expanded the liquid phase and reduced the concentration of benzyl alcohol, which was not favorable to the reaction. The first two factors were dominant and the reaction rate increased with increasing pressure in the two phase region. After the pressure reached phase separation pressure, there was only one fluid phase and the gas/liquid interface mass transfer was eliminated, which was favorable to the reaction. But as the pressure was further increased, the solvent power of SC CO_2 became stronger, which limited adsorption of the reactants on the surface of the catalyst and reduced the reaction rate. Furthermore, the lower diffusivity of the components at high pressure also reduced the reaction rate. Therefore, there was a maximum in the pressure *vs*. yield curve in Fig. 3. It should be emphasized that the maximum may not occur exactly at the phase separation pressure because the catalyst was porous as can be seen from the scanning electron microscopy (SEM, JEOL JSM 6700F) image of the CPSIL (Fig. 5), and the capillary force and the interaction of the reaction mixture and the surface of the catalyst affected the phase separation pressure in the pores.

3.3. Reaction in different solvents

The reaction was also conducted in toluene and dichloromethane, and the results are given in Table 1. Obviously, the reaction had higher yield in SC CO_2 than in conventional solvents. Only 76% (entry 1) or 87% (entry 2) were achieved after 8 h in toluene or dichloromethane, while a yield of 87% (entry 3)
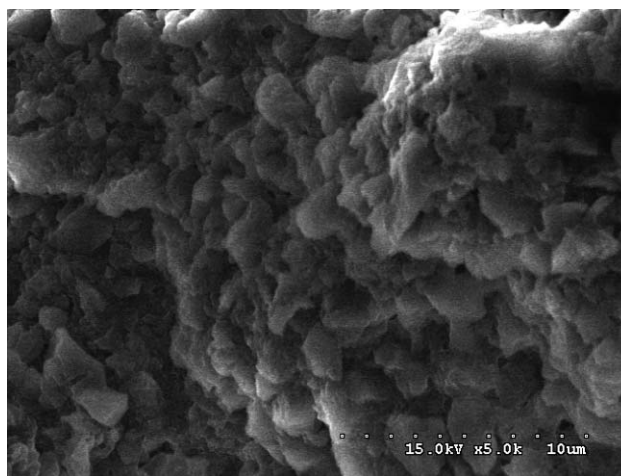
Fig. 5 Scanning electron microscopy image of the CPSIL.

Table 1 Oxidation of benzyl alcohol in different solvents

Entry	Solvent	Yield (%)	TOF/h^{-1}
1	Toluene[a]	76	2.1
2	CH_2Cl_2[a]	87	2.4
3	Sc CO_2[b]	87	3.8
4	Sc CO_2[c]	>99	5.5

[a] Reaction conditions: 1 MPa O_2, solvent 4 mL, 0.0266 g benzyl alcohol, 0.025 g catalyst, reaction time 8 h, 80°C (caution: the mixing of high pressure O_2 and organic liquid is dangerous). [b] Reaction conditions: 1 MPa O_2, total pressure 14 MPa, 0.0266 g benzyl alcohol, 0.025 g catalyst, reaction time 5 h, 80°C. [c] Reaction conditions: 1 MPa O_2, total pressure 14 MPa, 0.0533 g benzyl alcohol, 0.050 g catalyst, reaction time 4 h, 80°C

was obtained after only 5 h and nearly 100% could be achieved after 4 h under certain conditions in SC CO_2 (entry 4). The TOF in SC CO_2 was about 1.6–2.6 times higher than that in toluene and dichloromethane. This is mainly due to the high diffusivity of SC CO_2 and high miscibility of CO_2 and the reactants, which eliminated or reduced the effect of gas/liquid interface mass transfer. Besides, the reaction in SC CO_2 is environmentally more acceptable. It should be emphasized that the selectivity of the reaction in all the solvents was very high and the byproducts could not be detected in GC analysis. This indicated that the catalyst prepared in this work was very selective for the aerobic oxidation.

3.4. Recycling of the catalyst

The recyclability of the catalyst was also investigated. Two different processes were tested: (1) after reaction, the system was washed with DMF. The catalyst was filtrated followed by washing with THF three times. The recycled catalyst was utilized in the next reaction after being dried under vacuum; (2) the recycle was carried out by SC CO_2 extraction. After the reaction, the product was extracted by SC CO_2 at 14 MPa and 35 °C. The catalyst was used directly for the next run after the extraction process. As can be seen from Table 2, method 2 was superior to method 1. The catalyst was still very active after several runs, although the yield decreased continuously with run times. The possible reason may be the self-aggregation of Ru derivatives

Table 2 Recycling of the catalyst

Method	Run times	Yield (%)
1[a]	1	67
	2	27
2[b]	1	77
	2	52
	3	32
	4	24

[a] Recycling catalyst by DMF washing. Reaction conditions: 1 MPa O_2, total pressure 6 MPa, 0.0533 g benzyl alcohol, 0.050 g catalyst, reaction time 4 h, 80 °C. [b] Recycling catalyst by SC CO_2 extraction. Reaction conditions: 1 MPa O_2, total pressure 14 MPa, 0.0533 g benzyl alcohol, 0.050 g catalyst, reaction time 3 h, 80°C

as reported.[4b,c] In this work, we characterized the used catalyst using the XPS technique, and the result is given in Fig. 6. The peak of 464.4 eV (Ru $3p_{3/2}$) and 486.2 eV (Ru $3p_{1/2}$) confined the presence of RuO_4^-, while the binding energy of 463.2 eV (Ru $3p_{3/2}$) and 486.9 eV (Ru $3p_{1/2}$) showed the presence of RuO_2. The reasons for the activity reduction of the catalyst with recycling time needs to be studied further.
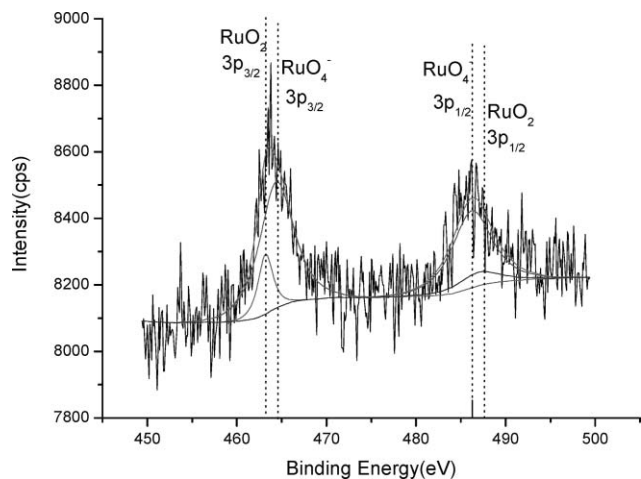
Fig. 6 XPS spectrum of the Ru 3p edge of the used catalyst. The vertical lines indicate the peak positions of the binding energies of Ru.

4. Conclusion

In this work, we prepared a catalyst for aerobic oxidation of benzyl alcohol by immobilization of perruthernate on polymer supported IL [VBIM]$^+$Cl$^-$. The benzyl alcohol can be converted to benzyl aldehyde with negligible by-products. SC CO_2 is an excellent solvent for this reaction because the reaction rate can be optimized by pressure, the O_2/liquid interface mass transfer can be eliminated, and it is environmentally more acceptable. The catalyst can be reused directly after *in situ* extraction of the products using SC CO_2, and it remains satisfactory active after being reused four times.

Acknowledgements

References

1 (a) E. J. Corey and G. Schmidt, *Tetrahedron Lett.*, 1979, **20**, 399; (b) M. Hirano, S. Yakaba, H. Chikamori, J. H. Clark and T. Morimoto, *J. Chem. Res. Synop.*, 1998, **6**, 308; (c) R. A. Lee and D. S. Donald, *Tetrahedron Lett.*, 1997, **38**, 3857.

2 B. W. Cue, *Chem. Eng. News*, 2005, **83**, 46.

3 (a) B. Z. Zhan and A. Thmpson, *Tetrahedron*, 2004, **60**, 2917; (b) G. J. ten Brink, I. W. C. E. Arends and R. A. Sheldon, *Adv. Synth. Catal.*, 2002, **344**, 355; (c) M. Gilhespy, M. Lok and X. Baucherel, *Chem. Commun.*, 2005, 1085; (d) G. Ragagnin, B. Betzemeier, S. Quici and P. Knochel, *Tetrahedron*, 2002, **58**, 3985; (e) S. Velusamy and T. Punniyamurthy, *Org. Lett.*, 2004, **6**, 217.

4 (a) R. Ciriminna, P. Hesemann, J. J. E. Moreau, M. Carraro, S. Campestrini and M. Pagliaro, *Chem.–Eur. J.*, 2006, **12**, 5220; (b) M. Hasan, M. Musawir, P. N. Davey and I. V. Kozhevnikov, *J. Mol. Catal. A: Chemical*, 2002, **180**, 77; (c) S. Campestrini, M. Carraro, R. Ciriminna, M. Pagliaro and U. Tonellata, *Adv. Synth. Catal.*, 2005, **347**, 825.

5 *Handbook of Chemistry and Physics*, ed. R. C. Weast, CRC Press, West Palm Beach, Florida, 68th edn, 1987.

6 (a) M. Poliakoff, J. M. Fitzpatrick, T. R. Farren and P. T. Anastas, *Science*, 2002, **297**, 807; (b) D. J. Cole-Hamilton, *Science*, 2003, **299**, 1702; (c) P. G. Jessop and W. Leitner, *Chemical Synthesis Using Supercritical Fluids*, Wiley-VCH, Weinheim, 1999; (d) P. G. Jessop, *J. Supercrit. Fluids*, 2006, 38, 211; (e) A. Baiker, *Chem. Rev.*, 1999, **99**, 453; (f) R. A. Scheldon, *Green Chem.*, 2005, **7**, 267; (g) M. Solinas, J. Y. Jiang, O. Stelzer and W. Leitner, *Angew. Chem., Int. Ed.*, 2005, **44**, 2291; (h) R. X. Liu, F. Y. Zhao, S. I. Fujita and M. Arai, *Appl. Catal., A: Gen.*, 2007, **316**, 127; (i) R. Amandi, K. Scovell, P. Licence, T. J. Lotz and M. Poliakoff, *Green Chem.*, 2007, **9**, 797; (j) J. S. Tian, C. X. Miao, J. Q. Wang, F. Cai, Y. Zhao and L. N. He, *Green Chem.*, 2007, **9**, 566.

7 (a) A. S. Wells and V. T. Coombe, *Org. Process Res. Dev.*, 2006, **10**, 794; (b) D. B. Zhao, Y. C. Liao and Z. D. Zhang, *Clean*, 2007, **35**, 42; (c) S. Stole, J. Arning, U. Bottin-Weber, A. Muller, W. Pitner, U. Welz-Biermann, B. Jastorff and J. Ranke, *Green Chem.*, 2007, **9**, 760.

8 (a) P. Wasserscheid and T. Welton, *Ionic Liquids in Synthesis*, Wiley-VCH, Weinheim, 2003; (b) P. B. Webb, M. F. Sellin, T. E. Kunene, S. Williamson, A. M. Z. Slawin, D. J. Cole-Hamilton, *J. Am. Chem. Soc.*, 2003, 125, 15577; (c) J. Pernak, M. Smiglak, S. T. Griffin, W. L. Hough, T. B. Wilson, A. Pernak, J. Zabieska-Matejuk, A. Fojutowski, K. Kita, R. D. Rogers, *Green Chem.*, 2006, 8, 798.

9 (a) B. Ni, Q. Zhang and A. D. Headley, *Green Chem.*, 2006, **8**, 798; (b) K. Fukumoto and H. Ohno, *Chem. Commun.*, 2006, 3081; (c) G. H. Tao, L. He, N. Sun and Y. Kou, *Chem. Commun.*, 2005, 3562; (d) S. Anjaiah, S. Chandrasekhar and R. Gree, *Tetrahedron Lett.*, 2004, **45**, 569; (e) S. G. Lee, *Chem. Commun.*, 2006, 1049; (f) L. Poletti, C. Chiappe, L. Lay, D. Pieraccini, L. Polito and G. Russo, *Green Chem.*, 2007, **9**, 337.

10 C. P. Mehnert, E. J. Mozeleski and R. A. Cook, *Chem. Commun.*, 2002, 3010.

11 C. P. Mehnert, R. A. Cook, N. C. Dispenziere and M. Afeworki, *J. Am. Chem. Soc.*, 2002, **124**, 12932.

12 J. Huang, T. Jiang, H. X. Gao, B. X. Han, Z. M. Liu, W. Z. Wu, Y. H. Chang and G. Y. Zhao, *Angew. Chem., Int. Ed.*, 2004, **43**, 1397.

13 (a) R. Akiyama and S. Kobayashi, *Angew. Chem., Int. Ed.*, 2002, **41**, 2602; (b) C. W. Tsang, B. Baharloo, D. Riendl, M. Yam and D. P. Gates, *Angew. Chem., Int. Ed.*, 2004, **43**, 5682; (c) A. Michrowska, K. Mennecke, U. Kunz, A. Kirschning and K. Grela, *J. Am. Chem. Soc.*, 2006, **128**, 13261.

14 D. W. Kim and D. Y. Chi, *Angew. Chem., Int. Ed.*, 2004, **43**, 483.

15 A. Wolfson, I. F. J. Vankelecom and P. A. Jacobs, *Tetrahedron Lett.*, 2003, **44**, 1195.

16 (a) Y. Xie, Z. F. Zhang, T. Jiang, J. L. He, B. X. Han, T. B. Wu and K. L. Ding, *Angew. Chem., Int. Ed.*, 2007, **46**, 7255; (b) X. D. Mu, J. Q. Meng, Z. C. Li and Y. Kou, *J. Am. Chem. Soc.*, 2005, **127**, 9694.

17 Z. S. Hou, B. X. Han, Z. M. Liu, T. Jiang and G. Y. Yang, *Green Chem.*, 2002, **4**, 467.

18 (a) D. G. Hert, J. L. Anderson, S. N. V. K. Aki and J. F. Brennecke, *Chem. Commun.*, 2005, 2603; (b) M. Wei, G. T. Musie, D. H. Busch and B. Subramaniam, *J. Am. Chem. Soc.*, 2002, **124**, 2513.

One-pot chemoenzymatic syntheses of enantiomerically-enriched *O*-acetyl cyanohydrins from aldehydes in ionic liquid†

Zhi-Liang Shen,[a] Wei-Juan Zhou,[a] Ya-Ting Liu,[a] Shun-Jun Ji*[b] and Teck-Peng Loh*[a]

A practical and efficient method for the synthesis of optically active *O*-acetyl cyanohydrins *via* one-pot lipase-catalyzed kinetic resolution of the *in situ* generated racemic cyanohydrins or *O*-acetyl cyanohydrins using an ionic liquid as both reaction media and promoter has been described.

The development of one-pot chemoenzymatic synthesis of enantiomerically-enriched compounds is highly sought-after in the synthetic community.[1] However, many organic reactions work only in the presence of metal complexes or Brønsted acids which are known to deactivate the catalytic activity of enzymes if operated in a one-pot manner. In order to achieve this goal, our group has been developing new C–C bond formation reactions, such as the Mukaiyama–aldol and cyanosilylation of aldehydes in water and ionic liquids without the use of metal complexes and/or special activation.[2] Herein, we report an efficient method to obtain the synthetically versatile enantiomerically-enriched *O*-acetyl cyanohydrins *via* one-pot lipase-catalyzed kinetic resolution of the *in situ* generated cyanohydrins or *O*-acetyl cyanohydrins using an ionic liquid as both reaction media and promoter.[3–5]

Our initial studies were aimed at finding out the most suitable lipases for the one-pot reaction of ionic liquid-promoted cyanosilylation of aldehydes followed by lipase-catalyzed kinetic resolution of the corresponding cyanohydrins. Therefore, the reaction involving hydrocinnamaldehyde using various lipases in ionic liquid [omim]PF$_6$ (1-methyl-3-octylimidazolium hexafluorophosphate) were investigated. The results are listed in Table 1.

A wide variety of lipases (including Lipozyme, Baker's yeast, Lipase Type VII, Amano lipase AYS, Amano lipase G, Amano lipase M, Amano lipase A, Amano lipase F-AP15, Amano lipase PS, Amano lipase AK, and Pseudomonas cepacia lipase) have been screened to evaluate their activities and selectivities. Except for Amano lipase PS, Amano lipase AK and Pseudomonas cepacia lipase, most of the lipases did not afford the desired *O*-acetyl cyanohydrins. Using these three lipases (Amano lipase PS,

Amano lipase AK and Pseudomonas cepacia lipase), the one-pot chemoenzymatic reaction in [omim]PF$_6$ proceeded smoothly to give the desired product **1** in moderate to good yields and moderate to excellent enantioselectivities (Table 1).

In addition, it was interesting to find that lipase activity in ionic liquid was anion dependent, since the same reaction using Amano lipase PS in ionic liquid [hmim]BF$_4$ (1-hexyl-3-methylimidazolium tetrafluoroborate) or [hmim]Cl (1-hexyl-3-methylimidazolium chloride) gave the desired product only in poor enantioselectivities (<5% ee). It is important to note that the use of Pseudomonas cepacia lipase afforded the desired products *O*-acetyl cyanohydrin and cyanohydrin in 46% yield with 82% ee and 44% yield with 79% ee, respectively (Table 1, entry 3). Therefore, the one-pot reactions involving the addition of TMSCN to different aldehydes followed by lipase-catalyzed kinetic resolution of the corresponding *O*-acetyl cyanohydrins were carried out under the above optimized reaction conditions. The results are summarized in Table 2.

As indicated in Table 2, this reaction worked well with aromatic, aliphatic and conjugate aldehydes. In all cases, the desired *O*-acetyl cyanohydrins were obtained in good to excellent yields with moderate to high enantioselectivities. Unfortunately, the corresponding unreacted cyanohydrins (R configuration) were obtained in low to good yields with low to moderate enantioselectivities.

Next, we proceeded to carry out one-pot TMSCN addition to aldehydes followed by acetylation reaction (using Ac$_2$O) promoted by ionic liquid, and finally subjecting the *in situ* generated *O*-acetyl cyanohydrin to lipase-catalyzed chemoenzymatic hydrolysis in ionic liquid [omim]PF$_6$. Similarly, a variety of lipases were screened and the results are shown in Table 3.

As listed in Table 3, among the several lipases screened (entries 1–4), the one-pot reaction involving benzaldehyde proceeded more efficiently with Candida antarctica lipase than with other lipases to give the desired product **3** in good yield (59%) and moderate ee (48%). The same reaction using Candida antarctica lipase carried out at room temperature or in ionic liquid [bmim]BF$_4$ (1-butyl-3-methylimidazolium tetrafluoroborate) afforded the desired product in low ee (entries 5–6). After several trials, it was gratifying to find that the addition of one equivalent of Ac$_2$O (in step 3) resulted in an increase in enantioselectivity of the desired product (73% ee, entry 7).[6] In addition, it was interesting to note that the lipase was tolerant to acetic acid under the current reaction conditions (entry 8).[6] With the optimized reaction conditions in hand, we continued to apply this one-pot strategy to other substrates. The results are summarized in Table 4.

[a]*Division of Chemistry and Biological Chemistry, School of Physical and Mathematical Sciences, Nanyang Technological University, Singapore 637371. E-mail: teckpeng@ntu.edu.sg; Fax: (+65) 6791 1961; Tel: (+65) 6316 8899*
[b]*Key Laboratory of Organic Synthesis of Jiangsu Province, College of Chemistry and Chemical Engineering, Suzhou University, Renai Road, Suzhou Industrial Park, Suzhou, 215123, China*
† Electronic supplementary information (ESI) available: Experimental details and spectral data. See DOI: 10.1039/b717235d

Table 1 Optimization of reaction conditions for the kinetic resolution of *in situ* generated cyanohydrin

Entry	Lipase[a]	Time/days	1 Yield (%)[b]	1 ee (%)	2 Yield (%)[b]	2 ee (%)[c]
1	I	3.5	41	70	26	85
2	II	3.5	61	80	7	51
3	III	4	46	82	44	79

[a] Lipase: Amano lipase AK (I), Amano lipase PS (II), Pseudomonas cepacia lipase (III). [b] Isolated yield based on aldehyde. [c] ee was determined by chiral HPLC analysis after converting to its corresponding acetylated product.

Table 2 One-pot syntheses of optically active *O*-acetyl cyanohydrins using different aldehydes

Entry	RCHO	Time/days	1 Yield (%)[a]	1 ee (%)	2 Yield (%)[a]	2 ee (%)[b]
1	3-F-C6H4CHO	4	35	74 (S)	29	54 (R)
2	C6H5CHO	3	25	73 (S)	31	44 (R)
3	4-Me-C6H4CHO	5	35	85 (S)	9	78 (R)
4	4-MeO-C6H4CHO	3	22	92 (S)	50	22 (R)
5	piperonal	5	31	87 (S)	11	54 (R)
6	2-naphthaldehyde	5	33	82 (S)	17	60 (R)
7	PhCH2CH2CHO	4	46	82 (S)	44	79 (R)
8	cinnamaldehyde	4	40	60 (S)	23	23 (R)

[a] Isolated yield based on aldehyde. [b] ee was determined by chiral HPLC analysis after converting to its corresponding acetylated product.

As shown in Table 4, the one-pot reactions involving various aldehydes proceeded efficiently in the presence of Candida antarctica lipase and [omim]PF$_6$ to furnish the desired products in good yields and ee. Even aliphatic aldehyde and conjugate aldehyde are good substrates for this reaction (entries 6–7).

In conclusion, we have developed a practical and efficient method for the synthesis of optically active *O*-acetyl cyanohydrins *via* one-pot lipase-catalyzed kinetic resolution of the *in situ* generated cyanohydrins or *O*-acetyl cyanohydrins in ionic liquid [omim]PF$_6$. This reaction is quite general and it works

Table 3 Optimization of one-pot reaction conditions for the kinetic resolution of *O*-acetyl cyanohydrin[a]

Entry	Lipase[b]	Additive (1 eq.)	3 Yield (%)[c]	3 ee (%)
1	I	—	38	17
2	II	—	66	8
3	III	—	59	48
4	IV	—	53	18
5[d]	III	—	71	2
6[e]	III	—	89	10
7	III	Ac₂O	39	73
8	III	AcOH	48	52

[a] The yield and ee of product **4** was not determined. [b] Lipase: Amano lipase AK (I), Amano lipase PS (II), Candida antarctica lipase (III), Pseudomonas cepacia lipase (IV). [c] Isolated yield based on aldehde. [d] Using [bmim]BF₄ in place of [omim]PF₆ (other conditions are the same). [e] The reaction was carried out at room temperature (other conditions are the same).

with a wide variety of aldehydes at room temperature in the absence of any metal complexes. The mild reaction conditions, good selectivities and the simplicity of the reaction procedure make this method attractive for scale-up purposes. Efforts to apply this strategy by combining other C–C bond formation reactions without metal complexes with enzymatic reactions are in progress.

Acknowledgements

Notes and references

1 For reviews regarding the use of enzymes in organic synthesis, see: (*a*) G. Seoane, *Curr. Org. Chem.*, 2000, **4**, 283; (*b*) S. M. Roberts, *J. Chem. Soc., Perkin Trans. 1*, 1998, 157; (*c*) S. M. Roberts, *J. Chem. Soc., Perkin Trans. 1*, 1999, 1; (*d*) K. Faber, *Biotransformations in Organic Chemistry*, Springer-Verlag, New York, 1992; (*e*) C. H. Wong, and G. M. Whitesides, *Enzymes in Synthetic Organic Chemistry*, Pergamon, Oxford, 1994; (*f*) K. Drauz, and H. Waldmann, *Enzyme Catalysis in Organic Synthesis*, Wiley-VCH, Weinheim, 1995; (*g*) H. G. Davies, R. H. Green, D. R. Kelly and S. M. Roberts, *Biotransformations in Preparative Organic Chemistry*, Academic Press, London, 1989; (*h*) J. Halgas, *Biocatalysts in Organic Synthesis*, Elsevier, Amsterdam, 1992; (*i*) T. Sugai, *Curr. Org. Chem.*, 1999, **3**, 373; (*j*) C. H. Wong, R. L. Halcomb, Y. Ichikawa and T. Kajimoto, *Angew. Chem., Int. Ed. Engl.*, 1995, **34**, 412; (*k*) G. Whitesides and C. H. Wong, *Angew. Chem., Int. Ed. Engl.*, 1985, **24**, 617; (*l*) J. Sukumaran and U. Hanefeld, *Chem. Soc. Rev.*, 2005, **34**, 530; (*m*) B. G. Davis, *Annu. Rep. Prog. Chem., Sect. B*, 2003, **99**, 49; (*n*) A. Ghanem and H. Y. Aboul-Enein, *Chirality*, 2005, **17**, 1; (*o*) A. Ghanem and H. Y. Aboul-Enein, *Tetrahedron: Asymmetry*, 2004, **15**, 3331; (*p*) B. G. Davis and V. Boyer, *Nat. Prod.*

Table 4 One-pot synthesis of optically active *O*-acetyl cyanohydrins using different aldehydes

Entry	RCHO	3 Yield (%)[a]	3 ee (%)	4 Yield (%)[a]	4 ee (%)[b]
1	(3-F-C₆H₄CHO)	44	86 (R)	30	50 (S)
2	(4-Cl-C₆H₄CHO)	44	98 (R)	28	66 (S)
3	(4-Br-C₆H₄CHO)	43	95 (R)	37	70 (S)
4	(C₆H₅CHO)	39	73 (R)	—[c]	
5	(4-CH₃-C₆H₄CHO)	34	84 (R)	36	25 (S)
6	(PhCH₂CH₂CHO)	39	81 (R)	46	63 (S)
7	(PhCH=CHCHO)	57	74 (R)	20	21 (S)

[a] Isolated yield based on aldehyde. [b] Ee was determined by chiral HPLC analysis after converting to its corresponding acetylated product. [c] Not determined.

Rep., 2001, **18**, 618; (*q*) T. Scheper, *New Enzymes for Organic Synthesis: Screening, Supply and Engineering*, Springer Berlin, Heidelberg, 1997.
2 (*a*) S. L. Chen, S. J. Ji and T. P. Loh, *Tetrahedron Lett.*, 2004, **45**, 375; (*b*) Z. L. Shen, S. J. Ji and T. P. Loh, *Tetrahedron Lett.*, 2005, **46**, 3137; (*c*) T. P. Loh, K. C. Xu, D. S. C. Ho and K. Y. Sim, *Synlett*, 1998, 369; (*d*) T. P. Loh, L. C. Feng and L. L. Wei, *Tetrahedron*, 2000, **56**, 7309.
3 For reviews regarding the application of ionic liquids in organic synthesis, see: (*a*) R. A. Sheldon, *Chem. Commun.*, 2001, 2399; (*b*) C. M. Gordon, *Appl. Catal. A: Gen.*, 2001, **222**, 101; (*c*) P. Wasserscheid and W. Keim, *Angew. Chem., Int. Ed.*, 2000, **39**, 3772; (*d*) J. D. Holbrey and K. R. Seddon, *Clean Prod. Process.*, 1999, **1**, 223; (*e*) T. Welton, *Chem. Rev.*, 1999, **99**, 2071; (*f*) H. Zhao and S. V. Malhotra, *Aldrichim. Acta*, 2002, **35**, 75; (*g*) C. E. Song, *Chem. Commun.*, 2004, 1033; (*h*) J. Ding and D. W. Armstrong, *Chirality*, 2005, **17**, 281; (*i*) C. Baudequin, J. Baudoux, J. Levillain, D. Cahard, A. C. Gaumont and J. C. Plaquevent, *Tetrahedron: Asymmetry*, 2003, **14**, 3081.
4 For one-pot method for the synthesis of *O*-acetyl cyanohydrins using lipase, see: (*a*) U. Hanefeld, Y. X. Li, R. A. Sheldon and T. Maschmeyer, *Synlett*, 2000, 1775; (*b*) Y. X. Li, A. J. J. Straathof and U. Hanefeld, *Tetrahedron: Asymmetry*, 2002, **13**, 739; (*c*) M. Inagaki, J. Hiratake, T. Nishioka and J. Oda, *J. Org. Chem.*, 1992, **57**, 5643; (*d*) M. Kimura, A. Kuboki and T. Sugai, *Tetrahedron: Asymmetry*, 2002, **13**, 1059; (*e*) G. de Gonzalo, I. Lavandera, R. Brieva and V. Gotor, *Tetrahedron*, 2004, **60**, 10525; (*f*) L. Veum, L. T. Kanerva, P. J. Halling,

T. Maschmeyer and U. Hanefelda, *Adv. Synth. Catal.*, 2005, **347**, 1015; (*g*) L. Veum and U. Hanefeld, *Tetrahedron: Asymmetry*, 2004, **15**, 3707; (*h*) A. Fishman and M. Zviely, *Tetrahedron: Asymmetry*, 1998, **9**, 107; (*i*) Y. N. Belokon, A. J. Blacker, L. A. Clutterbuck, D. Hogg, M. North and C. Reeve, *Eur. J. Org. Chem.*, 2006, 4609; (*j*) T. Sakai, Y. Miki, M. Tsuboi, H. Takeuchi, T. Ema, K. Uneyama and M. Utaka, *J. Org. Chem.*, 2000, **65**, 2740.

5 For selected other methods concerning the synthesis of *O*-acetyl cyanohydrins, see: (*a*) B. C. Ranu, J. Dutta and A. Das, *Chem. Lett.*, 2003, **32**, 366; (*b*) Y. N. Belokon, A. V. Gutnov, M. A. Moskalenko, L. V. Yashkina, D. E. Lesovoy, N. S. Ikonnikov, V. S. Larichev and M. North, *Chem. Commun.*, 2002, 244; (*c*) R. Yoneda, K. Santo, S. Harusawa and T. Kurihara, *Synthesis*, 1986, 1054; (*d*) S. Norsikian, I. Holmes, F. Lagasse and H. B. Kagan, *Tetrahedron Lett.*, 2002, **43**, 5715; (*e*) W. Huang, Y. M. Song, J. Wang, G. Y. Cao and Z. Zheng, *Tetrahedron*, 2004, **60**, 10469; (*f*) Y. N. Belokon, A. J. Blacker, P. Carta, L. A. Clutterbuck and M. North, *Tetrahedron*, 2004, **60**, 10433; (*g*) W. Huang, Y. M. Song, C. M. Bai, G. Y. Cao and Z. Zheng, *Tetrahedron Lett.*, 2004, **45**, 4763; (*h*) N. H. Khan, S. Agrawal, R. I. Kureshy, S. H. R. Abdi, V. J. Mayani and R. V. Jasra, *Eur. J. Org. Chem.*, 2006, 3175; (*i*) A. Baeza, C. Najera, M. G. Retamosa and J. M. Sansano, *Synthesis*, 2005, 2787; (*j*) Y. N. Belokon, P. Carta, A. V. Gutnov, V. Maleev, M. A. Moskalenko, L. V. Yashkina, N. S. Ikonnikov, N. V. Voskoboev, V. N. Khrustalev and M. North, *Helv. Chim. Acta*, 2002, **85**, 3301; (*k*) K. Iwanami, M. Aoyagi and T. Oriyama, *Tetrahedron Lett.*, 2005, **46**, 7487; (*l*) S. Lundgren, E. Wingstrand, M. Penhoat and C. Moberg, *J. Am. Chem. Soc.*, 2005, **127**, 11592; (*m*) T. Purkarthofer, W. Skranc, H. Weber, H. Griengl, M. Wubbolts, G. Scholz and P. Pöchlauer, *Tetrahedron*, 2004, **60**, 735.

6 Currently, the reasons which led to the phenomenon are unclear.

www.rsc.org/greenchem | Green Chemistry

Microwave-promoted efficient synthesis of C6-cyclo secondary amine substituted purine analogues in neat water†

Gui-Rong Qu,* Lin Zhao, Dong-Chao Wang, Jing Wu and Hai-Ming Guo*

The synthesis of C6-cyclo secondary amine-substituted purine analogues in neat water was achieved with the aid of microwave irradiation, providing a rapid, efficient and convenient method for the preparation of acyclic nucleosides in high yields.

Many nucleoside analogues with modifications on the heterocyclic bases have been investigated for their antiviral and anticancer activities. Purine derivatives with various substituents at C6 have received considerable attention due to their important physiological and pharmacological properties.[1] C6-aminopurines have been shown to have antitumor activity as kinase inhibitors.[2] The traditional method for the synthesis of C6-substituted aminopurine analogues is the amination of halo,[3] oxo,[4] mercapto or methylmercapto[5] with various amines. However, these synthetic routes often involve long reaction time, toxic solvent (such as CH_3CN,[5] dioxane,[6] DMF,[7] or DMSO[8]) and labor-intensive operation. Over the past two decades, microwave irradiation as a non-conventional energy source is becoming a very popular and useful technique in organic chemistry,[9] it has been applied to a wide range of reaction types, including aromatic nucleophilic substitution, cycloaddition, and organometallic reactions.[10] Many of these reactions have been demonstrated to result in higher yield and reduce reaction time under microwave irradiation compared with using a traditional heating method. Water, a safe and environmentally benign solvent, has attracted much attention in synthetic chemistry recently.[11] The use of both water as solvent and microwave irradiation for heating makes the reaction process more attractive. Herein, we describe a simple and efficient method for the synthesis of C6-cyclo secondary amine-substituted purine analogues under microwave irradiation in water.

To initiate our study, we examined the ability of a microwave promoting nucleophilic substitution reaction between 2,6-dichloropurine and piperidine in water (Scheme 1). To our delight, the reaction proceeded smoothly to give 2-chloro-6-piperidinopurine with 82% isolated yield without any additional base. Changing irradiation time had some influences on the yield. It seemed that the reaction reached chemical equilibrium
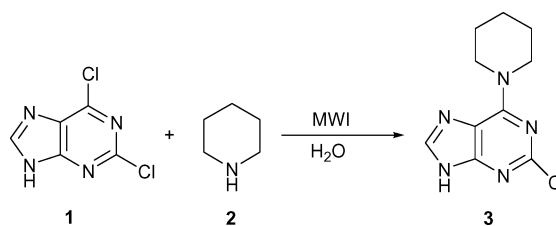
Scheme 1 Microwave promoting nucleophilic substitution reaction of 2,6-dichloropurine with piperidine.

after being irradiated for 8 min. When the reaction time was longer than 8 min, only slight yield variations were detected, therefore 8 min was the optimized reaction time. Further screening of irradiation power and reaction temperatures confirmed that 400 W and 100 °C were the best conditions.

To evaluate the generality of the reaction, a number of 6-chloropurine derivatives with piperidine, pyrrolidine or hexamethyleneamine were employed. The results are shown in Table 1. For piperidine, the reaction proceeded smoothly with all of the employed 6-chloropurine derivatives and gave good to excellent yields. Maybe this is because piperidine has a higher basicity which makes purine easily dissolve in water (entries 1–10). For pyrrolidine, the reaction failed to proceed if no extra base was added into the reaction system. Maybe this is because purine can not dissolve in water due to the weak alkalinity of pyrrolidine. In order to increase the solubility of purine in water, we decided to add a base to the reaction mixture because we found most purine analogues were easily dissolvable in alkaline aqueous solution. As anticipated, the nucleophilic substitution with pyrrolidine was better conducted by using NaOH as a base (entries 11–19). So it could be concluded that the differences of solubility in water of the starting materials played an important role when water acted as the reaction medium. For hexamethyleneamine, the reaction could not proceed even if NaOH was used as an added base, presumably due to the steric hindrance of the secondary amine (entry 20).

As shown in Table 1, to study the hindrance effect of the substituents on purine, a number of 6-chloropurines derivatives were also studied for the reaction. The desired C6-cyclo secondary amine-substituted purines analogues could be easily obtained in good to excellent isolated yields (75–95%). The products from 2,6-dichloropurine (**1a**) (entries 1 and 12) were obtained in higher yields compared with those from other 6-chloropurine analogues (**1b–j**) under the same reaction conditions. Moreover, when R_2 was cyanoethyl or allyl, the yields were higher compared with other substituted substrates. The results indicated that the

College of Chemistry and Environmental Science, Henan Normal University, Xinxiang, Henan, 453007, China. E-mail: quguir@sina.com, guohm518@hotmail.com; Fax: +86 373-3326336

† Electronic supplementary information (ESI) available: General; synthesis and characterization of compounds; references; NMR spectra. See DOI: 10.1039/b719429c
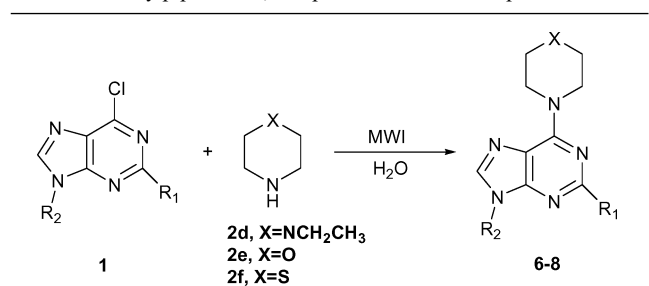
Table 1 Nucleophilic substitution reaction of 6-chloropurines derivatives with piperidine[a], pyrrolidine[b] or hexamethyleneamine[b]
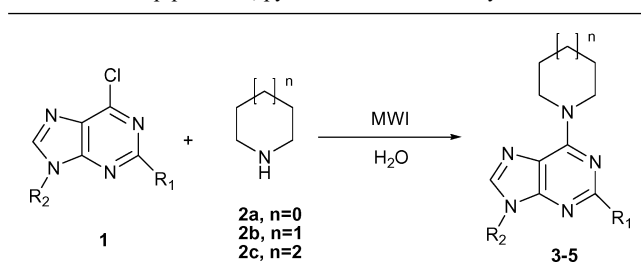
Entry	n	Product	R_1	R_2	Yield (%)[c]
1	1	**3a**	Cl	H	95
2	1	**3b**	H	Ribose	82
3	1	**3c**	Cl	Ribose	84
4	1	**3d**	NH_2	Ribose	78
5	1	**3e**	H	$-CH_2CH_2CN$	86
6	1	**3f**	Cl	$-CH_2CH_2CN$	88
7	1	**3g**	H	$-CH_2CH=CH_2$	84
8	1	**3h**	Cl	$-CH_2CH=CH_2$	86
9	1	**3i**	H	$-CH_2C_6H_5$	80
10	1	**3j**	Cl	$-CH_2C_6H_5$	83
11	0	**4a**	H	H	91
12	0	**4b**	Cl	H	93
13	0	**4c**	NH_2	H	90
14	0	**4d**	H	Ribose	79
15	0	**4e**	Cl	Ribose	81
16	0	**4f**	NH_2	Ribose	77
17	0	**4g**	Cl	$-CH_2CH=CH_2$	83
18	0	**4h**	Cl	$-CH_2CH_2CN$	84
19	0	**4i**	Cl	$-CH_2C_6H_5$	80
20	2	**5a**	H	H	NR[d]

[a] Reaction conditions: 2,6-dichloropurine derivatives (1 mmol), piperidine (4 mmol), H_2O (2 mL), MWI 400 W (100 °C). [b] Reaction conditions: 6-chloropurine derivatives (1 mmol), pyrrolidine (1.2 mmol), H_2O (2 mL), NaOH (2 mmol), MWI 400 W (100 °C). [c] Isolated yields based on nucleobases. [d] NR = no reaction.

Table 2 Nucleophilic substitution reaction of 6-chloropurine derivatives with 1-ethylpiperazine[a], morpholine[b] and thiomorpholine[b]

Entry	X	Product	R_1	R_2	Yield (%)[c]
1	NCH_2CH_3	**6a**	Cl	H	93
2	NCH_2CH_3	**6b**	H	H	91
3	NCH_2CH_3	**6c**	NH_2	H	90
4	NCH_2CH_3	**6d**	Cl	$-CH_2CH=CH_2$	82
5	NCH_2CH_3	**6e**	Cl	$-CH_2CH_2CN$	85
6	NCH_2CH_3	**6f**	Cl	$-CH_2C_6H_5$	78
7	O	**7a**	Cl	H	94
8	O	**7b**	H	Ribose	78
9	O	**7c**	NH_2	Ribose	76
10	O	**7d**	H	$-CH_2CH_2CN$	86
11	O	**7e**	Cl	$-CH_2CH_2CN$	83
12	O	**7f**	H	$-CH_2CH=CH_2$	82
13	O	**7g**	Cl	$-CH_2CH=CH_2$	84
14	O	**7h**	H	$-CH_2C_6H_5$	76
15	O	**7i**	Cl	$-CH_2C_6H_5$	78
16	O	**7j**	H	$-CH_2C_6H_4(o\text{-}Cl)$	73
17	S	**8a**	H	H	90
18	S	**8b**	Cl	H	92
19	S	**8c**	NH_2	H	89
20	S	**8d**	Cl	$-CH_2CH_2CN$	80
21	S	**8e**	Cl	$-CH_2CH=CH_2$	82
22	S	**8f**	Cl	$-CH_2C_6H_5$	77

[a] Reaction conditions: 2,6-dichloropurine derivatives (1 mmol), 1-ethylpiperazine (4 mmol), H_2O (2 mL), MWI 400 W (100 °C). [b] Reaction conditions: 2,6-dichloropurine derivatives (1 mmol), morpholine (1.2 mmol), H_2O (2 mL), NaOH (2 mmol), MWI 400 W (100 °C). [c] Isolated yields based on nucleobases.

kind of substitutents at N9 had impact on the reactions, which could be attributed to steric hindrance.

Intrigued by our above-described results, other cyclosecondary amines such as 1-ethylpiperazine, morpholine and thiomorpholine were chosen as the nucleophiles to probe whether the nucleophilic substitution reactions could be easily accessed. The results are shown in Table 2. As expected, these reactions also proceeded to give the corresponding 6-substituted purines in high yields. For example, 1-ethylpiperazine with 6-chloropurine proceeded smoothly to provide the desired product in the absence of base (entries 1–6). And treatment of morpholine (entries 7–16) and thiomorpholine (entries 17–22) with 6-chloropurine under the similar conditions as pyrrolidine successfully gave rise to the corresponding products. Substituting 4′-C with NCH_2CH_3, O, or S only resulted in slight variations in yield, indicating that no obvious substituent-effect existed. The variation in yields may be caused by the different solubility in water of those cyclosecondary amines. Better solubility gave corresponding higher yield. The influence of different substituent groups at C2 was also studied. The results indicated that those substitution groups had little impact on the yields of the products. When the chlorine atom was substituted by H or NH_2, relatively lower yields of the corresponding aminopurine were obtained after purification; this might be

ascribed to the electron-donating effects on C2 which could lead to a decrease of the yield.

In order to demonstrate the advantage of our method compared with the conventional heating method, the formation of **3a** was carried out in an oil bath under the same conditions as used with the microwave irradiation. It was shown the reaction afforded only 15% yield after 24 h. This clearly indicated that our method was superior to the conventional method.

In conclusion, we have developed a simple, facile and efficient method for the preparation of aminopurine and its analogues in neat water under microwave irradiation. This method has several advantages such as mild reaction conditions, ease of manipulation and short reaction times. Furthermore, most of the reactions involved are efficient, giving the desired compounds in higher purity and yield. The versatility of this methodology is suitable for library synthesis in drug discovery efforts.

Acknowledgements

Notes and references

1 (*a*) A. Brathe, L.-L. Gundersen, F. Rise, A. B. Eriksen, A. V. Vollsnes and L. Wang, *Tetrahedron*, 1999, **55**, 211; (*b*) A. J. Cocuzza, D. R. Chidester, S. Culp, L. Fitzgerald and P. Gilligan, *Bioorg. Med. Chem. Lett.*, 1999, **9**, 1063; (*c*) D. E. Verdugo, M. T. Cancilla, X. Ge, N. S. Gray, Y.-T. Chang, P. G. Schultz, M. Negishi, J. A. Leary and C. R. Bertozzi, *J. Med. Chem.*, 2001, **44**, 2683; (*d*) O. D. Perez, Y.-T. Chang, G. Rosania, D. Sutherlin and P. G. Schultz, *Chem. Biol.*, 2002, **9**, 475.
2 (*a*) C. Garcia-Echeverria, P. Taxler and D. B. Evans, *Med. Res. Rev.*, 2000, **20**, 28; (*b*) T. Schindler, W. Bornmann, P. Pellicena, W. T. Miller, B. Claerlson and J. Kuryan, *Science*, 2000, **289**, 1938.
3 A. Lanver and H.-G. Schmalz, *Molecules*, 2005, **10**, 508.
4 G. B. Elion, Burgi and G. H. Hitchings, *J. Am. Chem. Soc.*, 1952, **74**, 411.
5 (*a*) N. S. Girgis and E. B. Pedersen, *Synthesis*, 1982, **6**, 480; (*b*) R. Fu, X. Xu, Q. Dang and X. Bai, *J. Org. chem.*, 2005, **70**, 10810.
6 T. Y. H. Wu, P. G. Schultz and S. Ding, *Org. Lett.*, 2003, **5**, 3587.
7 M. T. Fiorini and C. Abell, *Tetrahedron Lett.*, 1998, **39**, 1827.
8 C. Ran, Q. Dai and R. G. Harvey, *J. Org. Chem.*, 2005, **70**, 3724.
9 (*a*) S. Caddick, *Tetrahedron*, 1995, **51**, 10403; (*b*) S. Deshayes, M. Liagre, A. Loupy, J.-L. Luche and A. Petit, *Tetrahedron*, 1999, **55**, 10851; (*c*) P. Lidstrom, J. Tierney, B. Wathey and J. Westman, *Tetrahedron*, 2001, **57**, 9225; (*d*) A. Kirschning, H. Monenschein and R. Wittenberg, *Angew. Chem., Int. Ed.*, 2001, **40**, 650; (*e*) A. Loupy, *Microwaves in Organic Synthesis*, Wiley-VCH, Weinheim, 2002, p. 147; (*f*) L.-K. Huang, Y.-C. Cherng, Y.-R. Cheng, J.-P. Jang, Y.-L. Chao and Y.-J. Cherng, *Tetrahedron*, 2007, **63**, 5323.
10 (*a*) D. Dallinger and C. O. Kappe, *Chem. Rev.*, 2007, **107**, 2563; (*b*) G. W. Kabalka and A. R. Mereddy, *Tetrahedron Lett.*, 2006, **47**, 5171; (*c*) K. V. V. Krishna Mohan, N. Narender and S. J. Kulkarni, *Green Chem.*, 2006, **8**, 368; (*d*) T. Y. Wu, P. G. Schultz and S. Ding, *Org. Lett.*, 2003, **5**, 3587; (*e*) A. Burczyk, A. Loupy, D. Bogdal and A. Petit, *Tetrahedron*, 2005, **61**, 179; (*f*) C. O. Kappe, *Angew. Chem., Int. Ed.*, 2004, **43**, 6250; (*g*) G.-R. Qu, S.-H. Han, Z.-G. Zhang, M.-W. Geng and F. Xue, *Can. J. Chem.*, 2006, **84**, 819.
11 (*a*) K. Surendra, N. S. Krishnaveni, R. Sridhar and K. R. Rao, *J. Org. Chem.*, 2006, **71**, 5819; (*b*) C.-J. Li, *Chem. Rev.*, 2005, **105**, 3095; (*c*) G.-R. Qu, Z.-G. Zhang, M.-W. Geng, R. Xia, L. Zhao and H.-M. Guo, *Synlett*, 2007, **5**, 721; (*d*) C. M. Kormos and N. E. Leadbeater, *Synlett*, 2006, **11**, 1663; (*e*) M. Eissen, J. O. Metzger, E. Schmidt and U. Schneidewind, *Angew. Chem., Int. Ed.*, 2002, **41**, 414; (*f*) S. Paul, M. Gupta, P. P. Singh, R. Gupta and A. Loupy, *Synth. Commun.*, 2005, **35**, 325.

Room-temperature self-curing ene reactions involving soybean oil†

Atanu Biswas,*[a] Brajendra K. Sharma,[b,c] J. L. Willett,[a] S. Z. Erhan[b] and H. N. Cheng*[d]

A mixture of soybean oil with diethyl azodicarboxylate exhibits a remarkable self-curing and thickening behavior at room temperature due to the occurrence of crosslinking ene reactions. The kinetics and the reaction mechanisms have been studied with the help of model compounds, ^{1}H and ^{13}C NMR, and size exclusion chromatography. The reactions are found to be most facile with linolenate, followed by linoleate, and least with oleate. The product from this reaction may be used as an environmentally friendly self-curing agent in appropriate applications.

Introduction

Self-curing, thickening, and self-gelling properties are often desirable in commercial applications.[1] A number of commercial and medical products can use such properties, *e.g.*, caulking agents, cements, coatings, adhesives, and biomaterials. For many current applications, these materials are acrylics, urethanes, poly(vinyl alcohol), cellulosic derivatives, or thermosetting polymers.

As part of our work involving green chemistry, we seek to use natural bio-based materials and extend their applications. Soybean oil (SBO) is one of our favorite raw materials because it is cheap, renewable, and environmentally friendly.[2] Soybean oil contains triacylglycerols with a mixture of fatty acids moieties (typically 51% linoleic acid, 25% oleic acid, 10% palmitic acid, 7% linolenic acid, and 5% stearic acid). The unsaturation in the soybean oil provides a handle to carry out further reactions. Previously we have incorporated nitrogen into the triglyceride structure through several reactions. These include the reactions of soybean oil with amines[3] and diethyl azodicarboxylate (DEAD) at high temperatures,[4] their hydrolysis products,[5] and enzymatic reactions to produce specific derivatives.[6]

In this work we discovered that soybean oil and DEAD at room temperature can undergo a self-curing and thickening reaction. The modified soybean oil first forms oligomers and (with time) eventually polymerizes. This reaction permits soybean oil to be used as the raw material for a variety of novel products that require curing, thickening, or adhesive properties.

[a]Plant Polymers Research Unit, National Center for Agricultural Utilization Research, USDA/Agricultural Research Services, 1815 N. University Street, Peoria, IL, 61604, USA
[b]Food and Industrial Oil Research Unit, National Center for Agricultural Utilization Research, USDA/Agricultural Research Services, 1815 N. University Street, Peoria, IL, 61604, USA
[c]Department of Chemical Engineering, Pennsylvania State University, University Park, PA, 16802, USA
[d]Hercules Incorporated Research Center, 500 Hercules Road, Wilmington, DE, 19808-1599, USA
† The use of trade, firm, or corporation names in this publication is for the information and convenience of the reader. Such use does not constitute an official endorsement or approval by the United States Department of Agriculture or the Agricultural Research Service of any product or service to the exclusion of others that may be suitable.

Experimental

Materials

Alkali refined soybean oil was obtained from ADM Packaged Oils, Decatur, IL and was used as received without further purification steps. All other materials were acquired from Aldrich Chemical Company.

Reaction of soybean oil with DEAD

A mixture of soybean oil 5.32 g. (6.2 mmol), 3.1 g. of DEAD (18.6 mmol, 3 molar equivalents) were mixed together and allowed to sit on the lab bench. They were sampled over two weeks. The final soybean oil/DEAD adduct was obtained as a very viscous, honey-colored oil.

NMR spectroscopy

All ^{1}H and ^{13}C NMR spectra were recorded quantitatively with a Bruker ARX-500 spectrometer (Bruker, Rheinstetten, Germany) at a frequency of 500 MHz (^{1}H) and 125 MHz (^{13}C) and a 5 mm dual probe. The sample solutions were prepared in deuterochloroform (CDCl$_3$, 99.8% D, Cambridge Isotope Laboratories, Inc., Andover, MA). Standard operating conditions were used with 30° pulse angle, 3 s between pulses, and ^{1}H decoupling.

Brookfield viscosity

The dynamic viscosity at 40 °C was measured on a Brookfield (Middleboro, MA), DV-III programmable rheometer controlled by Rheocalc 2.4 software. It was equipped with a CP-40 spindle and programmed to vary the sheer rate from 0.5–10 RPM. The viscosity was determined by the software using a Bingham model. In this model, the viscosity is found from the slope of a shear rate *vs.* shear stress relationship. An experiment was also performed varying the shear stress instead of the shear rate, and the results were identical. The temperature of the system was controlled by a Brookfield (Middleboro, MA) TC-602 water bath.

Size exclusion chromatography (SEC)

Molecular weights were measured on a PL-GPC 120 high temperature chromatograph (Polymer Laboratories, Amherst, MA) equipped with an autosampler and a built-in differential refractometer detector. Two PL gel 3 µm mixed E columns (300 mm × 7.5 mm, Polymer Laboratories) were used in series to resolve the samples. The injection volume was 100 µL. The samples were eluted using 1.00 mL min⁻¹ flow rate of THF at 40 °C. The SEC was calibrated using a mixture of linear polystyrene standards (M_n 1700, 2450, 5050, 7000, 9200, and 10 665) obtained from Polymer Laboratories (Amherst, MA), and methyl oleate (M_n 296.5), methyl linoleate (M_n 294.5), monoolein (M_n 356.5), diolein (M_n 620.9), and triolein (M_n 885.4) obtained from Aldrich Chemical Company (Milwaukee, WI).

Discussion and results

In a systematic investigation of this room-temperature reaction system, we first undertook the studies of model systems and their reactions with diethyl azodicarboxylate (DEAD). These studies provided useful information on the reaction behavior. We then proceeded to study the room temperature reaction of DEAD with soybean oil under similar reaction conditions.

1. Model reaction systems

As the first model system, we take a mixture of methyl linoleate and methyl linolenate (56 : 43 molar ratio). DEAD is added at a molar ratio of 0.88 : 1.0, relative to the fatty esters present. The reaction is monitored on the daily basis by both ¹H and ¹³C NMR. The ¹H NMR spectra for the first three days are shown in Fig. 1.

Most of the peaks for linoleate (L) and linolenate (N) are overlapped except for the end methyls (0.885 ppm for L, and 0.970 ppm for N), and the methylenes between the double bonds (2.752 ppm for L, and 2.801 ppm for N). Soon after the addition of DEAD to the two methyl esters, only a small amount of reaction occurs as evidenced by the small reacted DEAD peak at 4.15 ppm (Fig. 1, after 15 minutes). After one day, however, most of L and N have reacted with DEAD. As in high-temperature reactions,[4] linoleate gives the conjugated products (L′); two conjugated products are possible, depending on the point of addition (C9 or C13). For linolenate, we see a new peak at 2.886 ppm that corresponds to the half-reacted product of N (denoted as N′ in the scheme below). This half-reacted product can react further to form other products (N″) if more DEAD is added.
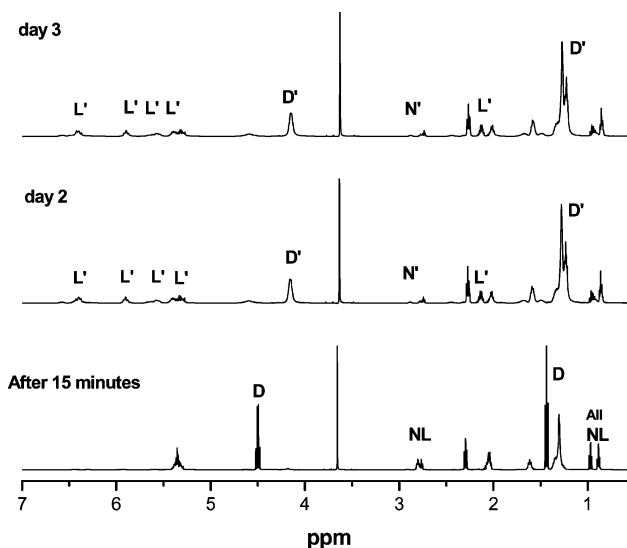
Fig. 1 ¹H NMR spectra of the reaction products between methyl linoleate and methyl linolenate with DEAD at room temperature. D = unreacted DEAD, D′ = reacted DEAD, L = linoleate, N = linolenate, and N′ = half-reacted N.

It is important to note that on day 2 all DEAD has reacted whereas some linoleate and linolenate are still unreacted. Thus, there is no significant change in the spectrum in subsequent days. After day 3 the spectrum stays essentially the same, except for line-broadening, corresponding to increasing formation of dimers, tetramers, and oligomers. Quantitative estimates of the various species are obtained from ¹H NMR and given in Table 1. In Scheme 1 D denotes DEAD, and D′ denotes DEAD residue.

The ¹³C NMR spectra for L + N mixture give corroborative information (Fig. 2). Basically all the DEAD has reacted fully by the second day. Because there is a deficit of DEAD relative to the amounts of olefins present, there are still some linoleate and linolenate unreacted. It is useful to note that linolenate reacts faster than linoleate.
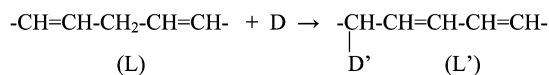
As the second model system, we use the room-temperature reaction of methyl linolenate with DEAD. In this case, a surplus of DEAD is used (molar ratio of methyl linolenate *versus* DEAD = 1 : 4), and the reaction is carried out for 6 days. As expected, the reaction proceeds very fast. Because three double bonds are present, the reaction can occur in different ways, generating a large number of isomers. As a result, the ¹³C NMR spectrum is smeared in the olefin region with no distinct peaks on day 1 (Fig. 3, day 1). On day 2 or after, the only distinct peaks in the ¹³C spectrum (Fig. 3, day 2) are C18 (14.2 ppm), C2

Table 1 Estimates[a] of major species in the room temperature reaction of L and N with DEAD

Time	L	N	L′	N′	N″	Unreacted DEAD
Time 0	1.0	1.0	0	0	0	1.0
Day 1 (within 30 min)	0.95	0.92	0.05	0.06	0.02	0.88
Day 2	0.15	0.04	0.85	0.04	0.92	0
Day 3	0.15	0.04	0.85	0.04	0.92	0

[a] L and N are estimated from methyls (0.9–1.0 ppm) and methylenes (~2.8 ppm). L′ and N′ are estimated by the decrease in the 2.8 ppm peaks. N″ is obtained by difference (N″=N–N′).
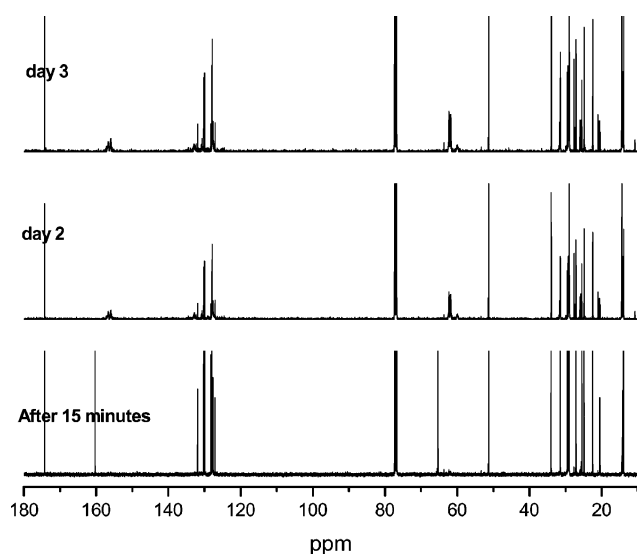
methyl linoleate:

-CH=CH-CH$_2$-CH=CH- + D → -CH-CH=CH-CH=CH-
            (L) |
                                              D'   (L')

methyl linolenate:

-CH=CH-CH$_2$-CH=CH-CH$_2$-CH=CH- + D → -CH-CH=CH-CH=CH-CH$_2$-CH=CH-
            (N) |
                                                          D'   (N')

                                                          ↓

                    -CH-CH=CH-CH=CH-CH=CH-CH-
                       | |
                       D'   D'

                    (an example of N'' structures)
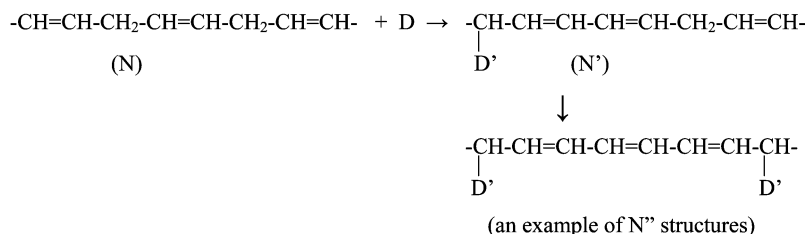
Scheme 1

Fig. 2 ^{13}C NMR spectra of the reaction products between methyl linoleate and methyl linolenate with DEAD at room temperature.

(34.0 ppm), C3 (25.0 ppm), C4 (29.5 ppm), C5 (29.0 ppm), and C6 (29.0 ppm).

Likewise, the ^{1}H spectra of the linolenate–DEAD reaction give a complex picture (Fig. 4). The olefin region shows an unmistakable pattern for conjugated double bonds (at 5.42, 5.65, 5.91, and 6.20 ppm); these are the same peaks found for linoleate-DEAD reactions.[4] However, other peaks are also present, and the peaks are broad. After 2 days of reaction (Fig. 4, day 2), the more distinct peaks are due to protons far away from the site of reactions, *e.g.*, methyl (0.932 ppm), H2 (2.28 ppm), H3 (1.59 ppm), H4-H6 (1.24 ppm), and methoxy (3.64 ppm).

2.   Reactions with soybean oil

In a typical SBO–DEAD reaction, 3 mol of DEAD are reacted with 1 mol of soybean oil. Over time, the viscosity of the mixture increases. After 14 days, the mixture is so thick that we can flip the flask over and none of the material can flow downward (Fig. 5). Quantitative Brookfield viscosity data (obtained without stirring) are given in Table 2 and also shown in Fig. 6.

A better understanding of the SBO–DEAD reaction can be obtained *via* the SEC analysis of the reaction products. The
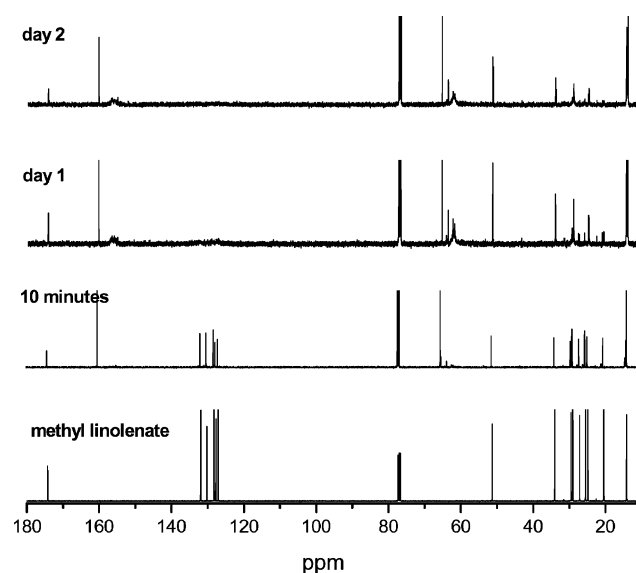
Fig. 3 ^{13}C NMR spectra of the reaction products of methyl linolenate with DEAD at room temperature.
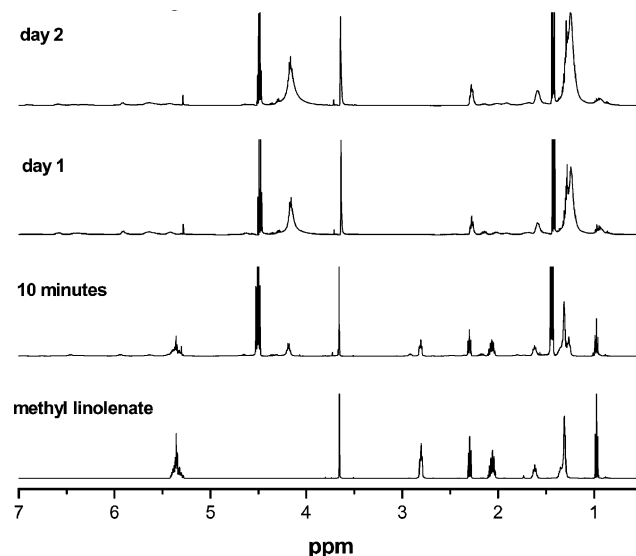
Fig. 4 ^{1}H NMR spectra of the reaction products of methyl linolenate with DEAD at room temperature.

Table 2 Brookfield viscosity data for room temperature reaction of SBO–DEAD (1 : 3 molar ratio)

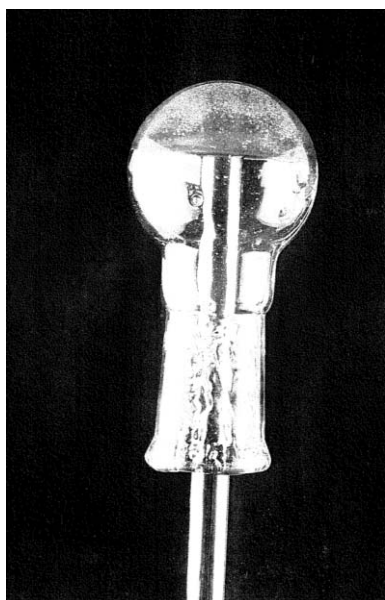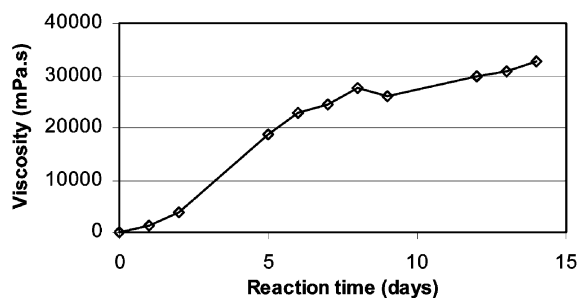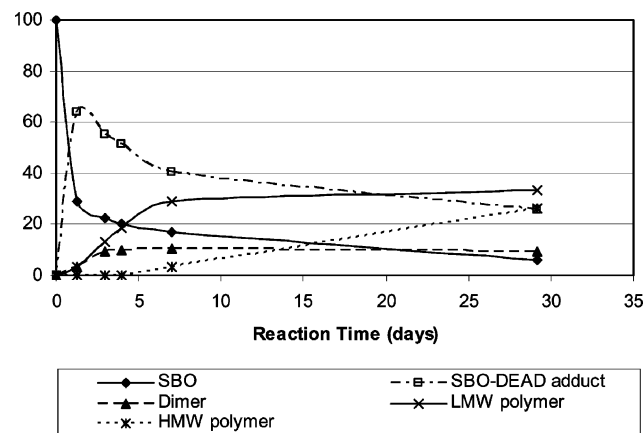| Hours	Days	Viscosity/mPa s
0	0	97
24	1	1 318
48	2	3 809
120	5	18 741
144	6	22 927
168	7	24 565
192	8	27 590
216	9	26 063
288	12	29 743
312	13	30 703
336	14	32 819

Fig. 6 Plot of Brookfield viscosity for the room temperature SBO–DEAD mixture *versus* time.

Fig. 7 SBO–DEAD reaction progress in terms of wt% distribution with time.

Fig. 5 Photograph of a mixture of soybean oil and DEAD at room temperature after 14 days.

data are shown in Table 3 and plotted in Fig. 7. (It may be noted that SBO, with a formula weight of 850 gives an apparent molecular weight of 1076 with the current calibration curve.) As expected, the SBO concentration decreases steadily with time. The SBO–DEAD adduct appears, reaching a maximum on day 1, and then slowly decreasing. Starting on day 3, the dimer of the SBO–DEAD adduct is found and stays relatively unchanged in concentration. At about the same time, SBO oligomerization becomes increasingly significant to generate low-molecular-weight polymers. The high-molecular-

weight SBO polymer appears more slowly. After 29 days about 26% of the reaction mixture contains high-molecular-weight SBO polymer. The M_n for the SBO high-molecular-weight polymer is about 86 500 Da, corresponding to a degree of polymerization of about 80.

The kinetics of the self-curing reaction can be seen more graphically in Fig. 8. After 1.29 days of room temperature reaction, the SEC curve drifts to slightly higher molecular weights. After 4 days low-molecular-weight polymers are clearly seen (at 10–14 min). After 29 days a significant portion of the materials is high-molecular-weight polymer (at 9.0–10.5 min).

The ^{1}H NMR spectra for selected reaction times are given in Fig. 9. It should be noted that DEAD reacts somewhat slower in soybean oil than in methyl linoleate and linolenate. As before, linoleate and linolenate moieties react relatively quickly and disappear on day 2. Oleate, however, remains largely

Table 3 SEC data as a function of time for the SBO–DEAD room temperature reaction

Sample	Reaction time/days	SBO	SBO adduct	Dimer of SBO adduct	LMW polymer	HMW polymer
Max RT/min		*15.48*	*14.8*	*13.58*	*13.01*	*10.17*
Peak RT range/min		*15.33–16.74*	*14.00–15.34*	*13.2–14.0*	*10.47–13.23*	*9.80–10.44*
Apparent M_n		*1076*	*2196*	*4408*	*13 546*	*86 520*
SBO	0.0	100	—	—	—	—
79-2	1.3	29.2	63.9	3.3	3.5	0.0
79-4	3.0	22.3	55.2	9.5	12.9	0.0
79-5	4.0	20.0	51.3	10.0	18.6	0.0
79-6	7.0	16.8	40.4	10.4	29.1	3.4
79-x	29.1	6.2	25.5	9.1	33.1	26.1
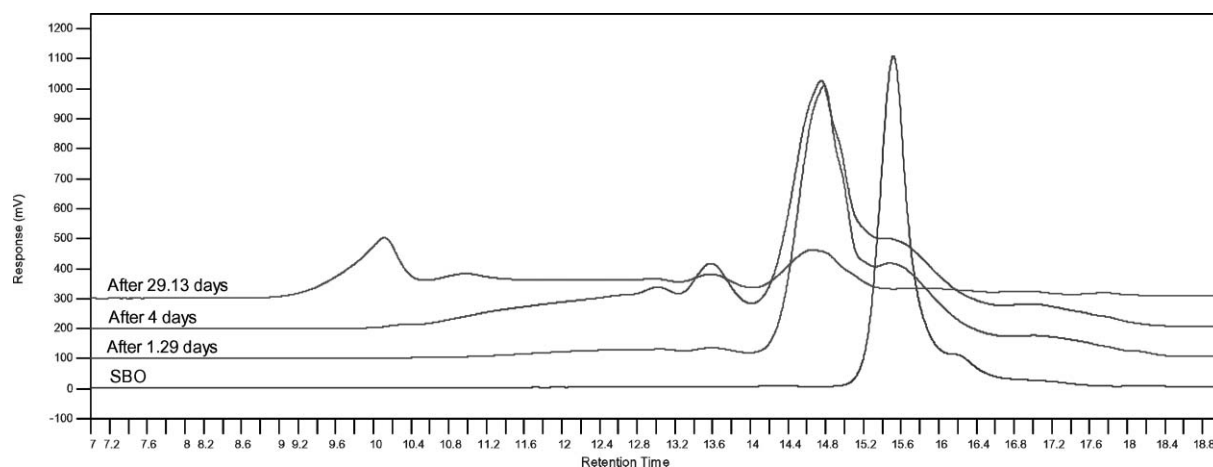
Fig. 8 SEC chromatograms of SBO and SBO–DEAD reaction products at different reaction times (1st from bottom = starting SBO, 2nd = after 1.29 days, 3rd = after 4 days, and 4th = after 29.13 days).
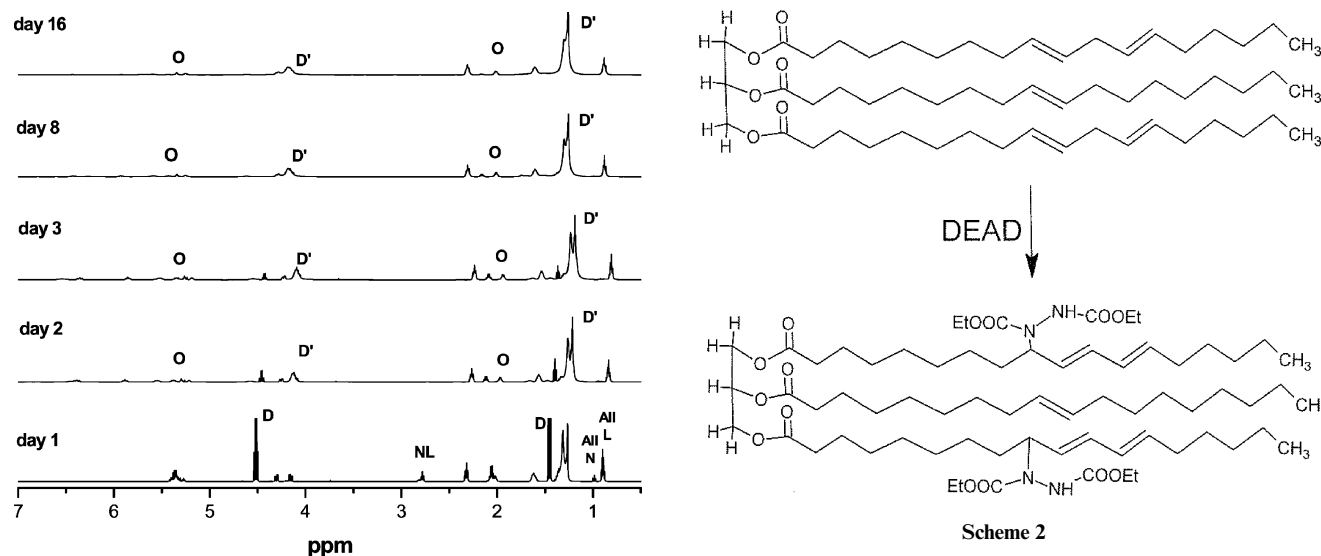
Fig. 9 ¹H NMR spectra of the reaction of soybean oil with DEAD at room temperature. D = unreacted DEAD, D′ = reacted DEAD, and O = oleate.


Scheme 2

unreacted. Thus the reactivity follows the following decreasing trend: linolenate > linoleate > oleate. Quantitative estimates of all major species are given in Table 4.

Note that 58% of linoleate and linolenate have been converted to the conjugated form on day 2 (Table 4, column 4). For illustration, see Scheme 2.

However, the amount of conjugated structures (L′ + N″) steadily decreases with time as soybean oil starts to form dimers

and oligomers. This is due to the Diels–Alder reaction of olefin and diene on the fatty acid moiety of SBO–aza-dicarboxylate ester, leading to self-condensation:
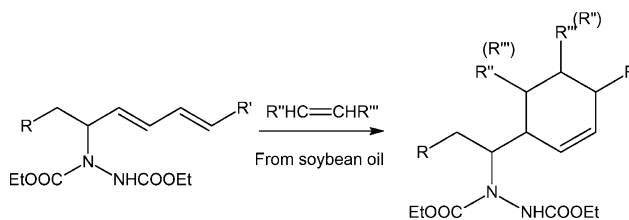
Table 4 Estimates of major species in the room temperature reaction of soybean oil with DEAD

Day	L	N	L′ + N″	Unreacted oleate	Unreacted DEAD	Reacted DEAD
1	1	1	0	0.21	2.7	0
2	0.05	0	0.58	0.21	0.75	2.0
3	0	0	0.54	0.21	0.40	2.3
4	0	0	0.44	0.21	0.22	2.5
5	0	0	0.44	0.21	trace	2.6
8	0	0	0.33	0.21	0	2.6
12	0	0	0.20	0.21	0	2.6

Some condensation of the diene with DEAD probably also takes place. The data in Table 4 clearly shows the decrease in olefin intensities with time. Thus, the combined use of NMR and SEC provides complementary information on this reaction.

The ^{13}C NMR spectrum of the reaction product (Fig. 10, day 1) gives the characteristic peaks for triglyceride (ester at 172.6 and 173.1 ppm, glycerol at 62.3 and 68.7 ppm), aza-carboxylate ester (156.5 ppm), diethyl (~62, 14.3 ppm). The detailed assignments have been given elsewhere.[4] It is important to note that after day 5 line-broadening starts to happen as higher molecular weight materials begin to build up. At day 16, most of the sharper features of the spectrum correspond to the unreacted oleate.
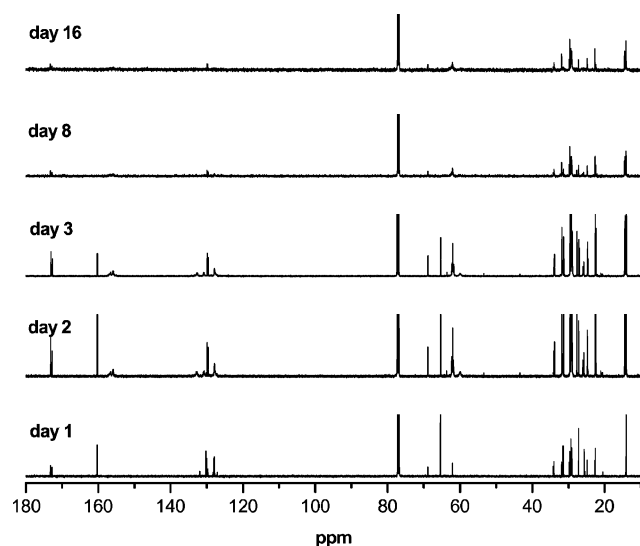
Fig. 10 ^{13}C NMR spectra of the reaction of soybean oil with DEAD at room temperature.

3. Applications

From the picture shown in Fig. 5, it is clear that this modified soybean oil can be an effective self-curing system. It is also evident that this reaction can be rendered more versatile through the formulation or suitable choice of different edible oils. For example, fish oil and linseed oil have a lot of unsaturation. Incorporation of some of these oils in the SBO–DEAD reaction will increase the degree of crosslinking and the viscosity of the final (cured) material. Since our data showed that oleate in the triglyceride oil is not substantially reacted with DEAD, olive oil can serve as a plasticizer in a formulation. Hydrogenated vegetable oils and animal fats do not react with DEAD, and they can be used as diluents in end-use formulations, *e.g.*, to vary the rate of curing, or to control the viscosity of the final material.

As soybean oil (and edible oils in general) are biodegradable and relatively cheap, this room temperature reaction may be useful in commercial applications. This is especially the case for biomaterials, where biocompatibility and toxicity of organic polymers are always of concern.

Conclusion

It is of interest that soybean oil can react with diethyl azodicarboxylate even at room temperature to form a crosslinked reaction product. The combined use of NMR, viscosity, and SEC permits a rather detailed understanding to be obtained for the reaction. The material obtained through this reaction is of interest because it is self-curing and thickening and may be an environmentally friendly alternative to organic self-curing, thickening, or adhesive systems.

Acknowledgements

References

1 For example (*a*) C. A. G. Arrais, M. Giannini, F. A. Rueggeberg and D. H. Pashley, *Oper. Dent.*, 2007, **32**, 37–44; (*b*) S.-C. Wang, P.-C. Chen, J.-T. Yeh and K.-N. Chen, *J. Appl. Polym. Sci.*, 2006, **102**, 4383–4393; (*c*) J. Lee, G. R. Yandek and T. Kyu, *Polymer*, 2005, **46**, 12511–12522; (*d*) S.-S. Hou and P.-L. Kuo, *Macromol. Chem. Phys.*, 1999, **200**, 2501–2507; (*e*) M. Yabuta, Y. Yukawa, Y. Nakao, Self-curing resin, *US Pat.*, 5 116 930, May 26, 1992.
2 For example (*a*) R. D. O'Brien, *Fats and Oils: Formulating and Processing for Applications*, CRC Press, Boca Raton, 2nd edn, 2003; (*b*) H. W. Lawson, *Food Oils and Fats: Technology, Utilization and Nutrition*, Chapman and Hall, New York, 1995.
3 A. Biswas, A. Adhvaryu, S. H. Gordon, S. Z. Erhan and J. L. Willett, *J. Agric. Food Chem.*, 2005, **53**, 9485.
4 A. Biswas, B. K. Sharma, J. L. Willett, K. Vermilion, S. Z. Erhan and H. N. Cheng, *Green Chem.*, 2006, **9**, 85.
5 A. Biswas, R. L. Shogren, J. L. Willett, S. Z. Erhan and H. N. Cheng, *Polym. Prepr.*, 2006, **47**(2), 259.
6 A. Biswas, R. L. Shogren, J. L. Willett, S. Z. Erhan and H. N. Cheng, *ACS Symp. Ser.*, 2008, accepted for publication.

Thermo-solvatochromism of chloro-nickel complexes in 1-hydroxyalkyl-3-methyl-imidazolium cation based ionic liquids

Xianjun Wei,[a] Linpo Yu,[a] Dihua Wang,[a] Xianbo Jin[a] and George Z. Chen*[a,b]

Sunlight can be directly absorbed by many coloured solids or liquids to re-generate heat but the temperature achievable is usually below 100 °C. Consequently, thermally responsive physical and/or chemical processes that can effectively utilise this almost free but low temperature solar heat are becoming increasingly important, considering the inevitable change in energy supply from fossil fuels to renewable sources in the near future. In this work, the thermochromic and solvatochromic behaviour of chloro-Ni(II) complexes was investigated by visual observation and vis-spectroscopy in 1-hydroxyalkyl-3-methylimidazolium (C_nOHmim^+, $n = 2$ or 3) based ionic liquids between room temperature and 85 °C. The thermochromism was a result of the tetrahedral complex, $NiCl_4^{2-}$ (blue, hot) being solvolysed into various octahedral complexes, *e.g.* $[NiCl_x(C_nOHmim^+-ClO_4^-)_y]^{2-x}$ ($x + y = 6$) or $[NiCl_x(C_nOHmim)_y]^{z+}-(ClO_4^-)_z$ ($z = 2 + y - x$) (yellow or green, cold) in the ionic liquids. The capability of the C_nOHmim^+ ligand to encourage the formation of octahedral chloro-Ni(II) complexes with a high number of chloride ligands could be attributed to the electrostatic attraction in the octahedral configurations. These new systems were found to be sensitive to water, but the lost thermo-solvatochromism was thermally recoverable. The enthalpy change, ΔH, of the tetrahedral–octahedral configuration conversion of the Ni(II) complexes in these ionic liquids was estimated to be in the range of 30–40 kJ mol^{-1} and the entropy change, ΔS (298K), 140–160 J mol^{-1} K^{-1}. These thermodynamic properties promise low energy thermochromic applications.

Introduction

Effective use of solar energy is a matter of immediate importance to the security of sustainable energy supply. While the majority of current research has been focused on developing photo-responsive systems, much less effort has been made for the utilisation of solar heat for chemical purposes. When focused, *via* for example a parabolic dish, the energy carried by sunlight can be converted to the so called high temperature (>500 °C) heat that is then exploited, for example, in electricity generation *via* a steam turbine. However, the more conveniently accessible solar heat is usually low temperature (<100 °C) in nature. Thus, developing new systems that can store and/or utilise the readily available low temperature solar heat would be very much desirable because large scale uses of fossil fuels will not be affordable very soon in terms of resource and climate changes.

Thermochromism is defined as the phenomenon of reversible colour changes of a substance or system in response to heating and cooling.[1] Many transition metal complexes can undergo thermochromic changes in certain solvents. Particularly, the

temperature range in which the colour changes occur falls well into that achievable *via* the solar heat. These changes often result from the tetrahedral–octahedral configuration changes assisted by the complex interacting with the solvent molecules (*i.e.* solvolysis), leading to the energy alteration of the *d-d* transition.[2-5] However, in all previously studied transition metal complexes in either an aqueous or an organic solution, the irreversible solvent evaporation upon heating is a predictable problem that can shorten the cycle life of the thermochromic systems or devices.

Unlike those conventional solvents of polar or non-polar molecules, most room temperature ionic liquids (ILs) have negligible vapour pressure because the ions, particularly the cations, are too large to enter the gas phase.[6-8] This intrinsic property of ILs has led to their use as a green solvent in many chemical processes, including organic synthesis,[9] coordination catalysis,[10] extraction and separation[11] and electrochemical energy storage systems.[12] For the same reason, ILs may also be the ideal candidate solvent for the stabilisation of metal complex based thermochromism. This thought formed the basis of this work. The key factor was identified to be the introduction of the necessary donor group, *e.g.* alcohol, to the cation of the IL so that it can participate in the solvolysis of the metal complex and hence enable the thermochromism.

Herein, we report the preparation and thermochromic characterisations of a number of novel reversible and stable thermochromic systems composed of $[bmim]_2NiCl_4$ dissolved in

[a] College of Chemistry and Molecular Sciences, Wuhan University, Wuhan, 430072, P. R. China. E-mail: mel@whu.edu.cn; Fax: (+86) 27-68756319
[b] School of Chemical and Environmental Engineering, University of Nottingham, University Park, Nottingham, UK NG7 2RD. E-mail: george.chen@nottingham.ac.uk; Fax: (+44) 115-9514115; Tel: (+44) 115-9514171

[C$_n$OHmim]BF$_4$ or [C$_n$OHmim]PF$_6$ (bmim: 1-butyl-3-methyl-imidazolium; C$_n$OHmim: 1-hydroxyalkyl-3-methylimidazolium, $n = 2$ or 3). It was found that, when dissolved in [bmim]BF$_4$, the [bmim]$_2$NiCl$_4$ exhibited the same characteristics on the vis-spectrum as that of the NiCl$_4^{2-}$ complex in the solid state (reflection spectrum)[13] or in a high Cl$^-$ concentration solution (absorption spectrum).[5,14,15] When the [bmim]$_2$NiCl$_4$ was dissolved in C$_n$OHmimBF$_4$ or C$_n$OHmimPF$_6$, thermochromism (yellow or green at room temperature; blue at elevated temperatures up to 85 °C) was confirmed by visual observation and spectral measurements. Particularly, the solvatochromic changes of the Ni(II) complex were studied by dissolving Ni(ClO$_4$)$_2$ in mixed [bmim]Cl and [C$_3$OHmim]ClO$_4$. Upon increasing the Cl/Ni molar ratio from 0 to >20, the gradual formation of different octahedral complex species, from [Ni(Sol)$_6$]$^{2+}$, [NiCl(Sol)$_5$]$^+$, [NiCl$_2$(Sol)$_4$], [NiCl$_3$(Sol)$_3$]$^-$ to [NiCl$_4$(Sol)$_2$]$^{2-}$ (Sol stands for solvent or the donor or ligand species in the solution, *e.g.* the [C$_3$OHmim]$^+$ cation or the ion-pair of C$_2$OHmim$^+$–BF$_4^-$), and finally to the tetrahedral NiCl$_4^{2-}$ species, could be attributed to the respective absorption features on the vis-spectra. These findings in the ILs differ from those in conventional solvents in which the high chloride and hence high energy octahedral configurations[5,16] such as [NiCl$_3$(Sol)$_3$]$^-$ and [NiCl$_4$(Sol)$_2$]$^{2-}$ are usually absent. In addition, the respective spectroscopic data were used in a simple and approximate model to derive the thermodynamic properties (equilibrium constants, enthalpy and entropy changes). Particularly, the enthalpy changes, ΔH, of the tetrahedral–octahedral configuration conversion were found to be significantly smaller than those in aqueous and alcohol solutions, promising low energy thermochromic applications at temperatures below 100 °C.

Experimental

Chemicals

Aqueous acids, HBF$_4$ (50 wt%, Acros Organics), HPF$_6$ (60 wt%, Acros) and HClO$_4$ (70 wt%, Sinopharm Chemical Reagent Co. Ltd) were all analytical reagents (A.R.) and used as received. NiCl$_2$·6H$_2$O (>98%, Sinopharm) was completely dehydrated to NiCl$_2$ in a muffle furnace (230–260 °C) for 3 h. Gravimetric analysis with diacetyldioxime found the Ni content in the dehydrated sample to be 44.70 wt% (theoretical value: 45.27 wt%). Anhydrous Ni(ClO$_4$)$_2$ was prepared by reacting NiCO$_3$·2Ni(OH)$_2$·4H$_2$O (Ni content: 44 wt%, Sinopharm) with HClO$_4$, followed by re-crystallisation and drying under vacuum at 95 °C. 2-chloro-1-ethanol (>99%, Acros) and 3-chloro-*n*-propanol (98%, Acros) were purified by treating with K$_2$CO$_3$ (≥99%, Sinopharm), dried over anhydrous Na$_2$CO$_3$ (≥99.8%, Sinopharm) and distilled. *N*-methylimidazole (99%, Acros) was treated with KOH (≥86%, Sinopharm) and distilled. In all distillation experiments, only the middle fraction was collected for use in this work.

### [bmim]Cl (1-butyl-3-methylimidazolium chloride)

A 250 ml three-neck round-bottom flask was charged with freshly distilled *N*-methylimidazole (41.5 g, 0.5 mol) and 1-chloro-*n*-butane (74.0 g, 0.75 mol). The solution was stirred and heated under reflux for 72 h at 75–80 °C. A yellow waxy

solid (77.0 g) was obtained.[17] The solid was recrystallised from dichloroethane to yield a white solid (55.0 g) which was further dried under vacuum at 70 °C.

^{1}H NMR (300 MHz, 25 °C, CD$_3$OD) δ: 0.98 (t, 3H, $^3J_{HH} = 7.5$ Hz), 1.38 (m, 2H), 1.85 (m, 2H), 3.94 (s, 3H), 4.23 (t, 2H, $^3J_{HH} = 7.2$ Hz), 7.59 (s, 1H), 7.65 (s, 1H), 8.99 (s, 1H).

[HO(CH$_2$)$_n$mim]Cl ($n = 2, 3$)

(In later text, HO(CH$_2$)$_n$ is simplified as C$_n$OH.) Fig. 1 shows schematically the synthesis reactions. The procedure was as follows. 2-chloro-1-ethanol (67 ml, 0.99 mol) or 3-chloro-1-propanol (84 ml, 0.99 mol), *N*-methylimidazole (72 ml, 0.90 mol) and acetic ether (40 ml) were added to a three-neck round-bottom flask (250 ml) in order. The mixture was stirred and heated at 75–85 °C under reflux for 72 h. The volatile matters were removed from the resulting solution under reduced pressure, giving rise to a yellow crystal ([C$_2$OHmim]Cl, 134.0 g or [C$_3$OHmim]Cl, 141.0 g) which was re-crystallised 4 times from dry ethanol. The resulting white crystal was dried under vacuum at 70 °C, and then stored in a dry glove-box before use.
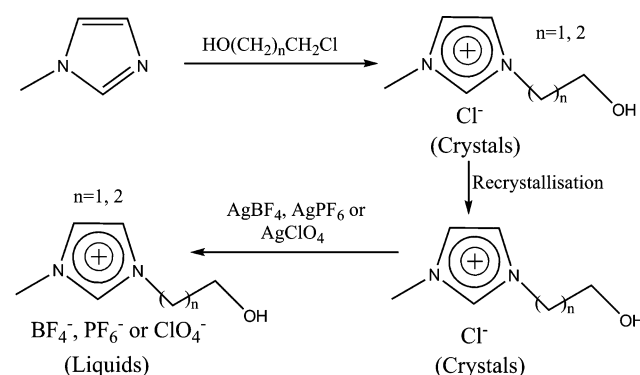
Fig. 1 Scheme of synthesis of 1-hydroxyalkyl-3-methylimidazolium based ionic liquids.

[C$_2$OHmim]Cl[18]. ^{1}H NMR (300 MHz, 25 °C, D$_2$O) δ: 3.77 (s, 3H), 3.79 (d, 2H, $^3J_{HH} = 4.2$ Hz), 4.18 (t, 2H, $^3J_{HH} = 5.4$ Hz), 4.64 (s, 1H), 7.32 (s, 1H), 7.36 (s, 1H), 8.62 (s, 1H).

[C$_3$OHmim]Cl. ^{1}H NMR (300 MHz, 25 °C, D$_2$O) δ: 1.97 (m, 2H), 3.49 (t, 2H, $^3J_{HH} = 6.6$ Hz), 3.76 (s, 3H), 4.17 (t, 2H, $^3J_{HH} = 7.2$ Hz), 4.65 (s, 1H), 7.31 (s, 1H), 7.36 (s, 1H), 8.61 (s, 1H).

[bmim]BF$_4$

The synthesis followed the procedure described in the literature.[17] The resulting product is a transparent and colourless liquid. ^{1}H NMR (300 MHz, 25 °C, CDCl$_3$) δ: 0.95 (t, 3H, $^3J_{HH} = 7.2$ Hz), 1.37 (m, 2H), 1.86 (m, 2H), 3.94 (s, 3H), 4.23 (t, 2H, $^3J_{HH} = 7.2$ Hz), 7.59 (s, 1H), 7.65 (s, 1H), 8.99 (s, 1H).

[C$_n$OHmim]BF$_4$ ($n = 2, 3$)[18–20]

Ag$_2$O (23.2 g, 0.1 mol) and HBF$_4$ (38.4 g, 50 wt %, 0.2 mol) were placed in a 400 ml beaker containing water (200 ml) and stirred. Then, [C$_2$OHmim]Cl (32.5 g) or [C$_3$OHmim]Cl (35.5 g) was added to the beaker. The reaction mixture was stirred

at room temperature for 4 h. The AgCl precipitate from the reaction was filtered. The filtrate was titrated drop by drop with the aqueous solution of either $AgBF_4$ or $[C_2OHmim]Cl$ or $[C_3OHmim]Cl$ until Ag^+ or Cl^- was not detected by the NaCl or $AgNO_3$ aqueous solution. The precipitate was filtered again. Water was evaporated from the filtrate with the rotary evaporator under reduced pressure. The remainder was dissolved in acetone (200 ml). The mixture was decoloured using activated carbon, and then heated to evaporate acetone. A transparent and colourless liquid was obtained and dried under vacuum at 70 °C.

$[C_2OHmim]BF_4$. ^1H NMR (300 MHz, 25 °C, CD_3OD) δ: 3.86 (d, 2H, $^3J_{HH}$ = 5.4 Hz), 3.92 (d, 3H), 4.28 (t, 2H, $^3J_{HH}$ = 5.1 Hz), 4.66 (s, 1H), 7.52 (s, 1H), 7.57 (s, 1H), 8.76 (s, 1H).

$[C_3OHmim]BF_4$. ^1H NMR (300 MHz, 25 °C, CD_3OD) δ: 2.07 (m, 2H), 3.59 (t, 2H, $^3J_{HH}$ = 6.6 Hz), 3.91(s, 3H), 4.31(t, 2H, $^3J_{HH}$ = 7.5 Hz), 4.53 (s, 1H), 7.52 (s, 1H), 7.57 (s, 1H), 8.73 (s, 1H).

$[C_3OHmim]PF_6$ and $[C_3OHmim]ClO_4$

The synthesis of $[C_3OHmim]PF_6$ and $[C_3OHmim]ClO_4$ was similar to that of $[C_3OHmim]BF_4$.

$[C_3OHmim]PF_6$. ^1H NMR (300 MHz, 25 °C, D_2O) δ: 1.93 (m, 2H), 3.45 (t, 2H, $^3J_{HH}$ = 6.6 Hz), 3.71 (s, 3H), 4.11 (t, 2H, $^3J_{HH}$ = 7.5 Hz), 4.64 (s, 1H), 7.25 (s, 1H), 7.29 (s, 1H), 8.50 (s, 1H).

$[C_3OHmim]ClO_4$. ^1H NMR (300 MHz, 25 °C, D_2O) δ: 2.00 (m, 2H), 3.52 (t, 2H, $^3J_{HH}$ = 6.0), 3.79 (s, 3H), 4.18 (t, 2H, $^3J_{HH}$ = 7.5), 4.65 (s, 1H), 7.32 (s, 1H), 7.37 (s, 1H).

$[bmim]_2NiCl_4$

Anhydrous $NiCl_2$ (3.244 g), $[bmim]Cl$ (8.747 g) and anhydrous ethanol (200 ml) were added into a 250 ml three-neck round-bottom flask with a reflux condenser. The temperature of the mixture was kept near its boiling point for 12 h until it became a transparent liquid. Ethanol was evaporated, and the remainder was dried under vacuum at 70 °C for 72 h. A blue crystal (11.6 g) was obtained. The Ni content was found to be 11.98 wt% which was close to the theoretical value of 12.24 wt%.

Vis-spectroscopy

Vis-spectroscopic measurements were made on a Cary 5000 UV-Vis-NIR Spectrophotometer (Varian Australia Pty, Ltd) over the wavelength range of 350–800 nm. A super-thermostat (Shanghai Cany Precision Instrument Co., Ltd) was employed to circulate water of a given temperature to the water-jacket of the quartz cell with a 2 mm light path. The water circulation was continued for at least 10 min and the temperature in the quartz cell was calibrated to ±0.05 °C with a thermometer inserted in the sample solution. The quartz cell was sealed using a clear balloon. The temperature was changed from ambient to 85 °C. The sample solutions were prepared in a dry glove-box. The total molar concentration of Ni(II) in the sample solution was calculated from total mass of $[bmim]_2NiCl_4$ (<4 wt%) in the IL, and the volume of the IL derived from the density of the IL at the given temperature (see below and Table 1). Here, the volume change of adding the small amount of $[bmim]_2NiCl_4$ into the IL was regarded to be negligible.

Density

The IL density was measured in a dry glove-box using a 5 ml picnometer with pure water as the reference.[21] The liquid temperature in the picnometer was controlled using a water jacket connected to the super-thermostat. Temperature was calibrated using a thermometer in the same liquid in a separate bottle of similar volume and shape to the picnometer placed in the same water jacket. The density was read after stabilising the temperature for at least 30 min.

Results and discussion

Hydroxyalkylised imidazolium cation based ionic liquids

It should be pointed out that the synthesis of $[C_nOHmim]X$ (X = BF_4^-, PF_6^-, $CF_3CO_2^-$) has been previously reported.[18–20] In our work, however, as shown in Fig. 1, the intermediate $[C_nOHmim]Cl$ was better purified by re-crystallisation and the removal of Cl^- ions from the respective ILs was more complete *via* AgCl precipitation. Impurities in the ILs, particularly the Cl^- ions, are influential to the thermochromic behaviour of the chloro-nickel complexes.

There is a special concern over the greenness of ILs containing fluorinated anions, although ILs have in general much greater physical and chemical stability than conventional organic solvents, and are commonly regarded as green media for research and practical applications.[22] In such evaluations, two factors should be considered. First, compounded fluorine is in most cases much lower in chemical and biochemical reactivity than the free fluoride ion, F^-. Second, in research, BF_4^- and PF_6^-

Table 1 Relationship between the density (ρ) of ILs and temperature (T) (from 25 °C to 85 °C). ρ (g ml^{-1}) = $a + bT + cT^2$

ILs	a	$b \times 10^3$	$c \times 10^6$	M (molar mass)	V_m/ml[a]	
					30 °C	70 °C
$[C_2OHmim]BF_4$	1.40	−1.67	9.14	214.08	157.23	160.81
$[C_2OHmim]ClO_4$	1.45	−1.43	6.90	226.73	160.17	163.59
$[C_2OHmim]PF_6$	1.58	−1.26	4.48	272.25	176.63	180.43
$[C_3OHmim]BF_4$	1.34	−1.34	6.11	228.11	175.35	179.38
$[C_3OHmim]PF_6$	1.53	−1.58	7.35	286.28	192.80	197.30
$[bmim]BF_4$	1.22	−1.14	4.18	226.13	190.56	195.31

[a] V_m (molar volume) = M (molar mass)/ρ

are often selected for experimental convenience and scientific simplicity. In this work, these two anions were used for demonstration purposes, but other stable and fluorine free anions, such as the ClO_4^- ion used in this work, can also in principle be associated to the C_nOHmim^+ ion to form the ILs and offer similar effects on the chloro-nickel complexes.

Relationship between IL density and temperature

The relationship between the IL density and the temperature (T, in °C) was found to accord with the following second-order polynomial equation, and the values of the coefficients are listed in Table 1.

$$\rho \ (g\ ml^{-1}) = a + bT + cT^2 \tag{1}$$

Because of the relative high viscosity of the IL at low temperatures, direct volume measurement was inaccurate. Thus, the ρ value as calculated according to eqn (1) was used to determine the volume of the IL at a given temperature. Such obtained volume was used to convert the mass concentration (wt%) to the molar concentration of $[bmim]_2NiCl_4$ dissolved in the IL. In the conversion, it was assumed that the change in the IL's molar volume was negligible upon dissolution of the small amount of $[bmim]_2NiCl_4$ (<4 wt%).

### Thermochromic behaviour of $[bmim]_2NiCl_4$ in different ILs

In this work, $[bmim]_2NiCl_4$ exhibited thermochromic variations in any of the tested $[C_nOHmim]X$ (X = BF_4^-, PF_6^-, ClO_4^-). Fig. 2a shows the absorption spectra of $[bmim]_2NiCl_4$ in $[C_3OHmim]BF_4$ at various temperatures. The spectra exhibited two absorption bands, I and II. Band I has two peaks of similar intensity at 705 nm and 656 nm, and a shoulder at 610 nm. These absorptions agree with the blue-coloured $NiCl_4^{2-}$ complex in the regular tetrahedral symmetry with the transition of $^3T_1(F) \rightarrow {}^3T_1(P)$. Band II is represented by a smaller absorption peak at about 445 nm as expected from the yellow or green coloured octahedral species which are capable of the transition of $^3A_{2g}(F) \rightarrow {}^3A_{1g}(P)$. The above analysis is in agreement with the literature.[4]

It is worth mentioning that in the example shown in Fig. 2, the octahedral complex may have a general formula of any of the following.

(a) $[NiCl_x(C_3OHmim)_y]^{2+y-x}$,
(b) $[NiCl_x(C_3OHmim^+–BF_4^-)_y]^{2-x}$ ($x + y = 6$), or even
(c) $[NiCl_x(C_3OHmim)_y]^{z+}–(BF_4^-)_z$ ($z = 2 + y - x$).

It is thought that expression (a) might be electrostatically unstable for the chloride-free or low chloride octahedral complexes, e.g. $[Ni(C_3OHmim)_6]^{8+}$, but expression (b) could be too large in volume to be appropriate if the BF_4^- ions were included in or associated with the complex solely because of electrostatic interactions. Expression (c) presents a compromise between (a) and (b) by considering the BF_4^- ions as the pairing ions in an ion-pair (or ion-cluster), but requires further experimental evidence. While more discussion will be given later on the formula of the octahedral complexes, for the convenience of discussion, we use $[NiCl_x(C_3OHmim^+–BF_4^-)_y]^{2-x}$ or a similar formula to represent the octahedral complex species in this paper.

Clearly, Fig. 2a shows that with increasing temperature, the absorption in band I grows in intensity at the expense of that
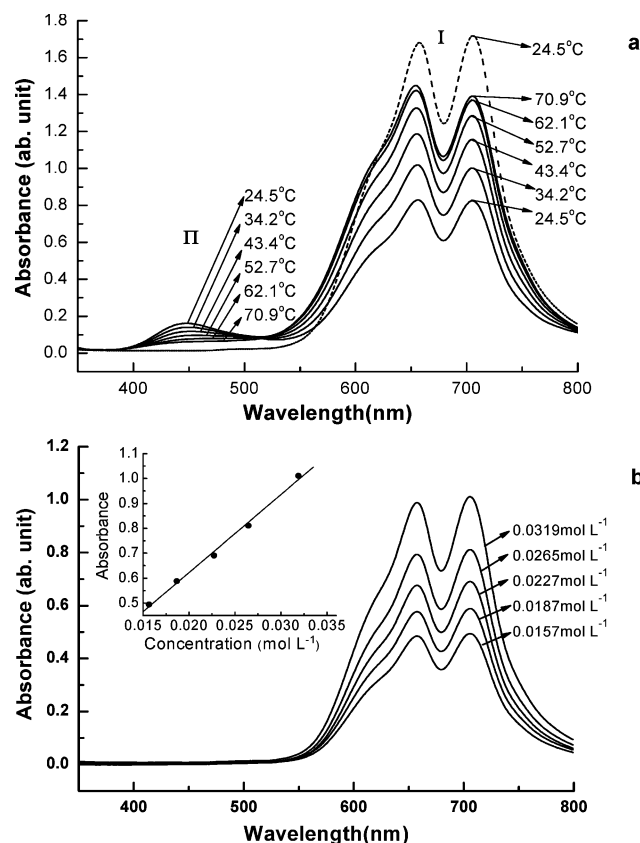
Fig. 2 Vis-spectra of $[bmim]_2NiCl_4$ (a) in $[C_3OHmim]BF_4$ at various temperatures as indicated ($C_{[bmim]_2NiCl_4}$ = 0.0640 mol L^{-1}), and (b) in $[bmim]BF_4$ at different concentrations as indicated (T = 35.0 °C). Note that the spectrum of $[bmim]_2NiCl_4$ (0.0543 mol L^{-1}) in $[bmim]BF_4$ at 24.5 °C is superimposed in (a) for comparison (dashed line). The inset in (b) plots the intensity of the absorption peak at 706 nm against the concentration of $[bmim]_2NiCl_4$.

of band II. The presence of an isosbestic point at about 519 nm is indicative of the equilibrium between two types of co-existing absorbents.[23] The system is therefore thermochromic, which is further illustrated by the colour photos (see later discussion on Fig. 7). The intensity of band I did not increase further when the temperature exceeds 71 °C, but that of band II continued to decrease.

Because various octahedral species may form when the thermo-solvolysis occurs, and their absorption wavelengths usually overlap, it is difficult to attribute the origin of band II by using the spectra alone. Therefore, the absorption spectra of $[bmim]_2NiCl_4$ in $[bmim]BF_4$ were recorded at different concentrations and are presented in Fig. 2b for comparison. The absorption intensity increased linearly with the concentration of $[bmim]_2NiCl_4$ (see the inset in Fig. 2b). Only band I was observed in this system, which remained constant in intensity and position (Table 2) when the temperature was changed.

According to the literature,[4,5,13] the tetrahedral $NiCl_4^{2-}$ configuration may exist as the only form in solid or in solutions containing high Cl$^-$ concentration, and shows only band I on the vis-spectrum. It is therefore interesting to observe only band I on the spectrum of $[bmim]_2NiCl_4$ in the simple ionic liquid, $[bmim]BF_4$. This behaviour, however, may not be surprising because, apart from the electrostatic interaction amongst the

Table 2 Absorption wavelengths and molar extinction coefficients (in brackets) of [bmim]$_2$NiCl$_4$ in various ILs

ILs	Wavelength/nm				
[C$_3$OHmim]BF$_4$	446 (26)	610[a]	655 (193)	705 (194)	519[b]
[C$_2$OH mim]BF$_4$	445 (23)	610[a]	655 (159)	705 (159)	523[b]
[C$_3$OH mim]PF$_6$	444 (14)	610[a]	655 (202)	705 (208)	525[b]
[bmim]BF$_4$	—	613[a]	657 (153)	705 (157)	—

[a] Shoulder. [b] Isosbestic point.

ionic species, *e.g.* bmim$^+$, BF$_4^-$ and NiCl$_4^{2-}$, there is no other donor group in this ionic liquid that may coordinate to Ni(II) to alter the NiCl$_4^{2-}$ species.

The absence of band II on the spectra of [bmim]$_2$NiCl$_4$ dissolved in [bmim]BF$_4$ confirms that the influence of [C$_3$OHmim]BF$_4$ on the absorptions must have resulted from the hydroxyl group coordinating with Ni(II), leading to the solvolysis of NiCl$_4^{2-}$ into the octahedral species to give rise to the absorption in band II. The spectra of [bmim]$_2$NiCl$_4$ in [C$_2$OHmim]BF$_4$ and [C$_3$OHmim]PF$_6$ are similar to that in [C$_3$OHmim]BF$_4$. The respective absorption data are listed in Table 2.

In the applied concentration and temperature ranges, it was observed that the peak in band II changed by 2–3 nm in position, and the shoulder and the peak at the lower wavelengths in band I by about 2 nm and 1 nm, respectively. These absorptions moved slightly to shorter wavelengths with increasing the temperature and lowering the total Ni concentration. However, the peak at 705 nm remained unchanged in position. The maximal molar extinction coefficients, ε_{max} (the numbers in brackets in Table 2), were measured by varying the concentration of [bmim]$_2$NiCl$_4$. At 705 nm and 655 nm, the ε_{max} values were verified by dissolving the respective chloride salts into the relevant ILs to make the Cl/Ni molar ratio greater than 20 so that only band I appeared on the spectra. These ε_{max} values of the high wavelength absorption allowed the conversion of the absorption intensity to the concentration of NiCl$_4^{2-}$. Such an obtained NiCl$_4^{2-}$ concentration was subtracted from the total concentration of [bmim]$_2$NiCl$_4$ to give the apparent concentration of the octahedral species for deriving the apparent ε_{max} value of band II.

Identification of the octahedral and tetrahedral complexes

To study the influence of the Cl$^-$ ion on the formation of the octahedral complexes, anhydrous Ni(ClO$_4$)$_2$ was dissolved in [C$_3$OHmim]ClO$_4$ and was kept at an approximate constant concentration of 0.07 mol L^{-1} in every tested solution. Then, the Cl/Ni molar ratio was changed by addition of [C$_3$OHmim]Cl. Fig. 3 shows the spectra recorded at the same temperature (34.2 °C) but different Cl/Ni molar ratios to bring about the formation of various octahedral and tetrahedral complexes. For the convenience of comparison, the absorptions in bands I and II are presented at different scales in Fig. 3 which also shows the colour photos of the corresponding solutions. These spectral changes in response to the addition of chloride ions are analysed in detail below.

[Ni(Sol)$_6$]$^{2+}$, Cl/Ni = 0 (curve 0 in Fig. 3). In the absence of Cl$^-$, the solution was pale grey-yellowish disregarding the concentration, and exhibited a single absorption band II with
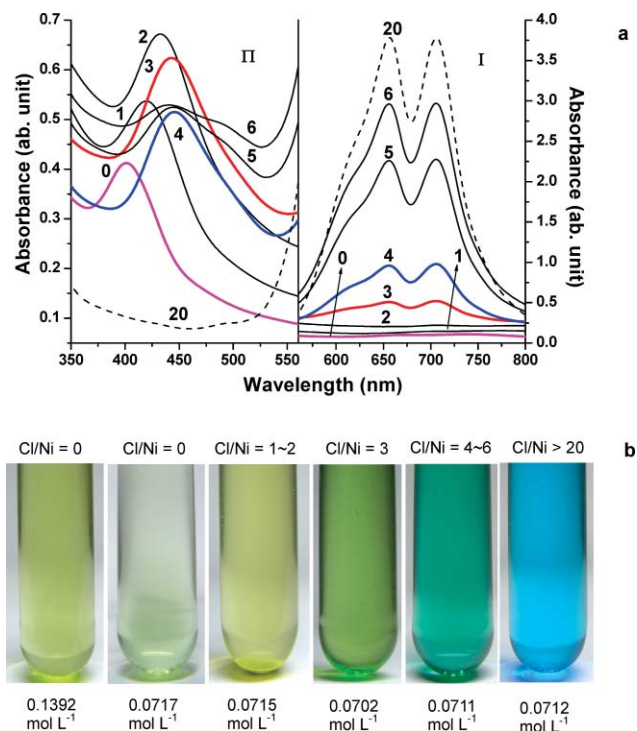
Fig. 3 (a) Vis-spectra of Ni(ClO$_4$)$_2$ (0.07 mol L^{-1}) recorded at 34.2 °C in [C$_3$OHmim]ClO$_4$ with added [C$_3$OHmim]Cl to give different Cl/Ni molar ratios as indicated on each spectrum. (b) The photos below the spectra were taken at room temperature from similar solutions with the indicated Cl/Ni ratios (top) and Ni(ClO$_4$)$_2$ concentrations (bottom).

a peak at 401 nm. This band suggests the $^3A_{2g}(F) \rightarrow {}^3A_{1g}(P)$ transition,[4] and hence the presence of an octahedral complex which could only be [Ni(C$_3$OHmim$^+$–ClO$_4^-$)$_6$]$^{2+}$. The absence of any absorption in the region of band I is evidence of this single form of complex in the solution.

[NiCl(Sol)$_5$]$^+$/[NiCl$_2$(Sol)$_4$], Cl/Ni = 1–2 (curves 1 and 2 in Fig. 3). At the equal molar ratio of Cl/Ni, the solution was yellow-green in colour. Replacement of the C$_3$OHmim$^+$–ClO$_4^-$ ion-pair by the Cl$^-$ ion shifts the $^3A_{2g}(F) \rightarrow {}^3A_{1g}(P)$ transition to lower energies (longer wavelengths) with the peak appearing at about 420 nm and increases its absorption intensity. The significant shift in absorption wavelength suggests the formation of the mono-chloro complex [NiCl(C$_3$OHmim$^+$–ClO$_4^-$)$_5$]$^+$. Note that there is almost no absorption in the band I region, suggesting the high stability of the mono-chloro complex in the test solution. It should be pointed out that the presence of the NiCl$_4^{2-}$ and [Ni(C$_3$OHmim$^+$–ClO$_4^-$)$_6$]$^{2+}$ at undetectable concentration cannot be completely excluded. Similar possibilities also apply to the following discussion.

At Cl/Ni = 2, the solution retained the yellow-green colour. The band II absorption peak increased further in intensity and shifted to 433 nm. However, some featureless absorption in the band I region starts to appear. We attribute the absorption at 433 nm to the formation of the di-chloro octahedral complex [NiCl$_2$(C$_3$OHmim$^+$–ClO$_4^-$)$_4$] which may be in equilibrium with other octahedral species and also possibly the tetrahedral NiCl$_4^{2-}$ complex at a very low concentration.

$[NiCl_3(Sol)_3]^-/[NiCl_4(Sol)_2]^{2-}$, Cl/Ni = 3–6 (curves 3 to 6 in Fig. 3). When the Cl/Ni molar ratio was 3, the solution turned to bright green. The peak shifted further to about 445 nm but the absorption intensity varied: the intensity of the peak decreased whilst those between 450 nm and 550 nm increased. The absorption in the band I region becomes more prominent with noticeable features of the $NiCl_4^{2-}$ complex. These changes suggest the formation of $[NiCl_3(C_3OHmim^+–ClO_4^-)_3]^-$ and also possibly $[NiCl_4(C_3OHmim^+–ClO_4^-)_2]^-$ in equilibrium with the $NiCl_4^{2-}$ complex and other octahedral species.

As the Cl/Ni molar ratio reached 4, the solution turned to blue-green. The absorption intensity in band II decreased further. It is also noticed that the absorption between 470 nm and 550 nm on curve 4 overlapped with that on curve 2 in band II. In band I, the full absorption features of the $NiCl_4^{2-}$ complex appeared.

For Cl/Ni = 5, the solution retained the blue-green colour. The main peak in band II remained at about 445 nm, but a shoulder appeared at about 490 nm. The shoulder turned into a peak at Cl/Ni = 6. It is possible that the tetra-chloro complex $[NiCl_4(C_3OHmim^+–ClO_4^-)_2]^{2-}$ was responsible for the absorption peak at 490 nm, although its stability and concentration may not be very high. It can also be seen that from Cl/Ni = 4 to 6, the absorption intensity of band I increased steeply.

$NiCl_4^{2-}$, Cl/Ni > 20. When the Cl/Ni molar ratio reached or exceeded 20, band II began to disappear and the spectrum changed to the same shape as those shown in Fig. 2b. The solution turned blue, and all the Ni(II) species were converted to $NiCl_4^{2-}$.

As discussed before for $[NiCl_x(C_3OHmim^+–BF_4^-)_y]^{2-x}$, the expression of $[NiCl_x(C_3OHmim^+–ClO_4^-)_y]^{2-x}$ ($x + y = 6$) (i.e. expression (b)) is used here for the convenience of discussion. The inclusion of the ClO_4^- ions in the octahedral complexes follows the electrostatic logic to avoid too high a positive charge on the complex species, e.g. $[Ni(C_3OHmim^+)_6]^{8+}$ (i.e. expression (a)). This logical derivation is in broad agreement with our preliminary investigations by electrophoresis. In the experiment, the solution of interest was placed in a U-tube and then covered in each leg by pure $[bmim]ClO_4$ to give a total solution length of ~25 cm. Electrophoresis with a graphite rod cathode and platinum foil anode was then carried out at room temperature (voltage: 30–50 V; electrolysis time: 24–48 h). It was thought that under the influence of the electric field, the coloured complex ions were to move (migration) according to its charged status. The results showed in general a significant movement of blue colour towards the anode when the Cl/Ni molar ratio was 3–5. However, little change to the bulk IL (yellow, green or blue-green) was observed. While the increased blue colour in the anode leg is expected from the movement of the anionic tetrahedral complex ($NiCl_4^{2-}$), it can be considered that the octahedral complexes might have been likely in a charge-neutral or low charge state which can only be achieved through the association of the ClO_4^- ions to the octahedral complexes.

However, the electrophoresis results are insufficient for determining if the ClO_4^- ions were paired with the C_3OHmim^+ ion corresponding to $[NiCl_x(C_3OHmim^+–ClO_4^-)_y]^{2-x}$ ($x + y = 6$, expression (b)), or with the complex cation to give rise to $[NiCl_x(C_3OHmim^+)_y]^{z+}–(BF_4^-)_z$ ($z = 2 + y - x$, expression (c)).

For the convenience of discussion, and also in analogy with the function of a solvent, we use expression (b) in this paper, although further work may be highly likely to prove expression (c) to be more appropriate.

The Ni(II) coordination ability of different hydroxyl groups

It is worth mentioning that in aqueous solutions,[14] $[NiCl(H_2O)_5]^+$ may form only in solutions containing enough Cl$^-$ ions (exceeding 10 mol L^{-1}). In relatively weaker coordinating solvents such as alcohol[5] and acetone,[15] $[NiCl(Sol)_5]^+$ or $[NiCl_2(Sol)_4]$ can form when the Cl/Ni or Br/Ni molar ratio exceeds 4. However, high-chloro octahedral complexes, such as $[NiCl_3(Sol)_3]^-$ and $[NiCl_4(Sol)_2]^{2-}$, have not yet been detected in conventional solvents.[5,16] It may therefore be speculated that their formation in $[C_nOHmim]^+$ based ILs could have benefited from the electrostatic interaction between the Cl$^-$ ions and the $[C_nOHmim]^+$ ion, which stabilised the high-chloro octahedral structure.

To further confirm the effect of the positive charge on the imidazolium ring, the Ni(II) coordination ability of ethanol and propanol was compared with that of $[C_3OHmim]BF_4$ in $[bmim]BF_4$. Fig. 4 presents the results. It can be seen that at the same $[bmim]_2NiCl_4$ concentration, the addition of each of the three hydroxyl donor solvents resulted in fairly different absorption features on the spectra. When the IL was added, there is a significant increase in absorption intensity in the band II region, accompanied by an even larger decrease in absorption intensity in the band I region. In contrast, the alcohol counterpart (propanol) caused almost no change. The change caused by the addition of ethanol was similar to that of propanol in the band I region, but between those of propanol and $[C_3OHmim]BF_4$. It can then be concluded that the IL is indeed more capable of coordinating with Ni(II) and the coordination ability follows the order of n-propanol < ethanol < $C_3OHmimBF_4$.

Thermodynamic properties

As discussed before, the absorption features in band I can be attributed to the tetrahedral $NiCl_4^{2-}$ complex, but those in band II are associated with possibly more than one species in

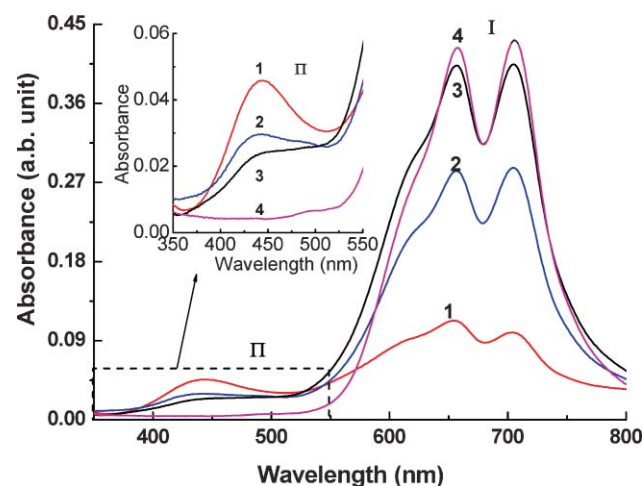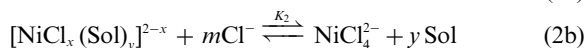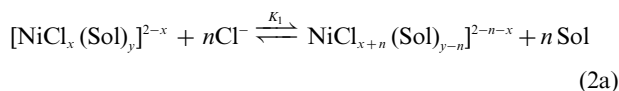**Fig. 4** Vis-spectra of $[bmim]_2NiCl_4$ (0.0137 ± 0.0002 mol L^{-1}) recorded at 34.2 °C in $[bmim]BF_4$ with different hydroxyl donor ligands. (1) $[C_3OHmim]BF_4$/Ni molar ratio = 220. (2) CH_3CH_2OH/Ni = 220. (3) $CH_3CH_2CH_2OH$/Ni(total) = 220. (4) OH/Ni = 0.

the octahedral configuration. The respective equilibria can be representatively expressed below.

$$[NiCl_x (Sol)_y]^{2-x} + n\,Cl^- \underset{}{\overset{K_1}{\rightleftharpoons}} NiCl_{x+n} (Sol)_{y-n}^{2-n-x} + n\,Sol$$
(2a)

$$[NiCl_x (Sol)_y]^{2-x} + m\,Cl^- \underset{}{\overset{K_2}{\rightleftharpoons}} NiCl_4^{2-} + y\,Sol$$
(2b)

$(x + y = 6; 0 \leq x \leq 4; 0 \leq y \leq 6; x + n \leq 4; m + x = 4; m \geq n)$

Reaction (2a) represents the octahedral–octahedral conversion at relatively low Cl^- concentrations, and should exhibit no or little colour change. At higher Cl^- concentrations, *e.g.* Cl/Ni ≥ 4, and/or elevated temperatures, Reaction (2b) takes place, leading to the octahedral–tetrahedral conversion and the thermochromic behaviour. The reverse of Reaction (2b) is solvolysis and proceeds with lowering the temperature and/or addition of the solvent.

In theory, it is possible to derive the equilibrium constant for each of the above reactions from the vis-spectra using the non-linear curve fitting method. However, the appearance of a clear isosbestic point in Fig. 2a, which was also commonly observed in other systems of this work, indicates the thermochromism may be treated in a simpler way as the equilibrium between two types of absorbents.[23] One should be the tetrahedral $NiCl_4^{2-}$ complex, but the other is likely a representative or the dominant of several octahedral species. Considering the above discussion on the formation of different octahedral complexes at different Cl/Ni ratios (Fig. 3), and the fact that the Cl/Ni ratio was always 4 in the solution used for recording Fig. 2, it is reasonable to assume this representative to be $[NiCl_3(C_3OHmim^+-BF_4^-)_3]^-$ (and the same for $[bmim]_2NiCl_4$ in other C_nOHmim^+ based ILs). Thus, the following reaction could have played the dominant role in the thermochromic changes shown in Fig. 2.

$$NiCl_3(C_3OHmim^+ - BF_4^-)_3]^- + Cl^-$$
(octahedral, green, cold)
(2)
$$\overset{K}{\rightleftharpoons} \quad NiCl_4^{2-} + 3\,[C_3OHmim]BF_4$$
(tetrahedral, blue, hot)
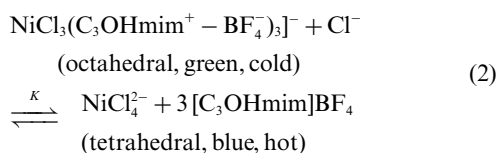
Reaction (2) is a special case of Reaction (2b) for $m = 1$ and $x = 3$. Because $[C_3OHmim]BF_4$ is present in excess in the solution, the equilibrium constant of Reaction (2) can be estimated by eqn (3).

$$K = \frac{C_{NiCl_4^{2-}}}{C_{[NiCl_3(C_3OHmim^+ - BF_4^-)_3]}^- C_{Cl^-}} = \frac{C_{NiCl_4^{2-}}}{(C_{[NiCl_3(C_3OHmim^+ - BF_4^-)_3]}^-)^2}$$
(3)

Changes in the enthalpy, ΔH, Gibbs free energy, ΔG, and entropy, ΔS, of eqn (2) can be derived from the equilibrium constant, K, using the following equations.

$$\frac{d \ln K}{d(1/T)} = -\frac{\Delta H}{R}$$
(4)

$$\Delta G = -RT \ln K$$
(5)

$$\Delta S(T) = \frac{\Delta H - \Delta G}{T}$$
(6)

The concentration of $NiCl_4^{2-}$ was obtained from Beer's law against the absorption in band I. Given the initial concentration of $[bmim]_2NiCl_4$, the concentration of $[NiCl_3(C_3OHmim^+\cdot BF_4^-)_3]^-$ was obtained by subtraction. The K value was then calculated according to eqn (3) and some results are listed in Table 3. Fig. 5 plots ln K against $1/T$. The data points could be fitted into a set of straight lines over the temperature range of 25 to 53 °C, and the initial $[bmim]_2NiCl_4$ concentration range of 0.0540 to 0.0872 mol L^{-1}. Values of ΔH were determined from the slopes of these linear plots according to eqn (4) and are given in Table 3 for different initial $[bmim]_2NiCl_4$ concentrations. It can be seen that these results are in good agreement with each other. On average, it was found that $\Delta H = 36.5 \pm 1.0$ kJ mol^{-1} and ΔS (298 K) = 150 ± 3 J mol^{-1} K^{-1}.
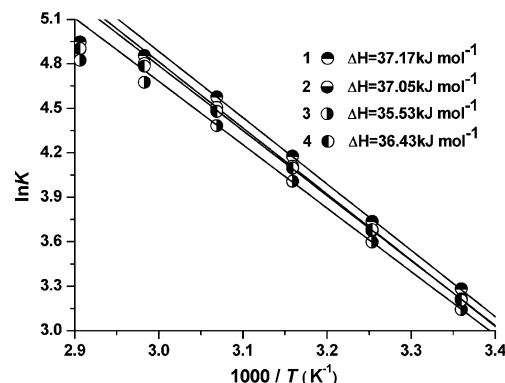
Fig. 5 Correlations between the temperature (T) and the equilibrium constant (K) of $[NiCl_3(C_3OHmim^+-BF_4^-)_3]^- + Cl^- \Leftrightarrow NiCl_4^{2-} + 3$ $[C_3OHmim]BF_4$. Initial $[bmim]_2NiCl_4$ concentration at room temperature: (1) 0.0540; (2) 0.0640; (3) 0.0791; (4) 0.0872 mol L^{-1}.

The vis-spectra of $[bmim]_2NiCl_4$ in $[C_2OHmim]BF_4$ and in $[C_3OHmim]PF_6$ were similar to those in $[C_3OHmim]BF_4$. Applying the same analysis and calculations, the thermodynamic data were obtained as shown in Table 4 and Fig. 6. On average, it was found that $\Delta H = 33.5 \pm 1.5$ kJ mol^{-1} and ΔS (298 K) = 138 ± 5 J mol^{-1} K^{-1} for $[C_2OHmim]BF_4$ and $\Delta H = 40.0 \pm 0.5$ kJ mol^{-1} and ΔS (298 K) = 158 ± 5 J mol^{-1} K^{-1} for $[C_3OHmim]PF_6$.

It should be pointed out that Reaction (2) is a special case of Reaction (2b) for $m = 1$, but it is possible to carry out similar analyses for $m = 2$ or 3. The results showed significantly different K values for different initial $[bmim]_2NiCl_4$ concentrations, suggesting $m = 1$ to be an appropriate assumption.

Both Fig. 5 and Fig. 6 show that, at temperatures higher than about 50 °C, the data points deviated from the straight lines. This phenomenon indicates that the $NiCl_4^{2-}$ concentrations as measured from the vis-spectra were probably lower than what would have been generated by Reaction (2) at higher temperatures. An early study on the vis-spectra of $[(C_6H_5)_4As]_2NiCl_4$ in ethanol suggested the formation of the tetrahedral $[NiCl_3(C_2H_5OH)]^-$ complex at high temperatures.[5] While such conversions may account for the measured lower $NiCl_4^{2-}$ concentration, the vis-spectra recorded in this work did not show any sign of such a complex. Alternatively, it was more likely that the assumption of the $[NiCl_3(Sol)_3]^-$ complex being the dominant species in the solution may only apply at relatively low temperatures. At higher temperatures, the relative concentrations of other

Table 3 Thermodynamic analysis and data of the correlated thermochromism and solvolysis of [bmim]$_2$NiCl$_4$ at different initial concentrations in [C$_3$OHmim]BF$_4$

T/°C	$C_{\mathrm{NiCl_4^{2-}}}$/ mol L^{-1}	$C_{\mathrm{[NiCl_3(Sol)_3]^-}}$/ mol L^{-1}	K	$C_{\mathrm{NiCl_4^{2-}}}$/ mol L^{-1}	$C_{\mathrm{[NiCl_3(Sol)_3]^-}}$/ mol L^{-1}	K
24.5	0.0240	0.0300	26.7	0.0295	0.0344	24.9
34.2	0.0279	0.0258	42.0	0.0341	0.0294	39.4
43.4	0.0314	0.0219	65.2	0.0381	0.0250	60.9
52.7	0.0343	0.0188	97.2	0.0414	0.0214	90.6
62.1	0.0360	0.0168	129	0.0436	0.0189	122
70.9	0.0365	0.0161	141	0.0441	0.0181	134
$C_{\mathrm{[bmim]_2NiCl_4}}$/mol L^{-1}			0.0540			0.0640
ΔH/kJ mol^{-1}			37.2 ± 0.5			37.1 ± 0.3
ΔS (298 K)/J mol^{-1} K^{-1}			152 ± 2			151 ± 2

T/°C	$C_{\mathrm{NiCl_4^{2-}}}$/ mol L^{-1}	$C_{\mathrm{[NiCl_3(Sol)_3]^-}}$/ mol L^{-1}	K	$C_{\mathrm{NiCl_4^{2-}}}$/ mol L^{-1}	$C_{\mathrm{[NiCl_3(Sol)_3]^-}}$/ mol L^{-1}	K
24.5	0.0384	0.0407	23.2	0.0446	0.0425	24.7
34.2	0.0438	0.0347	36.5	0.0508	0.0358	39.7
43.4	0.0484	0.0297	55.0	0.0556	0.0304	60.2
52.7	0.0521	0.0255	80.1	0.0595	0.0260	88.2
62.1	0.0547	0.0226	107	0.0623	0.0228	120
70.9	0.0558	0.0212	124	0.0632	0.0217	135
$C_{\mathrm{[bmim]_2NiCl_4}}$/mol L^{-1}			0.0791			0.0872
ΔH/kJ mol^{-1}			35.5 ± 0.2			36.4 ± 0.4
ΔS (298 K)/J mol^{-1} K^{-1}			146 ± 2			150 ± 2

Table 4 Thermodynamic analysis and data of the correlated thermochromism and solvolysis of [bmim]$_2$NiCl$_4$ at different initial concentrations in [C$_2$OHmim]BF$_4$

T/°C	$C_{\mathrm{NiCl_4^{2-}}}$/ mol L^{-1}	$C_{\mathrm{[NiCl_3(Sol)_3]^-}}$/ mol L^{-1}	K	$C_{\mathrm{NiCl_4^{2-}}}$/ mol L^{-1}	$C_{\mathrm{[NiCl_3(Sol)_3]^-}}$/ mol L^{-1}	K
24.5	0.0488	0.0437	25.6	0.0419	0.0408	25.1
34.2	0.0546	0.0371	39.6	0.0467	0.0353	37.4
43.4	0.0595	0.0317	59.2	0.0511	0.0304	55.3
52.7	0.0634	0.0273	85.4	0.0545	0.0266	77.2
62.1	0.0653	0.0249	105	0.0569	0.0238	100
70.9	0.0655	0.0245	110	0.0579	0.0226	113
$C_{\mathrm{[bmim]_2NiCl_4}}$/mol L^{-1}			0.0925			0.0827
ΔH/kJ mol^{-1}			34.5 ± 0.3			32.3 ± 0.5
ΔS (298 K)/J mol^{-1} K^{-1}			143 ± 2			135 ± 3

T/°C	$C_{\mathrm{NiCl_4^{2-}}}$/ mol L^{-1}	$C_{\mathrm{[NiCl_3(Sol)_3]^-}}$/ mol L^{-1}	K	$C_{\mathrm{NiCl_4^{2-}}}$/ mol L^{-1}	$C_{\mathrm{[NiCl_3(Sol)_3]^-}}$/ mol L^{-1}	K
24.5	0.0391	0.0365	29.4	0.0327	0.0331	29.8
34.2	0.0434	0.0316	43.6	0.0366	0.0286	44.6
43.4	0.0474	0.0271	64.6	0.0400	0.0248	64.9
52.7	0.0505	0.0236	90.7	0.0428	0.0216	91.4
62.1	0.0524	0.0213	115	0.0441	0.0201	109
70.9	0.0533	0.0202	131	0.0449	0.0191	123
$C_{\mathrm{[bmim]_2NiCl_4}}$/mol L^{-1}			0.0756			0.0658
ΔH/kJ mol^{-1}			32.5 ± 0.5			32.1 ± 0.2
ΔS (298 K)/J mol^{-1} K^{-1}			137 ± 3			136 ± 2

octahedral complexes may become more comparable with that of the [NiCl$_3$(Sol)$_3$]$^-$ complex, which will make both Reaction (2) and eqn (3) invalid and hence the deviation. Further work is obviously needed to understand better the systems at higher temperatures.

Practical significance

Table 5 compares the ΔH values of the octahedral–tetrahedral conversion in various solutions. It can be seen that the ΔH values in water and in alcohols are 4–5 times and 1.5–2 times of those in the C$_n$OHmim$^+$ based ILs, respectively. Therefore, these new thermochromic systems are more energy effective systems for practical applications. Further, as stated in the Introduction, the initial thought that stimulated this work was to prepare more stable thermochromic systems than those based on conventional solvents, such as water and alcohols.

In this work, it was indeed observed that, to bring about similar thermochromic changes in the same temperature range,

---

Table 5 Comparison of the ΔH and ΔS data for the octahedral-tetrahedral conversion of the Ni(II) complexes induced thermosolvolysis in various solutions

Octahedral species	Tetrahedral species	Solution	ΔH/kJ mol^{-1}	ΔS/J mol^{-1} K^{-1}	Ref.
[NiCl(glycol)$_5$]$^+$	[NiCl$_4$]$^{2-}$	Glycol + Cl$^-$	58	171[a]	16
[NiCl(glycerol)$_5$]$^+$	[NiCl$_4$]$^{2-}$	Glycerol + Cl$^-$	63	176[a]	16
[NiCl(H$_2$O)$_5$]$^+$	[NiCl$_4$]$^{2-}$	H$_2$O + Cl$^-$	167	472[b]	4
[NiCl$_2$(C$_2$H$_5$OH)$_4$]	[NiCl$_3$(C$_2$H$_5$OH)]$^-$	C$_2$H$_5$OH + Cl$^-$	61	—	5
[NiBr$_2$(CH$_3$OH)$_4$]	[NiBr$_3$(CH$_3$OH)]$^-$	CH$_3$OH + Br$^-$	51	—	5
[NiBr$_2$(C$_2$H$_5$OH)$_4$]	[NiBr$_3$(C$_2$H$_5$OH)]$^-$	C$_2$H$_5$OH + Br$^-$	72	—	5
[NiBr$_2$(n–C$_4$H$_9$OH)$_4$]	[NiBr$_2$(n–C$_4$H$_9$OH)$_2$]	n–C$_4$H$_9$OH + Br$^-$	71	—	5
[NiBr$_2$(n–C$_4$H$_9$OH)$_4$]	[NiBr$_3$(n–C$_4$H$_9$OH)]$^-$	n–C$_4$H$_9$OH + Br$^-$	62	—	5
[NiCl$_3$(C$_2$OHmim$^+$·BF$_4^-$)$_3$]$^-$	[NiCl$_4$]$^{2-}$	[C$_2$OHmim]BF$_4$	34	138[a]	c
[NiCl$_3$(C$_3$OHmim$^+$·BF$_4^-$)$_3$]$^-$	[NiCl$_4$]$^{2-}$	[C$_3$OHmim]BF$_4$	36	150[a]	c
[NiCl$_3$(C$_3$OHmim$^+$·PF$_6^-$)$_3$]$^-$	[NiCl$_4$]$^{2-}$	[C$_3$OHmim]PF$_6$	40	158[a]	c

[a] 298 K. [b] 383 K. [c] This work.
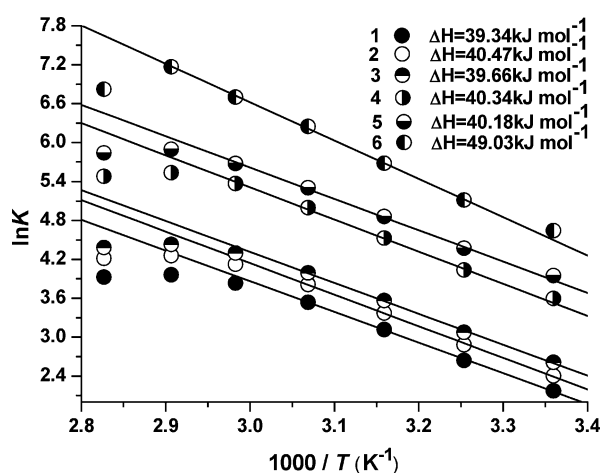
Fig. 6 Correlations between the temperature (T) and the equilibrium constant (K) of [NiCl$_3$(C$_3$OHmim$^+$–PF$_6^-$)$_3$]$^-$ + Cl$^-$ $\Leftrightarrow$ NiCl$_4^{2-}$ + 3 [C$_3$OHmim]PF$_6$. Initial [bmim]$_2$NiCl$_4$ concentration at room temperature: (1) 0.0902; (2) 0.0801; (3) 0.0718; (4) 0.0474; (5) 0.0419; (6) 0.0347 mol L^{-1}.

Fig. 7 Photos of [bmim]$_2$NiCl$_4$ in ethanol (top row: 0.0223 mol L^{-1}; 2nd row: 0.0547 mol L^{-1}; 3rd row: 0.1842 mol L^{-1}) and C$_3$OHmimBF$_4$ (bottom row: 0.0217 mol L^{-1}) at the indicated temperatures.

a much higher Ni(II) concentration was needed in the alcohol systems than in the IL systems. Fig. 7 compares the colour photos taken from the two systems, showing their colour changes in response to temperature increase. Note that the colour change in ethanol was only observed at relatively high concentrations. In addition, at the same Ni(II) concentration, the colour change occurred quicker and at lower temperatures in the IL systems than in the alcohols.

Upon repeated heating–cooling cycling, evaporation of solvent was observed in the alcohol systems, which could lead to precipitation of the Ni(II) salt eventually. In similar experiments, the IL systems exhibited much greater stability. They could absorb moisture from air to be decoloured but the effect was slow and could be completely reversed upon heating under vacuum. Fig. 8 compares the vis-spectra of [bmim]$_2$NiCl$_4$ before and after 12 heating–cooling cycles (at a rate of about 2 cycles per day) in ethanol (0.0223 or 0.1842 mol L^{-1}, 30–75 °C) and in C$_3$OHmimBF$_4$ (0.0217 mol L^{-1}, 30–85 °C). It can be seen in Fig. 8a and 8b that the ethanol system exhibited significant changes in both absorption intensity and peak wavelength in the band II region. The more serious consequence of the thermal

cycling in the alcohol was the precipitation of the salt because of solvent evaporation. On the contrary, the IL system showed a much smaller change in the peak wavelength of band II with the intensity remaining the same. There was a noticeable decrease in the intensity of band I, which was confirmed to be due to the IL absorbing moisture from air because the system could be completely recovered by simply thermal drying under vacuum as shown in Fig. 8c. It is worth mentioning that in the experiment, it was observed that the absorption of moisture led to the decolouring of the top layer (1–2 mm in thickness after the 12 heating-cooling cycles) of the solution, but very little spectral
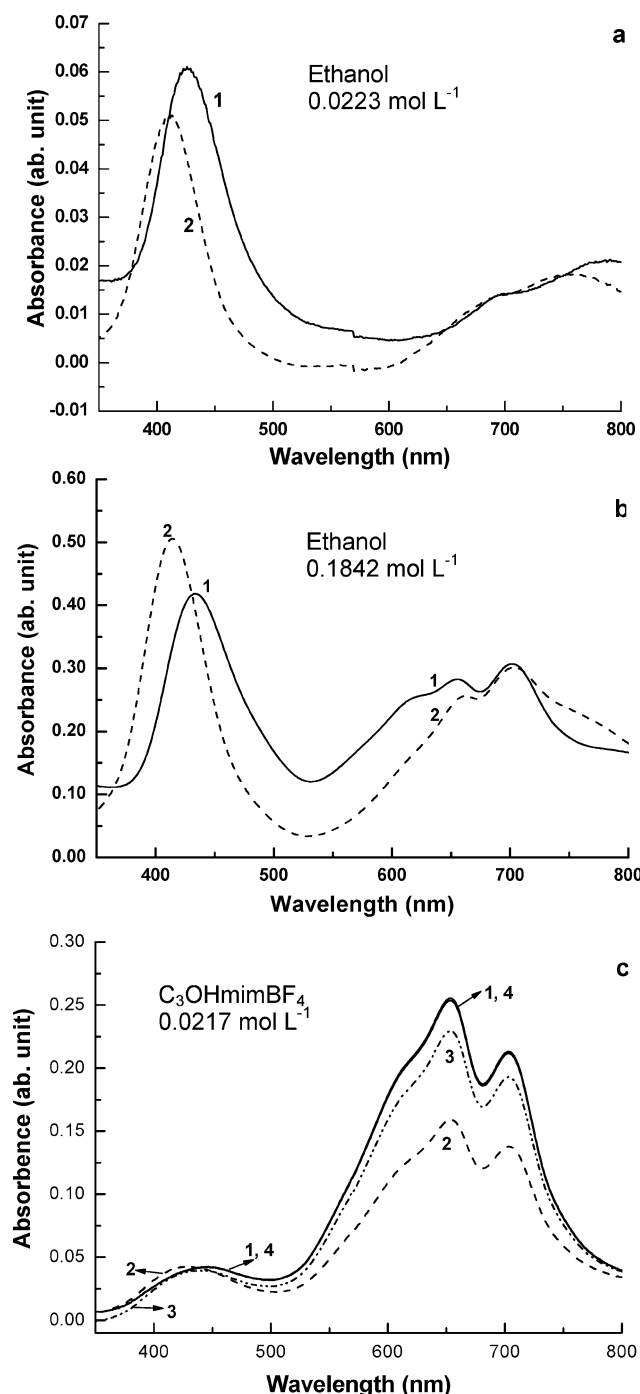
Fig. 8 Vis-spectra of [bmim]$_2$NiCl$_4$ at the indicated concentrations in (a, b) ethanol (cycling between 30–75 °C) and (c) in C$_3$OHmimBF$_4$ (cycling between 30–85 °C). The numbers next to the spectra indicate (1, solid line) before and (2, dashed line) after 12 heating–cooling cycles, and after drying the cycled solution under vacuum at 70 °C for (3) 15 h and (4) 35 h.

change occurred to the underneath solution. The spectra in Fig. 8c were measured after mixing the moisturise containing top layer solution with the bulk solution.

Conclusions

Novel thermochromic systems have been prepared in this work by dissolving [bmim]$_2$NiCl$_4$ in C$_n$OHmim$^+$ based ILs. In comparison with previously reported systems based on conventional solvents, the new ILs are more sensitive and energy effective to temperature changes, much wider in working temperatures and more stable in repeated heating–cooling cycle operations. These benefits can be attributed to the greater ability of the C$_n$OHmim$^+$ ion than the hydroxyl group in water and alcohols to coordinate with the NiCl$_x^{2-x}$ ion in the octahedral configuration. Because their effective working temperatures match very well with that readily achievable under sunlight, these hydroxyalkylised imidazolium based thermochromic systems present a new example of green chemistry.

Acknowledgements

References

1 W. Linert, Y. Fukuda and A. Camard, *Coord. Chem. Rev.*, 2001, **218**, 113–152.
2 U. El-Ayaan, F. Murata and Y. Fukuda, *Monatsh. Chem.*, 2001, **132**, 1279–1294.
3 K. Sone, Y. Fukuda, Inorganic Thermochromism, in *Inorganic Chemistry Concepts*, vol. 10, Springer, Berlin, 1987.
4 T. R. Griffiths and R. K. Scarrow, *Trans. Faraday Soc.*, 1969, **65**, 1727–1733.
5 D. E. Scaife and K. P. Wood, *Inorg. Chem.*, 1967, **6**, 358–365.
6 T. Sato, G. Masuda and K. Takagi, *Electrochim. Acta*, 2004, **49**, 3603–3611.
7 G. T. Wei, Z. Yang and C. J. Chen, *Anal. Chim. Acta*, 2003, **488**, 183–192.
8 R. D. Rogers, K. R. Seddon, *Ionic Liquids: Industrial Applications to Green Chemistry*, ACS, Washington, DC, 2002.
9 Y. Cai, Y. Zhang, Y. Q. Peng, F. Lu, X. L. Huang and G. H. Song, *J. Comb. Chem.*, 2006, **8**, 636–638.
10 J. C. Xiao and J. M. Shreeve, *J. Org. Chem.*, 2005, **8**, 3072–3078.
11 A. E. Visser, R. P. Swatloski, W. M. Reichert, R. Mayton, S. Sheff, A. Wierzbicki, J. H. Davis and R. D. Rogers, *Chem. Commun.*, 2001, (1), 135–136.
12 H. Ohno, *Electrochim. Acta*, 2001, **46**, 1407–1411.
13 D. M. Gruen and R. L. Mcbeth, *J. Phys. Chem.*, 1959, **63**, 393–398.
14 D. A. Netzel and H. A. Droll, *Inorg. Chem.*, 1962, **2**, 412–413.
15 D. A. Fine, *Inorg. Chem.*, 1965, **4**, 345–350.
16 T. R. Griffiths and R. K. Scarrow, *Trans. Faraday Soc.*, 1969, **65**, 3179–3186.
17 J. S. Wilkes, J. A. Levisky, R. A. Wilson and C. L. Hussey, *Inorg. Chem.*, 1982, **21**, 1263–1264.
18 L. C. Branco, J. N. Rosa, J. J. Moura Ramos and C. A. M. Afonso, *Chem.–Eur. J.*, 2002, **8**, 3671–3677.
19 J. Fraga-Dubreuil and J. P. Bazureau, *Tetrahedron Lett.*, 2001, **42**, 6097–6100.
20 A. Lesimple, O. Mamer, W. Miao and T. H. Chan, *J. Am. Soc. Mass Spectrom.*, 2006, **17**, 85–95.
21 R. L. David, *CRC handbook of Chemistry and Physics*, CRC Press, Boca Raton, 87th edn, 2006, 6-4–6-5.
22 R. D. Rogers and K. R. Seddon, *Science*, 2003, **302**, 792–793.
23 C. A. Angell and D. M. Gruen, *J. Am. Chem. Soc.*, 1966, **88**, 5192–5198.

Ionic liquids: prediction of their melting points by a recursive neural network model†

Riccardo Bini,[a] Cinzia Chiappe,[a] Celia Duce,*[b] Alessio Micheli,*[c] Roberto Solaro,[b] Antonina Starita[c] and Maria Rosaria Tiné[b]

A recursive neural network (RNN) was used to predict the melting points of several pyridinium-based ionic liquids (ILs). The RNN is a neural network model for processing structured data that allows for the direct handling of chemical compounds as labelled rooted ordered trees. It constitutes a direct approach to quantitative structure–property relationship (QSPR) of ILs, which avoids the use of dedicated molecular descriptors. The adopted representation of molecular structures captures significant topological aspects and chemical functionalities for each molecule in a general and flexible way. Particular emphasis was given to the representation of cyclic moieties. The model was applied to a set of 126 pyridinium bromides; it was validated by splitting the dataset into a disjoint training set (100 compounds) and test set (26 compounds). Comparison with the results obtained by other QSPR approaches on the same dataset is also presented.

Introduction

Ionic liquids (ILs) are defined as salts that melt below 100 °C. Generally, ILs are composed of an inorganic anion and an organic cation. Although the number of ILs grows daily, the cations are almost always bulky asymmetric ammonium or phosphonium ions. The weak intermolecular interactions and low charge density of IL ions account for the low melting points of this class of salts.

The study of ILs has experienced a huge growth in recent years as a promising research field for the development of new environmentally sustainable technologies.[1] The exciting properties of ILs include negligible vapour pressure, excellent and adjustable solvation power (for both organic and inorganic compounds), non-flammability and high thermal stability.[2,3] These properties make ILs a viable alternative to organic volatile solvents and stimulated a great interest in the use of ILs for a wide range of applications, including chemical synthesis, separation and catalysis.[4,5]

Careful choice of the cation/anion combination allows for the synthesis of ILs with physical and chemical properties tailored to specific tasks.[6,7] According to Katritzky et al.,[8] there are approximately 10^{18} ion combinations that can lead to useful ILs. It is therefore necessary to develop predictive computational tools able to contribute to the design of new ILs possessing the required properties.

The melting point (mp) is an important IL physical property that has been the subject of several studies aimed at establishing quantitative structure–property relationships (QSPR). Earlier, QSPR models for the prediction of IL melting points were developed for datasets of the bromides of nitrogen-based organic cations such as, imidazolium,[8] pyridinium,[9] and quaternary ammonium cations.[10] Until now, multilinear regression techniques were used; only one paper[11] reported the application of nonlinear methods (decision trees and neural networks) leading to models of better performance.

To correlate the chemical structure with one property, a description of the molecule is needed. Molecular descriptors[12] were used in all reported QSPR studies to represent structures. The major limit of this approach is represented by the need for finding a set of complete and relevant molecular descriptors, which usually requires dealing with high dimensionality data.

Direct structure treatment could enable one to by-pass the limitations associated with the use of molecular descriptors. In this paper we show that neural networks for structures (or recursive neural networks, RNN) constitute a new approach to QSPR analysis of ILs. In particular, the emphasis is placed on the direct treatment of the molecular structure, which still represents a challenge for standard vector-based techniques. Our goal is to investigate whether the RNN is a feasible approach to the prediction of IL properties. In fact, the used class of neural networks can manage chemical graphs directly as an input; it is able to learn the mapping of structures to the desired property from training examples. In particular, given a structural representation of chemical graphs, RNNs automatically encode the structural information depending on the computational problem at hand. Accordingly, the numerical representation of the molecular structure is not defined a priori by using a set of

[a] Department of Bioorganic Chemistry and Biopharmacy, University of Pisa, via Bonanno Pisano 33, 56126, Pisa, Italy. E-mail: bini@farm.unipi.it, cinziac@farm.unipi.it; Fax: +39 050 2219660
[b] Department of Chemistry and Industrial Chemistry, University of Pisa, via Risorgimento 35, 56126, Pisa, Italy. E-mail: celia@dcci.unipi, mrt@dcci.unipi.itrosola@dcci.unipi.it
[c] Department of Informatics, University of Pisa, Largo B. Pontecorvo 3, 56127, Pisa, Italy. E-mail: micheli@di.unipi.it, starita@di.unipi.it

descriptors, but is learned as a result of the training process. The RNN model was successfully applied to the prediction of the boiling point of a class of alkanes,[13] the biological activity of a class of 1,4-benzodiazepin-2-ones,[14] the $\Delta_{solv}G°$ in water of monofunctional acyclic organic compounds,[15] and the T_g of (meth)acrylic polymers.[16–18]

In the present research, the method based on RNN model has been extended to the prediction of the physical properties of ILs containing cyclic structures by using an explicit treatment of cyclic moieties.

Method

The neural networks model used in this work is based on a recursive algorithm. A detailed description of this method can be found in ref. 13–15, 19 and 20. Briefly, the input pattern of standard neural networks is a fixed-size array. On the other hand, the adopted RNN can deal with variable-size structured domains in the form of *labelled rooted positional trees* (*trees* in the following) with defined out-degree *k* (where the out-degree of a vertex is the number of edges leaving that vertex). Previous applications[13–15,17,18] of this method show that chemical structures can be represented by trees in which every atom (or group of atoms) is a *vertex* (or *node*) and every chemical bond is an edge starting from the node. A label, *i.e.* an array of numerical variables, distinguishes each node. This translational process conveys topological and chemical information of the molecules to the representation.

The first goal of this investigation was to find a flexible representation of pyridinium structures by extending the tree representation developed for organic acyclic compounds[15] while preserving the hierarchical structure. In particular, we devised a specific structure representation to treat the cyclic moieties occurring in the IL dataset. Although all cycles in the data set have the same size (six), they differ in the content of double bonds and heteroatoms (oxygen, nitrogen). One possible choice was to define a group for every chemically different cycle.[20] However, the introduction of specific labels for groups with a few occurrences in the data set must be avoided because of low data sampling. This issue led us to introduce a detailed ring representation. Indeed, all cycles in the considered dataset are constituted by atom groups that occur also in other structures. Accordingly, all cyclic structures were represented by a node (Cycle) with six children, where the children are the atom groups constituting the ring skeleton (Fig. 1). The highest priority was assigned to the "Cycle" group.

Molecules in the dataset were split into the following elemental groups: CH_3, CH_2sp^3, CH_2sp^2, $CHsp^3$, $CHsp^2$, $CHsp$, Csp^3, Csp^2, Csp, $C=O$, $HC=O$, CN, N, NH, NH_2, $OHsp^3$ (bound to an sp^3 carbon), $OHsp^2$ (bound to an sp^2 carbon), O, S, F, Cl, Br, $C=N–OH$, $COOH$, COO, and $CONH_2$. The bromide anion was not represented, being invariant over the entire dataset.

Since the pyridinium ion characterized the entire dataset, every tree was rooted at the "Cycle" group representing this cation. The nitrogen atom (group N) is the first root child. The same "Cycle" group also represents the other cyclic moieties. In this case, the first child (highest priority) of the "Cycle" is the node representing the chemical group closest to the pyridinium cation (see Fig. 1). The other positions in every
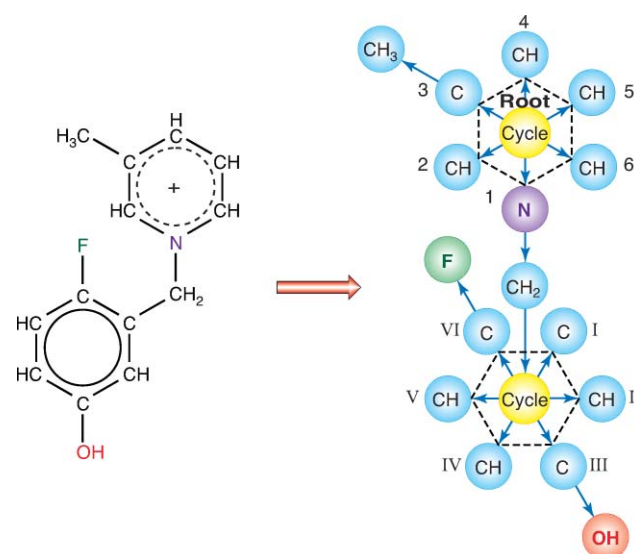
Fig. 1 Tree representation of the *N*-(2-fluoro-5-hydroxybenzyl)-3-methylpyridinium cation. The numbers indicate the priority of the nodes on cyclic moieties.

cyclic backbone are ordered clockwise starting from the first child in such a way that the carbon atom in the skeleton ring bound to the substituent with the highest priority (according to Cahn–Ingold–Prelog rules[21]) has the lowest position number. The Cahn–Ingold–Prelog rules are also applied to establish the priority among groups in the remaining nodes.

When a multiple carbon–carbon bond is present, it is divided into two groups that take into account the hybridization of the carbon atoms. In order to have different representation for *cis* and *trans* alkenes, the group in the *cis* position has higher priority than the *trans* substituent.

The RNN exploits a recursive encoding process, which mimics the morphology of each input tree. For each node of the input structure, the model computes a numerical code by using information of both the node label and, recursively, the code of the sub-trees descending from the current node (*e.g.* the code of the fragment C–OH in Fig. 1 is computed starting from OH node and then encoding the node C using the code of its sub tree OH). This process computes a code of the whole molecular structure (at the root level). The code is then mapped to the output property value. The encoding and mapping free parameters of the neural network are adapted to the task by the learning algorithm on the basis of training examples. By this process, the RNN models a direct and adaptive relationship between the molecular structure and the target property. In particular, the recursive model can learn the encoding of the input structured representation according to the given QSPR task. Hence, RNN can automatically discover by learning the specific structural descriptors (numerical code) for the particular task to be solved. As a result, there is no need for *a priori* definition/calculation and/or selection of input properties.

Experiments

In order to assess the performance of our model, we used a dataset of 126 pyridinium bromides taken from Katritzky *et al.*[9] and used also by Carrera *et al.*,[11] the source of the dataset

being the Beilstein database.[22] The investigated structures, all experimental melting points for each structure, literature sources and some experimental details are reported in Table SI1 of the ESI.† When different melting points were reported for the same structure, the value reported by Katritzky et al.[9] was used. A progressive number (id in Table SI1†) was associated with every structure ordered from the lowest to the highest melting point ranging from 300 to 500 K. The whole set was divided into disjoint training and test sets for learning and validation processes. The validation was performed in two ways. First, we carried out a cross-validation according to Katritzky et al.[9] in which the entire dataset was divided in three subsets (set A = 1st, 4th, . . . 124th compound; set B = 2nd, 5th, . . . 125th compound; set C = 3rd, 6th, . . . 126th compound). Independent experiments were carried out by taking in turn two subsets (84 compounds in all) as the training set, the other one being the test set. The second validation method is a single-validation in which the training/test set were split based on careful consideration of chemical structures. Namely, compounds were selected in order to make the training set representative of the different molecular sizes, topologies, and functional groups of the investigated substituted pyridinium ions. About 20% of the entire dataset (26 compounds) was used as test set.

In order to get a significant appraisal of the results, sixteen trials were carried out for each experiment and the results were averaged over the different trials. Learning was stopped when the maximum error for each compound of the training set was below the preset value (50 K). We chose this threshold by considering the differences among the melting points of the same compound from different sources. For each experiment, the complete list of training and test sets results is given in the ESI (Tables SI2–

5†), where the experimental melting point, the mean calculated melting point, the mean error, and the standard deviation over sixteen trials are reported for each compound.

Results and discussion

The quality of the experimental data used as input is critical for QSAR/QSPR calculations. It is well known that determination of the melting point is not very easy for these kinds of compounds because many of them are hygroscopic and crystallized from different solvents. This experimental uncertainty is the reason for the high threshold (50 K) set in RNN training. Accordingly, we stopped the learning process when the error was below 50 K for each molecule of the training set. Indeed, no significant prediction improvement was obtained when the threshold was set at 20 K.

Table 1 reports the mean absolute error (MAE), the correlation coefficient (R) and the standard deviation (RMS) obtained by an ensemble averaging method over sixteen trials for both training and test sets. The resulting cross-validation output is also shown. When available, results taken from Katritzky et al.[9] and Carrera et al.[11] are reported as well.

It has to be stressed that the main difference between RNN and other QSAR/QSPR methods is that our method is not based on selection of molecular descriptors. Katritzky et al.[9] used molecular descriptors calculated by CODESSA software package.[23] Carrera et al.[11] applied DRAGON[24] and PETRA[25] software packages. Both studies choose the best descriptors applying multiple linear regression,[9] decision trees[11] and counter propagation neural networks (CPGNN)[11] to the whole dataset (126 compounds). It is worth noting that the procedure used

Table 1 Comparison of mean absolute errors (MAE), correlation coefficients (R) and standard deviations (RMS) recorded in our experiments (in bold) with literature data[a]

		Training set			Test set		
		MAE	RMS		MAE	RMS	
	Exp.	(K)	(K)	R	(K)	(K)	R
0	A + B + C	10.07[b]	12.61[b]				
		19.67[c]	24.41[c]				
		8.140[d]	9.910[d]				
1	B + C	**8.40**	**11.38**	**0.9721**	**23.77**	**30.55**	**0.7788**
			22.55[e]		15.95[b]	22.13[b]	
					24.29[c]	29.21[c]	
					14.55[d]	18.17[d]	
						27.10[e]	
2	A + C	**7.84**	**10.04**	**0.9785**	**20.35**	**28.87**	**0.8045**
			23.29[e]		21.76[b]	28.27[b]	
					19.38[c]	23.97[c]	
					14.88[d]	18.70[d]	
						25.53[e]	
3	A + B	**10.49**	**12.93**	**0.9641**	**25.10**	**30.49**	**0.7775**
			23.71[e]		18.61[b]	26.07[b]	
					26.80[c]	31.50[c]	
					17.65[d]	21.96[d]	
						24.05[e]	
4	Cross validation				**23.07**	**29.98**	**0.7872**
5	Single validation	**7.630**	**10.08**	**0.9782**	**19.37**	**23.78**	**0.8725**

[a] Molecular descriptors used to obtain the data from the reported literature sources were selected by applying the methods to the entire dataset (126 molecules). [b] Data from ref. 11, obtained by the decision tree method. [c] Data from ref. 11, obtained by the CPG NN method. [d] Data from ref. 11, best results obtained by an ensemble of 8 decision trees method. [e] Data from ref. 9, obtained by multiple linear regression method.

Downloaded by Lomonosov Moscow State University on 14 October 2010
Published on 08 January 2008 on http://pubs.rsc.org | doi:10.1039/B708123E

for feature selection by Katritzky *et al.*[9] and Carrera *et al.*[11] hampers rigorous comparison of our results with their findings. Indeed, these authors split the dataset into training and test sets only after completing the feature selection process on the whole dataset. In this case, a "feature selection bias"[26–28] can lead to an optimistic estimation of the prediction accuracy. This aspect was also pointed out by Varnek *et al.*[29] in a recent paper in which several linear and nonlinear machine learning methods are applied to the same dataset used in this work. Since we avoided feature selection by construction, this issue does not affect the results of RNN, which was built and tested on disjoint data sets.

In the experiments used for cross validation (experiments 1–3, Table 1), the training set was not chosen by considering the structural features present in the dataset, thus forcing the RNN to make predictive extrapolations. Moreover, the training sets of experiments 1–3 were not the best ones for a structure-based approach. Nonetheless, the test set results are only slightly worse than those reported by Katritzky *et al.*[9] and Carrera *et al.*[11] Because of the small dataset size, the method should be assessed by using a training set that is representative of all analyzed structures. Accordingly, experiment 5 in Table 1 ($R = 0.8725$) should be considered as the most meaningful one to gauge the RNN predictive performance.

Punctual analysis of the training set outputs for single validation (exp. 5, Table 1) and cross validation experiments (exp. 1–3, Table 1) highlight the presence of the same outliers, *i.e.* compounds with an error more than twice the standard deviation, namely *N*-(2-pyridinyl)pyridinium bromide (**27**), *N*-morpholinomethyl-4-methylpyridinium bromide (**38**), *N*-ethoxy-4-methoxypyridinium bromide (**61**), *N*-phenylpyridinium bromide (**93**), *N*-propyl-3-carbamoylpyridinium bromide (**107**), and *N*-(2-oxopropyl)-2-methylpyridinium bromide (**121**). This behaviour for compounds **27**, **38**, **61**, **107** and **121** is very likely attributable to the poor dataset sampling of some structures. For instance, compound **38** is the only one containing a morpholino substituent. On the other hand, the error on compound **93** can be attributed to the uncertainty of the experimental melting point. Indeed, **93** is very hygroscopic and this compound is an outlier also in the multiple linear regression approach.[9]

Analysis of the results of the single validation test set shows the occurrence of two outliers, namely *N*-allyl-4-cyanopyridinium bromide (**72**) and *N*-ethoxycarbonylmethylpyridinium bromide (**80**). It is worth noting that these two compounds are outliers also when present in the training set of A + B (exp. 3, Table 1) and B + C (exp. 1, Table 1) experiments. According to the RNN, these two compounds do not obey the trend of all other ILs. The available information (see Table SI1 in the ESI†) does not allow for an easy explanation of this behaviour.

Conclusions

The reported results indicate that the proposed RNN method coupled with structured domain input can be successfully applied to an ensemble of substituted pyridinium bromide salts.

This RNN provides a good prediction model of the melting point of ionic liquids starting directly from their molecular structure, thus avoiding the use of dedicated molecular descriptors. Moreover, the devised method for the representation of cyclic structures as labelled rooted ordered trees avoids the need for specific labels for each different cycle. This approach compromises the most detailed representation of the dataset with the generality of description without any significant loss of accuracy.

Acknowledgements

Financial support by MIUR is gratefully acknowledged.

References

1 R. A. Sheldon, *Green Chem.*, 2005, **7**, 267.
2 T. Welton, *Chem. Rev.*, 1999, **99**, 2071.
3 C. Chiappe and D. Pieraccini, *J. Phys. Org. Chem.*, 2005, **18**, 275.
4 T. Welton, *Coord. Chem. Rev.*, 2004, **248**, 2459.
5 *Ionic Liquids in Synthesis*, Wiley-VCH Verlag GmbH & Co, KGaA, Weinheim, 2002.
6 T. S. Handy, *Curr. Org. Chem.*, 2005, **9**, 959.
7 S. Zhang, N. Sun, X. He, X. Lu and X. Zhang, *J. Phys. Chem. Ref. Data*, 2006, **35**, 1475.
8 A. R. Katritzky, R. Jain, A. Lomaka, R. Petrukhin, M. Karelson, A. E. Visser and R. D. Rogers, *J. Chem. Inf. Comput. Sci.*, 2002, **42**, 225.
9 A. R. Katritzky, R. Jain, A. Lomaka, R. Petrukhin, M. Karelson, A. E. Visser and R. D. Rogers, *J. Chem. Inf. Comput. Sci.*, 2002, **42**, 71.
10 D. Eike, J. Brennecke and E. Maginn, *Green Chem.*, 2003, **5**, 323.
11 G. Carrera and J. Aires-de-Sousa, *Green Chem.*, 2005, **7**, 20.
12 *Handbook of Molecular Descriptors*, Wiley-VCH Verlag GmbH & Co, KGaA, Weinheim, 2002.
13 A. M. Bianucci, A. Micheli, A. Sperduti and A. Starita, *Appl. Int. J.*, 2000, **12**, 117.
14 A. Micheli, A. Sperduti, A. Starita and A. M. Bianucci, *J. Chem. Inf. Computut. Sci.*, 2001, **41**, 202.
15 L. Bernazzani, C. Duce, A. Micheli, V. Mollica, A. Sperduti, A. Starita and M. R. Tiné, *J. Chem. Inf. Computut. Sci.*, 2006, **46**, 2030.
16 C. Duce, A. Micheli, A. Starita, M. R. Tiné and R. Solaro, *Macromol. Rapid Commun.*, 2006, **27**, 712.
17 C. Duce, A. Micheli, A. Starita, M. R. Tiné and R. Solaro, *J. Math. Chem.*, in press.
18 C. Bertinetto, C. Duce, A. Micheli, R. Solaro, A. Starita and M. R. Tiné, *Polymer*, 2007, **48**, 7121.
19 A. Sperduti and A. Starita, *IEEE Trans. Neural Networks*, 1997, **8**, 714.
20 A. Micheli, A. Sperduti, A. Starita and A. M. Bianucci, *Proceedings of the IJCNN—International Joint Conference on Neural Networks*, 2001, **4**, 2732.
21 http://www.acdlabs.com/iupac/nomenclature/.
22 The Beilstein Database, MDL Information System GmbH, http://www.Beilstein.com.
23 A. R. Katritzky, V. S. Lobanov, M. Karelson, *CODESSA Reference Manual. Version 2.0*, University of Florida, 1996.
24 DRAGON: http://www.disat.unimib.it/chm/dragon.htm.
25 PETRA: http://www2.chemie.uni-erlangen.de.
26 A. Miller, *Subset Selection in Regression*, Chapman & Hall/CRC, II edn, 2002.
27 P. Zhang, *Biometrika*, 1992, **79**, 741.
28 C. Ambroise and G. J. McLachlan, *Proc. Natl. Acad. Sci. U. S. A.*, 2002, **99**, 6562.
29 A. Varnek, N. Kireeva, I. V. Tetko, I. I. Baskin and V. P. Solov'ev, *J. Chem. Inf. Model.*, 2007, **47**, 1111.

This journal is © The Royal Society of Chemistry 2008   *Green Chem.*, 2008, **10**, 306–309 | 309

Glycine betaine as a renewable raw material to "greener" new cationic surfactants

Fabrice Goursaud,[a] Mathieu Berchel,[a] Jérôme Guilbot,[a] Nathalie Legros,[a] Loïc Lemiègre,[a] Jérôme Marcilloux,[b] Daniel Plusquellec[a] and Thierry Benvegnu*[a]

This article describes the synthesis, properties and potential applications of new cationic surfactants based on natural glycine betaine and vegetable oils as renewable raw materials. Convenient procedures were developed on a multigram scale using environmentally friendly starting materials to provide glycine betaine-derived esters and amides. Some readily biodegradable formulations containing ester-type surfactant were found to exhibit remarkable emulsifying properties for road making applications and they are now under industrial development using green solvent-free processes. Bipolar bolaamphiphiles possessing two cationic glycine betaine moieties were synthesized as monomers for the preparation of original drug delivery liposomal systems.
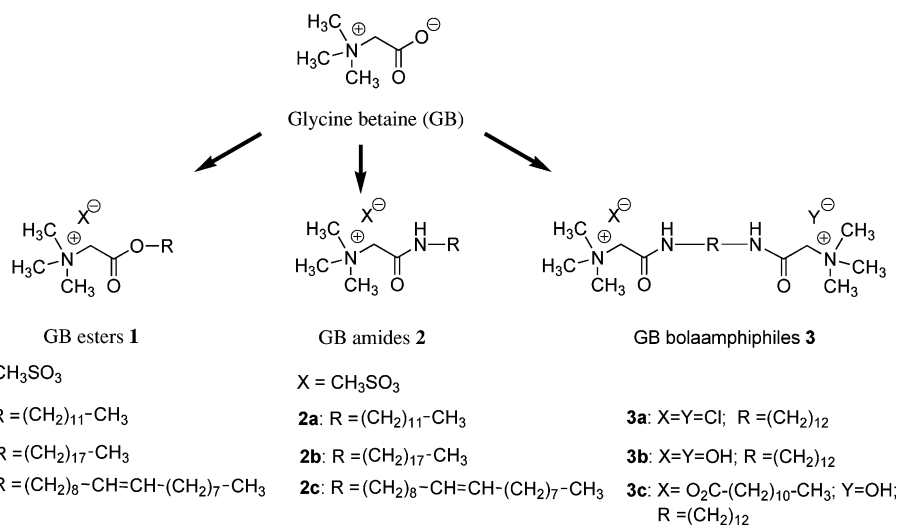
Introduction

Cationic surfactants fall into several categories depending on the nature of their cationic polar heads. Some of them have functional groups capable of being protonated and show cationic properties particularly in acidic media (for example amine types) while others, such as quaternary ammonium salts, exhibit a permanent positive charge.[1] In household products, the cationic surfactants are primarily applied in fabric softeners, hair conditioners, and other hair preparations. Other applications of cationic surfactants include disinfectants and biocides, emulsifiers, wetting agents, and processing additives. By volume, the most important cationic surfactants in household products are the alkyl ester ammonium salts that are used in fabric softeners (esterquats). These surfactants were generally found to have an acute aquatic toxicity and their poor biodegradability has been a serious disadvantage. Due to their toxicity, some cationic surfactants such as dimethyldialkylammonium salts present in most fabric softeners have seen their use limited, even abandoned, in certain European countries like Germany and the Netherlands. These undesirable effects on environment, coupled with consumer demand for "greener" products, are leading manufacturers to focus on the production of cationic surfactants from alternative, less harmful raw materials in an effort to reduce environmental pollution at all levels. Many recently-developed surfactants are an attempt to satisfy the modern consumers' desire for products to be "more natural". Like most plant-based products, surfactants based on renewable raw materials (RRM) are characterized by their positive impact on the environment,

biodegradability, low or no toxicity and innocuousness for human health.[2] In addition, the use of renewables in surfactant production can contribute to save fossil resources, such as crude oil and natural gas, and to the reduction of fossil carbon dioxide emissions (CO_2) and hence, could be part of a strategy to mitigate the greenhouse gas effect. There is a good chance that the use of biomass could contribute to these goals because the quantity of carbon dioxide originated from biomass is equivalent to the amount which was previously withdrawn from the atmosphere during growth. Finally, the natural origin of these surfactant molecules is a significant communication and marketing asset.

Glycine betaine (GB), a natural low expense substance possessing a quaternary trimethylalkylammonium moiety and a carboxylate function, constitutes a prime raw material for the preparation of biodegradable and biocompatible cationic surfactants (Scheme 1). Accounting for 27% in weight of molasses of sugar beet, and obtained after extraction of saccharose, it remains currently a little developed by-product of the sugar-industry. Within this context, the aim of this study was to produce novel GB esters **1** and amides **2** (Scheme 1) from tropical oils (copra, palm kernel: C_{12} lauric alkyl chain) or European oils (sunflower, rapeseed: C_{18} stearic and oleic alkyl chains), conveniently, economically and with an environmentally acceptable process (no solvent, no waste). The introduction of an ester-type or an amide-type linkage between the hydrophilic moiety (polar head group) and the hydrophobic backbone (alkyl chain) should ensure a high biodegradability. In particular, fatty chains with 18 carbon atoms derived from European vegetable oils were used for their emulsifying properties compatible with numerous industrial and technical applications (road bitumen emulsifying applications, emulsions for uses in cosmetics). Additionally, the covalent linking of two cationic glycine betaine moieties through a polymethylene diamine was envisaged to yield original dicationic bolaamphiphiles **3** (Scheme 1). Bolaamphiphiles are molecules with two hydrophilic heads connected by one or two

[a]ENSCR, UMR CNRS 6226 Sciences Chimiques de Rennes, Equipe "Chimie organique et supramoléculaire", Avenue du Général Leclerc, 35700, Rennes, France. E-mail: thierry.benvegnu@ensc-rennes.fr; Fax: +33 (0)2 23 23 80 46; Tel: +33 (0)2 23 23 80 60
[b]EIFFAGE Travaux Publics, 2/12, rue Hélène Boucher-B. P. 92, 93337, Neuilly sur Marne, France

Glycine betaine (GB)

GB esters **1**

X = CH₃SO₃

1a: R =(CH₂)₁₁−CH₃

1b: R =(CH₂)₁₇-CH₃

1c: R =(CH₂)₈−CH=CH−(CH₂)₇-CH₃

GB amides **2**

X = CH₃SO₃

2a: R =(CH₂)₁₁−CH₃

2b: R =(CH₂)₁₇-CH₃

2c: R =(CH₂)₈−CH=CH−(CH₂)₇-CH₃

GB bolaamphiphiles **3**

3a: X=Y=Cl; R =(CH₂)₁₂

3b: X=Y=OH; R =(CH₂)₁₂

3c: X= O₂C-(CH₂)₁₀-CH₃; Y=OH; R =(CH₂)₁₂

Scheme 1 Ester/amide-type surfactants **1–2** and bolaamphiphiles **3** derived from glycine betaine.
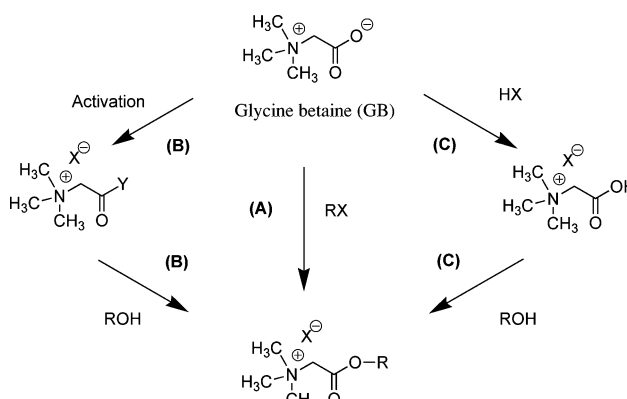
hydrophobic chains. In recent years, this kind of compound has drawn more and more attention[3] in both fundamental investigations and applications. Compared to conventional monopolar surfactants, these bipolar compounds exhibit characteristic interfacial properties and aggregation behaviours. Usually the critical micellization concentrations are larger,[4–6] and the sizes of the micelles are smaller[5,6] than those of monopolar surfactants of the same carbon number. Moreover, they are supposed to self-assemble into stable monolayer lipid membranes (MLM) reproducing the unusual architecture of natural archaeal bipolar lipids.[3,7] The introduction of various counter-ions (chloride, hydroxide or laurate) was envisaged in order to evaluate the influence of this structural parameter on aggregation behaviours.

Results and discussion

Synthesis of cationic GB surfactants

Three synthetic pathways have been envisaged for the esterification reaction of glycine betaine as outlined in Scheme 2. In pathway A, the introduction of the ester linkage is achieved by the reaction of the starting GB with electrophilic reagents such as alkyl halides and their tosylate or chloroformate counterparts. According to pathway B, GB esters are produced through a strategy based on a preliminary activation of GB which is then reacted with fatty alcohols. Conversely, acid-catalyzed esterification reaction between GB and fatty alcohols (pathway C) proceeds in one-step *via* the *in situ* protonation of the carboxylate function.

The latter strategy is more advantageous in so far as it can use only environmentally friendly starting materials, without any additional solvent. First, we found that methane sulfonic acid (MSA) was the best candidate for a green synthetic route to GB esters. Indeed, MSA is an easy-to-handle liquid, often recyclable and less aggressive than sulfuric acid or HF. It is considered as readily biodegradable, ultimately forming sulfates and carbon dioxide. In fact, MSA is considered to be a natural product and in part of the natural sulfur cycle.[8] The process we developed in this work is reported in Scheme 3.

Glycine betaine (GB)

Activation (B)

HX (C)

RX (A)

ROH (B)

ROH (C)

Scheme 2 Synthetic pathways A–C for the preparation of GB ester surfactants **1**.

Glycine betaine (GB)

CH₃SO₃H
ROH
130°C
reduced pressure

H₂O

1a: R =(CH₂)₁₁−CH₃

1b: R =(CH₂)₁₇-CH₃

1c: R = (H₂C)₈−CH=CH−(CH₂)₇-CH₃
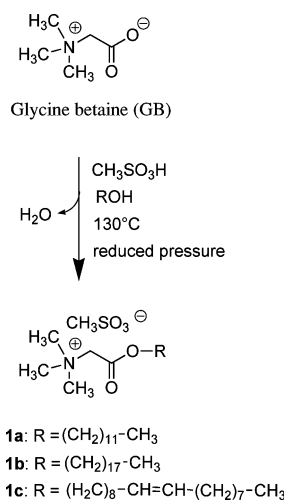
Scheme 3 Methane sulfonic acid-catalyzed synthesis of GB ester-type surfactants **1**.

Esterification reactions of GB were carried out with saturated or unsaturated fatty alcohols of various lengths (lauric, stearic or oleic alcohols) at 130 °C, in the presence of methane sulfonic acid and under reduced pressure in order to eliminate the water

Table 1 Esterification reactions of GB

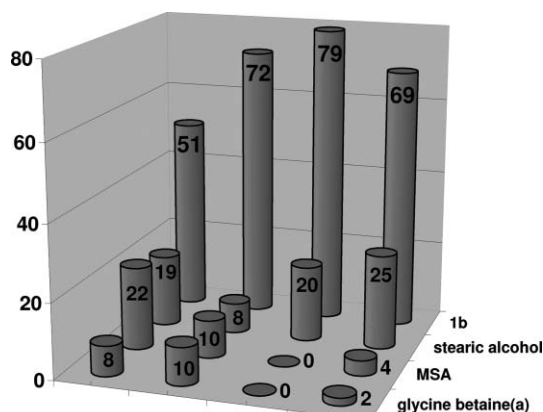| Entry	Fatty alcohol; equiv.	MSA; equiv.	Conditions	Yield (%)
1	Lauric; 2.0	2.0	5–10 mbar, 3 h	95
2	Lauric; 1.0	1.1	25 mbar, 2.5 h	50
3	Lauric; 2.0	1.5	5–10 mbar, 7 h	50
4	Stearic; 1.2	2.0	50 mbar, 7 h	60
5	Stearic; 1.2	2.5	50 mbar, 7 h	70
6	Oleic; 1.4	2.5	50 mbar, 7 h	85

formed all through the reaction. For the laurate derivative **1a**, reaction using 2 equiv. of lauric alcohol and 2 equiv. of MSA under 5–10 mbar gave the expected ester in an excellent 95% yield (Table 1). A decrease of the MSA amount (1.1–1.5 equiv.) dramatically lowers the reaction yield. The work-up involved the neutralization of MSA used in excess with an aq NaHCO$_3$ solution followed by the addition of diethyl ether in which lauric alcohol is soluble. The layers were separated and the aqueous layer was extracted with *n*-butanol/ethyl acetate. After concentration to dryness and recrystallization, the ester was isolated as a white solid. In the case of C$_{18}$ derivatives, it was found that the optimal conditions correspond to a GB : ROH : MSA ratio of 1 : 1.2 (or 1.4) : 2.5. The best yields we were able to obtain for the synthesis of GB stearate and oleate esters **1b–c** were 70% and 85%, respectively when the reaction mixtures were stirred under reduced pressure (50 mbar) for 7 h (Table 1).
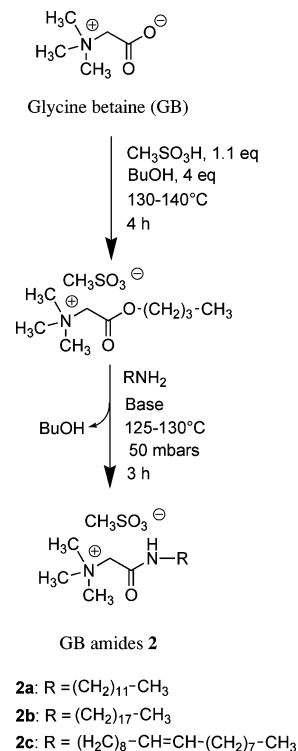
Due to the insolubility of the reaction mixtures in water, alternative purification procedures of C$_{18}$ surfactant **1b** were envisaged: processes based upon precipitation in organic solvents as diethyl ether, *n*-butanol or ethanol or use of crude reaction mixtures, furnished a large variety of emulsifying formulations (Fig. 1) characterized by various compositions (several controlled ratios of residual free GB, C$_{18}$ fatty alcohol, MSA). It is noteworthy that treatment of the mixtures with ethanol or *n*-butanol led to the total or nearly quantitative removal of residual GB and MSA. Direct flash chromatography of the crude mixture was also envisaged to isolate the surfactant with a high purity. The scale-up of one oleic ester-based mixture (weight ratio:

1c/oleic alcohol/MSA/GB = 49/33/15/3) obtained without any purification (solvent-free process) was performed on a 60 kg scale for road making applications. The resulting formulation was obtained by simple warming of the reaction mixture to room temperature without any additional treatment and no degradation of the oleic acid double bond was observed (notably in NMR and mass spectrum experiments) under the acidic conditions.

GB amides were prepared following a one-pot two step procedure: first, glycine betaine reacted with *n*-butanol in the presence of MSA as catalyst at 130–140 °C for 3–4 h: the solvent was distilled out during heating (Dean–Stark apparatus). After cooling, the short butyl chain is replaced by a longer chain in a base-catalyzed aminolysis reaction of the butylester using fatty amines, especially lauric amine or C$_{18}$ stearic and oleic amines. The reaction is then carried out under reduced pressure (50–100 mbar) at 125–130 °C in order to eliminate the butanol formed all through the reaction (Scheme 4).

Fig. 1 Weight ratio (%) of the components in the mixtures obtained without or after purification relative to entry 5 (Table 1) measured by ¹H NMR (±5%). From left to right: crude reaction mixture; after precipitation in diethyl ether; after precipitation in ethanol; after precipitation in *n*-butanol. (a) Protonated form of GB, ((CH₃)₃N⁺–CH₂C(O)OH/CH₃SO₃⁻).

Scheme 4 Synthesis of GB amide-type surfactants **2**.

2a: R = (CH₂)₁₁–CH₃
2b: R = (CH₂)₁₇–CH₃
2c: R = (H₂C)₈–CH=CH–(CH₂)₇–CH₃

This two stage-process includes the recycling of butanol which is used both as a reagent and as a solvent. The addition of an organic base (triethanolamine, TEA or dibutylamine, DBA) into

Table 2 Aminolysis of GB butylester

| Entry	Fatty amine; equiv.	Base; equiv.	Yield (%)
1	Lauric; 1.1	TEA; 0.2	80
2	Stearic 1.2	DBA; 0.3	60
3	Oleic; 1.2	—	65

the reaction mixture allows the neutralization of the excess MSA, thus inhibiting the partial protonation of the fatty amine. As a stronger base, dibutylamine was used instead of triethanolamine for the less reactive C_{18} stearic amine (Table 2). GB amide **2b** was purified by precipitation in diethyl ether (**2b** is soluble in ethanol and *n*-butanol; weight ratio: **2b**/dibutylamine and stearic amine salts/GB = 59/20–30/11–21) or direct column flash chromatography of the crude reaction mixtures. In the case of compound **2c**, only the crude mixture (**2c**/oleic amine salt/oleic amine/GB = 59/34/<1/6) and pure **2c** resulting from flash chromatography were available because of the high solubility of oleic amine and amide **2c** in organic solvents.

GB bolaamphiphile **3a** was synthesized by *N*-acylation of commercially available 1,12-dodecamethylene diamine with 2 equiv. of the acyl chloride derivative **4**[9] of glycine betaine in CH_2Cl_2 in the presence of triethylamine (Scheme 5) in a 73% yield. As reported for monocationic GB amides **2**, the development of a greener approach based on aminolysis of the GB butylester with α,ω-diamines are now under investigation. The cationic bolaamphiphile hydroxide **3b** was prepared by ion-exchange (DOWEX 550 A resin) with a basic ion exchanger (OH⁻) from the corresponding chloride **3a** in a nearly quantitative yield (96%). The quantitative counter-ion exchange was shown by silver nitrate titration. Our attention was next directed toward the synthesis of the more lipophilic unsymmetrical bolaamphiphile **3c**. This compound which results from the exchange of one hydroxide counter-ion at one end of the bipolar surfactant by the fatty lauric chain, is supposed to self-assemble into monolayer membranes and the presence of two counter-ions with different lipophilicity is expected to induce membrane curvature. Mixing lauric acid with C_{12} bolaamphiphile hydroxide **3b** (1 : 1 molar ratio) in $CHCl_3$/MeOH (1 : 1) for 20 min at room temperature led, in 90% yield to unsymmetrical bolaamphiphile **3c**. The new compound resulting from the acid–base mixture was isolated after precipitation in EtOAc and ¹HNMR data (peak

integration) confirmed the 1 : 1 ratio between bolaamphiphile and lauric acid. Reaction using 2 equiv. of lauric acid gave the unsymmetrical compound **3c** in a lower yield (16%) due to the formation of the symmetrical bolaamphiphile possessing two fatty anions instead of hydroxide counter-ions: this additional more lipophilic product was found to be soluble in EtOAc unlike derivative **3c**.

Chemical hydrolysis

Hydrolysis of GB ester **1b** was investigated using GC to monitor the appearance of the resulting fatty alcohol (see Experimental section). The degree of hydrolysis was evaluated at different times and pH values (Fig. 2). Surfactant **1b** was found to be extremely stable against acid. Conversely, a rapid hydrolysis of GB ester was observed under alkaline conditions. As previously reported,[10] acid hydrolysis would involve protonation of the carbonyl oxygen, forming a dicationic intermediate that would be energetically very unfavourable. In basic conditions, the very electrophilic carbonyl carbon (presence of the strongly electron-withdrawing quaternary ammonium) would be prone to nucleophilic attack by hydroxide ions. This pronounced pH dependency makes GB esters interesting as so-called cleavable surfactants.[11] GB amide-type surfactants **2** did not exhibit such similar pH sensitivity in particular under neutral and basic conditions. Within this context, we envisaged to take advantage
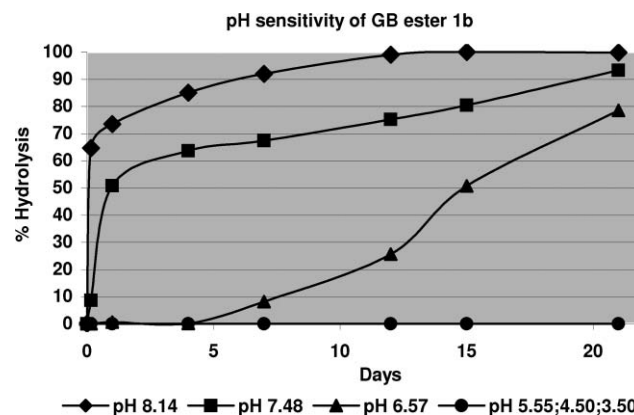
Fig. 2 Hydrolysis rate of GB ester **1b** at different pH values (phosphate-citrate buffers) and with time.
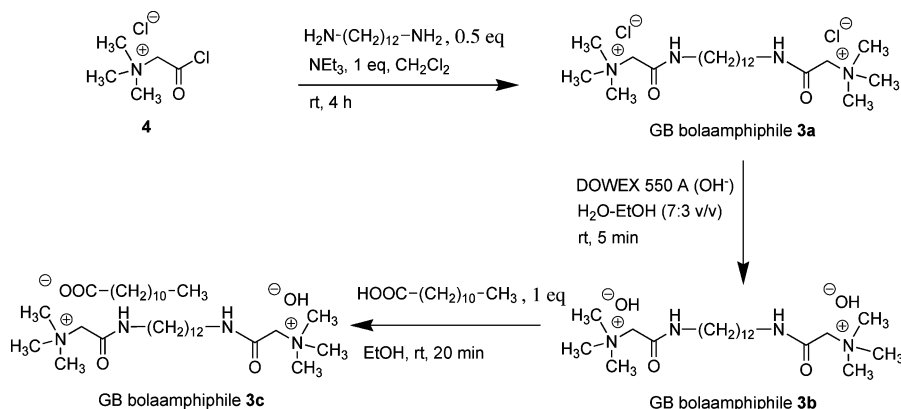
Scheme 5 Synthesis of GB bolaamphiphiles **3**.

of these characteristics to control the speed at which bitumen emulsions could break over mineral aggregates (see part relative to emulsifying properties).

Surface tension measurements

Surfactants tend to partition preferentially at the interface between fluid phases such as air/water interfaces. The formation of such ordered molecular film at the interface lowers the interfacial tension and is responsible for the unique properties of surfactant molecules. One of the most widely used indexes for evaluating surfactant activity is the critical micelle concentration (c.m.c.). The c.m.c. is the solubility of a surfactant within an aqueous phase or the minimum surfactant concentration (C) required for reaching the lowest interfacial or surface tension value γ. At concentrations above the c.m.c., surfactants associate readily to form micelles. The c.m.c. value is estimated from the inflection point in the γ *vs.* log C curve. As shown in Fig. 3 and Table 3, the c.m.c. values of both GB esters and amides decreased with increasing the alkyl chain length. In particular, the c.m.c. of oleic **1c** solution was lower than for its saturated stearic counterpart **1b**. c.m.c. values were found to be independent of the ester or amide linkage in the saturated C_{12} and unsaturated C_{18} series, unlike in the saturated C_{18} alkyl chain. Except for **2a**, GB esters and amides reduced the surface tension at values characteristic to quite significant surfactant activities and compatible with emulsifying applications for the C_{18} derivatives (see part relative to emulsifying properties).

**Table 3** Surface properties of GB esters **1**, amides **2** and bolaamphiphiles **3**

Compound	c.m.c./mmol L^{-1}	γ /mN m^{-1}
1a	1.2	32
1b	0.794	37
1c	0.1	37
2a	1.2	50
2b	0.14	36
2c	0.12	36
3a	5.0	42
3b	—	48[a]
3c	—	36[b]

[a] γ at 10 mmol L^{-1}. [b] γ at 1 mmol L^{-1}.

As expected, with bipolar bolaamphiphile **3a** which possesses a similar C_{12} lipophilic domain as in monocationic surfactants **1a** and **2a**, the c.m.c. value was larger due to the presence of the additional hydrophilic GB polar head (Table 3). Bolaamphiphiles **3b** and **3c** did not form micelles even at concentrations as high as 10 or 1 mmol L^{-1}. Hydroxide counter-ions thus seem to increase the hydrophile character of the monomers as well as the hydration of their positively charged heads in an important way that prevents the formation of micelles. The presence of one lauric acid chain in compound **3c** increased the effective hydrophobic chain volume of the molecules, thereby increasing the critical packing parameter p[12,13] to satisfy the requirement for the formation of vesicles instead of smaller micellar aggregates (see part relative to supramolecular membrane assemblies).

Emulsifying properties for road making applications

In road construction, bitumen products are typically applied in conjunction with a mineral aggregate. The good adhesion properties of bitumen to aggregates allow it to act as a binder, while the aggregate provides mechanical strength. At ambient temperature, bitumen is a highly viscous to an almost solid substance that rends it extremely difficult to work with. Bitumen can, however, be transferred into a workable state by applying heat, by blending with petroleum solvents or as an emulsion of bitumen in water. Working with bitumen at high temperatures (150–180 °C) is very dangerous, with a risk of serious burns. It also requires costly equipment for heating, storage and application of the bitumen, which moreover must be performed on-site. Bitumen that has been mixed with petroleum solvents is more workable. Nevertheless, the solvents, usually kerosene, are fire hazards and produce hydrocarbon emissions when they evaporate, contributing to air pollution. In contrast, bitumen emulsions can be applied without a need for heating (although they are still prepared at high temperatures), they do not have the handling and the environmental hazards associated with hot mixes. Bitumen emulsions improve also adhesion to aggregates, and can be applied in a good range of weather conditions.[14] The bitumen is dispersed throughout the continuous water phase as minute particles typically 0.1–5 μm in diameter, as an oil in water emulsion. Bitumen–water emulsions must break in a controlled manner upon laying with the mineral aggregate. Various technologies for road making are used, as a function
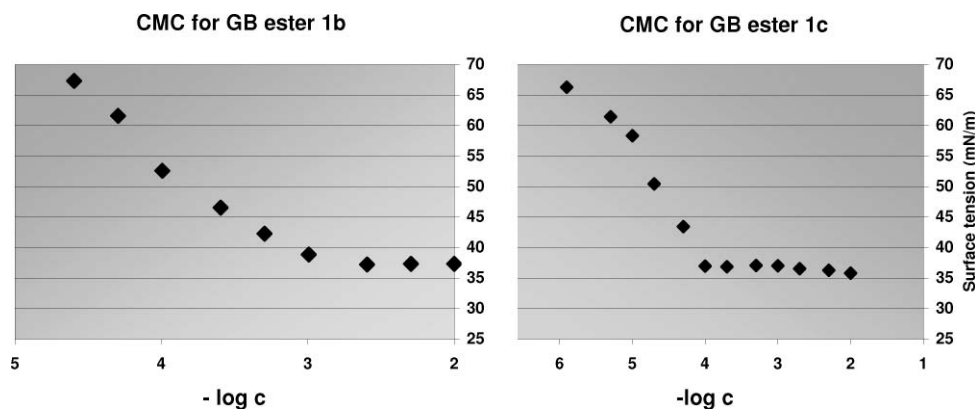
Fig. 3 Surface tension curves of GB esters **1b** and **1c** at room temperature.

of the speed at which emulsion breaks over mineral aggregates: surface dressing with rapid breaking emulsions (the emulsion is sprayed onto the road surface, chippings are spread on top and normally rolled to ensure proper embedment and alignment) and cold mixes (this category covers several different technologies among which open graded storable cold asphalt for patch working, combined cement/bitumen emulsion mixes and dense graded cold asphalt for wearing course) that require slower breaking emulsions. The emulsifier in a bitumen emulsion system has thus three functions: it reduces the interfacial tension between bitumen and water, stabilizes the emulsion and assists the adhesion of the bitumen. Cationic emulsifiers for bitumen emulsions are usually used in Europe (2 000 000 tonnes of bitumen emulsion produced per year), particularly in France which produces 50% of the total European bitumen emulsion (0.2 to 2% of surfactants). Commercially available cationic emulsifiers are mainly surfactants that are ionised in an acidic environment and include polyamines, amidoamines and imidazolines, which are the most widely used emulsifiers. These cationic surfactants that come entirely or partially from petrochemicals, were found to exhibit a low biodegradability and a high aquatic toxicity. Within this context, C_{18} GB esters **1b–c** and amides **2b–c** represent a new family of plant-derived emulsifiers that could limit environmental impact. Different GB-derived emulsifier formulations were tested in the formation of road bitumen emulsions, especially pure surfactants **1b**, **1c**, **2b**, and **2c** or the corresponding crude formulations resulting from non-purified reaction mixtures. Emulsion particle size, rupture index, pseudo-viscosity, stability measurements were performed to highlight the influence of each surfactant formulation (Tables 4 and 5).

These GB ester- or amide-based formulations were found to have chemical stability, viscosity, bitumen emulsifying properties (strong adhesivity, rapid emulsion breaking), very promising for their uses in surface dressing technologies (see Experimental section). Surprisingly, the higher chemical stability of amide surfactants did not slow down the emulsion breaking during the interactions between the emulsion particles and the mineral aggregates. When in contact with acidic bitumen emulsions, some mineral materials as limestone lead to a rapid pH increase thereby destabilising pH cleavable emulsifiers. Seemingly, this pH increase phenomenon did not operate in a sufficient way to modify the behaviour of bitumen emulsions as a function of emulsifier pH sensitivity.

The GB ester **1c**-containing formulation based on crude reaction mixture rapidly emerged as the best candidate for an industrial production of emulsion. Firstly, this crude product was found to be as efficient as pure compound **1c**; secondly, it exhibited higher water-solubility and liquidity than the corresponding pure solid compound **1c**. Additionally, as stated in the Experimental section, the aerobic ultimate biodegradability of emulsifier **1c** as a crude reaction mixture was evaluated applying the "CO_2 evolution" test. This test is included in the European Regulation on biodegradability of detergent surfactant.[15] A surfactant is considered as readily biodegradable if the biodegradation level exceeds 60% within 28 days in this test. High biodegradation level (70%) was reached that allowed this formulation to be classified as readily biodegradable. Finally, after an experimental phase (1000 meter road coatings using a bitumen emulsion based on the crude product **1c**), the project arrives today at the stage of industrial development for the production, on a large scale, of this new vegetable-derived surfactant, called Emulgreen®.[16] Additional applications of these novel biodegradable cationic surfactants in cosmetic formulations (shampoos, hair conditioners, body washes, creams) are currently being developed.

Supramolecular membrane assemblies

The self-assembling properties of bolaamphiphiles **3** as well as the characterization of their supramolecular aggregates in dilute aqueous media, were studied by X-ray scattering (XRS)

Table 4 Characteristics of bitumen emulsions of different purities derived from GB esters **1b** and **1c**

Emulsion composition	1b	1b	1c	1c	Specifications for 65% rapid breaking emulsion
Bitumen 160/220 (%)	65	65	65	65	
Pure emulsifier (%)	0.25	—	0.25	—	
Crude emulsifier (%)	—	0.50	—	0.52	
HCl (%)	0.05	0.00	0.05	0.05	
Water (%)	34.7	34.5	34.7	34.43	
Standard methods					
Rupture index (NF T 66.017)	55	51	61	60	<100
Adhesivity (NF T 66.018)					
1st part (RT) (%)	90	75	100	100	≥90
2nd part (60 °C) (%)	90	75	100	100	≥75
Median diameter/µm					
Internal method	23.5	25.0	7.5	9.8	—
pH emulsion	2.7	1.8	3.1	2.0	—
Stability to storage (NF T 66.022)	8.5	4.3	0.8	2.9	<5
Homogeneity (NF T 66.016)					
Particles					
>0.63 mm (%)	0.01	0.01	0.17	0.05	<0.1
0.16 to 0.63 mm (%)	0.04	—	0.16	0.09	<0.25
Pseudo viscosity STV at 25 °C (NF T 66.020)	—	15	52	17	>6
Water content (%) (NF T 66.023)	35.3	34.7	34.7	35.0	34 to 36

Table 5 Characteristics of bitumen emulsions of pure GB amide **2b** and crude GB amide **2c**

Emulsion composition	2b	2c	Specifications for 65% rapid breaking emulsion
Bitumen 160/220 (%)	65	65	
Pure emulsifier (%)	0.25	—	
Crude emulsifier (%)	—	0.45	
HCl (%)	0.05	0.05	
Water (%)	34.7	34.5	
Standard methods			
Rupture index (NF T 66.017)	44	59	100
Adhesivity (NF T 66.018)			
1st part (RT) (%)	90	100	$\geq$90
2nd part (60 °C) (%)	90	100	$\geq$75
Median diameter/μm			
Internal method	19.9	3.8	—
pH emulsion	2.9	2.9	—
Stability to storage (NF T 66.022)	4.0	1.1	<5
Homogeneity (NF T 66.016)			
Particles			
>0.63 mm (%)	0.09	0.03	<0.1
0.16 to 0.63 mm (%)	0.11	0.13	<0.25
Pseudo viscosity STV at 25 °C (NF T 66.020)	55	33	>6
Water content (%) (NF T 66.023)	35.0	35.0	34 to 36

and freeze fracture electron microscopy (FFEM). Compounds **3a** and **3b** did not display any lamellar lyotropic mesophase probably caused by their high hydrophilic character and an unfavourable critical packing parameter p (p is described as $v/a_0 l_c$, where v is the surfactant tail volume, l_c is the tail length, and a_0 is the equilibrium area per molecule at the aggregate surface; $0 \leq p \leq 1/3$ for spherical micelles, $1/3 \leq p \leq 1/2$ for cylindrical micelles, and $1/2 \leq p \leq 1$ for bilayer structures[12,13]). Conversely, the presence of the lauric acid-derived counter-ion in compound **3c** resulted in an increase of p, which was more favourable to the formation of lamellar structures. Upon the addition of 40–50% water, the X-ray diffraction pattern of **3c** displayed two sharp reflections ($h = 1,2$) in the low-angle region and a sharp reflection at 4.2 Å that correspond to the formation of a lamellar L_β phase in which chains are ordered. Above the transition temperature (45 °C), bolaamphiphile **3c** formed a L_α lamellar phase of 36 Å dimension characterized by two reflections ($h = 1,2$) in the low-angle region and a broad diffuse band in the wide angle region ($1/4.5$ Å) which is ascribed to the presence of disordered chains. In more dilute aqueous media, unsonicated suspension of bolaamphiphe **3c** gave at room temperature vesicles which are not fractured in the usual way along the midplane of the membrane (Fig. 4a). These vesicles were cross-fractured; that-is-to-say, the fracture propagated across the membrane, generating more or less distorted circles.[17] The absence of a fracturable midplane in the membrane indicates that the bolaamphiphile spans the membrane to form a monolayer. The cross-fracture behaviour has further been shown to be indicative for monomolecular vesicular membranes and membrane spanning lipid molecules.[18,19] When the preparations were sonicated and frozen from 60 °C (> transition temperature), standard convex and concave surfaces characteristic of bilayered vesicular aggregates were observed (Fig. 4b). The presence of these fracture midplanes in the membrane indicates that most of the bolaamphiphiles **3c** adopt a U-bent shape to form bilayers.

(a)

(b)
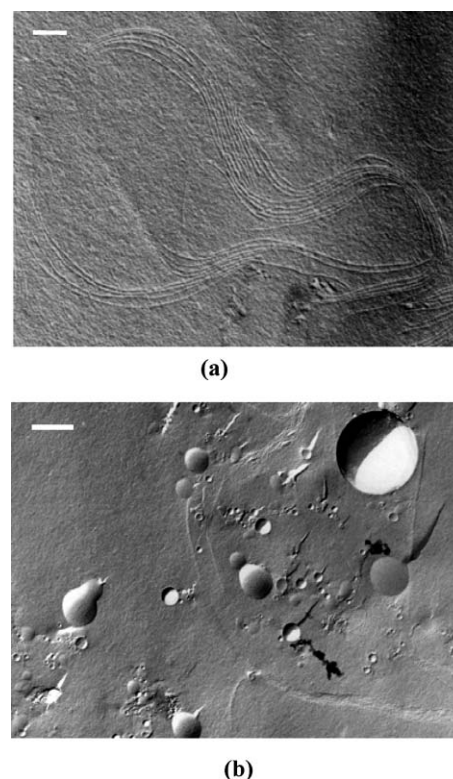
Fig. 4 Freeze fracture electron microscopy of bolaamphiphile **3c**: (a) 20 °C, without sonication, bar is 90 nm; (b) 60 °C, after sonication, bar is 280 nm.

The transition from monolayered to bilayered vesicles by heating can be attributed to the difference in stiffness of the alkyl chains, the rigid chains of the L_β lamellar phase inhibiting the adoption of a U-bent conformation in vesicle membrane.

This temperature-dependent behaviour represents an innovative approach for the control of the stretched or the U-shaped conformation of the bolaamphiphiles in vesicles. Applications of these monolayer/bilayer systems for the encapsulation and the controlled release of negatively charged materials including nucleic acids are under investigation.

Experimental

General

All commercially available chemicals were used without further purification. Unless otherwise noted, nonaqueous reactions were carried out under a nitrogen atmosphere. Analytical TLC was performed on Merck 60 F254 silica gel nonactivated plates. A solution of 5% H_2SO_4 in EtOH was used to develop the plates. Merck 60 H (5–40 μm) silica gel was used for column chromatography. Fast-atom bombardement (FAB, m-nitrobenzylic alcohol as the matrix) and electropositive electrospray (ESI+) mass spectra were acquired on a MS/MS TOF mass spectrometer. ^{1}H and ^{13}C NMR spectra were recorded at 400 and 100 MHz, respectively on a Bruker instrument. FTIR were recorded on a Thermo Nicolet instrument (Avatar 320 FT-IR).

Synthesis of cationic GB surfactants 1–3. Dodecylbetainate methanesulfonate **1a**. Dodecanol (2.23 g, 12.0 mmol, 2.0 equiv.) was added to a suspension of dried glycine betaine (700 mg, 6.0 mmol, 1.0 equiv.) in methanesulfonic acid (1.15 g, 12.0 mmol, 2.0 equiv.). The reaction mixture was gradually heated to 130 °C under reduced pressure (5–10 mbar) to remove the water formed by the reaction. After 3 h, the reaction mixture became homogeneous and the brown mixture was cooled down to room temperature and to atmospheric pressure. Solid NaHCO$_3$ (510 mg, 6.0 mmol) and water (70 mL) were added. The excess of fatty alcohol was extracted with Et$_2$O and the compound **1a** was then extracted with (nBuOH/EtOAc: 1 : 1). The combined organic phases were washed with water and were evaporated under reduced pressure. The crude material was purified by recrystallisation from EtOAc/EtOH to obtain pure compound **1a** (2.16 g, 5.7 mol, 95%) as a white solid. mp 103–104; ν_{max}(nujol)/cm^{-1} 1755 (C=O); δ_H(400 MHz; DMSO-d$_6$) 0.85 (3H, t, J 6.8, CH$_3$), 1.24 (18H, s, (CH_2)$_9$CH$_3$), 1.60 (2H, s, CH_2CH$_2$O), 2.30 (3H, s, CH$_3$SO$_3^-$), 3.23 (9H, s, (CH$_3$)$_3$), 4.17 (2H, t, J 6.6, CH$_2$), 4.45 (2H, s, CH$_2$CO); δ_C(400 MHz; DMSO-d$_6$) 15.17 (CH$_3$), 23.31, 26.43, 29.02, 29.81, 29.93, 30.15, 30.19, 30.22, 30.26, 32.52 (CH$_2$), 40.96 (CH$_3$SO$_3^-$), 54.30 ((CH$_3$)$_3$), 63.66 (CH$_2$O), 66.93 (CH_2CO), 166.15 (C=O).

Octadecylbetainate methanesulfonate 1b. Octadecanol (69.3 g, 0.256 mol, 1.2 equiv.) was added to a suspension of dried glycine betaine (25 g, 0.213 mol, 1.0 equiv.) in methanesulfonic acid (36 mL, 0.555 mol, 2.6 equiv.). The reaction mixture was gradually heated to 130 °C under reduced pressure (50–60 mbar) to remove the water formed by the reaction. After 1 to 2 h, the reaction mixture became homogeneous and after 7 h the brown mixture was cooled down to room temperature at atmospheric pressure. The crude material was used as such (weight ratio: **1b**/octadecanol/MSA/GB = 51/19/22/8) or purified alternatively by (1) extensive washing with Et$_2$O (1 L) and filtration (removing of most of MSA and fatty alcohol; weight

ratio: **1b**/octadecanol/MSA/GB = 72/8/10/10), (2) extensive washing with EtOH (1 L) and filtration (removing of all of MSA and fatty alcohol; weight ratio: **1b**/octadecanol/MSA/GB = 79/21/0/0), (3) extensive washing with n-butanol (1 L) and filtration (removing of quasi all of MSA and fatty acid; weight ratio: **1b**/octadecanol/MSA/GB = 69/25/4/2) or (4) flash chromatography on silica gel (EtOAc/iPrOH/H$_2$O: 6.2 : 3.0 : 0.8) to obtain pure compound **1b** (70.1 g, 0.151 mol, 70%) as a white solid. R_f 0.16–0.40 (EtOAc/iPrOH/H$_2$O: 6 : 3 : 1); mp 104–105 °C; ν_{max}(nujol)/cm^{-1} 3030–2840 (C–H), 1750 (C=O); δ_H(400 MHz; CDCl$_3$/CD$_3$OD: 1 : 1) 0.83 (3H, t, J 6.7, CH$_3$), 1.15–1.37 (30H, m, CH$_2$), 1.59–1.70 (2H, m, CH_2CH$_2$O), 2.70 (3H, s, CH$_3$SO$_3^-$), 3.32 (9H, s, (CH$_3$)$_3$), 4.20 (2H, t, J 6.7, CH$_2$CH_2O), 4.34 (2H, s, CH$_2$CO); δ_C(100 MHz; CDCl$_3$/CD$_3$OD: 1 : 1) 14.33 (CH$_3$), 23.17, 26.22, 28.82, 29.71, 29.88, 30.02, 30.08, 30.19, 32.45 (CH$_2$), 39.50 (CH$_3$SO$_3^-$), 54.18 ((CH$_3$)$_3$), 63.46 (CH$_2$CH_2O), 67.27 (CH_2CO), 165.24 (CH$_2$CO); m/z (FAB) 370.3680 (M$^+$ requires C$_{23}$H$_{48}$NO$_2$ 370.3680).

(Z)-Octadec-9-enylbetainate methanesulfonate 1c. Oleic alcohol (137.5 g (70%), 0.359 mol, 1.4 equiv.) was added to a suspension of dried glycine betaine (30 g, 0.256 mol, 1.0 equiv.) in methanesulfonic acid (41.5 mL, 0.640 mol, 2.5 equiv.). The reaction mixture was gradually heated to 130 °C under reduced pressure (50–60 mbar) to remove the water formed by the reaction. After 1 to 2 h, the reaction mixture became homogeneous and after 7 h the brown mixture was cooled down to room temperature at atmospheric pressure. The crude material was used as such (weight ratio: **1c**/oleic alcohol/MSA/GB = 49/33/15/3) or purified by flash chromatography on silica gel (EtOAc/iPrOH/H$_2$O: 6.2 : 3.0 : 0.8) to obtain pure compound **1c** (101 g, 0.218 mol, 85%) as a white solid. R_f 0.15–0.48 (EtOAc/iPrOH/H$_2$O: 6 : 3 : 1); mp < 45 °C; ν_{max}(nujol)/cm^{-1} 3040–2780 (C–H), 1750 (C=O), 1648 (C=C); δ_H(400 MHz; CDCl$_3$) 0.83 (3H, t, J 6.8, CH$_3$), 1.13–1.37 (22H, m, CH$_2$), 1.60–1.69 (2H, m, CH_2CH$_2$O), 1.88–2.01 (4H, m, CH_2CH=CHCH_2), 2.71 (3H, s, CH$_3$SO$_3^-$), 3.30 (9H, s, (CH$_3$)$_3$), 4.19 (2H, t, J 6.8, CH$_2$CH_2O), 4.32 (2H, s, CH$_2$CO), 5.25–5.39 (2H, m, CH$_2$CH=CHCH$_2$); δ_C(100 MHz; CDCl$_3$) 14.21 (CH$_3$), 22.90, 25.89, 27.40, 28.49, 29.38, 29.52, 29.62, 29.73, 29.86, 29.91, 29.96, 32.13, 32.81 (CH$_2$), 39.27 (CH$_3$SO$_3^-$), 54.09 ((CH$_3$)$_3$), 63.22 (CH$_2$CH_2O), 67.09 (CH_2CO), 129.93 (CH$_2$CH=CHCH$_2$), 130.24, 164.88 (CH$_2$CO); m/z (ESI+) 368.3529 (M$^+$ requires C$_{23}$H$_{46}$NO$_2$ 368.3523).

Betainylaminododecane methanesulfonate 2a. A mixture of glycine betaine (0.70 g, 6.0 mmol, 1.0 equiv.) in nBuOH (30 mL) and methanesulfonic acid (0.64 g, 6.6 mmol, 1.1 equiv.) was refluxed for 3 to 4 h. The reaction mixture was allowed to cool down to room temperature, triethanolamine (0.2 equiv.) and dodecylamine (1.67 g, 9.0 mmol, 1.5 equiv.) were added and the nBuOH was removed under reduced pressure. The reaction mixture was maintained under reduced pressure and heated at 140 °C until complete reaction (TLC). After cooling to room temperature, NaHCO$_3$ 5% was added and the stirring continued for 4 h. The excess of fatty amine was extracted by Et$_2$O and the surfactant was then extracted by (nBuOH/EtOAc: 4 : 1). The combined organic phases were washed with water and evaporated under reduced pressure. Recrystallisation from EtOAc afforded pure amide surfactant **2a** (1.84 g, 4.8 mmol,

80%) as a white solid. mp 87 °C; ν_{max}(nujol)/cm^{-1} 1680 (C=O), 1578; δ_H(400 MHz; DMSO-d_6) 0.84 (3H, t, J 6.6, CH$_3$), 1.23 (18H, s, (CH_2)$_9$CH$_3$), 1.40 (2H, s, CH_2CH$_2$NH), 2.32 (3H, s, CH$_3$SO$_3^-$), 3.08 (2H, q, J 7.1, CH$_2$NH), 3.20 (9H, s, (CH$_3$)$_3$), 4.15 (2H, s, CH$_2$CO), 9.23 (1H, s, NH); δ_C(100 MHz; DMSO-d_6) 15.17 (CH$_3$), 23.32, 27.58, 29.84, 29.92, 29.95, 30.24, 30.28, 32.52 (CH$_2$), 39.80 (CH$_2$NH), 40.96 (CH$_3$SO$_3^-$), 54.30 ((CH$_3$)$_3$), 65.10 (CH$_2$CO), 164.38 (C=O).

Betainylaminooctadecane methanesulfonate 2b. A mixture of glycine betaine (25 g, 0.213 mol, 1.0 equiv.) in nBuOH (78 mL) and methanesulfonic acid (15.2 mL, 0.235 mol, 1.1 equiv.) was refluxed for 3 to 4 h. The reaction mixture was allowed to cool down to room temperature, dibutylamine (0.3 equiv.) and octadecylamine (69.0 g, 0.256 mol, 1.2 equiv.) were added and the nBuOH was removed under reduced pressure. The reaction mixture was maintained under reduced pressure and heated at 130 °C for 3 h. After cooling to room temperature, compound **2b** was purified by extensive washing with Et$_2$O and filtered (weight ratio: **2b**/dibutylamine and stearic amine salts/GB = 59/20–30/11–21) or/and by chromatography on silica gel (EtOAc/iPrOH/H$_2$O: 6 : 3 : 1 then 5 : 3 : 2) to afford the titled product (59.2 g, 0.128 mol, 60%) as a white solid. R_f 0.16–0.40 (EtOAc/iPrOH/H$_2$O: 5 : 3 : 2); mp 140–142 °C; ν_{max}(nujol)/cm^{-1} 3080–2800 (C–H), 1670 (C=O), 1576; δ_H(400 MHz; DMSO-d_6) 0.86 (3H, t, J 6.9, CH$_3$), 1.19–1.31 (30H, m, CH$_2$), 1.40–1.49 (2H, m, CH_2CH$_2$NH), 2.37 (3H, s, CH$_3$SO$_3^-$), 3.05–3.13 (2H, m, CH$_2$CH_2NH), 3.21 (9H, s, (CH$_3$)$_3$), 4.05 (2H, s, CH$_2$CO), 8.61–8.67 (1H, m, NH); δ_C(100 MHz; DMSO-d_6) 13.40 (CH$_3$), 22.13, 24.22, 26.01, 28.27, 28.59, 30.88 (CH$_2$), 38.50 (CH$_2$CH$_2$NH), 40.25 (CH$_3$SO$_3^-$), 53.35 ((CH$_3$)$_3$), 64.24 (CH$_2$CO), 162.66 (CH$_2$CO); m/z (ESI+) 369.3845 (M$^+$–MsO$^-$ requires C$_{23}$H$_{49}$N$_2$O 369.3839).

(Z)-Betainylaminooctadec-9-ene methanesulfonate 2c. A mixture of glycine betaine (25 g, 0.213 mol, 1.0 equiv.) in nBuOH (78 mL) and methanesulfonic acid (15.2 mL, 0.235 mol, 1.1 equiv.) was refluxed for 3 to 4 h. The reaction mixture was allowed to cool down to room temperature, oleylamine (68.5 g, 0.256 mol, 1.2 equiv.) was added and the nBuOH was removed under reduced pressure. The reaction mixture was maintained under reduced pressure and heated at 130 °C for 3 h. After cooling to room temperature, the crude material was used as such (weight ratio: **2c**/oleic amine salt/oleic amine/GB = 59/34/<1/6) or purified by flash chromatography on silica gel (EtOAc/iPrOH/H$_2$O: 6 : 3 : 1 then 5 : 3 : 2) to afford the titled product **2c** (64.1 g, 0.138 mol, 65%) as a white solid. R_f 0.16–0.41 (EtOAc/iPrOH/H$_2$O: 5 : 3 : 2); mp < 35 °C; ν_{max}(nujol)/cm^{-1} 3090–2790 (C–H), 1675 (C=O), 1579; δ_H(400 MHz; DMSO-d_6) 0.84 (3H, t, J 6.7, CH$_3$), 1.15–1.33 (22H, m, CH$_2$), 1.36–1.46 (2H, m, CH_2CH$_2$NH), 1.88–2.03 (4H, m, CH_2CH=CHCH_2), 2.33 (3H, s, CH$_3$SO$_3^-$), 3.04–3.12 (2H, m, CH$_2$CH_2NH), 3.20 (9H, s, (CH$_3$)$_3$), 4.07 (2H, s, CH$_2$CO), 5.26–5.37 (2H, m, CH$_2$CH=CHCH$_2$), 8.58–8.64 (1H, m, NH); δ_C(100 MHz; DMSO-d_6) 14.08 (CH$_3$), 22.20, 26.43, 26.65, 26.69, 28.67, 28.73, 28.80, 28.92, 28.96, 29.17, 29.23, 31.38 (CH$_2$), 38.66 (CH$_2$CH$_2$NH), 40.05 (CH$_3$SO$_3^-$), 53.25 ((CH$_3$)$_3$), 63.86 (CH$_2$CO), 129.74, 129.75, (CH$_2$CH=CHCH$_2$),

163.19 (CH$_2$CO); m/z (ESI+) 367.3694 (M$^+$–MsO$^-$ requires C$_{23}$H$_{47}$N$_2$O$_1$ 367.3688).

Dibetainylaminododecane chloride 3a. A solution of thionyl chloride (3.0 g, 26.0 mmol) in dry acetonitrile (20 mL) was added dropwise at 0 °C to a suspension of glycine betaine (2.00 g, 17.0 mmol) in dry acetonitrile (10 mL). The reaction mixture was stirred for 2 h at room temperature and both the solvent and the excess of thionyl chloride were removed under reduced pressure. The resulting acyl chloride was diluted with CH$_2$Cl$_2$ (10 mL) and a solution of 1,12-diaminododecane (1.71 g, 8.6 mmol) and Et$_3$N (1.72 g, 17.0 mmol) in CH$_2$Cl$_2$ (30 mL) was added dropwise at room temperature. The reaction mixture was stirred for 2 h and the solvent was removed under reduced pressure. The residue was diluted with water (80 mL) and NaHCO$_3$ 5% was added until neutral pH. The bolaamphiphile **3a** was extracted with nBuOH (2 × 30 mL) and the water phase was saturated with NaCl and extracted with nBuOH (30 mL). The combined organic phases were washed with water (5 mL) and were evaporated under reduced pressure. The residue was washed with Et$_2$O, filtered and dried to obtain pure bolaamphiphile **3a** (2.95 g, 6.3 mmol, 73%). ν_{max}(nujol)/cm^{-1} 1678 (C=O), 1546; δ_H(400 MHz; DMSO-d_6) 1.23 (16H, s, (CH$_2$)$_8$), 1.41 (4H, s, 2 CH_2CH$_2$NH), 3.08 (4H, q, J 6.6, 2 CH$_2$NH), 3.21 (18H, s, 2 (CH$_3$)$_3$), 4.15 (4H, s, CH$_2$CO), 8.85 (1H, s, NH); δ_C(100 MHz; DMSO-d_6) 27.57, 29.75, 29.84, 29.89, 30.02, 30.20 (CH$_2$), 39.77 (CH$_2$NH), 54.40 ((CH$_3$)$_3$), 65.04 (CH$_2$CO), 164.31 (C=O); δ_H(400 MHz; CD$_3$OD) 1.23 (16H, s, (CH$_2$)$_8$), 1.44 (4H, s, 2 CH_2CH$_2$NH), 3.14 (4H, t, J 7.1, 2 CH$_2$NH,), 3.21 (18H, s, 2 (CH$_3$)$_3$), 4.00 (4H, s, CH$_2$CO); δ_C(100 MHz; CD$_3$OD) 27.99, 30.11, 30.37, 30.65, 30.69 (CH$_2$), 40.48 (CH$_2$NH), 54.75 ((CH$_3$)$_3$), 65.76 (CH$_2$CO), 164.57 (C=O); m/z (LSIMS Cs$^+$) 435.3458 (M$^+$–Cl requires C$_{22}$H$_{48}$ClN$_4$O$_2$ 435.3466).

Dibetainylaminododecane hydroxyde 3b. Bolaamphiphile **3a** (500 mg, 1.06 mmol) was dissolved in (H$_2$O/EtOH: 7 : 1) and passed through a DOWEX 550 A (OH$^-$) resin with the same solvent mixture. After lyophilisation the titled compound **3b** (440 mg, 96%) was obtained. ν_{max}(nujol)/cm^{-1} 1680 (C=O), 1563, 1548; δ_H(400 MHz; CD$_3$OD) 1.30 (16H, s, (CH$_2$)$_8$), 1.53 (4H, s, 2 CH_2CH$_2$NH), 3.21–3.23 (4H, m, CH_2NH), 3.30 (18H, s, (CH$_3$)$_3$); δ_C(100 MHz; CD$_3$OD) 28.02, 30.16, 30.39, 30.68, 30.71 (CH$_2$), 40.52 (CH$_2$NH), 54.65 ((CH$_3$)$_3$), 164.58 (C=O).

Dibetainylaminododecane dodecanoate 3c. A solution of lauric acid (31.4 mg, 0.186 mmol, 1.0 equiv.) in (CHCl$_3$/MeOH: 1 : 1) was added to a solution of bolaamphiphile **3a** (81.0 mg, 0.186 mmol, 1.0 equiv.). The mixture was stirred for 20 min and the solvents were removed under reduced pressure. The resulting residue was precipitated in EtOAc and filtered to obtained the unsymmetrical bolaamphiphile **3c** (103 mg, 0.167 mmol, 90%). mp > 200 °C. ν_{max}(nujol)/cm^{-1} 1709 (C=O), 1679, 1648, 1641, 1546; δ_H(400 MHz; CD$_3$OD) 0.88 (3H, t, J 6.6, CH$_3$), 1.29 (32H, s, (CH$_2$)$_8$, (CH$_2$)$_8$), 1.54 (6H, m, CH_2CH$_2$CO$_2$, CH_2CH$_2$NH), 2.18 (2H, t, J 7.6, CH$_2$CO$_2$), 3.21 (4H, t, J 7.1, CH_2NH), 3.30 (18H, s, (CH$_3$)$_3$), 4.07 (4H, s, CH$_2$CO); δ_C(100 MHz; CD$_3$OD) 14.44 (CH$_3$), 23.74, 27.24, 28.02, 30.15, 30.40, 30.48, 30.60, 30.67, 30.70, 30.72, 30.73, 30.76, 30.78, 33.08 (CH$_2$), 37.82 (CH$_2$CO$_2$), 40.49 (CH$_2$NH), 54.73 ((CH$_3$)$_3$), 65.72

(CH_2CO), 164.58 (CONH); m/z (LSIMS Cs$^+$) 399.3701 (M$^+$–$C_{12}H_{25}O_3$ requires $C_{22}H_{47}N_4O_2$ 399.3699).

pH sensitivity study of GB ester-type surfactants. The chemical hydrolysis of the ester linkage between GB and C_{18} fatty alcohols was monitored by GC using n-dodecanol as an internal standard. Surfactant solutions of fixed concentration (34 mmol L^{-1}) in various buffers (phosphate-citrate buffers: pH comprised between 3 and 8) were held at room temperature under constant stirring. Fatty alcohol resulting from the hydrolysis reaction was extracted by diethyl ether and the samples were centrifuged (10 000 t min^{-1} for 10 min) in order to break the emulsions formed during the extraction process. GC analysis of the diethyl ether solutions was performed on a GC 8000 TOP CEInstruments gas chromatography and the separation was achieved on a Alltech AT1 column, 30 m × 0.25 mm id, 0.25 μm film thickness. Helium was used as a carrier gas and the inlet pressure was set to 75 kPa. The injections were done at 320 °C and the temperature detector was fixed at 330 °C. The GC oven temperature program was as follows: 200 °C initial column temperature, 3 min at 200 °C, 30 °C min^{-1} to 320 °C, held to 5 min.

Surface tension measurements. The surface tension of aqueous solutions of GB surfactants in water was measured using the de Noüy ring method with a Kruss K10T tensiometer (compounds **3a–c**) or with a drop tensiometer (compounds **1a–c** and **2a–c**). For the latter method, a syringe with a U-shaped needle was lowered into the sample cell containing the aqueous solution of surfactant and an air bubble was produced from the syringe. The dynamic surface tension was measured by filming the rising bubble and analysing the contour of the bubble according to axisymmetric drop shape analysis, ADSA, with the Tracker instrument, IT Concept. The surface tension was determined at room temperature for several concentrations of surfactants in pure water.

Evaluations of emulsifying formulations (bitumen emulsions) and biodegradability test. Bitumen emulsions were prepared using bitumen 160/220 and GB ester or amide emulsifiers. In this process, hot bitumen (140–160 °C) was sheared with water (60 °C) containing the emulsifier and hydrochloric acid (HCl). The two phases were delivered into the mill by metered pumps. The fluids were forced into a small gap between the rotor and the stator where they experienced strong shear forces, which caused the molten bitumen to break into minute particles. Each bitumen particle was coated with the emulsifier during mixing. *Emulsion particle size measurements* were performed using a laser particle sizer. The *rupture (break) index* of the emulsions was measured as follows: reference siliceous fines were poured continously through a funnel at a rate of 0.3 to 0.5 g s^{-1} into a beaker containing 100 g of emulsion. The mixture was agitated constantly, and the addition of fines halted when the aggregate–emulsion system took on the appearance of a block. The quantity of fines added to the 100 g of bitumen is called the rupture (break) index. *Adhesivity* of bitumen was tested as follows: the purpose of this test is to assess the adhesivity in the presence of water, of a hydrocarbon binder coated on aggregate, and in it the displacement of bitumen by water on the surface of the aggregate is measured. In the test, bitumen-coated aggregate was plunged into water while hot, and the percentage of the surface covered by the binder after 16 h immersion at 60 °C, was evaluated. *Viscosity* was measured on a Standard Tar Viscosimeter (STV). This apparatus allows measurement of the pseudo-viscosity of the bitumen emulsion, of the efflux time of a certain amount of binder through a calibrated aperture at a fixed temperature. The viscosity values given in Tables 4 and 5 corresponded to a 4 mm aperture and a temperature of 25 °C. *The CO_2* Evolution Test, a standardized method (OECD 301 B),[20] was used for evaluating the biodegradability of the emulsifying formulation containing GB ester **1c**. The principle of this test was the determination of the ultimate biodegradability of organic compounds by aerobic microorganisms, using a static aqueous test system and the evolution of CO_2 as the analytical parameter. A 1.50 L mixture was prepared in 2 L vessels containing an inorganic medium and the organic compound as the sole source of carbon at a concentration of 10 to 40 mg of organic carbon L^{-1}. Usually activated sludge, obtained from a wastewater treatment plant for another source of the environment, was used as a mixed inoculum. The vessels were aerated with 1 to 2 bubbles of CO_2-free air per s (50 mL min^{-1}) and incubated at 20 ± 2 °C for usually 28 days. Agitation was increased by stirring with a magnetic bar (length, 40 mm) at about 800 rpm. The biogenous CO_2 formed during the microbial degradation was trapped in two external adjacent vessels (volume, 200 mL) containing an aqueous sodium hydroxide solution (0.05 M, 100 mL). Samples were taken at regular intervals to determine the amount of dissolved inorganic carbon (DIC) and to calculate the amount of CO_2 produced. This evolved CO_2 was compared with the calculated theorical amount (ThCO_2), and the degree of biodegradation was expressed as a percentage.

Characterizations of supramolecular membrane assemblies. The aqueous preparations of bolaamphiphiles **3** were obtained by simple mixing and gentle stirring with or without sonication. X-ray scattering experiments were performed with a focusing Guinier temperature-controlled camera using monochromatic Cu Kα$_1$ radiation ($\lambda = 1.54$ Å) and linear collimation. The samples were placed between two mica windows in vacuum-tight cells. For freeze fracture electron microscopy, a small drop of the preparation containing glycerol as a cryoprotectant (30/70, glycerol/water) was desposited on a thin copper planchett, rapidly frozen in liquid propane, and kept in liquid nitrogen. The samples were frozen from various temperatures according to specific requirements. Freeze fracture was performed with a Balzers 301 freeze etch unit. The samples were fractured at −125 °C in a vacuum lower than 16–6 Torr and subsqently shadowed with Pd–C. The replicas were washed with a SDS solution, rinsed with water, and examined in a Philips 410 electron microscope.

Conclusion

This investigation has pointed out the potential of glycine betaine as an innovative renewable raw material for the development of biodegradable surfactants. Monocationic GB ester and amide derivatives were prepared using eco-friendly reactants and catalysts. The industrial production of an emulsifying

formulation using an environmentally benign solvent-free synthetic approach, called Emulgreen® is now in progress. This work represents a concrete example for the valorization of European oils in non-food industry. Novel bolaamphiphiles possessing two glycine betaine moieties were designed and synthesized for the formation of vesicular aggregates as novel delivery systems. All these results are particularly important in the context of the growing number of European laws, regulations and directives. The new European Detergent Regulation that entered into force on October, 2005 is the most recent one.[15] The main elements of this regulation are additional requirements with respect to ultimate biodegradability (60% degradation within 28 days) of surfactants, special new requirements for the additional declarations of detergent ingredients on the packaging including possible sensitizing ingredients, and additional compulsory information concerning detergent formulations to be provided for medical professional and consumers. While previous legislation was only applicable to anionic and non-ionic surfactants, this Regulation includes all four surfactant families: anionic, non-ionic, cationic and amphoteric. Consequently, innovative research and development in new biodegradable products, particularly for the introduction of new cationic surfactants, should be favoured to propose an alternative to non-compliant surfactants found in formulations impacted by the European Detergent Regulation.

Acknowledgements

References

1 D. Rubingh and P. M. Holland, *Cationic Surfactants*, Surfactants Science Series, 1990, vol. 37.
2 M. Patel, *J. Ind. Ecol.*, 2004, **7**, 47–62.
3 (*a*) J. H. Furhrop and T. Wang, *Chem. Rev.*, 2004, **104**, 2901–2937; (*b*) F. M. Menger and B. N. A. Mbaduha, *J. Am. Chem. Soc.*, 2001, **123**, 875–885; (*c*) C. Satgé, R. Granet, B. Verneuil, P. Krausz and Y. Champavier, *Carbohydr. Res.*, 2004, **339**, 1243–1254.
4 K. Meguro, K. Ikeda, A. Otsuji, M. Taya, M. Yasuda and K. Esumi, *J. Colloid Interface Sci.*, 1987, **118**, 372–378.
5 K. C. Mackenzie, C. A. Bunton, D. F. Nicoli and G. Savelli, *J. Phys. Chem. B*, 1987, **91**, 5709–5713.
6 S. Yiv, K. M. Kale, R. Lang and R. Zana, *J. Phys. Chem. B*, 1976, **80**, 2651–2655.
7 M. Roussel, V. Lognoné, D. Plusquellec and T. Benvegnu, *Chem. Commun.*, 2006, 3622–3624.
8 S. C. Baker, *Nature*, 1991, **350**, 627–628.
9 J. Guilbot, T. Benvegnu, N. Legros, D. Plusquellec, J.-C. Dedieu and A. Gulik, *Langmuir*, 2001, **17**, 613–618.
10 A. R. Tehrani-Bagha, H. Oskarsson, C. G. van Ginkel and K. Holmberg, *J. Colloid Interface Sci.*, 2007, **312**, 444–452.
11 (*a*) K. Holmberg, *Novel Surfactants, Preparation, Applications, and Biodegradability*, Dekker, New York, 2003; (*b*) P.-E. Hellberg, K. Bergström and K. Holmberg, *J. Surfact. Deterg.*, 2000, **3**, 81–91; (*c*) D. A. Jaeger, J. Mohebalian and P. L. Rose, *Langmuir*, 1990, **6**, 547–554.
12 J. N. Israelachvili, D. J. Mitchell and B. W. Ninham, *Biochim. Biophys. Acta*, 1977, **470**, 185–201.
13 J. N. Israelachvili, S. Marcelja and R. G. Q. Horn, *Q. Rev. Biophys.*, 1980, **13**, 121–200.
14 X. Gutierrez, F. Silva, M. Chirinos, J. Leiva and H. Rivas, *J. Dispersion Sci. Technol.*, 2002, **23**, 405–418.
15 European regulation (EC) No. 648/2004.
16 J.-P. Antoine, J. Marcilloux, D. Plusquellec, T. Benvegnu and F. Goursaud, Patents ≠ FR 2869910, WO 2005121252, 2005.
17 S. L. Lo and E. L. Chang, *Biochim. Biophys. Res. Commun.*, 1990, **167**, 238–245.
18 M. G. L. Elferink, J. G. de Wit, R. Demel, A. J. M. Driessen and W. Konings, *J. Biol. Chem.*, 1992, **267**, 1375–1381.
19 R. Kanichay, L. T. Boni, P. H. Cooke, T. K. Khan and P. L.-G. Chong, *Archaea*, 2003, **1**, 175–183.
20 *OECD guidelines for testing of chemicals. OECD 301 B CO_2 evolution test. Organisation for Economic Co-operation and Development*, Paris, France, 1993.

Biodiesel: a green polymerization solvent

Somaieh Salehpour and Marc A. Dubé*

In an effort to use clean technologies, fatty acid methyl esters (FAME) produced from canola have been used as a polymerization solvent. Solution polymerizations of four commercially important monomers have been studied using FAME as a solvent. A series of methyl methacrylate (MMA), styrene (Sty), butyl acrylate (BA) and vinyl acetate (VAc) homopolymerizations in FAME were carried out at 60 °C at different solvent concentrations. Chain transfer to solvent rate constants were obtained using the Mayo method. The transfer constants increased in the order: MMA < Sty < BA < VAc. Under the conditions studied, the MMA solution polymerization in FAME was observed to behave as a precipitation polymerization. The estimated chain transfer to solvent rate constants were employed in a polymerization simulator to predict the polymerization rates and average molecular weights.

Introduction

The solution polymerization method, an important polymer production technology, has faced several ecological criticisms in the last decade.[1] Many of the solvents which are used in this technique are known to have a negative impact on our ecosystem by diminishing the ozone layer and participating in reactions that form tropospheric pollution. Moreover, they can cause cancer, infertility and genetic disorders in individuals frequently exposed to them.[2] One of the ways to avoid some of these side effects is to use technologies which do not employ solvents, such as bulk polymerization, although other difficulties can arise. For example, the presence of solvent keeps the viscosity low as polymers are formed, which translates into improved heat transfer and prevention of thermal runaway.[3] Solution polymerization may also present some chain transfer to solvent reactions which can have an impact on the polymer product's molecular weight. Emulsion polymerization can be an attractive alternative to solution polymerization although desirable end-use properties are not always achieved.[4] Therefore, the superior properties of polymers prepared by solution polymerization suggest that rather than altering the polymerization technology, one could look for more environmentally friendly solvents to replace more harmful conventional solvents.[5]

The choice of polymerization solvent is influenced by a number of issues. It should be non-toxic and reasonably non-hazardous, but versatile. Water is a non-toxic, inexpensive and abundantly available solvent, and therefore a good candidate. However, its polarity makes it extremely difficult to be a substitute for organic solvents because of solubility issues. Recently, non-classical solvents such as supercritical fluids have been considered as an alternative media.[6]

Department of Chemical Engineering, University of Ottawa, 161 Louis Pasteur St., Ottawa, ON, Canada K1N 6N5.
E-mail: Marc.Dube@UOttawa.ca; Fax: +1-613-562-5127

Supercritical water and carbon dioxide were investigated as green solvents for polymerization.[7] In view of the fact that water exists in the supercritical state at temperatures above 647 K and pressures above 217 atm (21987 kPa), it can perform as a non-polar solvent mainly due to the absence of hydrogen bonding under these extreme conditions. However, implementation of this technology can cause corrosion problems. Considering economic reasons, one can surmise that supercritical water may not be a convenient solvent alternative.[7]

With growing concerns over the volatile organic content (VOC) of common solvents, ionic liquids have attracted attention as an environmentally friendly alternative.[8] Ionic liquids are organic salts which are in the liquid state at ambient temperatures. Ionic liquids are composed of ions, unlike conventional solvents which are molecular liquids; *e.g.*, chloroaluminate compounds and imidazolium-based salts such as imidazolium tetrafluoroborates can exist at room temperature with very low vapor pressures.[9,10] In general, ionic liquids are not miscible with many organic solvents, particularly when the latter are non-polar, such as hexane.[11] Ionic liquids have yet to be commonly applied in the polymer industry, perhaps because of their high cost and the lack of data concerning their toxicity and biodegradability.[12]

Another interesting alternative to conventional polymerization solvents is biodiesel. While primarily used as an environmentally friendly alternative or extender to petroleum diesel as a fuel source, some studies have been done on the solvent power of biodiesel.[5] Biodiesel is environmentally benign, has a low volatility and is also a renewable material with low viscosity and good solubility properties.[13] Based on the definition of the American Society for Testing and Materials (ASTM), biodiesel can be defined as alkyl esters of long chain fatty acids derived from a lipid feedstock. The most common method to produce biodiesel is *via* base-catalyzed transesterification of vegetable oils and animal fats with an alcohol.[13] Typically, methanol is the alcohol of choice, and the resulting esters are fatty acid methyl esters (FAME). The C16–18 methyl esters that comprise the

Table 1 Comparison of biodiesel to some polymerization solvents

Solvent	Toxicity	OSHA PEL 8 h (ppm)	Price/US$ L^{-1}
Toluene[a]	Narcotic, liver and kidney damage at high concentrations	200	35.00
Benzene[a]	Carcinogen	10	49.00
Ethyl acetate[a]	Narcotic, liver and kidney damage at high concentrations	400	46.00
Xylene[a]	Narcotic at high concentrations	100	43.00
Methyl oleate[a]	Non-hazardous material	None	1200.00
Biodiesel[b]	Non-hazardous material	None	0.60

[a] Sigma-Aldrich anhydrous, 99+%, MSDS. Toxicity information from Budavari *et al.*[14] and Sitting.[15] [b] Toxicity information from Mittelbach and Remschmidt.[13]

largest part of biodiesel are readily biodegradable due to their chemical nature and can be domestically produced and obtained at a competitive price.[9]

The Occupational Safety and Health Administration (OSHA) in the United States reports permissible exposure limits (PEL) for chemical concentrations to which one may be exposed with no harmful health effects.[2] In Table 1, the toxicity, PEL values and approximate prices for biodiesel and some common polymerization solvents are shown. It is evident from the table, that biodiesel is an attractive choice in terms of both cost and safety.

There are no reported uses of biodiesel as a polymerization solvent. Methyl oleate, a major component of biodiesel (∼55–65 wt% for canola-based biodiesel), has previously been used in its pure form as a polymerization solvent in the 1960's.[16] However, pure methyl oleate comes at a high cost (see Table 1). In the work presented here, the application of FAME as a polymerization solvent is reported for four commercially important monomers: methyl methacrylate (MMA), styrene (Sty), butyl acrylate (BA) and vinyl acetate (VAc). Chain transfer to solvent rate constants are also estimated. Finally, the experimental kinetic data are modeled using the WATPOLY polymerization simulator.[17]

Experimental

The monomers MMA, BA, VAc and Sty (Sigma–Aldrich) were received inhibited by 0.05 ppm hydroquinone. To remove the inhibitor, VAc was distilled under vacuum while BA, MMA and Sty were washed 3 times with a 10% (v/v) sodium hydroxide solution, then washed 3 times with distilled de-ionized water and dried over calcium chloride prior to vacuum distillation. Distillations were completed a maximum of 24 h prior to polymerization, and the monomers were stored at −10 °C.

The initiator 2,2-azobisisobutyronitrile (AIBN, DuPont Chemicals) was recrystallized 3 times in absolute methanol. FAME was obtained by transesterification of canola oil (No Name®) with methanol (reagent grade, Commercial Alcohols Inc.) in the presence of sodium hydroxide catalyst in a membrane reactor process.[18] The FAME product from the reactor was washed 5 times with de-ionized water, which was then removed under vacuum. Hexane and methanol (analytical grade, Sigma–Aldrich), and all other solvents used for sample characterization were employed without further purification.

Polymerizations were performed in sealed glass ampoules (17 cm length, 0.8 cm outer diameter) at 60 °C in a water bath.

The feed was prepared by weighing the monomer, FAME solvent and initiator into a flask and delivered into a series of 5 mL glass ampoules. The same ratio of initiator to monomer, 0.4 phm (parts per 100 parts by weight of monomer), was utilized for all concentrations of monomers. The ampoules were degassed by several freeze–pump–thaw cycles under high vacuum, were flame sealed and then submerged in a constant temperature water bath. At the appropriate time interval, ampoules were removed from the bath and quenched in an ice bath to stop the reaction. The ampoules were broken and the contents poured into a pre-weighed beaker. The solution was diluted with 5 mL of acetone. The extraction of polymer was done by precipitation in hexane (for MMA, VAc and Sty) and in methanol (for BA) at room temperature. The polymer–monomer–FAME solution was added slowly to the non-solvent (*i.e.*, hexane or methanol) while stirring, and generally appeared as a fine white fiber or a milky dispersion. After settling for ∼24 h, decantation and evaporation of the non-solvent, the extracted polymer was dried in a vacuum oven at 40 °C until a constant weight was reached. The solution polymerization experimental conditions are summarized in Table 2.

Conversion was calculated by gravimetry. The cumulative number- and weight-average molecular weights were determined using a Waters Associates gel permeation chromatograph equipped with a Waters model 410 refractive index detector. Three Waters Ultrastyragel packed columns (10³, 10⁴, and 10⁶ Å) were installed in series. THF was filtered and used as the eluent at a flow rate of 0.3 mL min^{-1} at 38 °C. The universal calibration method was used with 10 standard samples of polystyrene (SHODEX, Showa, Denko, Tokyo, Japan) with peak molecular weights between 1.3×10^3 and 3.15×10^6 g mol^{-1}. Standards and samples were prepared in THF 0.2% (w/v) solutions and filtered prior to injection through 0.45 μm PTFE filters to remove any

Table 2 Experimental conditions

Monomer	Experiment	Monomer/FAME (wt%)
Methyl methacrylate	M1	50/50
	M2	60/40
	M3	80/20
Styrene	S1	50/50
	S2	60/40
	S3	80/20
Vinyl acetate	V1	50/50
	V2	60/40
	V3	80/20
Butyl acrylate	B1	50/50
	B2	60/40
	B3	80/20

Table 3 Mark-Houwink parameters for samples in tetrahydrofuran

Polymer	$K/\times 10^3$ mL g^{-1}	a
Poly(butyl acrylate)[b]	11	0.708
Poly(vinyl acetate)[a]	15.6	0.708
Poly(methyl methacrylate)[a]	12.8	0.690
Polystyrene[a]	16	0.700

[a] Brandrup et al.[19] [b] McKenna and Villanueva.[20]

gel or impurity, if present. Millennium 32(tm) software (Waters) was used for data acquisition. The Mark–Houwink K and a parameters used as part of the universal calibration technique are given in Table 3.

Results and discussion

Many solvents are known to have some effect on kinetic reaction rate constants and therefore on the rate of polymerization. Studying the chain transfer to solvent constant, C_{fs}, is one conventional way to observe the effect of solvent on polymerization kinetics, where

$$C_{fs} = \frac{k_{fs}}{k_p} \tag{1}$$

k_{fs} is the chain transfer to solvent rate parameter and k_p is the propagation rate parameter.

Various methods can be employed to determine the value of C_{fs}.[21] Traditionally, the Mayo method,[22] which shows the quantitative effect of various transfer reactions on the number-average degree of polymerization, has been used. This method is based on overall chain growth and chain stopping rates under the assumption of steady state and uses the long-chain approximation.[21] An alternative is the chain-length distribution (CLD) method, which has been developed by Clay and Gilbert.[23] This latter procedure is based on the calculation of the high molecular weight slope for the number molecular weight distribution. Both procedures yield very similar results, especially in chain transfer-dominated systems.[21] In the work presented here, transfer constants were obtained using the Mayo equation:[3]

$$\frac{1}{\bar{X}_n} = \frac{k_t R_p}{k_p^2 [M]^2} + C_{fm} + C_{fs}\frac{[S]}{[M]} + C_{fi}\frac{k_t R_p^2}{k_p^2 f k_d [M]^3} \tag{2}$$
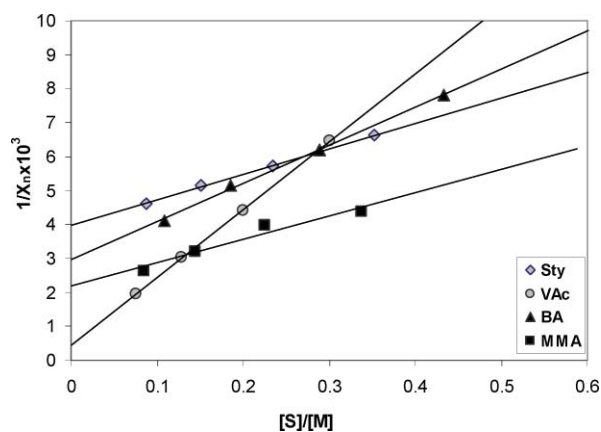
where $\bar{X}_n$ is the number-average degree of polymerization, R_p is the rate of polymerization, k_t, k_p and k_d are the termination, propagation and initiator decomposition rate coefficients, respectively. f is the initiator efficiency, $[M]$ and $[S]$ are the concentrations of the monomer and solvent, respectively, and C_{fm}, C_{fs} and C_{fi} are the transfer constants to monomer, solvent and initiator, respectively.

On the right hand side of eqn (2), the first term represents the contribution of the rate of polymerization and termination, the second term corresponds to the effect of transfer to monomer on polymer chain size, the third term describes the role of transfer to solvent reactions and the last term expresses contributions of the initiator. In our case, the third term on the right hand side of eqn (2) makes the biggest contribution to the degree of polymerization. By using low concentrations of initiator or initiators with very small C_{fi} values (e.g., AIBN), the last term in eqn (2) becomes negligible and rate retardation becomes

minimal.[3] In addition, by keeping $k_t R_p/[M]^2$ constant, the first term on the right hand side may be kept constant by adjusting the initiator concentration over a series of separate polymerizations. Nonetheless, this term will change with changes in $[S]/[M]$ because the termination rate parameter, k_t, is chain length dependent and will vary due to the effect of $[S]/[M]$ on the average chain length. This is a weakness of the Mayo method; however, the effect is not significant for all practical purposes.[21] Under these conditions, eqn (2) is reduced to

$$\frac{1}{\bar{X}_n} = \frac{1}{\bar{X}_{no}} + C_{fs}\frac{[S]}{[M]} \tag{3}$$

where $(1/X_{no})$ is the value of $(1/\bar{X}_n)$ in the absence of solvent. The value of C_{fs} is obtained from the slope of the line by plotting $(1/\bar{X}_n)$ versus $[S]/[M]$. All data regarding the calculation of C_{fs} for each monomer are given in Table 4. The corresponding Mayo plots are given in Fig. 1.

Fig. 1 Mayo plot: reciprocal of number-average degree of polymerization versus the solvent/monomer ratio for the monomers polymerized in FAME.

All polymers except pMMA were soluble in FAME and the values of the chain transfer constant for any compound increased in order: MMA < Sty < BA < VAc. This matches the order of increased resonance stabilization by the particular substituent of the radical produced from the monomer.[3]

Chain transfer values were all larger than that for polymerization in conventional solvents such as toluene or benzene. Therefore, average molecular weights are higher in these non-green solvents.[24] Transfer constants for these and some other polymerization solvents are shown in Table 5. This corresponds to a major issue in transfer to solvent phenomena which relates to solvent structure and reactivity. In many cases, the addition of active radical sites to monomer is thwarted since solvent radicals are more stable than monomer radicals. Therefore, the nature of the solvent is important. For example, benzene has a low C_{fs} value (see Table 5) because of strong C–H bonds and also transfer to solvent in this case appears to occur through the addition of the propagating radical to the benzene ring. In toluene, weaker benzylic bonds result in a higher C_{fs} value compared to benzene (see Table 5). The radical is resonance stabilized, which makes the abstraction of benzylic hydrogen easier. On the other hand, esters which typically comprise FAME would be expected to have higher transfer constants compared to

Table 4 Chain transfer data

Experiment	$\bar{M}_n$	$1/\bar{X}_n \times 10^3$	[S]/[M]	Conversion (wt%)	$C_{fs} \times 10^4$
Methyl methacrylate, AIBN/monomer = 0.4 phm					
M1	22900	4.37	0.33	9.96	68 ± 1
M2	25200	3.97	0.22	10.37	
M3	31200	3.20	0.14	8.74	
M4	37800	2.64	0.08	9.96	
Styrene, AIBN/monomer = 0.4 phm					
S1	15700	6.62	0.35	8.27	74 ± 1
S2	18200	5.71	0.23	11.74	
S3	20100	5.15	0.15	9.17	
S4	22500	4.62	0.08	9.12	
Vinyl acetate, AIBN/monomer = 0.4 phm					
V1	13700	6.47	0.30	10.25	190 ± 3
V2	20200	4.40	0.20	8.35	
V3	29400	3.02	0.12	11.24	
V4	45600	1.95	0.07	8.36	
Butyl acrylate, AIBN/monomer = 0.4 phm					
B1	16400	7.80	0.43	10.23	110 ± 2
B2	20600	6.21	0.28	12.30	
B3	24700	5.16	0.18	8.99	
B4	31100	4.10	0.10	11.20	

Table 5 Comparison of chain transfer to solvent data for different polymerization solvents

	$C_{fs} \times 10^4$ for polymerization of:			
Solvent	MMA	Sty	VAc	BA
Benzene[a]	0.83	0.023	6	0.4
Toluene[a]	0.96	0.125	35	1.8
Methyl oleate[b]	1.68	3.52	217	—
Xylene[a]	0.50	0.78	140	—
FAME	68	74	190	110

[a] Brandrup et al.[16] [b] Jordan et al.[17]

aliphatic and aromatic hydrocarbons because of C–H breakage and stabilization of the radical by an adjacent carbonyl group.

As expected, the cumulative number-average molecular weights increased by decreasing the solvent concentration (see Table 4). The molecular weight was higher at low MMA conversions compared to the other systems at the same stage of reaction. This can be due to the effect of delayed termination in the precipitation polymerization mechanism.[25] For pVAc, a low molecular weight polymer was produced because of a high rate of transfer to solvent (i.e., $C_{fs} = 190.98 \times 10^4$) which is an effect of low monomer reactivity in addition to the high transfer to monomer rate constant.[26]

In Fig. 2–5, conversion vs. time data are shown for the four different monomers at three different solvent concentrations, along with model predictions from the WATPOLY simulator.[17] The parameters for FAME, which include physical property data and the estimated C_{fs} values, were added to the simulator's database. The model was fitted to the experimental conversion and molecular weight data by changing the lumped rate parameter ($k_p/k_t^{1/2}$) for each individual monomer concentration. As can be seen in Fig. 2–5, within experimental error, the model demonstrates reliable predictions in almost all cases using a single lumped parameter for each monomer. The value of the modified parameters ($k_p/k_t^{1/2}$) were 0.2, 0.24 and 0.31 for
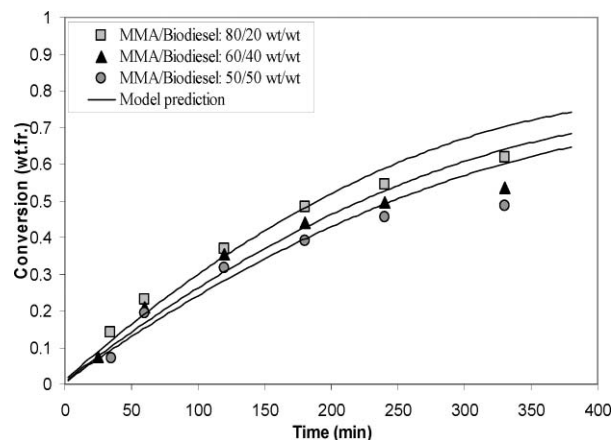
Fig. 2 MMA homopolymerization in FAME: conversion versus time at different solvent concentrations.
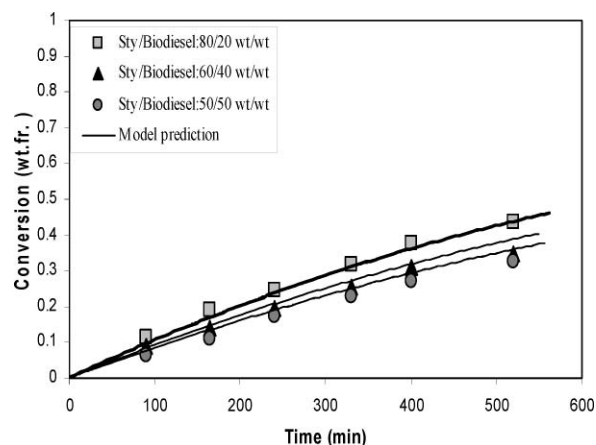
Fig. 3 Sty homopolymerization in FAME: conversion versus time at different solvent concentrations.

VAc and 1.09, 1.16 and 1.22 for BA at 50, 40 and 20 wt% concentration of solvent, respectively, while it was kept constant at 0.39 for Sty and 1.16 for MMA at all solvent concentrations.
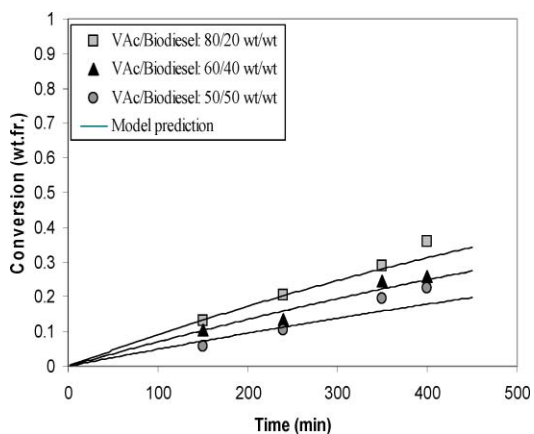
Fig. 4 VAc homopolymerization in FAME: conversion *versus* time at different solvent concentrations.
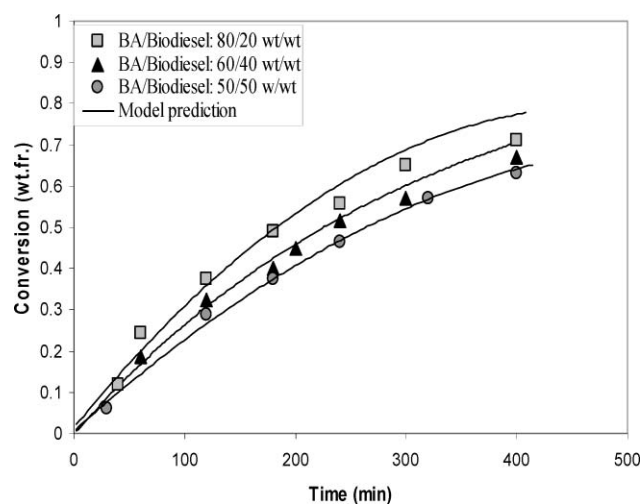

Fig. 5 BA homopolymerization in FAME: conversion *versus* time at different solvent concentrations.

This indicates different effects of solvent on propagation and termination rate constants for each individual monomer.

In Figs. 6–9, cumulative average molecular weight *vs.* conversion data together with model predictions are shown at 40 wt% solvent concentrations for MMA, BAc and BA, respectively.
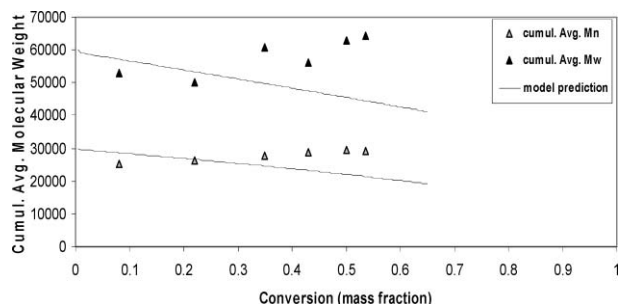

Fig. 6 Cumulative average molecular weight *versus* conversion for MMA solution homopolymerization in FAME at 60 °C (60/40 wt%).

Solvent can affect the individual propagation and termination rate parameters.[20] The pulsed-laser polymerization (PLP) data
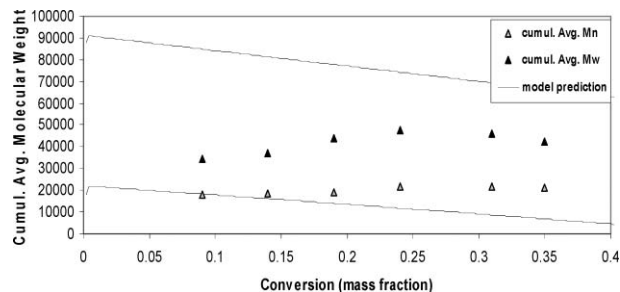

Fig. 7 Cumulative average molecular weight *versus* conversion for Sty solution homopolymerization in FAME at 60 °C (60/40 wt%).
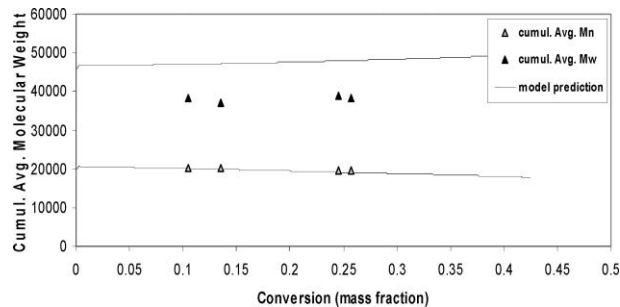

Fig. 8 Cumulative average molecular weight *versus* conversion for VAc solution homopolymerization in FAME at 60 °C (60/40 wt%).
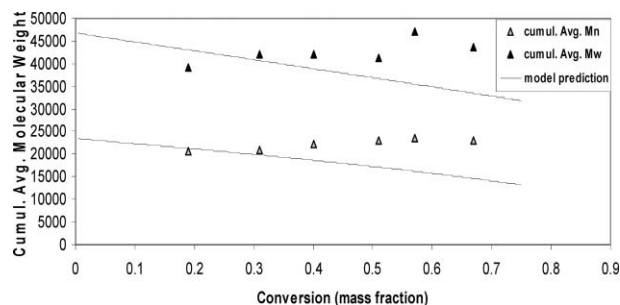

Fig. 9 Cumulative average molecular weight *versus* conversion for BA solution homopolymerization in FAME at 60 °C (60/40 wt%).

show that changing solvent viscosity and polarity has no significant effect on the propagation rate coefficient of Sty and MMA but preferential solvation of the radical site seems to occur when polymer precipitation takes place, thus increasing the monomer concentration at the free radical site and increasing the apparent k_p.[27] There is evidence of either a radical–solvent or radical–monomer complex, which participates in propagation reactions and modifies the propagation rate parameter. The stability and reactivity of these complexes determines the effect on k_p.[24] Regarding the effect on k_t, it is known that k_t is nearly always diffusion-controlled.[28] By increasing the solvent concentration, more transfer to solvent reactions are possible, resulting in faster termination reactions due to the generation of shorter and more mobile chains. This leads to an increase in k_t and, therefore, to a decrease in the rate of polymerization.[29] Regardless of the effect of solvent on the individual rate parameters, it is the lumped rate parameter, $k_p/k_t^{1/2}$, which should be manipulated because the individual parameters are coupled.

A considerable difference in the polymerization rate was observed for all monomers by changing the concentration of

solvent. Therefore, the solvent must be a major contributing factor to the change in rate in addition to the effect of dilution. The lowest polymerization rate was at the monomer/FAME ratio of 50/50 wt%, whereas the highest was observed for a ratio of 80/20 wt% for each polymer system. In general, the lowest rate of polymerization was observed for VAc, which is not surprising given its high transfer to solvent coefficient compared to other monomers. All polymers were soluble except pMMA, which precipitated in the FAME. The same behavior was observed for pMMA in methyl oleate.[16]

Conclusions

FAME derived from canola oil fulfills the demands of a solution polymerization solvent for homopolymerization of MMA, Sty, BA and VAc. Reactions at different solvent concentrations have been investigated to verify the effect of this solvent on polymerizations. Increasing solvent concentration from 20 to 50% with all other factors kept constant was more pronounced for VAc. MMA was precipitated in FAME during polymerization. Transfer constants to solvent were in the order MMA < Sty < BA < VAc. Model predictions showed reasonable agreement for all monomers with experimental data when new solvent data and changes in k_t and k_p were incorporated into the model.

Given its high boiling point, using FAME as a polymerization solvent can increase productivity by enabling polymerizations at elevated temperatures. Solution polymerization of the monomers employed in this study at 120 °C using canola-based FAME resulted in faster reaction rates with no evidence of polymerization of the solvent.[30] However, long reactions at high temperatures may result in complementary decomposition reactions of FAME.[31] A high degree of chain transfer to solvent when using FAME as the polymerization medium will lead to lower molecular weight polymer products, which may be desirable in some product applications.

Acknowledgements

Notes and references

1 M. G. Benton and C. S. Brazel, *ACS Symp. Ser.*, 2002, **818**, 125.
2 J. Sherman, B. Chin, P. Huibers, R. Garcia-Valls and T. Hatton, *Environ. Health Perspect.*, 1998, **106**(Suppl. 1), 253.
3 G. Odian, *Principles of polymerization*, John Wiley and Sons, Inc., New York, 4th edn, 2004.
4 R. Jovanovic and M. A. Dube, *Macromol. Sci. Polym. Rev.*, 2004, **44**, 1.
5 J. Hu, Z. Du, Z. Tang and E. Min, *Ind. Eng. Chem. Res.*, 2004, **43**, 7928.
6 J. Duan, Y. Shim and H. J. Kim, *J. Chem. Phys.*, 2006, **20**, 124.
7 J. M. DeSimone, *Science*, 2002, **297**, 5582.
8 P. Kubisa, *Prog. Polym. Sci.*, 2004, **29**, 3.
9 K. R. Seddon, *Kinet. Catal.*, 1996, **37**, 693.
10 C. Chiappe and D. Pieraccini, *J. Phys. Org. Chem.*, 2005, **18**, 275.
11 Z. Yang and W. Pan, *Enzyme Microb. Technol.*, 2005, **37**, 19.
12 R. A. Sheldon, *Green Chem.*, 2005, **7**, 267.
13 M. Mittelbach and C. Remschmidt, *Biodiesel: The Comprehensive Handbook*, Martin Mittelbach Paperback, Vienna, 2004.
14 *The Merck Index*, ed. S. Budavari, M. O'Neil, A. Smith and P. E. Heckelman, Merck and Co., Rahway, NJ, 1989.
15 M. Sitting, *Handbook of toxic and hazardous chemicals and carcinogens*, Noyes Publications, Park Ridge, 3rd edn, 1991.
16 E. F. Jordan, B. Artymyshyn and A. N. Wrigley, *J. Polym. Sci. Polym. Chem.*, 1969, **7**, 2605.
17 J. Gao and A. Penlidis, *J. Macromol. Sci., Rev. Macromol. Chem. Phys.*, 1996, **36**, 199.
18 M. A. Dubé, A. Y. Tremblay and J. Liu, *Bioresour. Technol.*, 2007, **98**, 639.
19 J. Brandrup, E. H. Immergut and E. A. Grulke, *Polymer Handbook*, Wiley-Interscience, New York, 4th edn, 1999.
20 T. F. McKenna, A. Villanueva and M. Santos, *J. Polym. Sci. Polym. Chem.*, 1999, **37**, 571.
21 J. P. A. Heuts, T. P. Davis and G. T. Russell, *Macromolecules*, 1999, **32**, 6019.
22 F. R. Mayo, *J. Am. Chem. Soc.*, 1943, **65**, 2324.
23 P. A. Clay and R. G. Gilbert, *Macromolecules*, 1995, **28**, 552.
24 M. D. Zammit, T. P. Davis, G. D. Willett and K. F. O'Driscoll, *J. Polym. Sci. Polym. Chem.*, 1997, **35**, 2311.
25 G. C. Eastwood, *Encyclopedia of Polymer Science and Technology*, Interscience, New York, 1967, vol. 7.
26 Y. Zhang, M. A. Dubé, D. D. McLean and M. Kates, *Bioresour. Technol.*, 2003, **90**, 229.
27 O. F. Olaj, M. Zoder and P. Vana, *Macromolecules*, 2001, **34**, 441.
28 M. Buback, M. Egorov, R. G. Gilbert, V. Kaminsky, O. F. Olaj, G. T. Russell, P. Vana and G. Zifferer, *Macromol. Chem. Phys.*, 2002, **203**, 2570.
29 R. Jovanović and M. A. Dubé, *J. Appl. Polym. Sci.*, 2004, **94**, 871.
30 S. Salehpour and M. A. Dubé, *Polym. Int.*, 2008, DOI: 10.1002/pi.2413.
31 O. Herbinet, B. Sirjean, F. Battin-Leclerc, R. Fournet and P. Marquaire, *Energy Fuels*, 2007, **21**, 1522.

Catalyst- and solvent-free conditions as an environmentally benign approach to 4-aryl-3-cyano-hexahydro-4H-1,2-benzoxazine-2-oxides†

Gianfranco Bellachioma, Luca Castrica, Francesco Fringuelli, Ferdinando Pizzo* and Luigi Vaccaro*

Under solvent-free conditions, (E)-2-aryl-1-cyano-1-nitroethenes **1a–l** rapidly react with 1-(trimethylsilyloxy)-cyclohex-1-ene (**2a**) with a complete regio- and diastereoselectivity and leading to the exclusive formation of the *cis*-fused hexahydro-*4H*-benzoxazine-2-oxides **3a–l**, which were isolated without the need for a work-up procedure in excellent yields.

1,2-Oxazine-2-oxides are generally accessible *via* a catalyzed formal [4 + 2] cycloaddition reactions of α-nitroalkenes with electron-rich alkenes.[1,2] These heterocycles are valuable intermediates to prepare in a regio- and stereoselectively manner a number of important building blocks or target heterocyclic compounds, such as pyrrolidines, β-lactam-*N*-oxides, pyrrolizidine and indolizidine alkaloids, enamines, γ-ketoalcohols, γ-nitroketones, *etc.*[1]

To contribute to the development of an environmentally benign organic chemistry, we are focusing our research on the replacement of the volatile common organic reaction media and we are interested in the use of water and solvent-free conditions (SolFC).[3,4] In addition, we are paying attention to new substrates whose reactivity can eliminate the need for a metal catalyst. In particular, we are investigating the chemical versatility of (E)-2-aryl-1-cyano-1-nitroethenes and 3-substituted coumarins.[4e,5] These substrates allowed uncatalyzed processes to be conveniently realized[4b,c] or metal catalysts to be replaced by organocatalysts such as tetrabutylammonium fluoride (TBAF).[4b,5e,f]

In more detail, we have reported that (E)-2-aryl-1-cyano-1-nitroethenes (**1a**, **1b**, and **1f**) are excellent Michael acceptors in water in the reactions with enantiopure alkyl vinyl ethers, allowing the preparation of various cyclic nitronates by a completely *endo* stereoselective [4 + 2] cycloaddition.[5b]

As a continuation of our investigation on the synthetic versatility of nitroethenes **1** under environmentally-friendly conditions, we report in this paper the reactions of nitroethenes **1a-l** under SolFC as Michael acceptors with 1-(trimethylsilyloxy)-cyclohex-1-ene (**2a**) for the synthesis of hexahydro-4*H*-1,2-benzoxazine-2-oxides **3a-l** (see Tables 1 and 2).

We have initially optimized the reaction conditions by studying the influence of the reaction medium on the [4 + 2] cycloaddition of (E)-2-(4′-methoxyphenyl)-1-cyano-1-nitroethene (**1a**)

CEMIN-Laboratory of Green Synthetic Organic Chemistry, Dipartimento di Chimica, Università di Perugia, Via Elce di Sotto, 8 06123, Perugia, Italia. E-mail: luigi@unipg.it, pizzo@unipg.it; Fax: +39 075 5855560; Tel: +39 075 5855558
† CCDC reference numbers 623145 (**3b**) and 623146 (**6a**). For crystallographic data in CIF or other electronic format see DOI: 10.1039/b712858d

Table 1 Effect of the reaction medium on the Michael addition of 1-nitroethene **1a** with 1-(trimethylsilyloxy)-cyclohex-1-ene (**2a**) (1.5 molar equiv.) at 30 °C
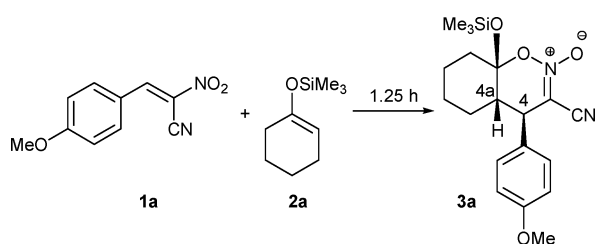
Entry	Reaction medium[a]	Conversion (%)[b]
1	SolFC	100[c]
2	H$_2$O	65
3	CH$_2$Cl$_2$	90
4	CH$_3$CN	95
5	Et$_2$O	34
6	Et$_2$O/petroleum ether (8/2)	29[d]

[a] 2 mL per 1 mmol of **1a**. [b] Conversion of **1a** to **3a** measured by ^{1}H NMR analyses. [c] **3a** was isolated in 90% yield by re-crystallization from Et$_2$O/petroleum ether (8/2). [d] After 24 h conversion of **1a** to **3a** was 88%.

with 1-(trimethylsilyloxy)-cyclohex-1-ene (**2a**) (1.5 molar equiv.) and the results are reported in Table 1.

In aqueous medium at 30 °C, under heterogeneous conditions, the conversion of **1a** to the corresponding hexahydro-4*H*-1,2-benzoxazine-2-oxide **3a** after 1.25 h was only 65% (Table 1, entry 2). Under homogeneous conditions, by using dichloromethane or acetonitrile, the cycloaddition proceeded faster to give after 1.25 h a 90% and 95% conversion to **3a**, respectively (Table 1, entries 3 and 4). In diethyl ether, where nitroethene **1a** is poorly soluble, the conversion to **3a** was very slow (34%, Table 1, entry 5).

By operating in the absence of reaction medium (SolFC) and under air atmosphere, the reaction of **1a** with **2a** was complete after 1.25 h and the corresponding *cis*-3-cyano-4-(4′-methoxyphenyl)-8*a*-(trimethylsilyl)oxy]-4*a*,5,6,7,8,8*a*-hexahydro-4*H*-1,2-benzoxazine-2-oxide (**3a**) was formed through a completely regio- and stereoselective [4 + 2] cycloaddition

Table 2 [4 + 2] Cycloaddition of 1-nitroethenes **1b–l** with 1-(trimethylsilyloxy)-cyclohex-1-ene (**2a**) (1.5 molar equiv.) under SolFC

Entry	Nitroethene **1** Ar	$T/°C$	t/h	Product	Yield (%)[a]
1	**1b** (phenyl)	25	0.75	**3b**	90
2	**1c** (2-OMe-phenyl)	40	1.25	**3c**	87
3	**1d** (4-Me-phenyl)	25	1.25	**3d**	85
4	**1e** (4-MeS-phenyl)	40	1.5	**3e**	85
5	**1f** (4-Cl-phenyl)	25	0.75	**3f**	90
6	**1g** (4-F_3C-phenyl)	30	1.0	**3g**	80
7	**1h** (2-NO_2-phenyl)	30	1.0	**3h**	82
8	**1i** (2,4-(MeO)$_2$-phenyl)	90	1.0	**3i**	80
9	**1j** (3,4-methylenedioxyphenyl)	60	0.5	**3j**	80
10	**1k** (2-furyl)	50	0.5	**3k**	86
11	**1l** (2-thienyl)	60	0.5	**3l**	84

[a] Yield of the isolated product by re-crystallization of crude reaction mixture.
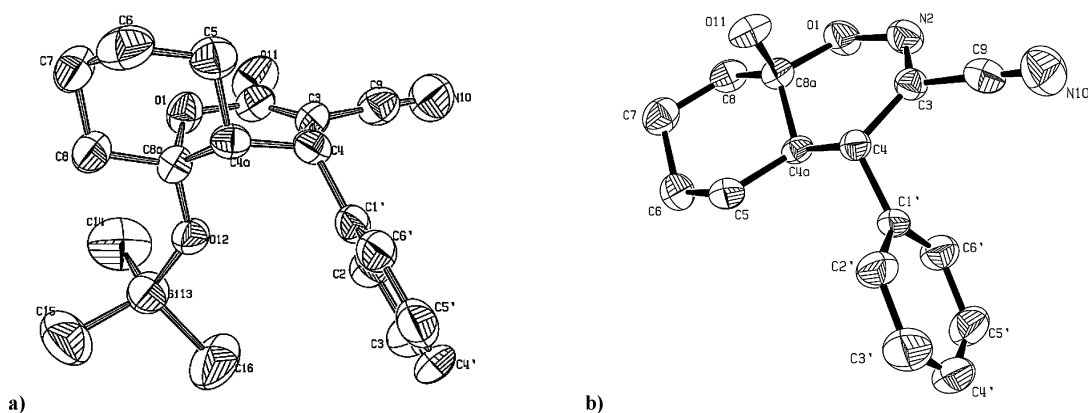
Fig. 1 X-Ray structures of **3b** (a) and **6a** (b).

process (Table 1, entry 1). **2a** was used in a slight exceess (1.5 molar equiv.) to achieve an optimal stirring.

The pure product **3a** was isolated in 90% yield, by direct re-crystallization of the crude reaction mixture (Et$_2$O/petroleum ether 8/2). For the sake of the most economically convenient procedure, the reaction of **1a** with **2a** was also performed in the mixture of solvent used for the re-crystallization of **3a** (Et$_2$O/petroleum ether 8/2), but very poor conversion was observed and only after 24 h 88% of **3a** was formed (Table 1, entry 6 and footnote d). The result obtained under SolFC is satisfactory considering that the highest chemical efficiency has been reached by avoiding the use of an organic reaction medium, the work-up procedure and any further purification step.

Considering this result, the study was extended to 1-nitroethenes **1b–l** and the results are reported in Table 2. In the absence of reaction medium (SolFC) and under air atmosphere, the cycloadditions of **1b–l** with **2a** were fast (0.5–1.5 h) and independently from the substituent, the yields were always excellent (80–90%) (Table 2). In all cases, these reactions were completely regio- and diastereoselective and led exclusively to the formation of the *cis*-fused hexahydro-4*H*-1,2-benzoxazine-2-oxides **3b–l**.

The formation of these heterocycles is due to a like-type (*lk*) Michael addition of **1** with **2a**. As typical of nitroalkene cycloadditions, the HOMO of silyl enol ether **2a** interacts with the LUMO of the nitroethene **1**, and the *endo* approach led to the transition state which is stabilized by secondary orbital interactions between the HOMO of **2a** and the LUMO of **1**.

Cyclic nitronates **3b–l** have been isolated in pure form by re-crystallization of the crude reaction mixture from ethyl acetate or Et$_2$O/petroleum ether solutions with no need for a work-up procedure. The structures of **3a–l** were confirmed by X-ray analysis of the representative compound **3b** (see Fig. 1).†[6] In addition, ^{1}H NMR analysis showed that strong NOESY correlations exist between aryl and OSiMe$_3$ protons and there are smaller interactions between the proton at position C-4*a* and the OSiMe$_3$. Similarly, analogous NOESY correlations were found in the other nitronates **3a**, **3c–l**, confirming in all cases their *cis*-fusion and the *cis* correlation between the trimethylsilyloxy and the aryl groups.

We have completed our study on the reactivity of (*E*)-2-aryl-1-cyano-1-nitroethenes **1** by investigating the Michael reaction of

1b with 1-methoxy-2-methyl-1-(trimethylsilyloxy) -propene (**2b**) under SolFC and dry conditions (Scheme 1)
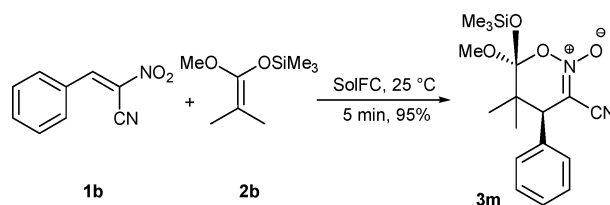
Scheme 1 Reaction of **1b** with **2b** under SolFC.

The addition of **2b** (1.2 molar equiv.) to **1b** was complete at 25 °C after 5 min and proceeded completely regio- and stereoselectively with the exclusive formation of Rel(4*S*,6*S*)-3-cyano-6-methoxy-5,5-dimethyl-4-phenyl-6-[(trimethylsilyl)-oxy]-5,6-dihydro-4*H*-1,2-oxazine-2-oxide (**3m**).

This result confirms the ability of (*E*)-2-aryl-1-cyano-1-nitroethenes **1** to react as Michael acceptors.

Finally, we have explored the possibility of converting **3** into its corresponding pyrrole derivative by: (i) hydrolytic ring-opening of the representative cyclic nitronate **3b**, and (ii) reduction of the nitro group of the corresponding γ-nitro ketones **4** and subsequent cyclization reaction.

The hydrolytic ring-opening of **3b** (step i, H$_2$O, 40 °C, 0.5 h) led to a 88/12 mixture of two ketones **4** that were isolated in 85% yield and could not be separated in our hands. The crude reaction mixture of **4** was then treated with formamidinesulfinic acid (4.0 molar equiv.) and triethylamine (TEA) (1.0 molar equiv.) in *i*-PrOH at 80 °C for 4.5 h (step ii), Scheme 2.

Surprisingly, we did not isolate the corresponding pyrrole product as expected from the data reported in the literature.[7] In our case the reduction of the nitro group was not complete and oxime **5** was formed. Cyclization of **5** *in situ* gave a 85/15 mixture of hydroxy 1,2-oxazines **6a/6b** in 56% overall yield (Scheme 2). Major diasteroisomer **6a**, coming from the oxime **5** by the axial attack of the hydroxy group to the carbonyl group, was obtained pure after re-crystallization from chloroform and it structure was determined by X-ray analysis (Fig. 1).†[8]

Hydroxy 1,2-oxazine **6a**, is a highly functionalized hetero-cyclic system and only a few examples of related compounds have been previously prepared and used as intermediate for the
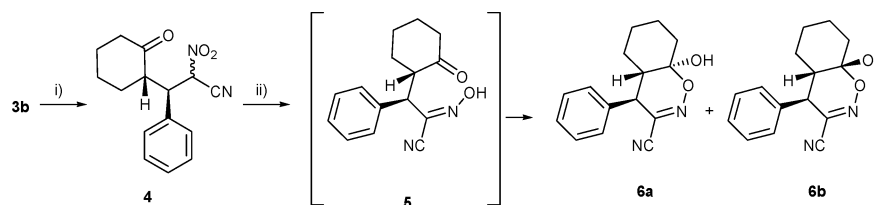
Scheme 2 Synthesis of hydroxy hexahydro-4*H*-1,2-benzoxazines **6a/6b** starting from hexahydro-4*H*-1,2-benzoxazine-2-oxide **3b**.

preparation of unnatural α-amino acids.[9] Optimization of the preparation of **6** and further investigations on their synthetic utility certainly deserve further attention.

In conclusion (*E*)-2-aryl-1-cyano-1-nitroethenes **1a–l** have been used to prepare in a stereoselective manner and with excellent yields a new series of *cis*-fused 4-aryl-3-cyano-hexahydro-*4H*-1,2-benzoxazine-2-oxides **3a–l**. The combination of solvent-free conditions and the absence of any catalyst makes this procedure easy, efficient and environmentally-friendly to access a specific class of valuable intermediates.

Experimental

General

All chemicals were purchased and used without any further purification. All ^{1}H NMR and ^{13}C NMR spectra were recorded at 200 MHz or 400 MHz, and at 50.3 or 100.6 MHz respectively, using a convenient deuterated solvent (reported in the characterization charts) and the residual peak as internal standard, or TMS in the case of CDCl$_3$. All melting points are uncorrected. Thin layer cromatography analyses were performed on silica gel on aluminium plates and UV and/or KMnO$_4$ were used as revealing agents. Column chromatography were performed by using silica gel 230–400 mesh and eluting as reported in the following characterization charts. Nitroethenes **1a–l** were prepared according to reported procedures.[5a,10] Nitronates **3a–l**, β-aryl-γ-nitroketones **4**, and hydroxy 1,2-benzoxazines **6a, b** are new compounds and their characterization charts (^{1}H NMR, ^{13}C NMR, IR, mp and elemental analysis) are reported below. X-Ray structure and cif files for compounds **3b** and **6a** are reported in the ESI.†

Representative experimental procedure for the [4 + 2] cycloaddition of 1 with 2a under solvent-free conditions

In a screw-capped vial equipped with a magnetic stirrer (*E*)-1-cyano-2-(4′-methoxyphenyl)-1-nitroethene (**1a**) (0.612 g, 3.0 mmol) was charged and 1-(trimethylsilyloxy)-cyclohex-1-ene (**2a**) (0.766 g, 4.5 mmol) was added dropwise at 25 °C under vigorous stirring. The reaction mixture was warmed to 30 °C and after 1.25 h the stirring was stopped and the pale yellow reaction mixture was re-crystallized from diethyl ether/petroleum ether (8/2) to afford 1.010 g of **3a** as a white solid (90%).

Rel(4*S*,4a*S*,8a*S*)-3-cyano-4-(4′-methoxyphenyl)-8*a*[(trimethyl-silyl)oxy]-4a,5,6,7,8,8*a*-hexahydro-4*H*-1,2-benzoxazine-2-oxide (3a)

Mp: 134–135 °C (Et$_2$O/petroleum ether: 8/2); yield 90%; ^{1}H NMR (CDCl$_3$, 400 MHz) δ (ppm) 0.18 (s, 9H), 1.20–1.36 (m,

1H), 1.51–1.83 (m, 5H), 1.84–2.00 (m, 1H), 2.10–2.30 (m, 2H), 3.58 (s, 1H), 3.81 (s, 3H), 6.87 (bd, *J* = 8.5 Hz, 2H), 7.21 (bd, *J* = 8.5 Hz, 2H); ^{13}C NMR (acetone-d6, 100.6 MHz) δ (ppm) 1.8, 22.6, 23.7, 31.8, 36.8, 45.0, 46.9, 55.2, 101.3, 108.1, 114.0, 114.6, 130.3, 132.6, 159.9; IR (CHCl$_3$) 2949 (w), 2223 (s), 1574 (s), 1513 (m), 1254 (s), 1181 (s); elemental analysis for C$_{19}$H$_{26}$N$_2$O$_4$Si: Calcd. C, 60.93; H, 7.00; N, 7.48. Found: C, 60.85; H, 7.05; N, 7.45.

Rel(4*S*,4a*S*,8a*S*)-3-cyano-4-phenyl-8*a*[(trimethylsilyl)oxy]-4a,5,6,7,8,8*a*-hexahydro-4*H*-1,2-benzoxazine-2-oxide (3b)

Mp: 133–134 °C (Et$_2$O/petroleum ether: 8/2); yield 90%; ^{1}H NMR (CDCl$_3$, 400 MHz) δ (ppm) 0.15 (s, 9H), 1.28–1.38 (m, 1H), 1.46–1.82 (m, 5H), 1.89–2.01 (m, 1H), 2.15–2.27 (m, 2H), 3.65 (s, 1H), 7.25–7.37 (m, 5H); ^{13}C NMR (CDCl$_3$, 100.6 MHz) δ (ppm) 1.7, 22.6, 23.9, 32.0, 36.6, 45.0, 47.6, 101.6, 107.4, 113.0, 127.5, 127.9, 128.7, 139.3; IR (CCl$_4$) 2947 (m), 2215 (s), 1577 (s), 1258 (s), 1175 (s); elemental analysis for C$_{18}$H$_{24}$N$_2$O$_3$Si: Calcd. C, 62.76; H, 7.02; N, 8.13. Found: C, 62.63; H, 7.00; N, 8.11.

Rel(4*S*,4a*S*,8a*S*)-3-cyano-4-(2′-methoxyphenyl)-8*a*[(trimethyl-silyl)oxy]-4a,5,6,7,8,8*a*-hexahydro-4*H*-1,2-benzoxazine-2-oxide (3c)

Mp: 134–135 °C (ethyl acetate); yield 87%; ^{1}H NMR (CDCl$_3$, 400 MHz) δ (ppm) 0.14 (s, 9H), 1.24–1.37 (m, 1H), 1.41–1.82 (m, 5H), 1.97–2.05 (m, 1H), 2.06–2.12 (m, 1H), 2.14–2.19 (m, 1H), 3.88 (s, 3H), 3.97 (s, 1H), 6.89 (s, *J* = 8.2Hz, 1H), 6.94 (dt, *J* = 0.9, 7.5 Hz, 1H), 7.21–7.29 (m, 2H); ^{13}C NMR (CDCl$_3$, 100.6 MHz) δ (ppm) 1.8, 22.8, 24.1, 31.1, 36.8, 41.6, 42.9, 55.4, 101.6, 107.7, 110.3, 113.2, 120.4, 127.2, 128.6, 129.3, 156.3; IR (CHCl$_3$) 2945 (s), 2223 (m), 1574 (s), 1256 (s), 1178 (s); elemental analysis for C$_{19}$H$_{26}$N$_2$O$_4$Si: Calcd. C, 60.93; H, 7.00; N, 7.48. Found: C, 60.91; H, 6.97; N, 7.52.

Rel(4*S*,4a*S*,8a*S*)-3-cyano-4-(4′-methylphenyl)-8*a*[(trimethyl-silyl)oxy]-4a,5,6,7,8,8*a*-hexahydro-4*H*-1,2-benzoxazine-2-oxide (3d)

Mp: 123–124 (ethyl acetate); yield 85%; ^{1}H NMR (CDCl$_3$, 400 MHz) δ (ppm) 0.17 (s, 9H), 1.25–1.40 (m, 1H), 1.45–1.80 (m, 5H), 1.85–1.97 (m, 1H), 2.10–2.25 (m, 2H), 2.34 (s, 3H), 3.59 (s, 1H), 7.05–7.20 (m, 4H); ^{13}C NMR (CDCl$_3$, 100.6 MHz) δ (ppm) 1.8, 21.0, 22.6, 23.9, 31.9, 36.5, 45.1, 47,3, 102.0, 107.3, 113.0, 127.9, 129.3, 136.2, 137.4; IR (CHCl$_3$) 2947 (m), 2223 (w), 1573 (s), 1257 (s), 1179 (s); elemental analysis for C$_{19}$H$_{26}$N$_2$O$_3$Si:

Calcd. C 63.65; H 7.31; N 7.81. Found: C 63.56; H 7.37; N 7.88.

Rel(4*S*,4*aS*,8*aS*)-3-cyano-4-(4′-methylsulfanyl phenyl)-8*a*[(trimethylsilyl)oxy]-4*a*,5,6,7,8,8*a*-hexahydro-4*H*-1,2-benzoxazine-2-oxide (3e)

Mp: 117–118 (Et$_2$O/petroleum ether: 8/2); yield 85%; ^{1}H NMR (CDCl$_3$, 400 MHz) δ (ppm) 0.16 (s, 9H), 1.23–1.38 (m, 1H), 1.42–1.82 (m, 5H), 1.87–1.98 (m, 1H), 2.10–2.25 (m, 2H), 2.47 (s, 3H), 3.59 (s, 1H), 7.15–7.30 (m, 4H); ^{13}C NMR (CDCl$_3$, 100.6 MHz) δ (ppm) 1.8, 15,7, 22.6, 23.9, 31.9, 36.5, 45.0, 47.2, 101.6, 107.3, 112.9, 126.7, 128.4, 136.0, 138,0; IR (CHCl$_3$) 2947 (m), 2223 (w), 1578 (s), 1257 (s), 1180 (s); elemental analysis for C$_{19}$H$_{26}$N$_2$O$_3$SSi: Calcd. C 58.43; H 6.71; N 7.17. Found: C 58.40; H 6.77; N 7.15.

Rel(4*S*,4*aS*,8*aS*)-3-cyano-4-(4′-chlorophenyl)-8*a*[(trimethylsilyl)oxy]-4*a*,5,6,7,8,8*a*-hexahydro-4*H*-1,2-benzoxazine-2-oxide (3f)

Mp: 112–113 (Et$_2$O/petroleum ether: 8/2); yield 90%; ^{1}H NMR (CDCl$_3$, 200 MHz) δ (ppm) 0.10 (s, 9H), 1.20–1.92 (m, 7H), 2.03–2.17 (m, 2H), 3.55 (s, 1H), 7.13–7.29 (m, 4H); ^{13}C NMR (CDCl$_3$, 50.3 MHz) δ (ppm) 1.8, 22.6, 24.0, 32.0, 36.6, 44.9, 47.1, 101.1, 107.3, 112.9, 128.8, 129.4, 133.5, 137.8; IR (CHCl$_3$) 2949 (w), 2227 (w), 1574 (s), 1183 (m); elemental analysis for C$_{18}$H$_{23}$ClN$_2$O$_3$Si: Calcd. C, 57.05; H, 6.12; N, 7.39. Found: C, 57.13; H, 6.10; N, 7.33.

Rel(4*S*,4*aS*,8*aS*)-3-cyano-4-(4′-trifluoromethylphenyl)-8*a*[(trimethylsilyl)oxy]-4*a*,5,6,7,8,8*a*-hexahydro-4*H*-1,2-benzoxazine-2-oxide (3g)

Mp: 110–111 (ethyl acetate); yield 80%; ^{1}H NMR (CDCl$_3$, 400 MHz) δ (ppm) 0.15 (s, 9H), 1.25–1.40 (m, 1H), 1.70–1.85 (m, 5H), 1.95–2.03 (m, 1H); 2.15–2–25 (m, 2H); 3.71 (s, 1H); 7.42 (d, J = 8.5 Hz, 2H); 7.62 (d, J = 8.1 Hz, 2H); ^{13}C NMR (CDCl$_3$, 100.6 MHz) δ (ppm) 1.7, 22.5, 24.0, 32.1, 36.7, 44.8, 47.3, 100.5, 107.4, 112.9, 119.8, 122.5, 125.2, 125.7, 127.9, 128.3, 129.4, 129.7, 130.0, 130.3, 143.3; IR (CHCl$_3$) 2948 (w), 2223 (w), 1574 (m), 1327 (s), 1258 (m), 1226 (m), 1174 (m), 1132 (m); elemental analysis for C$_{19}$H$_{26}$F$_3$N$_2$O$_3$Si: Calcd. C, 55.32; H, 5.62; F, 13.82; N, 6.79. Found: C, 55.13; H, 5.66; F, 13.80 N, 6.77.

Rel(4*S*,4*aS*,8*aS*)-3-cyano-4-(2′-nitrophenyl)-8*a*[(trimethylsilyl)oxy]-4*a*,5,6,7,8,8*a*-hexahydro-4*H*-1,2-benzoxazine-2-oxide (3h)

Mp: 131–132 (ethyl acetate); yield 82%; ^{1}H NMR (CDCl$_3$, 400 MHz) δ (ppm) 0.14 (s, 9H), 1.28–1.88 (m, 6H), 2.15 (dd, J = 4.4, 12.4 Hz, 1H); 2.15–2.27 (m, 2H), 4.44 (s, 1H);), 7.46–7.54 (m, 1H); 7.57 (d, J = 6.6 Hz, 1H); 7.60–7.66 (m, 1H); 8.09 (d, J = 8.2 Hz, 2H); ^{13}C NMR (CDCl$_3$, 100.6 MHz) δ (ppm) 2.0, 22.7, 24.2, 31.4, 37.2, 43.5, 43.7, 100.0, 108.0, 113.0, 125.8, 128.8, 131.9, 133.5, 134.2, 147.8; IR (CHCl$_3$) 2950 (w), 2223 (w), 1572 (m), 1528 (s), 1350 (m), 1258 (m), 1176 (m); elemental analysis for C$_{18}$H$_{23}$N$_3$O$_5$Si: Calcd. C, 55.51; H, 5.95; N, 10.79. Found: C, 55.43; H, 6.90; N, 10.73.

Rel(4*S*,4*aS*,8*aS*)-3-cyano-4-(2′,4′-dimethoxyphenyl)-8*a*[(trimethylsilyl)oxy]-4*a*,5,6,7,8,8*a*-hexahydro-4*H*-1,2-benzoxazine-2-oxide (3i)

Mp: 135–136 (ethyl acetate); yield 80%; ^{1}H NMR (CDCl$_3$, 400 MHz) δ (ppm) 0.16 (s, 9H), 1.17–1.80 (m, 6H), 1.91–2.21 (m, 3H), 3.80 (s, 3H), 3.84 (s, 3H), 3.90 (s, 1H), 6.40–6.50 (m, 2H), 7.12, (s, 1H); ^{13}C NMR (CDCl$_3$, 100.6 MHz) δ (ppm) 1.8, 22.7, 23.9, 31.0, 36.7, 41.0, 43.1, 55.4, 55.5, 98.5, 102.0, 103.8, 107.7, 113.2, 119.7, 129.8, 157.3, 160.2; IR (CHCl$_3$) 2945 (m), 2223 (w), 1615 (m), 1574 (s), 1258 (m), 1182 (m); elemental analysis for C$_{20}$H$_{28}$N$_2$O$_5$Si: 59.38; H 6.98; N 6.92. Found: 59.49; H 6.87; N 6.95.

Rel(4*S*,4*aS*,8*aS*)-4-(1′,3′-benzodioxol-5′-yl)-3-cyano-8*a*[(trimethylsilyl)oxy]-4*a*,5,6,7,8,8*a*-hexahydro-4*H*-1,2-benzoxazine-2-oxide (3j)

Mp: 125–126 (Et$_2$O/petroleum ether: 8/2); yield 80%; ^{1}H NMR (CDCl$_3$, 400 MHz) δ (ppm) 0.19 (s, 9H), 1.23–1.38 (m, 1H), 1.40–1.80 (s, 5H), 1.81–1.94 (m, 1H), 2.06–2.27 (m, 2H), 3.53 (s, 1H), 5.96 (s, 2H), 6.65–6.78 (m, 2H), 6.81, (d, J = 1.4 Hz, 1H); ^{13}C NMR (CDCl$_3$, 100.6 MHz) δ (ppm) 11.8, 22.6, 23.9, 32.0, 36.5, 45.3, 47.5, 101.3, 102.1, 107.2, 108.3, 108.6, 112.9, 121.5, 132.9, 147.1, 148.0; IR (CHCl$_3$) 2948 (m), 2223 (w), 1642 (m), 1577 (s), 1254 (s), 1180 (s); elemental analysis for C$_{19}$H$_{24}$N$_2$O$_5$Si: C, 58.74; H, 6.23; N, 7.21. Found: C, 58.77; H, 6.29; N, 7.20.

Rel(4*R*,4*aS*,8*aS*)-3-cyano-4-(2′-furyl)-8*a*[(trimethylsilyl)oxy]-4*a*,5,6,7,8,8*a*-hexahydro-4*H*-1,2-benzoxazine-2-oxide (3k)

Mp: 125–126 (ethyl acetate); yield 86%; ^{1}H NMR (CDCl$_3$, 400 MHz) δ (ppm) 0.09 (s, 9H), 1.32–1.75 (m, 5H), 1.77–1.92 (m, 1H), 2.18 (d, J = 12.5 Hz, 2H), 2.45 (dd, J = 4.4, 12.5 Hz, 1H), 3.73 (s, 1H), 6.23 (d, J = 3.3 Hz, 1H), 6.35 (dd, J = 1.9, 3.2 Hz, 1H), 7.34–7.37 (m, 1H); ^{13}C NMR (CDCl$_3$, 100.6 MHz) δ (ppm) 1.4, 22.6, 24.1, 30.6, 36.6, 40.8, 41.1, 98.7, 106.7, 107.2, 110.6, 113.0, 141.6, 151.0; IR (CHCl$_3$) 2948 (m), 2223 (w), 1574 (s), 1256 (s), 1186 (s); elemental analysis for C$_{16}$H$_{22}$N$_2$O$_4$Si: C, 57.46; H, 6.63; N, 8.38. Found: C, 57.55; H, 6.69; N, 8.32.

Rel(4*R*,4*aS*,8*aS*)-3-cyano-4-(2′-thienyl-8*a*[(trimethylsilyl)oxy]-4*a*,5,6,7,8,8*a*-hexahydro-4*H*-1,2-benzoxazine-2-oxide (3l)

Mp: 109–110 (ethyl acetate); yield 84%; ^{1}H NMR (CDCl$_3$, 400 MHz) δ (ppm) 0.18 (s, 9H), 1.20–1.36 (m, 1H), 1.39–1.81 (m, 5H), 1.85–1.94 (m, 1H), 2.17–2.26 (m, 1H), 2.31 (ddd, J = 1.2, 4.7, 12.6 Hz, 1H), 3.84 (s, 1H), 6.92 (dd, J = 3.5, 5.3 Hz, 1H), 6.98 (d, J = 3.5 Hz, 1H), 7.25 (dd, J = 1.3, 5.2 Hz, 1H); ^{13}C NMR (CDCl$_3$, 100.6 MHz) δ (ppm) 1.7, 22.6, 24.0, 31.5, 36.4, 43.1, 45.3, 101.8, 106.9, 112.6, 125.9, 126.6, 126.9, 141.6; IR (CHCl$_3$) 2948 (s), 2223 (m), 1576 (s), 1257 (s), 1184 (s); elemental analysis for C$_{16}$H$_{22}$N$_2$O$_3$SSi: C, 54.83; H, 6.33; N, 7.99. Found: C, 54.88; H, 6.39; N, 7.93.

Experimental procedure for the [4 + 2] cycloaddition of 1b with 2b

(*E*)-1-Cyano-2-phenyl-1-nitroethene (**1b**) (0.511 g, 3.0 mmol) was charged in a two-necked round bottom flask equipped with a

magnetic stirrer and 1-methoxy-2-methyl-1-(trimethylsilyloxy)-propene (**2b**) (0.627 g, 3.6 mmol) was added dropwise at 25 °C under nitrogen. After 5 min the solid formed was re-crystallized from dry diethyl ether to afford the desired nitronate **3m** in 95% yield.

Rel(4S,6S)-3-cyano-6-methoxy-5,5-dimethyl-4-phenyl-6-[(trimethylsilyl)oxy]-5,6-dihydro-4H-1,2-oxazine-2-oxide (3m)

This product was very sensitive to water and short lived in the presence of air and was therefore characterized by ^{1}H NMR only. Oil; yield 95%; ^{1}H NMR (CDCl$_3$, 400 MHz) δ (ppm) 0.32 (s, 9H), 1.20 (s, 3H), 1.24 (s, 3H), 3.63 (s, 3H), 4.41 (s, 1H), 7.26–7.35 (m, 5H).

2-Nitro-3-(2′-oxocyclohexyl)-3-phenylpropane nitrile (4)

Yield 85%; characterization data for major diastereoisomer ^{1}H NMR (CDCl$_3$, 400 MHz) δ (ppm) 1.22–1.28 (m, 1H), 1.60–1.69 (m, 2H), 1.79–1.84 (m, 2H), 2.17–2.20 (m, 1H), 2.48–2.54 (m, 2H), 2.99 (td, J = 5.0, 11.0 Hz, 1H), 3.95 (dd, J = 5.5, 11.0 Hz, 1H), 6.57 (d, J = 5.5 Hz, 1H), 7.26–7.41 (m, 5H); ^{13}C NMR (CDCl$_3$, 100.6 MHz) δ (ppm) 25.2; 28.5, 33.6, 42.7, 47.3, 51.4, 79.1, 111.3, 128.6, 129.1, 129.3, 133.1, 212.3.

Rel(4R,4aR, 8aS)-3-cyano-8a-hydroxy-4-phenyl-4a,5,6,7,8,8a-hexahydro-4H-1,2-benzoxazine (6a)

Mp: 142–144 (chloroform); yield 46%; ^{1}H NMR (CDCl$_3$, 400 MHz) δ (ppm) 1.12–1.23 (m, 1H), 1.25–1.33 (m, 1H), 1.42–1.47 (m, 1H); 1.61–1.87 (m, 5H); 1.94–1.99 (m, 1H); 2.71 (bd, J = 1.9 Hz, 1H), 3.39 (d, J = 11.9 Hz, 1H), 7.18–7.22 (m, 2H), 7.34–7.43 (m, 3H); ^{13}C NMR (CDCl$_3$, 100.6 MHz) δ (ppm) 22.6, 24.9, 26.1, 35.2, 42.0, 43.4, 98.9, 113.1, 128.5, 128.7, 129.3, 135.5, 141.6; elemental analysis for C$_{15}$H$_{16}$N$_2$O$_2$: C, 74.97; H, 6.71; N, 11.66. Found C, 75.11; H, 6.75; N, 11.51.

Acknowledgements

Notes and references

1 (a) A. T. Nielsen and T. G. Archibald, *Tetrahedron*, 1970, **26**, 3475; (b) M. Miyashita, T. Yanami and A. Yoshikoshi, *J. Am. Chem. Soc.*, 1976, **98**, 4679; (c) S. Daneo, G. Pitacco, A. Risaliti and E. Valentin, *Tetrahedron*, 1982, **38**, 1499; (d) M. Miyashita, T. Yanami, T. Kumazawa and A. Yoshikoshi, *J. Am. Chem. Soc.*, 1984, **106**, 2149; (e) A. Yoshikoshi and M. Miyashita, *Acc. Chem. Res.*, 1985, **18**, 284; (f) R. S. Varma and G. W. Kabalka, *Heterocycles*, 1986, **24**, 2645; (g) S. E. Denmark and L. R. Marcin, *J. Org. Chem.*, 1993, **58**, 3857; (h) S. E. Denmark and L. R. Marcin, *J. Org. Chem.*, 1995, **60**, 3221; (i) S. E. Denmark and A. Thorarensen, *Chem. Rev.*, 1996, **96**, 137–

165; (j) R. M. Uittenbogaard, J.-P. G. Seerden and H. W. Sheeren, *Tetrahedron*, 1997, **53**, 11929; (k) S. E. Denmark and J. A. Dixon, *J. Org. Chem.*, 1998, **63**, 6178; (l) S. E. Denmark and A. R. Hurd, *J. Org. Chem.*, 1998, **63**, 3045; (m) G. J. Kuster, F. Kalmoua, R. de Gelder and H. W. Scheeren, *Chem. Commun.*, 1999, 855; (n) S. E. Denmark and M. Seierstad, *J. Org. Chem.*, 1999, **64**, 1610; (o) M. Avalos, R. Babiano, P. Cintas, F. J. Higes, J. L. Jiménez, J. C. Palacios and M. A. Silva, *J. Org. Chem.*, 1999, **64**, 1494; (p) D. Seebach, I. M. Lyapkalo and R. Dahinden, *Helv. Chim. Acta*, 1999, **82**, 1829; (q) F. Benedetti, S. Drioli, P. Nitti, G. Pitacco and E. Valentin, *Arkivoc*, 2001, 140–155; (r) S. E. Denmark, J. J. Cottell, in *The Chemistry of Heterocyclic Compounds: Synthetic Applications of 1,3-Dipolar Cycloaddition Chemistry Toward Heterocycles and Natural Products*, ed. A. Padwa and W. H. Pearson, Wiley-Interscience, New York, 2002, pp. 83–167; (s) P. G. Tsoungas, *Heterocycles*, 2002, **57**, 1149–1178.

2 (a) D. Seebach and M. A. Brook, *Helv. Chim. Acta*, 1985, **68**, 319–324; (b) M. A. Brook and D. Seebach, *Can. J. Chem.*, 1987, **65**, 836–850; (c) D. Seebach, I. M. Lyapkalo and R. Dahinden, *Helv. Chim. Acta*, 1999, **82**, 1829–1842.

3 As representative examples see: (a) F. Fringuelli, F. Pizzo, M. Rucci and L. Vaccaro, *J. Org. Chem.*, 2003, **68**, 7041–7045; (b) G. Fioroni, F. Fringuelli, F. Pizzo and L. Vaccaro, *Green Chem.*, 2003, **5**, 425–428; (c) F. Fringuelli, F. Pizzo and L. Vaccaro, *J. Org. Chem.*, 2004, **67**, 2315–2321; (d) F. Fringuelli, F. Pizzo, S. Tortoioli and L. Vaccaro, *Org. Lett.*, 2005, **7**, 4411–4414; (e) S. Bonollo, F. Fringuelli, F. Pizzo and L. Vaccaro, *Green Chem.*, 2006, **8**, 960–964 and literature cited herein; (f) *Organic Reactions in Water*, ed. U. M. Lindström, Blackwell, Oxford, UK, 2007.

4 As representative examples see: (a) F. Fringuelli, F. Pizzo, C. Vittoriani and L. Vaccaro, *Chem. Commun.*, 2004, 2756–2757; (b) F. Fringuelli, F. Pizzo, C. Vittoriani and L. Vaccaro, *Eur. J. Org. Chem.*, 2006, 1231–1236; (c) F. Fringuelli, R. Girotti, F. Pizzo and L. Vaccaro, *Org. Lett.*, 2006, **8**, 2487–2489; (d) F. Fringuelli, R. Girotti, O. Piermatti, F. Pizzo and L. Vaccaro, *Org. Lett.*, 2006, **8**, 5741–5744.

5 (a) D. Amantini, F. Fringuelli, O. Piermatti, F. Pizzo and L Vaccaro, *Green Chem.*, 2001, **3**, 229–232; (b) F. Fringuelli, M. Matteucci, O. Piermatti, F. Pizzo and M. C. Burla, *J. Org. Chem.*, 2001, **66**, 4661–4666; (c) D. Amantini, F. Fringuelli, O. Piermatti, F. Pizzo and L. Vaccaro, *J. Org. Chem.*, 2003, **68**, 9263–9268; (d) D. Amantini, F. Fringuelli, O. Piermatti, F. Pizzo, E. Zunino and L. Vaccaro, *J. Org. Chem.*, 2005, **70**, 6526–6529; (e) G. D'Ambrosio, F. Fringuelli, F. Pizzo and L. Vaccaro, *Green Chem.*, 2005, **7**, 874–877.

6 Crystal data of **3b**: formula, M = 344.48 g mol^{-1}, triclinic space group *P*-1 (No 2), a = 9.893(2) Å, b = 10.366(2) Å, c = 10.379(2) Å, α = 102.062(17)°, β = 105.681(17)°, γ = 103.638(17)°, V = 952.6(4) Å^3, T = 295(2) K, Z = 2, D = 1.201 g cm^{-3}, μ = 0.140 mm^{-1}, crystal size = 0.25 × 0.20 × 0.15 mm^3, R = 0.0409, Rw = 0.0772, GOF = 0.876.

7 B. Quiclet-Sire, I. Thévenot and Z. S. Zard, *Tetrahedron Lett.*, 1995, **36**, 9469–9470.

8 Crystal data of **6a**: formula, M = 256.30 g mol^{-1}, triclinic space group *P*21/c (No 14), a = 14.092(3) Å, b = 8.462(3) Å, c = 11.276(3) Å, β = 96.819(17)°, V = 1335.1(7) Å^3, T = 295(2) K, Z = 4, D = 1.275 g cm^{-3}, μ = 0.086 mm^{-1}, crystal size = 0.24 × 0.17 × 0.05 mm^3, R = 0.0467, Rw = 0.0826, GOF = 0.809.

9 (a) M. Miyashita, B. Z. E. Awen and A. Yoshikoshi, *Tetrahedron*, 1990, **46**, 7569–7586; (b) J. K. Gallos, V. C. Sarli, A. C. Varvogli, C. Z. Papadoyanni, S. D. Papaspyrou and N. G. Argyropoulos, *Tetrahedron Lett.*, 2003, **44**, 3905–3909; (c) J. K. Gallos, V. C. Sarli, Z. S. Massen, A. C. Varvogli, C. Z. Papadoyanni, S. D. Papaspyrou and N. G. Argyropoulos, *Tetrahedron*, 2005, **61**, 565–574.

10 (a) W. Lehnert, *Tetrahedron*, 1972, **28**, 663–666; (b) D. Amantini, F. Fringuelli, O. Piermatti, F. Pizzo, E. Zunino and L. Vaccaro, *J. Org. Chem.*, 2005, **70**, 6526–6529.

Crystallization of an organic compound from an ionic liquid using carbon dioxide as anti-solvent

Maaike C. Kroon,[a,b] Vincent A. Toussaint,[a] Alireza Shariati,[c] Louw J. Florusse,[a] Jaap van Spronsen,[b] Geert-Jan Witkamp[b] and Cor J. Peters*[a]

In this paper the anti-solvency behavior of supercritical carbon dioxide (CO_2) as a way to recover an organic compound from an ionic liquid by crystallization is explored. As an example, the conditions for crystallization of the organic compound methyl-(Z)-α-acetamido cinnamate (MAAC) from the ionic liquid 1-butyl-3-methylimidazolium tetrafluoroborate ([bmim$^+$][BF$_4^-$]) using supercritical CO_2 as anti-solvent are studied experimentally by measuring the phase behavior of the ternary system [bmim$^+$][BF$_4^-$] + CO_2 + MAAC. MAAC can be recovered from [bmim$^+$][BF$_4^-$] by either using a shift to higher CO_2 concentrations at constant temperature (anti-solvent crystallization) or by using a shift to lower temperatures at constant CO_2 concentration (thermal shift).

Introduction

Ionic liquids (ILs) are molten salts with melting points close to room temperature.[1] They have been described as environmentally benign replacements for volatile organic solvents as reaction and separation media.[1–3] A key property of ILs is that the vapor pressure is negligibly small at room temperature ($\sim 10^{-10}$ Pa), although recently it was found that the vapor pressures of some ionic liquids at higher temperatures could in fact be measured ($\sim 10^{-4}$ Pa at 400 K).[4,5] Therefore, when used at room temperature, ILs can be recycled and reused without leading to solvent emissions into the atmosphere. Other advantages that distinguish ILs from traditional volatile organic solvents include the wide liquid temperature range, the good thermal stability, the high ionic conductivity, the wide electrochemical window, and the tunable solvency power for a wide range of materials by the choice of cation and anion.[1]

When ILs are used as reaction media, the recovery of pure products from ILs can be difficult. Low-temperature distillation is a good option for solute recovery, due to the lack of any measurable vapor pressure at room temperature,[4,5] but it is only suited for the recovery of volatile and thermally stable products. Another option is to remove a product from an IL by extraction with supercritical carbon dioxide (CO_2), since ILs do not dissolve in CO_2,[6,7] but this option only works for products that have a sufficiently high solubility in supercritical

CO_2. A relatively unexplored option that can be used to separate compounds from ILs is crystallization.

So far, only a few papers on crystallization of products from ILs have been written.[8–10] Since ILs cannot evaporate, conventional evaporative crystallization, where the solvent is evaporated in order to create supersaturation, is not possible. Instead, it should be possible to crystallize products from ILs by conventional cooling crystallization, although this option has not been explored yet.[8] Up to now, most products were crystallized from ILs in combination with a reaction step, where the product precipitates upon reaction, as the reactants have a higher solubility in IL than the product.[9,10] This method is however not practical for separation of products that have comparable or higher solubility in IL compared to the starting materials. Another method to crystallize a product from an IL is the use of an additional co-solvent that increases the solubility of the product in the IL and is evaporated in a second step in order to induce crystallization.[8] In this process, the additional co-solvent is generally a volatile organic solvent that is easily lost as emission. In our group it was shown for the first time that crystallization of a product from an IL is also possible using supercritical CO_2 as an anti-solvent, where the addition of CO_2 lowers the solubility of the product in the IL, thereby creating supersaturation.[11] Mellein and Brennecke[12] found that this ability of CO_2 to act as an anti-solvent is highly dependent on the solubility of CO_2 in the IL/organic mixture and on the hydrogen-bonding interaction between the IL and the organic. Crystallization using supercritical CO_2 as an anti-solvent is a good alternative for the recovery of pure products from ILs without problems associated with toxic and/or flammable emissions, as CO_2 is the only emission that might occur, which is a non-toxic, non-flammable and natural occurring compound. Also, Saurer et al.[13] were able to precipitate salts from IL/organic mixtures using supercritical CO_2 as anti-solvent, although the concentration of IL was rather low. However, the effects of the conditions on the crystallization

*a*Section of Physical Chemistry and Molecular Thermodynamics, Department of Chemical Technology, Faculty of Applied Sciences, Delft University of Technology, Julianalaan 136, 2628 BL, Delft, The Netherlands. E-mail: C.J.Peters@tudelft.nl; Fax: +31 15-2784289; Tel: +31 15-2782660
*b*Section of Process Equipment, Department of Process & Energy, Faculty of Mechanical, Maritime and Materials Engineering, Delft University of Technology, Leeghwaterstraat 44, 2628, CA, Delft, The Netherlands
*c*Petroleum and Chemical Engineering Department, Shiraz University, Shiraz, 71345, Iran

of organics from ILs using supercritical CO_2 as anti-solvent were never investigated before.

In this work we will further investigate the anti-solvency behavior of supercritical CO_2 as a way to recover an organic compound from an IL by crystallization. More specifically, we will systematically investigate the effect of the conditions (pressure, temperature and CO_2 concentration) on the crystallization of the product methyl-(Z)-α-acetamido cinnamate (MAAC) from the IL 1-butyl-3-methylimidazolium tetrafluoroborate ($[bmim^+][BF_4^-]$) using supercritical CO_2 as anti-solvent. MAAC is an intermediate in the production of Levodopa, a medicine against Parkinson's disease. The total phase behavior of the ternary system $[bmim^+][BF_4^-] + CO_2 + MAAC$ will be measured within a temperature range of (278.1 to 368.1) K, a pressure range of (1.44 to 14.40) MPa, a CO_2 concentration range from (30.05 to 49.25) mol% and a MAAC concentration range from (0 to 5.82) mol% in order to find the conditions for anti-solvency behavior of CO_2 and thus for crystallization of MAAC from $[bmim^+][BF_4^-]$ using supercritical CO_2 as anti-solvent.

Experimental

The phase behavior measurements of the ternary system $[bmim^+][BF_4^-] + CO_2 + MAAC$ involve visual observation of the phase transitions at different conditions using the Cailletet apparatus. This equipment allows measurement of phase equilibria within a pressure range from (0.1 to 15) MPa and temperatures from (255 to 470) K, depending on the heat-transferring fluid used. The Cailletet apparatus operates according to the synthetic method. Details of the experimental facilities and procedures can be found elsewhere.[14]

The temperature measurements in the Cailletet apparatus have an uncertainty of ±0.05 K, which is due to the temperature fluctuations in the water bath. The pressure is measured with a dead weight gauge with an uncertainty of ±0.01 MPa. The uncertainty in compositions of the samples is ±0.005 in mole fraction. Because measurements are always carried out from mid-temperature to high-temperature and thereafter from low-temperature to mid-temperature, one should measure (and we

have measured) the same value at the beginning and the end of the experiment, in order to check the reproducibility of the experiments.

MAAC was prepared with a purity of over 99.0 mol% as previously described.[15] The purity was measured using HPLC and ^1H NMR (300.2 MHz, $CDCl_3$, TMS): δ 2.14 (s, 3H), 3.85 (s, 3H), 7.38 (m, 6H). The CO_2 used for the measurements was supplied by Air Products and had a purity of 99.95 mol%. The IL $[bmim^+][BF_4^-]$ was prepared with a purity of over 99.5 mol% as previously described.[16] The purity was measured using a boron-analysis (ICP-AES): 4.76 ± 0.10 mol% boron (theoretical amount is 4.78 mol%) and NMR-analysis: ^1H NMR (300.2 MHz, $CDCl_3$, TMS): δ 0.93 (t, 3H), 1.34 (m, 2H), 1.86 (m, 2H), 3.95 (s, 3H), 4.20 (t, 2H), 7.47 (s, 2H), 8.71 (s, 1H). The amount of chloride in the IL was measured with ion chromatography and was 60 ppm. The largest impurity was fluoride, with an amount of 230 ppm. Prior to use, the $[bmim^+][BF_4^-]$ was dried under vacuum conditions at room temperature for several days. The water content of the dried IL was measured using Karl-Fischer moisture analysis and was 30 ppm. Within the temperature range of the experiments, the IL didn't show any decomposition or reaction with CO_2 or MAAC.

The crystal shape of the crystallized MAAC was analysed using Scanning Electron Microscopy (SEM) from Jeol, type JSM-5400.

Results and discussion

The phase behavior of the ternary system $[bmim^+][BF_4^-] + CO_2 + MAAC$ was measured for three different CO_2 concentrations (30 mol%, 40 mol% and 50 mol%) and two different concentrations of MAAC (2.73 mol% and 5.82%) with respect to IL, and compared to the binary $[bmim^+][BF_4^-] + CO_2$ system without any MAAC added.[17] The highest concentration used was 5.82 mol% of MAAC in $[bmim^+][BF_4^-]$ (= 72.5 g l^{-1}), because this is the maximum solubility at room temperature and atmospheric pressure. The results for 2.73 mol% and 5.82 mol% MAAC can be found in Tables 1 and 2, respectively, in which the concentration of CO_2 is expressed as mole fraction in the binary

Table 1 Phase equilibria for various concentrations of CO_2 in the system $[bmim^+][BF_4^-] + CO_2 + 2.73$ mol% MAAC (with respect to the IL)

x_{CO_2}	T/K	p/MPa	Equilibria	T/K	p/MPa	Equilibria	T/K	p/MPa	Equilibria
0.3042	278.18	1.467	VL→L	313.32	3.237	VL→L	343.99	5.437	VL→L
	283.89	1.692	VL→L	317.99	3.537	VL→L	347.93	5.772	VL→L
	288.44	1.897	VL→L	323.43	3.892	VL→L	353.04	6.207	VL→L
	293.40	2.132	VL→L	328.35	4.237	VL→L	358.17	6.662	VL→L
	298.37	2.377	VL→L	333.31	4.602	VL→L	363.15	7.122	VL→L
	303.05	2.632	VL→L	338.35	4.992	VL→L	367.88	7.597	VL→L
	308.11	2.917	VL→L						
0.4003	278.26	2.182	VL→L	313.21	4.886	VL→L	343.30	8.491	VL→L
	283.12	2.467	VL→L	318.03	5.383	VL→L	348.09	9.178	VL→L
	288.12	2.790	VL→L	323.23	5.952	VL→L	353.12	9.935	VL→L
	293.23	3.152	VL→L	328.04	6.511	VL→L	358.17	10.730	VL→L
	298.57	3.566	VL→L	333.25	7.152	VL→L	363.25	11.567	VL→L
	303.10	3.945	VL→L	338.18	7.791	VL→L	368.14	12.407	VL→L
	308.34	4.417	VL→L						
0.4925	278.09	3.032	VL→L	302.87	5.612	VL→L	323.07	9.192	VL→L
	283.00	3.437	VL→L	307.95	6.352	VL→L	325.79	9.812	VL→L
	287.72	3.872	VL→L	312.81	7.157	VL→L	328.09	10.387	VL→L
	292.70	4.362	VL→L	318.03	8.137	VL→L	330.71	11.052	VL→L
	298.53	5.037	VL→L	320.60	8.652	VL→L	332.99	11.687	VL→L

Table 2 Phase equilibria for various concentrations of CO_2 in the system $[bmim^+][BF_4^-]$ + CO_2 + 5.82 mol% MAAC (with respect to the IL)

x_{CO_2}	T/K	p/MPa	Equilibria	T/K	p/MPa	Equilibria	T/K	p/MPa	Equilibria
0.3005	278.34	1.438	VL→L	313.04	3.133	VL→L	342.98	5.293	VL→L
	283.26	1.628	VL→L	318.08	3.453	VL→L	348.02	5.698	VL→L
	288.32	1.828	VL→L	323.15	3.793	VL→L	353.09	6.128	VL→L
	293.07	2.048	VL→L	328.00	4.128	VL→L	358.09	6.563	VL→L
	298.39	2.303	VL→L	333.09	4.508	VL→L	363.08	7.008	VL→L
	303.13	2.553	VL→L	337.95	4.883	VL→L	368.00	7.473	VL→L
	308.10	2.828	VL→L						
0.4015	278.55	2.239	SLV→SL	301.70	11.899	SL→L	337.67	7.824	VL→L
	283.50	2.514	SLV→SL	303.11	3.979	VL→L	342.71	8.524	VL→L
	287.89	2.809	SLV→SL	308.16	4.454	VL→L	347.81	9.249	VL→L
	293.03	3.164	SLV→SL	313.04	4.929	VL→L	352.62	10.009	VL→L
	298.01	3.564	SLV→SL	318.09	5.434	VL→L	357.82	10.839	VL→L
	301.27	5.899	SL→L	323.00	5.984	VL→L	362.76	11.659	VL→L
	301.38	7.899	SL→L	327.93	6.564	VL→L	367.19	12.459	VL→L
	301.49	9.899	SL→L	332.86	7.199	VL→L			
0.4829	278.11	2.959	SLV→SL	293.09	4.324	SLV→SL	322.96	11.899	SL→L
	280.13	3.124	SLV→SL	298.01	4.884	SLV→SL	323.30	14.399	SL→L
	282.36	3.309	SLV→SL	303.05	5.514	SLV→SL	323.40	8.899	VL→L
	284.18	3.469	SLV→SL	308.20	6.229	SLV→SL	328.35	9.989	VL→L
	286.08	3.649	SLV→SL	313.29	7.029	SLV→SL	333.17	11.144	VL→L
	288.13	3.824	SLV→SL	318.07	7.874	SLV→SL	338.30	12.539	VL→L
	290.14	4.024	SLV→SL	322.61	9.399	SL→L			
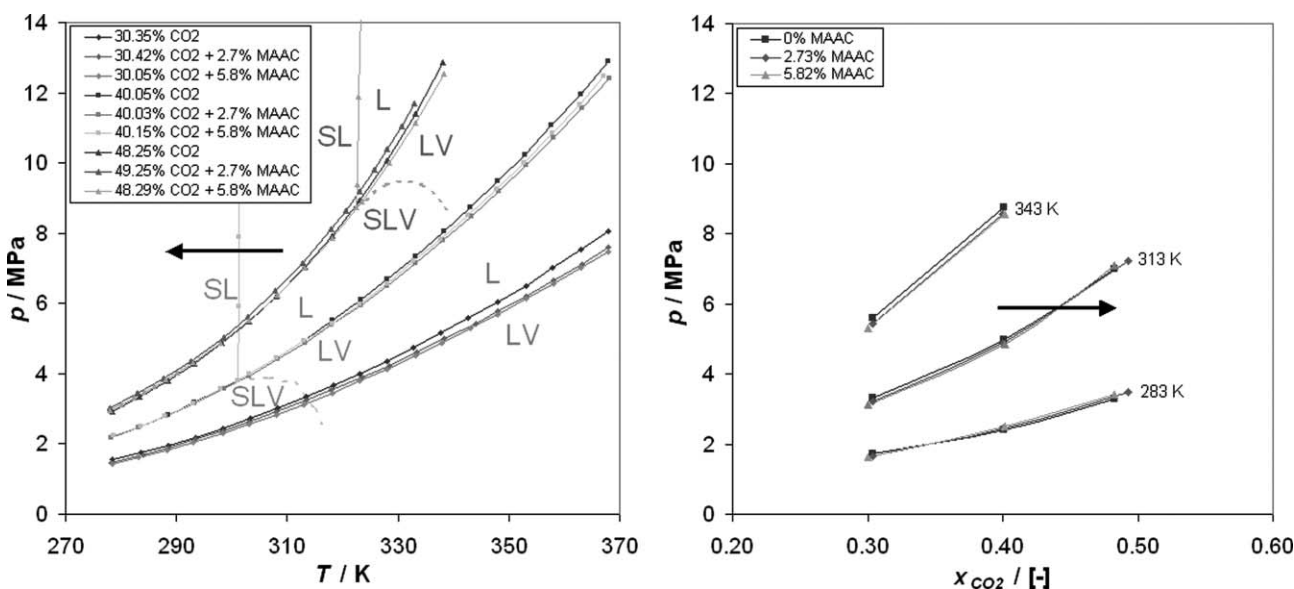
Fig. 1 Experimentally determined phase behavior of the ternary system $[bmim^+][BF_4^-]$ + CO_2 + MAAC (composition in mol%, dotted lines are not measured). This phase behavior gives rise to two methods to induce crystallization: (i) shift to lower temperatures (arrow in left-hand site of the picture) and (ii) shift to higher CO_2 concentrations (arrow in right-hand site of the picture).

IL/CO_2 system. The results are graphically shown in Fig. 1. Although the differences between the measurements seem not so large, they are statistically significant as the accuracy of the Cailletet equipment is very high (±0.01 MPa).

From the left-hand part of Fig. 1 it can be concluded that CO_2 at low concentrations (30 mol%) works as co-solvent, since the equilibrium pressures of the ternary system with MAAC are lower than the equilibrium pressures in the binary system. Therefore, at low CO_2 concentrations, the solubility of MAAC in the $[bmim^+][BF_4^-]$/CO_2 system is higher than the solubility of MAAC in pure $[bmim^+][BF_4^-]$. Adding CO_2 at low concentrations thus increases the solubility of MAAC in IL.

However, it can immediately be seen that CO_2 at higher concentrations (40 mol% and 50 mol%) and at lower temperatures starts to work as anti-solvent. The MAAC precipitates out at higher concentrations of CO_2 (presence of a solid/liquid to liquid transition), because at higher CO_2 concentrations the solubility of MAAC in the $[bmim^+][BF_4^-]$/CO_2 system is lower than the solubility of MAAC in pure $[bmim^+][BF_4^-]$. Furthermore, it can be noticed from the left-hand part of Fig. 1 that the solid/liquid-to-liquid transition (= crystallization line) moves to higher temperatures and pressures as the concentration of CO_2 increases.

In the right-hand part of Fig. 1 the bubble-point pressure is plotted against the mole fraction of CO_2 at fixed temperature,

which better shows the effect of adding MAAC on the $[bmim^+][BF_4^-]/CO_2$ system. From the right-hand part of Fig. 1 it is again clear that at low concentrations of CO_2, it works as co-solvent (line from 0 mol% MAAC is above lines from 2.73 mol% MAAC and 5.82 mol% MAAC). However, at high concentrations of CO_2 and low temperatures, the line of 0 mol% MAAC is below the line of 2.73 mol% MAAC (at temperatures lower than 301 K) and 5.82 mol% MAAC (at temperatures lower than 323 K) and CO_2 works as anti-solvent. Here, the MAAC precipitates out of the IL.

The phase behavior described in the previous paragraphs gives rise to two possible ways to induce the separation of MAAC from $[bmim^+][BF_4^-]$ by crystallization: (i) a shift in temperature to lower temperatures at constant CO_2 concentration (= thermal shift, see arrow in left-hand part of Fig. 1) and (ii) a shift in CO_2 concentration to higher concentrations at constant temperature (= crystallization by CO_2 as anti-solvent, see arrow in right-hand part of Fig. 1). The IL offers the additional advantage of a large liquid temperature range,[1] allowing large thermal shifts in order to change the solubility of the solute in IL. Moreover, the tunable solvency power of ILs is an additional opportunity. It is however a challenge to remove all IL from the MAAC, because conventional washing with CO_2 will not work as ILs are not soluble in CO_2.[6,7] Crystallization can only become a useful technique to separate products from ILs if complete IL removal from crystallized products is addressed first, for example by physical replacement of the IL or a second washing step with a chemical that only dissolves the IL and not the organic. The crystals of MAAC obtained in the shape of small plates (see Fig. 2) were therefore not free of adhering ionic liquid.
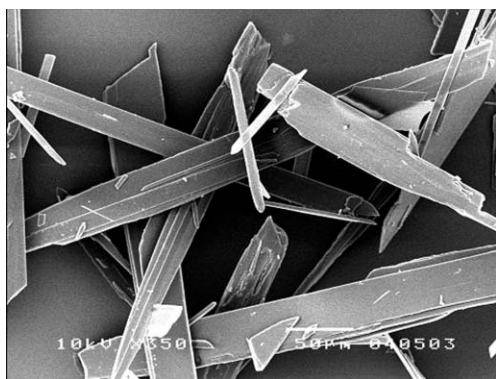

Fig. 2 SEM-image of MAAC (350× magnified, 10 kV).

Both methods (anti-solvent crystallization and thermal shifts) are common for the crystallization of organic compounds from volatile organic solvents using supercritical CO_2 as anti-solvent in a so-called GAS (Gas Anti-Solvent) process within a specific operating window,[18] but the conditions at which organics can be removed from ILs using CO_2 as anti-solvent were never found before. In fact, it was earlier believed that precipitation of products from ILs using supercritical CO_2 was impossible, because ILs do not expand significantly when CO_2 is dissolved.[7] Therefore, the influence of dissolving CO_2 on the solubility of the product was considered to be low. Here, we have shown that it is possible to recover the product MAAC from an IL by crystallization using CO_2 as anti-solvent when changing the CO_2 concentration from lower (30 mol%) to higher concentrations (40 mol% or 50 mol%). This offers a new way to recover products from ILs. As for each solute an optimized IL can be designed (by choice of cation and anion), it is expected that crystallization using supercritical CO_2 as anti-solvent is applicable for the recovery of other solutes from ILs, although it might not generally work in every case.

Conclusions

The phase behavior of the ternary system consisting of the IL $[bmim^+][BF_4^-]$, the supercritical fluid CO_2 and the organic compound MAAC was studied experimentally. CO_2 at low concentrations (30 mol%) acts as co-solvent where it increases the solubility of MAAC in $[bmim^+][BF_4^-]$, whereas CO_2 at higher concentrations (40 to 50 mol%) acts as anti-solvent where it reduces the solubility of MAAC in $[bmim^+][BF_4^-]$. Therefore, the product MAAC can be recovered by crystallization from $[bmim^+][BF_4^-]$ using a shift in CO_2 concentration to higher concentrations at constant temperature (anti-solvent crystallization). Another option to crystallize MAAC from $[bmim^+][BF_4^-]$ is the use of a thermal shift to lower temperatures at constant CO_2 concentration, as indicated by the measured solid/liquid-to-liquid transition lines. Both methods are a solution to the problem of recovering thermally labile and CO_2 insoluble products from ILs and can be generally applied for the recovery of other organic compounds from ILs, provided that complete IL removal from the crystallized product is addressed.

References

1 *Ionic Liquids in Synthesis*, ed. P. Wasserscheid and T. Welton, Wiley-VCH Verlag, Weinheim, 2003.
2 M. J. Earle and K. R. Seddon, *Pure Appl. Chem.*, 2000, **72**, 1391–1398.
3 J. F. Brennecke and E. J. Maginn, *AIChE J.*, 2001, **47**, 2384–2389.
4 M. J. Earle, J. M. S. S. Esperança, M. A. Gilea, J. N. C. Lopes, L. P. N. Rebelo, J. W. Magee, K. R. Seddon and J. A. Widegren, *Nature*, 2006, **439**, 831–834.
5 D. H. Zaitsau, G. J. Kabo, A. A. Strechan, Y. U. Paulechka, A. Tschersich, S. P. Verevkin and A. Heintz, *J. Phys. Chem. A*, 2006, **110**, 7303–7306.
6 L. A. Blanchard, D. Hancu, E. J. Beckman and J. F. Brennecke, *Nature*, 1999, **399**, 28–29.
7 L. A. Blanchard and J. F. Brennecke, *Ind. Eng. Chem. Res.*, 2001, **40**, 287–292.
8 W. M. Reichert, J. D. Holbrey, K. B. Vigour, T. D. Morgan, G. A. Broker and R. D. Rogers, *Chem. Commun.*, 2006, 4767–4779.
9 J. H. Liao and W. C. Huang, *Inorg. Chem. Commun.*, 2006, **9**, 1227–1231.
10 J. D. Holbrey, K. B. Vigour, W. M. Reichert and R. D. Rogers, *J. Chem. Crystallogr.*, 2006, **36**, 799–804.
11 M. C. Kroon, J. Van Spronsen, C. J. Peters, R. A. Sheldon and G. J. Witkamp, *Green Chem.*, 2006, **8**, 246–249.
12 B. R. Mellein and J. F. Brennecke, *J. Phys. Chem. B*, 2007, **111**, 4837–4843.
13 E. M. Saurer, S. N. V. K. Aki and J. F. Brennecke, *Green Chem.*, 2006, **8**, 141–143.
14 A. Shariati and C. J. Peters, *J. Supercrit. Fluids*, 2003, **25**, 109–117.
15 S. Gladiali and L. Pinna, *Tetrahedron: Asymmetry*, 1991, **2**, 623–632.
16 J. G. Huddleston, H. D. Willauer, R. P. Swatloski, A. E. Visser and R. D. Rogers, *Chem. Commun.*, 1998, 1765–1766.
17 M. C. Kroon, A. Shariati, M. Costantini, J. Van Spronsen, G. J. Witkamp, R. A. Sheldon and C. J. Peters, *J. Chem. Eng. Data*, 2005, **50**, 173–176.
18 J. C. De, La Fuente, A. Shariati and C. J. Peters, *J. Supercrit. Fluids*, 2004, **32**, 55–61.

Highly active and robust organic–inorganic hybrid catalyst for the synthesis of cyclic carbonates from carbon dioxide and epoxides

Takashi Sakai,* Yoshihiro Tsutsumi and Tadashi Ema

A high-throughput combinatorial strategy enabled us to find a highly active organic–inorganic hybrid catalyst for the production of cyclic carbonates from CO_2 and epoxides. The best hybrid catalyst **1a** was prepared by the coupling of 3-(triethoxysilyl)propyltriphenylphosphonium bromide and mesoporous silica, and the organic and inorganic moieties had a synergistic effect on catalytic activity. The pore size of silica was found to be important for catalysis; mesoporous silica with the mean pore size of 19 nm exhibited much better performance than silica with that of 6 nm. The solvent-free and metal-free reactions proceeded successfully under very mild conditions (1 MPa, 90 °C, 1 mol% loading of catalyst, 6 h), and the hybrid catalyst could be recycled ten times.
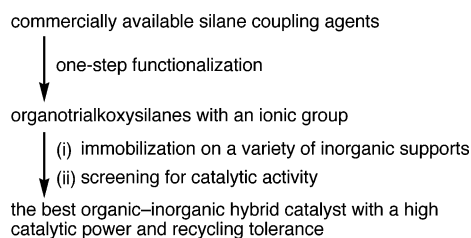
Introduction

Chemical fixation of CO_2 to synthesize a useful compound is one of the most important and challenging subjects in synthetic organic chemistry. Although CO_2 is one of the greenhouse gases, it is a non-toxic, abundant, and recoverable C_1 building block.[1] One method for the CO_2 fixation is the coupling reaction with epoxides to synthesize five-membered cyclic carbonates,[2] which can be used as aprotic polar solvents, monomers for polycarbonates, and fine chemical intermediates. Cyclic carbonates have been synthesized from the corresponding 1,2-diols and a highly toxic gas, phosgene. In the past decade, however, many catalysts for synthesizing cyclic carbonates from CO_2 and epoxides have been developed to surpass the phosgene method. For example, alkali metal salts,[3] MgO or Al/MgO catalysts,[4,5] heavy metal catalysts,[6] ionic liquids,[2c,d,7] and onium halides[8] have been developed. Some of them have problems, such as harsh reaction conditions (a high temperature and pressure) and the use of organic solvent or a Lewis base co-catalyst. Recently, solvent-free and metal-free catalysts as well as halogen-free catalysts are becoming more and more important.[9,10] Reusability of catalysts, which is important from the viewpoint of practical use, has also been investigated with organic–inorganic hybrid catalysts,[11] ion-exchange resins,[12] PEG-supported or polyfluoroalkyl-substituted phosphonium salts.[13,14]

Here we demonstrated a high-throughput combinatorial strategy to find a highly active organic–inorganic hybrid catalyst for the production of cyclic carbonates from CO_2 and epoxides. The best hybrid catalyst with high catalytic activity and reusability was prepared by the coupling of 3-(triethoxysilyl)propyltriphenylphosphonium bromide and mesoporous silica. We found that the pore size of silica is important for catalysis; mesoporous silica with the mean pore

Division of Chemistry and Biochemistry, Graduate School of Natural Science and Technology, Okayama University, Tsushima, Okayama, 700-8530, Japan

size of 19 nm exhibited much better performance than silica with that of 6 nm. Solvent-free and metal-free reactions proceeded successfully under very mild conditions, and the catalyst could be recycled ten times. We also wish to report an unexpected effect of the substituent attached to the phosphorus atom on catalytic activity.
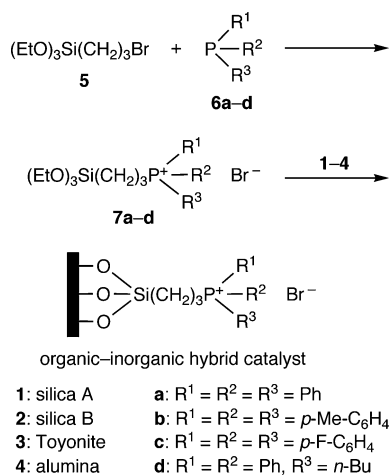
Results and discussion

The high-throughput combinatorial strategy that we employed is represented in Scheme 1. We envisioned that organotrialkoxysilanes with an ionic group, which are key compounds prepared from commercially available silane coupling agents, could be attached easily to a variety of inorganic supports and that the catalytic abilities of organic–inorganic hybrid catalysts could be evaluated rapidly. We also expected that the use of the immobilized catalyst would allow us to recycle the catalyst several times.

commercially available silane coupling agents

↓ one-step functionalization

organotrialkoxysilanes with an ionic group

↓ (i) immobilization on a variety of inorganic supports
(ii) screening for catalytic activity

the best organic–inorganic hybrid catalyst with a high catalytic power and recycling tolerance

Scheme 1 High-throughput combinatorial strategy for the screening of catalysts.

The synthetic scheme for the immobilized catalysts is shown in Scheme 2. Initially, we tried to prepare the key compound, 3-(triethoxysilyl)propyltriphenylphosphonium bromide (**7a**), by heating a mixture of 3-(triethoxysilyl)propyl bromide (**5**) and triphenylphosphine (**6a**) in DMF at 150 °C for 24 h under N_2; however, pure product could not be obtained because of the formation of a small amount of unknown impurities. The reaction in refluxing toluene resulted in no conversions, while the reaction in DMSO at 150 °C gave decomposed

$(EtO)_3Si(CH_2)_3Br$ + **5** ... **6a–d** →

$(EtO)_3Si(CH_2)_3P^+$ ... Br^- **1–4** →

7a–d

organic–inorganic hybrid catalyst

1: silica A
2: silica B
3: Toyonite
4: alumina

a: $R^1 = R^2 = R^3 = Ph$
b: $R^1 = R^2 = R^3 = p\text{-Me-C}_6H_4$
c: $R^1 = R^2 = R^3 = p\text{-F-C}_6H_4$
d: $R^1 = R^2 = Ph, R^3 = n\text{-Bu}$

Scheme 2 Preparation of immobilized phosphonium bromide catalysts.

by-products. Finally, we succeeded in the isolation of the desired phosphonium bromide **7a** by changing the solvent to MeCN. Washing the product with Et_2O gave **7a** as a powder in 92% yield, which was pure as measured by ^1H and ^{31}P NMR. The same procedure gave other phosphonium bromides **7b–c** as a powder and **7d** as a viscous oil in good yields.

Next, phosphonium bromides **7a–d** were immobilized on a variety of inorganic supports: two kinds of silica (silica A and silica B), Toyonite, and alumina. Silica A and B have the mean pore sizes of 19 nm and 6 nm, respectively. Toyonite is a porous ceramic support prepared from kaolin minerals by a hydrothermal treatment under acidic conditions and has a mean pore size of 60 nm.[15] Alumina used in this study is basic aluminium oxide developed for the purpose of chromatography. For example, phosphonium bromide **7a** was attached to silica A by the heat treatment in toluene at 80 °C for 48 h, and the resulting hybrid catalyst **1a** was filtered, washed with EtOH, acetone, and Et_2O, and then dried *in vacuo* to give a white power. The completion of the immobilization was confirmed by the NMR analysis of the filtrate. The degree of the immobilization of **7a** was determined by the combustion analysis of **1a** to be 8.0% (w/w), which is close to 7.6% (w/w), a value calculated by assuming that **7a** was immobilized in 100% yield (0.2 mmol of organic moiety per 1 g of inorganic support). The other catalysts immobilized on silica A, silica B, Toyonite, and alumina were also prepared in the same way.

Catalysts **1a–4a** (1 mol% of the catalytic moiety with respect to the amount of epoxide) were used in the coupling reaction of CO_2 (1 MPa) with 1,2-epoxyhexane (**8a**) at 90 °C for 6 h in a stainless steel autoclave. The results are summarized in Table 1. The control reactions using tetraphenylphosphonium bromide (entry 13) and 3-(triethoxysilyl)propyltriphenylphosphonium bromide (**7a**) (entry 14) were also conducted, which gave 1% and 38% conversions, respectively. In contrast, silica-immobilized catalysts **1a** and **2a** dramatically increased the yield up to 99% (entries 1 and 2). On the other hand, Toyonite-immobilized catalyst **3a** gave a lower yield (90%, entry 3), and the alumina-immobilized catalyst **4a** resulted in a much lower yield (52%, entry 4). The catalytic activity of the organic–inorganic hybrid catalysts decreased in the following order: **1a** ~ **2a** > **3a** > **4a**.

Table 1 Synthesis of cyclic carbonate **9a** from CO_2 and 1,2-epoxyhexane (**8a**) with phosphonium bromide catalysts[a]
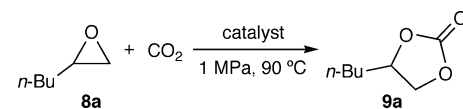

Entry	Catalyst	Conversion (%)[b]
1	**1a**	99
2	**2a**	>99
3	**3a**	90
4	**4a**	52
5	**1a**[c]	90
6	**2a**[c]	64
7	**1b**	>99
8	**1c**	96
9	**1d**	99
10	**3b**	44
11	**3c**	70
12	**3d**	55
13[d]	$PPh_4{}^+Br^-$	1
14[d]	**7a**	38

[a] Conditions: **8a** (10.0 mmol), catalyst (1 mol%, 550 mg, 0.2 mmol of organic moiety per 1 g of inorganic support), 1 MPa CO_2, in a 50 mL autoclave, 6 h. [b] Determined by NMR. [c] 0.5 mol% catalyst was loaded. [d] Non-immobilized catalyst was used.

Because the same organic moiety is attached to these catalysts, this difference in catalytic activity should originate from the nature of the inorganic moiety. We noticed that this order of catalytic activity is the same as that of the acidity of the OH group on the surface of the inorganic supports. Therefore, not only the phosphonium bromide moiety but also the acidic OH group on silica are likely to participate in catalysis as proposed by Sakakura and coworkers,[11a] whereas the less acidic OH group on Toyonite and the much less acidic OH group on basic alumina are insufficient for the activation of epoxide. Thus, we found that the synergistic effect of the organic and inorganic moieties on catalytic activity varies to a considerable degree.

Furthermore, we observed a clear difference in catalytic activity between silica-based catalysts **1a** and **2a** when the catalyst loading was decreased to 0.5 mol% (entries 5 and 6, 90% *vs* 64%). The mean pore size of silica A, 19 nm, seems to be more suitable for catalysis than that of silica B, 6 nm. Other researchers have also reported the importance of the pore size of silica in the asymmetric hydrogenation of olefins.[16] Because various types of mesoporous silicas have recently been synthesized,[17] mesoporous silica capable of promoting the cycloaddition of CO_2 to epoxides more efficiently may be found in future. The time course of the **1a**-catalyzed formation of cyclic carbonate **9a** is shown in Fig. 1, which indicates the solvent-free and metal-free fast catalytic reaction under mild reaction conditions. In this way, we could find rapidly the best catalyst **1a** based on the combinatorial protocol shown in Scheme 1.

Next, we investigated the effect of the substituents of the phosphonium moiety on the catalytic activity. The increase in the Lewis acidity of the phosphonium moiety was expected to increase the catalytic activity. Surprisingly, catalyst **1c** was less active than **1b** and **1d**, which is opposite to our expectation (Table 1, entries 7–9). The bulkiness of the fluorine atom at
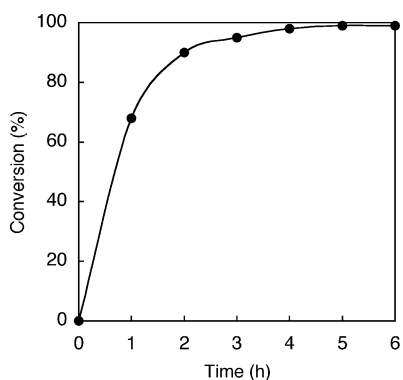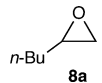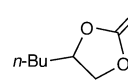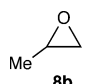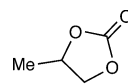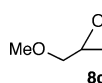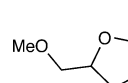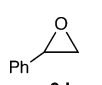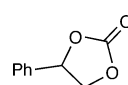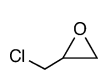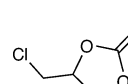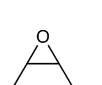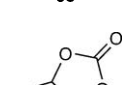
Fig. 1 Time course for the **1a**-catalyzed formation of cyclic carbonate **9a**. Reaction conditions: 1,2-epoxyhexane (**8a**) (2.5 mmol), catalyst **1a** (1 mol%), 1 MPa CO_2, 90 °C.

the *para* position may have hindered the reaction. Although no appreciable differences could be observed between silica-immobilized catalysts **1a**, **1b** and **1d** under the reaction conditions examined (entries 1, 7, and 9), Toyonite-immobilized catalysts exhibited a clear difference (entries 3 and 10–12) as follows. The bulky and electron-donating *p*-Me-substituted catalyst **3b** gave the lowest conversion (entry 10). This trend is reasonable because the pK_a of P(*p*-Me-C_6H_4)$_3$ (4.46) is known to be larger than that of PPh$_3$ (3.28).[18] On the other hand, the result obtained with *p*-F-substituted catalyst **3c** was again opposite to our expectation, giving a lower conversion as compared with **3a** (entry 11). The replacement of one of the three phenyl groups in **3a** by the *n*-butyl group also hampered the catalytic activity (entry 12).

We decided to use catalyst **1a** in further experiments because of its high catalytic activity and synthetic accessibility. The scope of the substrate acceptance was explored (Table 2). Epoxides bearing an electron-donating substituent such as *n*-Bu, Me, and CH_2OMe (**8a–c**) were converted to the corresponding cyclic carbonates **9a–c** in high yields (88–99%) within a short reaction time (6–12 h). When styrene oxide (**8d**) was used, the yield did not exceed 86%, probably because solid product **9d** covered the surface of the catalyst during the reaction. Epoxide **8e** with an electron-withdrawing CH_2Cl group required a longer reaction time (20 h) to give product **9e** in a high yield (85%), which is probably due to the reduced electron density of the epoxide oxygen atom. The reaction of 1,2-epoxycyclohexane (**8f**) afforded a low yield of **9f** (21%) probably because of a steric hindrance. In all cases, cyclic carbonates were formed exclusively; only the signals for cyclic carbonate and epoxide could be detected after the reaction.

To further demonstrate the advantage of the organic–inorganic hybrid catalyst, the reusability of **1a** was examined. The results are shown in Fig. 2. To our delight, catalyst **1a** could be used ten times, and the conversion reached 97% even after the ten-time reuse of **1a**. The catalyst **1a** used ten times still retained catalytic activity. Moreover, **1a** retained the original catalytic activity during storage for more than eight months. Thus, **1a** is a robust catalyst capable of showing high catalytic activity for a long time and is useful for the environmentally benign organic synthesis.

Table 2 Synthesis of various cyclic carbonates using immobilized catalyst **1a**[a]

Substrate	Product	Time (h)	Yield (%)[b]
8a	**9a**	6	99
8b	**9b**	6	99
8c	**9c**	12	88
8d	**9d**	6	86
8e	**9e**	20	85
8f	**9f**	24	21

[a] Conditions: **8** (10.0 mmol), catalyst **1a** (1 mol%, 550 mg, 0.2 mmol of organic moiety per 1 g of inorganic support), 1 MPa CO_2, in a 50 mL autoclave. [b] Isolated yield.
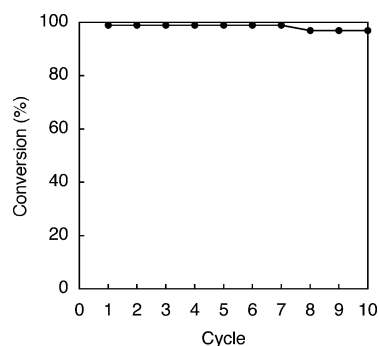
Fig. 2 The reusability of the immobilized catalyst **1a** (1 mol%) for the cycloaddition of CO_2 (1 MPa) to 1,2-epoxyhexane (**8a**) at 90 °C for 7 h.

Conclusions

We have prepared a variety of phosphonium bromide catalysts immobilized on silica, Toyonite, and alumina **1a–4a**, among which **1a** was found to be the best choice for the solvent-free and metal-free synthesis of cyclic carbonates under mild reaction conditions. The isolation of 3-(triethoxysilyl)propyltriphenylphosphonium bromide (**7a**) and its derivatives **7b–d** was the key, which enabled us to rapidly find the matched combination of phosphonium bromide and inorganic support. Interestingly, we observed a synergistic effect of the

organic and inorganic moieties on catalytic activity; not only the phosphonium bromide moiety but also the OH group on the surface of silica seem to participate in catalysis. We also found that the pore size of silica is important for catalysis; mesoporous silica with the mean pore size of 19 nm exhibited much better performance than silica with that of 6 nm. The present reaction (1 MPa, 90 °C, 1 mol% loading of catalyst, 6 h) is conducted under the mildest conditions that have been reported so far for the solvent-free and metal-free systems, and **1a** is a robust catalyst with high recycling tolerance.

Experimental

Materials and methods

Mesoporous silica MP20300 (silica A) was provided by Mitsubishi Chemical Corporation and Nippon Kasei Chemical Co., Ltd., and silica BW-127ZH (silica B) was purchased from Fuji Silysia Chemical, Ltd. Toyonite 800 and aluminium oxide 90 active basic were purchased from Toyo Denka Kogyo Co., Ltd. and Merck, respectively. All the epoxides were commercially obtained and used without purification. Dry toluene and dry MeCN were distilled from NaH and CaH$_2$, respectively.

General procedure for preparing phosphonium bromide

A solution of phosphine (2.00 mmol) and 3-bromopropyltriethoxysilane (2.00 mmol) in dry MeCN (4 mL) under N$_2$ was heated at reflux overnight. The progress of the reaction was monitored by ^{1}H and ^{31}P NMR. The mixture was concentrated, and the residue was triturated with dry Et$_2$O (10 mL) and then filtered to give phosphonium bromide **7a–c** or decanted to give a viscous oil **7d**

3-(Triethoxysilyl)propyltriphenylphosphonium bromide (7a). 92% yield; ^{1}H NMR (500 MHz, CDCl$_3$) δ 1.05 (t, J = 7.5 Hz, 2 H), 1.12 (t, J = 7.0 Hz, 9 H), 1.75–1.80 (m, 2 H), 3.75 (q, J = 7.0 Hz, 6 H), 3.81–3.87 (m, 2 H), 7.66–7.70 (m, 6 H), 7.76–7.84 (m, 9 H); ^{13}C NMR (125 MHz, CDCl$_3$) δ 9.6 (d, J_{CSi} = 15.5 Hz), 15.1, 16.6, 22.8 (d, J_{CP} = 48.3 Hz), 56.7, 116.5 (d, J_{CP} = 83.9 Hz), 128.8 (d, J_{CP} = 11.9 Hz), 131.8 (d, J_{CP} = 10.0 Hz), 133.4; ^{31}P NMR (121 MHz, CDCl$_3$) δ 22.9; IR (KBr) 2972, 2887, 1441, 1115, 1074 cm^{-1}.

3-(Triethoxysilyl)propyltris(*p*-methylphenyl)phosphonium bromide (7b). 87% yield; ^{1}H NMR (500 MHz, CDCl$_3$) δ 1.02 (t, J = 7.5 Hz, 2H), 1.14 (t, J = 7.0 Hz, 9 H), 1.72–1.77 (m, 2 H), 2.46 (s, 9 H), 3.60–3.66 (m, 2 H), 3.76 (q, J = 7.0 Hz, 6 H), 7.45–7.47 (m, 6 H), 7.60–7.67 (m, 6 H); ^{13}C NMR (125 MHz, CDCl$_3$) δ 10.7 (d, J_{CSi} = 16.4 Hz), 16.5, 17.6, 21.2, 24.4 (d, J_{CP} = 51.9 Hz), 57.7, 114.4 (d, J_{CP} = 87.5 Hz), 130.6 (d, J_{CP} = 12.8 Hz), 132.8 (d, J_{CP} = 10.1 Hz), 145.7 (d, J_{CP} = 2.8 Hz); ^{31}P NMR (121 MHz, CDCl$_3$) δ 22.3; IR (KBr) 2978, 2885, 1597, 1450, 1111, 1080 cm^{-1}.

3-(Triethoxysilyl)propyltris(*p*-fluorophenyl)phosphonium bromide (7c). 89% yield; ^{1}H NMR (500 MHz, CDCl$_3$) δ 1.07 (t, J = 7.5 Hz, 2 H), 1.16 (t, J = 7.0 Hz, 9 H), 1.72–1.77 (m, 2 H), 3.78 (q, J = 7.0 Hz, 6 H), 4.05–4.11 (m, 2 H), 7.38–7.42 (m, 6 H), 7.91–7.97 (m, 6 H); ^{13}C NMR (125 MHz, CDCl$_3$) δ 11.0 (d, J_{CSi} = 17.4 Hz), 16.8, 18.1, 24.8 (d, J_{CP} = 51.1 Hz), 58.4,

113.8 (d, J_{CP} = 85.8 Hz), 118.3 (dd, J_{CF}, J_{CP} = 13.6, 21.8 Hz), 136.6 (t, J_{CF} = J_{CP} = 10.0 Hz), 166.6 (d, J_{CF} = 258.9 Hz); ^{31}P NMR (121 MHz, CDCl$_3$) δ 23.2; ^{19}F NMR (282 MHz, CDCl$_3$) δ −101.4 to −100.3 (m); IR (KBr) 2978, 2893, 1589, 1504, 1242, 1165, 1111 cm^{-1}.

***n*-Butyldiphenyl-3-(triethoxysilyl)propylphosphonium bromide (7d).** 92% yield; ^{1}H NMR (500 MHz, CDCl$_3$) δ 0.89 (t, J = 7.5 Hz, 5 H), 1.16 (t, J = 7.0 Hz, 9 H), 1.43–1.55 (m, 6 H), 3.31–3.43 (m, 4 H), 3.77 (q, J = 7.0 Hz, 6 H), 7.66–7.69 (m, 4 H), 7.75–7.78 (m, 2 H), 7.89–7.93 (m, 4 H); ^{13}C NMR (125 MHz, CDCl$_3$) δ 9.72 (d, J_{CSi} = 15.5 Hz), 12.0, 14.7, 16.7, 19.8 (d, J_{CP} = 48.4 Hz), 21.5 (d, J_{CP} = 49.3 Hz), 21.9 (d, J_{CP} = 16.4 Hz), 22.4, 56.8, 116.5 (d, J_{CP} = 81.1 Hz), 128.7 (d, J_{CP} = 11.9 Hz), 131.5 (d, J_{CP} = 10.1 Hz), 133.1; ^{31}P NMR (121 MHz, CDCl$_3$) δ 26.7; IR (nujor) 3055, 2970, 2874, 1439, 1165, 1119 cm^{-1}.

General procedure for the immobilization of phosphonium bromide on inorganic support

A mixture of phosphonium bromide (2.00 mmol) and inorganic support (10.0 g) (silica A, silica B, Toyonite, or alumina) in dry toluene (40 mL) and dry DMF (2 mL) was stirred at 80 °C for 48 h (silica and alumina) or at 40 °C for 12 h (Toyonite).[19] The immobilized catalyst was washed with EtOH, acetone, and Et$_2$O, filtered, and dried *in vacuo* for 4 h. Immobilization of phosphonium bromide was confirmed by the increase of the weight of the powdery solid and by the decrease in phosphonium bromide in the filtrate as measured by ^{1}H and ^{31}P NMR.

General procedure for the coupling reaction of CO$_2$ with epoxide

A 50 mL stainless autoclave was charged with epoxide (10.0 mmol), catalyst (550 mg, 0.2 mmol of organic moiety per 1 g of inorganic support, 1 mol% of the catalytic moiety with respect to the amount of epoxide), and then CO$_2$ (initial pressure of 1 MPa). The mixture was heated with stirring at 90 °C for the reaction time indicated. The reactor was cooled in an ice bath for 30 min, and excess CO$_2$ was released carefully. The product was dissolved in Et$_2$O, and the catalyst was removed by filtration. The product was analyzed by ^{1}H NMR and GC: Apiezon grease L (1 m) for **9a** and **9c–f**, Inj. 270 °C, Col. 50 °C→150 °C (5 °C min^{-1}) or PEG-20M (3 m) for **9b**, Inj. 250 °C, Col. 70 °C→150 °C (3 °C min^{-1}). The product was purified by distillation or silica gel column chromatography if necessary.

4-*n*-Butyl-1,3-dioxolan-2-one (9a).[20] 99% yield; ^{1}H NMR (500 MHz, CDCl$_3$) δ 0.93 (t, J = 7.3 Hz, 3 H), 1.34–1.49 (m, 4 H), 1.66–1.72 (m, 1 H), 1.78–1.85 (m, 1 H), 4.07 (dd, J = 7.3, 8.0 Hz, 1 H), 4.52 (t, J = 8.0 Hz, 1 H), 4.67–4.73 (m, 1 H); ^{13}C NMR (125 MHz, CDCl$_3$) δ 13.2, 21.7, 25.9, 32.9, 69.0, 76.8, 154.8; IR (neat) 1794 cm^{-1}.

4-Methyl-1,3-dioxolan-2-one (9b).[20] 99% yield; ^{1}H NMR (500 MHz, CDCl$_3$) δ 1.49 (d, J = 6.0 Hz, 3 H), 4.02 (dd, J = 7.0, 8.5 Hz, 1 H), 4.55 (dd, J = 7.5, 8.5 Hz, 1 H), 4.83–4.87 (m, 1 H); ^{13}C NMR (125 MHz, CDCl$_3$) δ 19.2, 70.5, 73.4, 154.9; IR (neat) 1790 cm^{-1}.

4-Methoxymethyl-1,3-dioxolan-2-one (9c).[11c] 88% yield; ^{1}H NMR (500 MHz, CDCl$_3$) δ 3.43 (s, 3 H), 3.58 (dd, J = 4.0, 11.0 Hz, 1 H), 3.64 (dd, J = 4.0, 11.0 Hz, 1 H), 4.38 (dd,

J = 6.0, 8.5 Hz, 1 H), 4.49 (t, J = 8.5 Hz, 1 H), 4.78–4.81 (m, 1 H); ^{13}C NMR (125 MHz, CDCl$_3$) δ 59.5, 66.1, 71.4, 75.0, 154.9; IR (neat) 1794 cm^{-1}.

4-Phenyl-1,3-dioxolan-2-one (9d).[20] 86% yield; ^{1}H NMR (500 MHz, CDCl$_3$) δ 4.35 (dd, J = 8.0, 8.5 Hz, 1 H), 4.80 (dd, J = 8.0, 8.5 Hz, 1 H), 5.68 (t, J = 8.0 Hz, 1 H), 7.36–7.47 (m, 5 H); ^{13}C NMR (125 MHz, CDCl$_3$) δ 71.1, 77.9, 125.8, 129.2, 129.7, 135.8, 154.8; IR (KBr) 1778 cm^{-1}.

4-Chloromethyl-1,3-dioxolan-2-one (9e).[20] 85% yield; ^{1}H NMR (500 MHz, CDCl$_3$) δ 3.69–3.79 (m, 2 H), 4.41 (dd, J = 6.0, 9.0 Hz, 1 H), 4.59 (dd, J = 8.0, 9.0 Hz, 1 H), 4.93–4.97 (m, 1 H); ^{13}C NMR (125 MHz, CDCl$_3$) δ 43.7, 66.9, 74.3, 154.2; IR (neat) 1802 cm^{-1}.

4,5-Tetramethylene-1,3-dioxolan-2-one (9f).[21] 21% yield; ^{1}H NMR (500 MHz, CDCl$_3$) δ 1.40–1.46 (m, 2 H), 1.60–1.65 (m, 2 H), 1.88–1.92 (m, 4 H), 4.67–4.70 (m, 2 H); ^{13}C NMR (125 MHz, CDCl$_3$) δ 19.0, 26.6, 75.6, 155.3; IR (nujor) 1790 cm^{-1}.

Acknowledgements

References

1 (*a*) M. Komatsu, T. Aida and S. Inoue, *J. Am. Chem. Soc.*, 1991, **113**, 8492; (*b*) K. Nakano, T. Kamada and K. Nozaki, *Angew. Chem., Int. Ed.*, 2006, **45**, 7274.

2 Reviews: (*a*) D. J. Darensbourg and M. W. Holtcamp, *Coord. Chem. Rev.*, 1996, **153**, 155; (*b*) A.-A. G. Shaikh and S. Sivaram, *Chem. Rev.*, 1996, **96**, 951; (*c*) J. Sun, S. Fujita and M. Arai, *J. Organomet. Chem.*, 2005, **690**, 3490; (*d*) S. Zhang, Y. Chen, F. Li, X. Lu, W. Dai and R. Mori, *Catal. Today*, 2006, **115**, 61.

3 N. Kihara, N. Hara and T. Endo, *J. Org. Chem.*, 1993, **58**, 6198.

4 T. Yano, H. Matsui, T. Koike, H. Ishiguro, H. Fujihara, M. Yoshihara and T. Maeshima, *Chem. Commun.*, 1997, 1129.

5 K. Yamaguchi, K. Ebitani, T. Yoshida, H. Yoshida and K. Kaneda, *J. Am. Chem. Soc.*, 1999, **121**, 4526.

6 (*a*) A. Baba, T. Nozaki and H. Matsuda, *Bull. Chem. Soc. Jpn.*, 1987, **60**, 1552; (*b*) H. S. Kim, J. J. Kim, S. D. Lee, M. S. Lah, D. Moon and H. G. Jang, *Chem.–Eur. J.*, 2003, **9**, 678; (*c*) R. L. Paddock and S. T. Nguyen, *Chem. Commun.*, 2004, 1622; (*d*) J. Sun, L. Wang, S. Zhang, Z. Li, X. Zhang, W. Dai and R. Mori, *J. Mol. Catal. A: Chem.*, 2006, **256**, 295; (*e*) H. Jing and S. T. Nguyen, *J. Mol. Catal. A: Chem.*, 2007, **261**, 12; (*f*) T. Chang, H. Jing, L. Jin and W. Qiu, *J. Mol. Catal. A: Chem.*, 2007, **264**, 241; (*g*) L. Jin, H. Jing, T. Chang, X. Bu, L. Wang and Z. Liu, *J. Mol. Catal. A: Chem.*, 2007, **261**, 262.

7 (*a*) J. Peng and Y. Deng, *New J. Chem.*, 2001, **25**, 639; (*b*) H. Kawanami, A. Sasaki, K. Matsui and Y. Ikushima, *Chem. Commun.*, 2003, 896; (*c*) Y. J. Kim and R. S. Varma, *J. Org. Chem.*, 2005, **70**, 7882; (*d*) D.-W. Park, N.-Y. Mun, K.-H. Kim, I. Kim and S.-W. Park, *Catal. Today*, 2006, **115**, 130.

8 V. Caló, A. Nacci, A. Monopoli and A. Fanizzi, *Org. Lett.*, 2002, **4**, 2561.

9 Y. Du, J.-Q. Wang, J.-Y. Chen, F. Cai, J.-S. Tian, D.-L. Kong and L.-N. He, *Tetrahedron Lett.*, 2006, **47**, 1271.

10 (*a*) H. Yasuda, L.-N. He, T. Takahashi and T. Sakakura, *Appl. Catal., A*, 2006, **298**, 177; (*b*) C. Qi, H. Jiang, Z. Wang, B. Zou and S. Yang, *Synlett*, 2007, 255.

11 (*a*) T. Takahashi, T. Watahiki, S. Kitazume, H. Yasuda and T. Sakakura, *Chem. Commun.*, 2006, 1664; (*b*) A. Zhu, T. Jiang, B. Han, J. Zhang, Y. Xie and X. Ma, *Green Chem.*, 2007, **9**, 169; (*c*) A. Barbarini, R. Maggi, A. Mazzacani, G. Mori, G. Sartori and R. Sartorio, *Tetrahedron Lett.*, 2003, **44**, 2931.

12 Y. Du, F. Cai, D.-L. Kong and L.-N. He, *Green Chem.*, 2005, **7**, 518.

13 J.-S. Tian, C.-X. Miao, J.-Q. Wang, F. Cai, Y. Du, Y. Zhao and L.-N. He, *Green Chem.*, 2007, **9**, 566.

14 L.-N. He, H. Yasuda and T. Sakakura, *Green Chem.*, 2003, **5**, 92.

15 Y. Yamashita, M. Kamori, and H. Takenaka, *US Patent*, 6004786.

16 J. Horn and W. Bannwarth, *Eur. J. Org. Chem.*, 2007, 2058.

17 F. Hoffmann, M. Cornelius, J. Morell and M. Fröba, *Angew. Chem., Int. Ed.*, 2006, **45**, 3216.

18 C. Babij and A. J. Poë, *J. Phys. Org. Chem.*, 2004, **17**, 162.

19 T. Sakai, K. Hayashi, F. Yano, M. Takami, M. Ino, T. Korenaga and T. Ema, *Bull. Chem. Soc. Jpn.*, 2003, **76**, 1441.

20 J.-W. Huang and M. Shi, *J. Org. Chem.*, 2003, **68**, 6705.

21 W. J. Kruper and D. V. Dellar, *J. Org. Chem.*, 1995, **60**, 725.

Enantioselective catalytic hydrogenation of methyl α-acetamido cinnamate in [bmim][BF₄]/CO₂ media

Alireza Shariati,[a] Roger A. Sheldon,[b] Geert-Jan Witkamp[c] and Cor J. Peters*[d]

The homogeneously-catalyzed hydrogenation reaction of methyl α-acetamido cinnamate (MAC) was chosen to evaluate the feasibility of combining the advantages of ionic liquids (ILs) as solvents for reactions and the chiral complexes as catalysts for enantioselective reactions. 1-Butyl-3-methylimidazolium tetrafluoroborate ([bmim][BF₄]) and (−)-1,2-bis((2R,5R)-2,5-dimethylpholano)benzene (cyclooctadiene)rhodium(I) tetrafluoroborate (Rh-MeDuPHOS) were selected as the solvent and the catalyst, respectively. All experiments were carried out in an autoclave. The Rh-MeDuPHOS catalyst dissolved in [bmim][BF₄] was able to hydrogenate MAC with high conversions and enantioselectivities. The effects of hydrogen (H_2) pressure on the conversion and enantioselectivity of MAC hydrogenation were studied. It was shown that with increasing H_2 pressure, the conversion increases while the selectivity decreases. Adding carbon dioxide (CO_2) as a potential enhancer of this reaction was also studied. It was shown that by increasing the partial pressure of CO_2, the conversion decreases, while the selectivity increases. Catalyst recycling by extraction of the product with methyl *tert*-butyl ether (MTBE) was also possible.

1. Introduction

In recent years, ILs have increasingly attracted attention as the green, efficient reaction media of the future.[1–6] This is mainly because of their lack of noticeable vapor pressure, their good solvent power, their high thermal stability, and their widely tuneable properties with regard to polarity, hydrophobicity, and solvent miscibility through appropriate modifications of the cation, the anion, or their alkyl chains.

One type of reaction that may potentially benefit from ILs as their solvents is the homogeneous catalytic reaction. Asymmetric synthesis is one of the most versatile routes for producing optically active compounds, particularly by the use of enantioselective homogeneous chiral catalysts.[7–12] The wonderful outcome of homogeneous catalysis is that all of the active sites are available to the reactants. However, application of this methodology to industrial-scale is not easy because separation of the product from the homogeneous catalyst is difficult.

Innovative methods for immobilization and efficient recycling of homogeneous catalysts are facing ever increasing interest for the development of environmentally benign and economically

viable homogeneously catalysed processes.[7,13] One suggested method is to immobilize homogeneous catalysts in ILs. The product is then extracted by another solvent in which the IL and the catalyst do not dissolve.[14–19]

Extracting organic products from ILs using supercritical CO_2 without any cross-contamination, was first suggested by Brennecke and coworkers[20–21] and later was tested by Jessop and coworkers[22] for some asymmetric hydrogenation reactions. They could extract the product from the IL-phase using supercritical CO_2 without any IL or homogeneous catalyst contaminations, reaching a clean separation.

The solubility of H_2 in different ILs was determined by Dyson et al.[23] They showed that the concentration of H_2 in the different ILs is much lower than for molecular organic solvents. Jessop et al.[24] showed that dissolving CO_2 in the IL-phase can improve the hydrogenation reaction of some unsaturated carboxylic acids by easing the H_2 solubility in the IL-phase by decreasing the viscosity and expanding the IL. Similarly, Solinas et al.[25] discussed the effect of CO_2 on metal-catalyzed hydrogenation of imines in ILs. They demonstrated that the presence of CO_2 can be beneficial for efficient hydrogenation in ILs. Recently, Blackmond and coworkers[26,27] studied extensively the kinetic and selectivity aspects of H_2 availability on the hydrogenation reaction using Rh-chiral catalysts. Boyle et al.[28] performed the asymmetric hydrogenation of methyl α-benzamido cinnamate in an IL solvent using Rh-DuPHOS catalyst. They showed the feasibility of asymmetric hydrogenation in ILs with high conversion and selectivity.

The aim of this work was to experimentally investigate the possibility of combining the advantages of ILs as solvents for reactions and chiral catalysts for asymmetric reactions. For this purpose, the asymmetric homogeneous hydrogenation of MAC

[a]Chemical and Petroleum Engineering Department, Shiraz University, Shiraz, Iran
[b]Biocatalysis and Organic Chemistry, Faculty of Applied Sciences Delft University of Technology, Julianalaan 136, 2628 BL, Delft, The Netherlands
[c]Laboratory for Process Equipment, Department of Process & Energy, Faculty of Mechanical Engineering, Delft University of Technology, Leeghwaterstraat 44, 2628 CA, Delft, The Netherlands
[d]Physical Chemistry and Molecular Thermodynamics, Department of Chemical Technology, Faculty of Applied Sciences, Delft University of Technology, Julianalaan 136, 2628 BL, Delft, The Netherlands

in [bmim][BF$_4$] (Fig. 1) was selected as a model reaction. The Rh-MeDuPHOS homogeneous chiral complex (Fig. 2) was chosen as the catalyst, because this chiral complex has been found to be a very active and quite an efficient enantioselective catalyst in the homogeneous asymmetric reduction of enamides to chiral amino acid derivatives.[13]
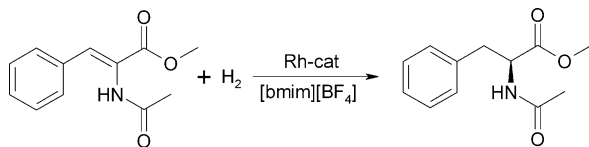

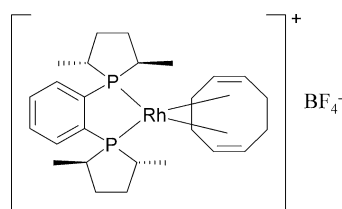**Fig. 1** The asymmetric hydrogenation of MAC.

Fig. 2 The Rh-MeDuPHOS chiral complex.

In order to investigate the role of CO$_2$ as a potential enhancer of this reaction, some of the hydrogenations were carried out in the presence of CO$_2$. In this work, the effects of H$_2$ pressure, CO$_2$ pressure, and temperature on the conversion and selectivity of the asymmetric hydrogenation of MAC were studied experimentally. To study the recyclability of the Rh-MeDuPHOS catalyst, and also the ability of the IL to immobilize the catalyst, some biphasic hydrogenation reactions were performed. MTBE was chosen as the solvent for extracting the reaction product from the IL-phase, because it forms a separable phase with [bmim][BF$_4$] and dissolves the product without extracting the catalyst. The hydrogenation of MAC in methanol (MeOH) was also studied for comparison.

2. Materials and methods

2.1. Materials

MAC was synthesized according to the procedure of Gladiali and Pinna.[29] Rh-MeDuPHOS catalyst was obtained from the Biocatalysis and Organic Chemistry group of Delft University of Technology. The method of synthesizing the catalyst has been explained by Simons *et al.*[7] Dried MeOH, MTBE and dichloromethane were purchased from Aldrich and flushed with nitrogen (N$_2$) for at least one hour before use. The ionic liquid [bmim][BF$_4$] was obtained from the Laboratory for Process Equipments of Delft University and Technology. In order to decrease the color of the IL, it was diluted by dichloromethane and the mixture was filtrated using a silica column. Then dichloromethane was removed by vacuum evaporation and the IL with a light yellow color was obtained. The IL was flushed with N$_2$ for several hours before use.

2.2. Reaction

The asymmetric hydrogenation reactions were carried out at room temperature in a 160 ml Parr autoclave with a stirring speed of 600 rpm. Preparations and processes before and after the reactions involving air-sensitive Rh-MeDuPHOS catalyst were performed under an atmosphere of dry N$_2$.

In the homogeneous reactions in [bmim][BF$_4$] or MeOH, 50 ml of the reactant and catalyst solution in [bmim][BF$_4$] or MeOH (concentration of MAC = 0.02 g ml^{-1}, and concentration of Rh-MeDuPHOS = 1.46 × 10^{-4} g ml^{-1}) was transferred to the autoclave under a nitrogen atmosphere. The sealed autoclave was purged several times by H$_2$ while the stirrer rotated at low speed to ensure that the reactor is free of N$_2$. Then, the desired pressure was applied and the stirring speed was set to 600 rpm. Upon completion of the reaction, the remaining H$_2$ pressure was released. For analysing the reaction results, in the case of [bmim][BF$_4$] solvent, a sample of the reaction solution was extracted using MTBE. If the solvent was MeOH, the solvent was evaporated using vacuum.

Conversions of the hydrogenation reactions were determined by ^{1}H NMR analysis. Enantiomer excesses (ee%) of the reactions were determined by chiral HPLC using a Chiralcel OD column with 2-propanol/hexane (10 : 90) as eluent.

In the biphasic reactions, the catalyst was immobilized in the IL by dissolving it in 15 ml of [bmim][BF$_4$] under N$_2$ atmosphere. MAC dissolved in 40 ml of MTBE (0.004 g ml^{-1}) was added to the immobilized catalyst in the reactor. The reactor was then pressurized by H$_2$ as explained for the homogeneous reactions. After the reaction, the remaining pressure was released and the MTBE-phase and the IL-phase were separated under N$_2$ atmosphere. Following the removal of the MTBE solution, fresh substrate solution was added to the used IL-phase containing the used catalyst and the hydrogenation procedure was repeated. All the catalyst was reused in this way 3 times. Before analysing the reaction results, MTBE was removed from the reaction samples by vacuum evaporation. Additional specifications of the reactions are given at the bottom of Table 1.

3. Results and discussion

In order to study the effect of H$_2$ pressure on the conversion and enantioselctivity of the asymmetric hydrogenation of MAC using the Rh-MeDuPHOS chiral catalyst, the reaction was first performed in MeOH at three different pressures, *i.e.* 5, 20, and 50 bar, respectively. Table 1 summarizes the experimental results (Entries 1–3). These reactions show that 100% conversions were achieved at all 3 pressures. This is most probably due to the significant solubility of H$_2$ in MeOH, which causes sufficient availability of H$_2$ at the catalyst site. On the other hand, the enantioselectivities decreased by increasing pressure. As Blackmond and co-workers[30] explained in detail, the key kinetic parameter affecting enantioselectivity of asymmetric catalytic hydrogenation reactions is the concentration of molecular H$_2$ in the liquid phase, which is related to the pressure of the system, the rate of mass transfer, and the intrinsic kinetics of the competing reactions. Blackmond and co-workers[30] discussed that in cases in which the enatioselectivity decreases with increasing H$_2$ pressure, the system can benefit from H$_2$-starved conditions. In other

Table 1 Experimental results of the asymmetric hydrogenation of MAC^a

Entry	Solvent	H_2/bar	CO_2/bar	Conv.%	ee%
1	MeOH	5	0	100	94.1
2	MeOH	20	0	100	89.9
3	MeOH	50	0	100	85.8
4	[bmim][BF$_4$]	5	0	0	—
5	[bmim][BF$_4$]	20	0	94.2	91.9
6	[bmim][BF$_4$]	50	0	100	56.2
7	[bmim][BF$_4$]	5	35	10.0	69.7
8	[bmim][BF$_4$]	20	35	25.8	90.8
9	[bmim][BF$_4$]	20	5	61.0	81.8
10	[bmim][BF$_4$]	40	20	95.2	79.4
11	[bmim][BF$_4$]	50	10	100	71.2
12^b	[bmim][BF$_4$]/MTBE	20	0		
Cycle 1				100	91.5
Cycle 2				100	88.6
Cycle 3				100	88.4
13^c	[bmim][BF$_4$]/MTBE	20	0		
Cycle 1				5.3	100
Cycle 2				1.2	87.1
Cycle 3				0	—
14^d		20	0	100	77.8

^{a} For homogeneous reactions in MeOH the reaction time was 45 min. For homogeneous reactions in [bmim][BF$_4$] the reaction time was 24 h, however no pressure change was observed after 2 h of reaction. For the biphasic reactions, the reaction time was 2 h for each cycle. ^{b} The catalyst concentration = 1.46×10^{-4} g ml^{-1}. ^{c} The catalyst concentration = 6.69×10^{-5} g ml^{-1}. ^{d} T = 50 °C.

words, a diffusion-limited regime could be beneficial because the rate of consumption of H_2 by the reaction would be higher than the rate of diffusion of H_2 to the liquid phase.

Therefore, [bmim][BF$_4$] can be a good choice for this reaction, because as reported by Berger *et al.*[16] the solubility of H_2 in [bmim][BF$_4$] is very low. Although Berger *et al.*[16] mentioned that the solubility of hydrogen in [bmim][PF$_6$] is four times lower than in [bmim][BF$_4$], but it needs much higher pressure to achieve the same concentration of hydrogen in the liquid phase. Also, the solubility of Rh-MeDuPHOS in [bmim][BF$_4$] is very good.

In the next step of the experiments, the homogeneous hydrogenation reactions were carried out in the IL-phase. Table 1 shows the results (Entries 4–6). As expected, by increasing H_2 pressure, the conversions increased while the enantioselectivity decreased. As can be seen in Table 1, the homogeneous reaction has a quite high conversion and selectivity at 20 bar. At 5 bar, no conversion was detected. This shows the absence of sufficient H_2 in the IL phase at low pressures.

In order to study the effect of CO_2 on the reaction, CO_2 was added to the system at different pressures. Table 1 (Entries 7–11) shows the results for cases where CO_2 and H_2 coexist. A comparison of Entry 7, which has 10% conversion, with Entry 4, which has 0% conversion at the same hydrogen pressure, shows that the addition of CO_2 increased the conversion. This can be due to the decreased viscosity and the expansion of the IL-phase as a result of CO_2 dissolution, making it easier for H_2 to dissolve in the liquid phase. This phenomenon, *i.e.* the increase of H_2 concentration in the presence of CO_2, is extensively discussed by Solinas *et al.*[25] A comparison of the results of Entries 8 and 9 with Entry 5, on the other hand, shows that the conversion drops dramatically when the CO_2 pressure increases at constant H_2 pressure. Possible causes for this phenomenon may be the:

(a) anti-solvent effect of CO_2 on MAC or the catalyst

(b) extraction of MAC or the catalyst from the IL phase by the gas phase

(c) reduction of the catalyst activity by CO_2

(d) reduction of the MAC and the catalyst concentrations in the IL phase due to the significant solubility of CO_2 in the IL phase

Kroon *et al.*'s[31] experimental studies on the same reactive system do not support postulates (a) and (b) of this study. They used supercritical CO_2 for their experiments. Since CO_2 was not at supercritical conditions in our study, it had even lower solvent or anti-solvent power than Kroon *et al.*'s study, therefore postulates (a) and (b) are not responsible for the observed effects.

Leitner and co-workers[32] studied the reactivity of catalysts with rhodium complexes in supercritical CO_2 and concluded that the reactivities of such catalysts do not decrease in a supercritical CO_2 environment. Therefore, postulate (c) is also unlikely to be the case.

As Leitner[33] extensively discussed the role of supercritical CO_2 in hydrogenation reactions using organometalic catalysts, when CO_2 dissolves in a liquid solvent, it expands the liquid phase, therefore the catalyst and the reactant distribute over a larger volume. In the case of this study, it is true that the volumetric expansion of ILs in the presence of CO_2 is generally small, but because of the high solubility of CO_2 in the IL-phase, the concentrations of the catalyst and the reactant decrease dramatically, thereby affecting the conversion and enatioselctivity of the reaction. Entry 13, which was carried out at much lower concentration of the catalyst with no CO_2 present, also supports postulate (d). A similar phenomenon was observed by Webb *et al.*[34] for the hydroformylation of 1-hexene in [bmim][PF$_6$] in the presence of CO_2 catalyzed by a Rh-complex catalyst.

A plot of conversion and enantioselectivity as a function of the H_2 and CO_2 pressure ratios (P_{H_2}/P_{total} and P_{CO_2}/P_{total}) taken from Entries 6, 8, 10 and 11 in Table 1, with P_{total}= 50–60 bar, shows some interesting results (Fig. 3a and 3b). These ratios are representative for the H_2 and CO_2 concentrations in the IL-phase, respectively. As shown in Fig. 3a, by increasing the H_2 pressure ratio, the conversion increases while the selectivity decreases. By increasing the CO_2 pressure ratio, the conversion decreases while the enantioselectivity increases. The explanation behind this behavior is that by increasing the partial pressure of CO_2 in the system, the catalyst and the reactant become diluted, and as we expect, the enantioselectivity increases while the conversion decreases. We can conclude from these experiments that in order to obtain high conversion and selectivity for this asymmetric hydrogenation reaction, it is recommended to do first the homogeneous reaction in the absence of CO_2, and after completion of the reaction adding CO_2 to the system for extracting the reaction products and catalyst recycling.

In order to study the recyclability of the catalyst, two sets of biphasic experiments with [bmim][BF$_4$]/MTBE were performed. The IL and MTBE act as the immobilizer of the catalyst and as the solvent for the reactant and the product, respectively. As shown in the bottom of Table 1, for one set of the experiments (Entry 12), the concentration of the catalyst is the same as its concentration for homogeneous reactions (Entries 1–11). Entry 13 shows a case with much lower catalyst concentration. As

(a)

(b)
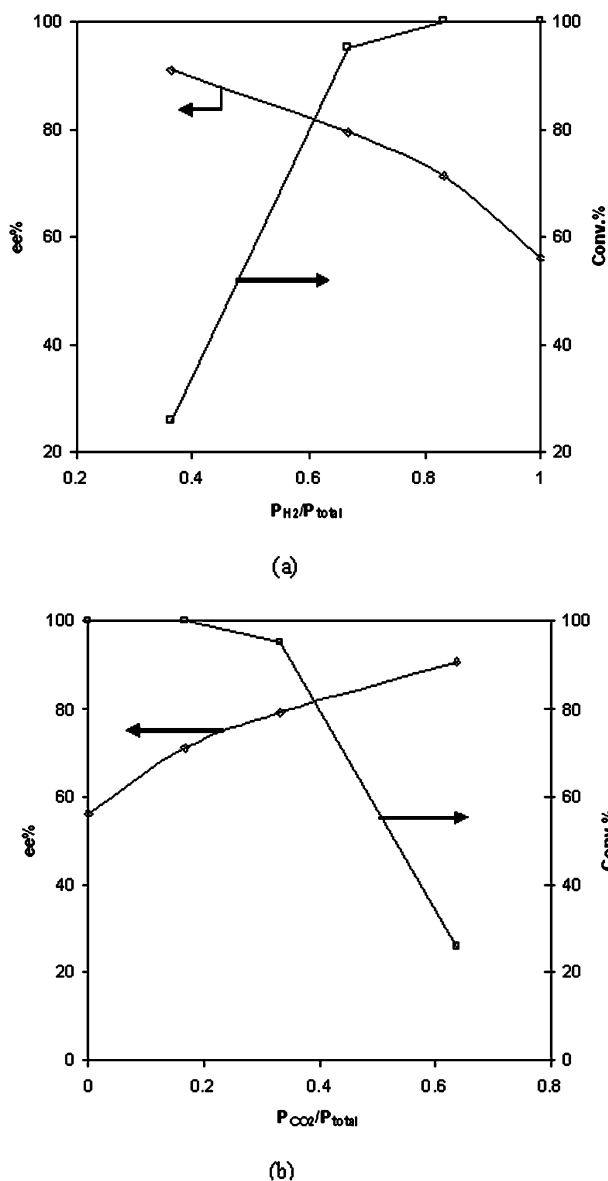
Fig. 3 Enantioselectivity and conversion of the asymmetric hydrogenation of MAC *versus* (a) H$_2$ pressure (b) CO$_2$ pressure ratio P_{total} = 50–60 bar.

can be seen, the effect of catalyst concentration is extremely significant. Entry 12 shows that it is possible to reuse the catalyst three times with high conversion and selectivity (without any loss in the conversion and only a slight drop in selectivity). However, for Entry 13 the conversions are too low. We think the reason that we do not get 100% conversion for Entry 5 at 20 bar, while we get complete conversion for Entry 12, is that MTBE is slightly dissolved in the IL-phase decreasing the viscosity, and therefore increasing the solubility of H$_2$ in the IL phase. Fig. 4 shows the results of Entry 12 graphically.

In order to study the effect of temperature on the hydrogenation reaction of MAC, a test according to Entry 14 was performed at 50 °C. As shown in Table 1, the conversion increased to 100% while the selectivity decreased in comparison with Entry 5. This is because the solubility of H$_2$ in the IL phase increases with increasing temperature.
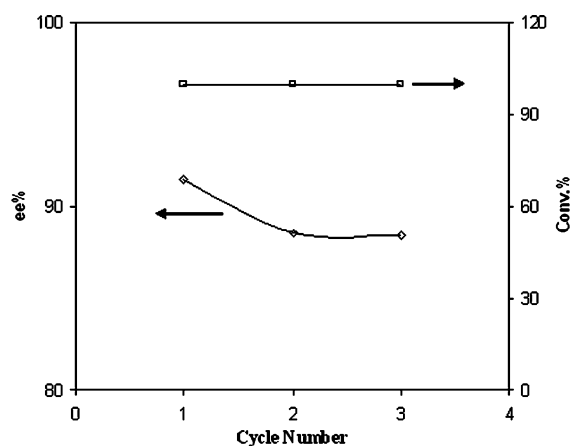
Fig. 4 Conversion and enantiosesectivity of the asymmetric hydrogenation of MAC in 3 consecutive recycles of IL/catalyst mixture.

4. Conclusion

Asymmetric hydrogenation of MAC in [bmim][BF$_4$] is feasible using Rh-MeDuPHOS as the homogeneous catalyst. [Bmim][BF$_4$], which dissolves low concentrations of H$_2$, is a good solvent for the asymmetric hydrogenation of MAC as it needs minimal amounts of dissolved H$_2$. The dilution effect of CO$_2$ on the catalyst and MAC causes the decrease of the conversion of the asymmetric hydrogenation of MAC in [bmim][BF$_4$]. It is suggested for this reaction to do first the homogeneous reaction and then add the extractive supercritical CO$_2$ in order to prevent conversion drop. Recycling of the catalyst using MTBE for extracting the reaction product was possible. A temperature rise decreased the selectivity of this reaction in [bmim][BF$_4$].

Acknowledgements

References

1 T. Welton, Ionic liquids in catalysis, *Coord. Chem. Rev.*, 2004, **248**, 2459–2477.
2 H. Olivier-Bourbigou and L. Magna, Ionic liquids: Perspectives for organic and catalytic reactions, *J. Mol. Catal. A: Chem.*, 2002, **182–183**, 419–437.
3 R. Sheldon, Catalytic reactions in ionic liquids, *Chem. Commun.*, 2001, 2399–2407.
4 C. M. Gordon, New developments in catalysis using ionic liquids, *Appl. Catal., A*, 2001, **222**, 101–117.
5 P. Wasserscheid and W. Keim, Ionic liquids-new "solutions" for transition metal catalysis, *Angew. Chem., Int. Ed.*, 2000, **39**, 3772–3789.
6 T. Welton, Room-temperture ionic liquids. Solvents for synthesis and catalysis, *Chem. Rev.*, 1999, **99**, 2071–2083.
7 C. Simons, U. Hanefeld, I. W. C. E. Arends, R. A. Sheldon and T. Maschmeyer, Noncovalent anchoring of asymmetric hydrogenation catalysts on a new mesoporous aluminosilicate: application and solvent effects, *Chem.–Eur. J.*, 2004, **10**, 5829–5835.
8 H. M. L. Davis and G. H. Lee, Enantioselective synthesis of cyclopropylphosphonates containing quaternary stereocenters using a D$_2$-symmetric chiral catalyst Rh$_2$(S-biTISP)$_2$, *Org. Lett.*, 2004, **6**, 2117–2120.

9 H. M. L. Davis and G. H. Lee, Dirhodium(II) tetra(*N*-(dodecyl benzenesulfonyl)prolinate) catalyzed enantioselective cyclopropenation of alkynes, *Org. Lett.*, 2004, **6**, 1233–1236.

10 C. Kashima, Y. Miwa, S. Shibata and H. Nakazono, Asymmetric diels alder reaction using pyrazole derivatives as a chiral catalyst, *J. Heterocycl. Chem.*, 2003, **40**, 681–688.

11 K. T. Sprott and E. J. Corey, A new cationic, chiral catalyst for highly enantioselective Diels–Alder reactions, *Org. Lett.*, 2003, **5**, 2465–2467.

12 K. Ohe, K. Morioka, K. Yonehara and S. Uemura, Asymmetric hydrogenation of enamides in aqueous media with a new water-soluble chiral rhodium-α,α-trehalose-derived phosphine-phosphinite catalyst, *Tetrahedron: Asymmetry*, 2002, **13**, 2155–2160.

13 A. Wolfson, S. Geresh, M. Gottlieb and M. Herskowitz, Heterogenization of Rh-MeDuPHOS by occlusion in polyvinyl alcohol films, *Tetrahedron: Asymmetry*, 2002, **13**, 465–468.

14 M. Berthod, J. M. Joerger, G. Mignani, M. Vaultier and M. Lemaire, Enantioselective catalytic asymmetric hydrogenation of ethyl acetoacetate in room temperature ionic liquids, *Tetrahedron: Asymmetry*, 2004, **15**, 2219–2221.

15 S. Guernik, A. Wolfson, M. Herskowitz, N. Greenspoon and S. Geresh, A novel system consisting of Rh-DuPHOS and ionic liquid for asymmetric hydrogenations, *Chem. Commun.*, 2001, 2314–2315.

16 A. Berger, R. F. de Souza, M. R. Delgado and J. Dupont, Ionic liquid-phase asymmetric catalytic hydrogenation: hydrogen concentration effects on enantioselectivity, *Tetrahedron: Asymmetry*, 2001, **12**, 1825–1828.

17 P. A. Z. Suarez, J. E. L. Dullius, S. Einloft, R. F. deSouza and J. Dupont, The use of new ionic liquids in two-phase catalytic hydrogenation reaction by rhodium complexes, *Polyhedron*, 1996, **15**, 1217–1219.

18 Y. Chauvin, L. Mussmann and H. Olivier, A novel class of versatile solvents for two-phase catalysis: hydrogenation, isomerization, and hydroformylation of alkenes catalyzed by rhodium complexes in liquid 1,3-dialkylimidazolium salts, *Angew. Chem., Int. Ed. Engl.*, 1996, **34**, 2698–2700.

19 A. L. Monteiro, F. K. Zinn, R. F. de Souza and J. Dupont, Asymmetric hydrogenation of 2-arylacrylic acids catalyzed by immobilized Ru-BINAP complex in 1-n-butyl-3-methylimidazolium tetrafluoroborate molten salt, *Tetrahedron: Asymmetry*, 1997, **8**, 177–179.

20 L. A. Blanchard, D. Hancut, E. J. Beckman and J. F. Brennecke, Green processing using ionic liquids and CO₂, *Nature*, 1999, **399**, 28–29.

21 L. A. Blanchard and J. F. Brennecke, Recoveryof organic products from ionic liquids using supercritical carbon dioxide, *Ind. Eng. Chem. Res.*, 2001, **40**, 287–292.

22 R. A. Brown, P. Pollet, E. McKoon, C. A. Eckert, C. L. Liotta and P. G. Jessop, Asymmetric hydrogenation and catalyst recycling using ionic liquid and supercritical carbon dioxide, *J. Am. Chem. Soc.*, 2001, **123**, 1254–1255.

23 P. J. Dyson, G. Laurenczy, C. A. Ohlin, J. Vallance and T. Welton, Detrmination of hydrogen concentration in ionic liquids and the effect (or lack of) on rates of hydrogenation, *Chem. Commun.*, 2003, 2418–2419.

24 P. G. Jessop, R. R. Stanely, R. A. Brown, C. A. Eckert, C. L. Liotta, T. T. Ngo and P. Pollet, Neoteric solvents for asymmetric hydrogenation: supercritical fluids, ionic liquids, and expanded ionic liquids, *Green Chem.*, 2003, **5**, 123–128.

25 M. Solinas, A. Pfaltz, P. G. Cozzi and W. Leitner, Enantioselective hydrogenation of imines in ionic liquid/carbon dioxide media, *J. Am. Chem. Soc.*, 2004, **126**, 16142–16147.

26 M. T. Reetz, A. Meiswinkel, G. Mehler, K. Angermund, M. Graf, W. Thiel, R. Mynott and D. G. Blackmond, Why are BINOL-based monophosphites such efficient ligands in Rh-catalyzed asymmetric olefin hydrogenation?, *J. Am. Chem. Soc.*, 2005, **127**, 10305–10313.

27 D. G. Blackmond, M. Ropic and M. Stefinovic, Kinetic studies of the asymmetric transfer hydrogenation of imines with formic acid catalyzed by Rh-diamine catalysts, *Org. Process Res. Dev.*, 2006, **10**, 457–463.

28 K. L. Boyle, E. B. Lipsky and K. S. Kalberg, Asymmetric hydrogenation of methyl α-benzamido cinnamate in ionic liquid solvent, *Tetrahedron Lett.*, 2006, **47**, 1311–1313.

29 S. Gladiali and L. Pinna, Asymmetric hydroformylation of *N*-acyl 1-aminoacrylic acid derivatives by rhodium/chiral diphosphine catalysts, *Tetrahedron: Asymmetry*, 1991, **2**, 623–632.

30 Y. Sun, R. N. Landau, J. Wang, C. LeBlond and D. G. Blackmond, A re-examination of pressure effects on enantioselectivity in asymmetric catalytic hydrogenation, *J. Am. Chem. Soc.*, 1996, **118**, 1348–1353.

31 M. C. Kroon, J. Van Spronsen, C. J. Peters, R. Sheldon and G.-J. Witkamp, Recovery of pure products from ionic liquids using supercritical carbon dioxide as a co-solvent in extractions or as an anti-solvent in precipitation, *Green Chem.*, 2006, **8**, 246–249.

32 G. Francio, K. Wittmann and W. Leitner, Highly efficient enantioselective catalysis in supercritical carbon dioxide using the perfuoroalkyl-substituted ligand (*R*,*S*)-3-H²F⁶-BINAPHOS, *J. Organomet. Chem.*, 2001, **621**, 130.

33 J. G. De Vries and C. J. Elsevier, *Handbook of Homogeneous Hydrogenation. Supercritical and Compressed Carbon Dioxide as Reaction Medium and Mass Separating Agent for Hydrogenation Reactions using Organometallic Catalysts*, ed. W. Leitner, Wiley-VCH, Weinheim, 2007, vol. 3, ch. 39 .

34 P. B. Webb, M. F. Sellin, T. E. Kunene, S. Williamson, A. M. Z. Slawin and D. J. Cole-Hamilton, Continuous flow hydroformylation of alkenes in supercritical fluid-ionic liquid biphasic systems, *J. Am. Chem. Soc.*, 2003, **125**, 15577–15588.

GDCh

GESELLSCHAFT DEUTSCHER CHEMIKER

Arbeitsgemeinschaft Nachhaltige Chemie

Scientific Conference:
Dream Reactions – Synthesis and Processes for Sustainable Chemistry

April 23 – 25, 2008 · Aachen

MAJOR TOPICS

CO_2-Fixation
Metrics and Concepts for Sustainability
Transformation of Renewable Feedstocks
Selective Oxidation
Controlling Selectivity
Atom Efficient Bond Formation

INVITED LECTURERS

C. Bolm, Aachen/D
D. Cole-Hamilton, St. Andrews/GB
M. Döring, Karsruhe/D
C. Eckert, Georgia/USA
L. Gooßen, Kaiserslautern/D
T. Graening, Berlin/D
C. Gürtler, Leverkusen/D
S. K. Hashmi, Heidelberg/D
P. G. Jessop, Ontario/CDN
J. Lacour, Genf/CH
C. Liotta, Georgia/USA
P. Saling, Ludwigshafen/D
Y. She, Peking/PRC

KEY NOTE LECTURERS

M. Beller, Rostock/D
K. Wagemann, Frankfurt/D

Tutorial Workshop:
Green Chemistry and Catalysis

April 25 – 26, 2008 · Aachen

RWTH AACHEN UNIVERSITY   Center of Catalysis Research   Bayer MaterialScience   ITMC RWTH

www.gdch.de/nachhaltig2008
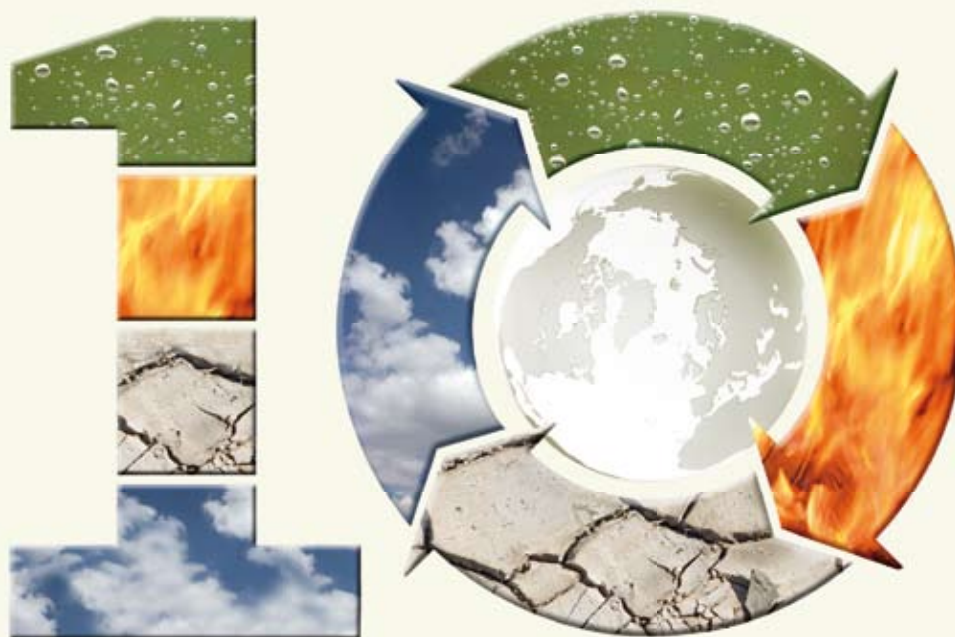
years of publishing!

Green Chemistry…

- The most highly cited *Green Chemistry* journal, Impact factor = 4.192*

- Fast publication, typically <90 days for full papers

- Full variety of research including reviews, communications, full papers and perspectives.

Celebrating 10 years of publishing, **Green Chemistry** offers the latest research that reduces the environmental impact of the chemical enterprise by developing alternative sustainable technologies, and provides a unique forum for the rapid publication of cutting-edge and innovative research for a greener, sustainable future

…for a sustainable future!

* 2006 Thomson Scientific (ISI) Journal Citation Reports ®

110739

RSC Publishing

www.rsc.org/greenchem

Registered Charity Number 207890